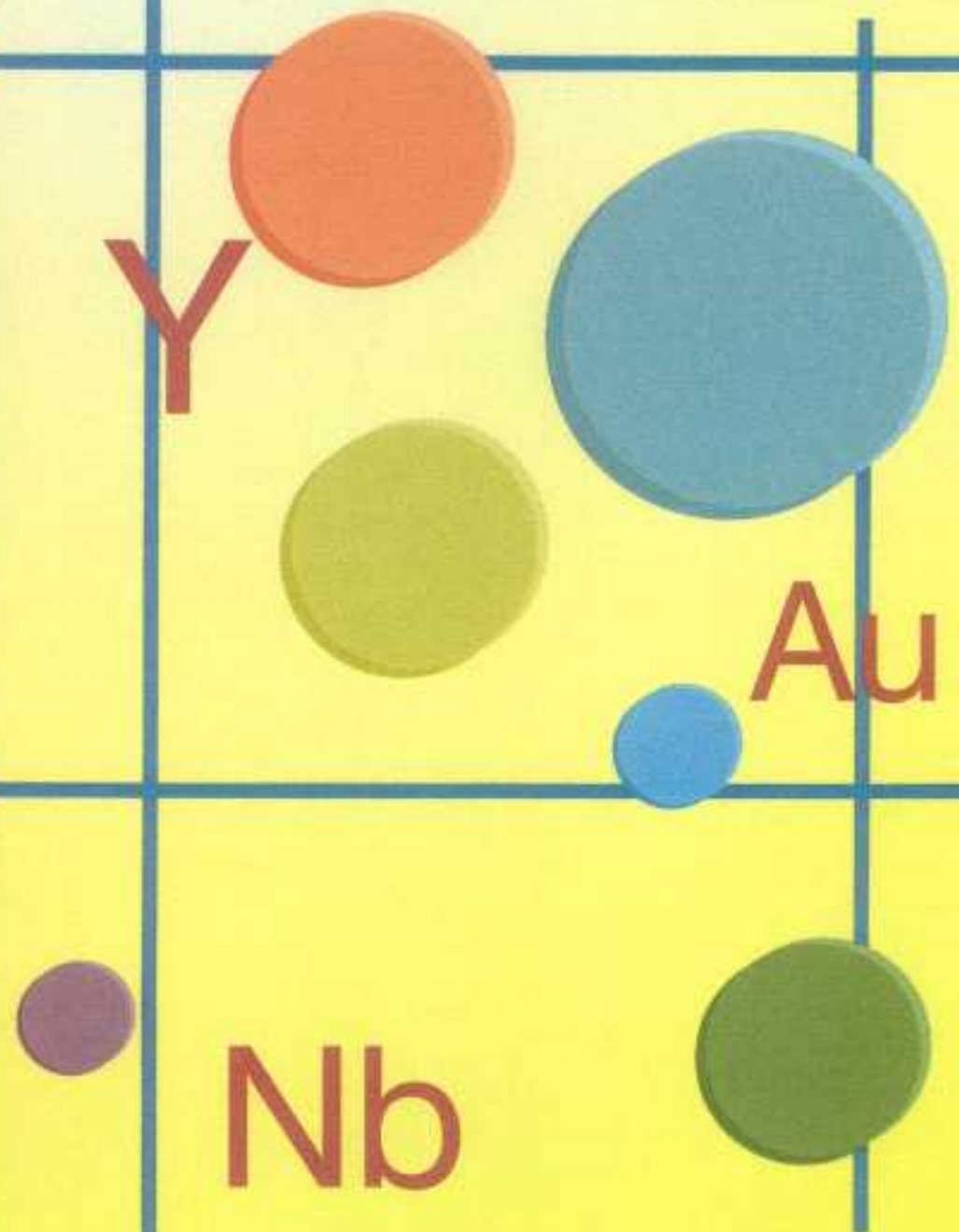




GEOCHEMICAL MAPPING OF THE KINGSTON 1:250 000 SHEET

by K. J. Pye, P. A. Morris, and S. A. McGuinness

1:250 000 REGOLITH GEOCHEMISTRY SERIES



GEOLOGICAL SURVEY OF WESTERN AUSTRALIA

DEPARTMENT OF MINERALS AND ENERGY





GEOLOGICAL SURVEY OF WESTERN AUSTRALIA

**GEOCHEMICAL MAPPING
OF THE KINGSTON
1:250 000 SHEET**

by
K. J. Pye, P. A. Morris, and S. A. McGuinness

Perth 2000

MINISTER FOR MINES
The Hon. Norman Moore, MLC

DIRECTOR GENERAL
L. C. Ranford

DIRECTOR, GEOLOGICAL SURVEY OF WESTERN AUSTRALIA
David Blight

Copy editor: J. A. Mikucki

REFERENCE

The recommended reference for this publication is:

PYE, K. J., MORRIS, P. A., and MCGUINNESS, S. A., 2000, Geochemical mapping of the Kingston 1:250 000 sheet: Western Australia Geological Survey, 1:250 000 Regolith Geochemistry Series Explanatory Notes, 53p.

National Library of Australia Card Number and ISBN 0 7307 5652 1

Grid references in this publication refer to the Geocentric Datum of Australia 1994 (GDA94)

Printed by Ausdoc On Demand Pty Ltd, Perth, Western Australia

Copies available from:
Information Centre
Department of Minerals and Energy
100 Plain Street
EAST PERTH, WESTERN AUSTRALIA 6004
Telephone: (08) 9222 3459 Facsimile: (08) 9222 3444
www.dme.wa.gov.au

Contents

Abstract	1
Introduction	1
Location and access	2
Physiography, vegetation, and soils	2
Physiography	2
Vegetation	2
Soils	3
Climate	3
Topographic and remote-sensing datasets	3
Geology	3
Archaean granite-greenstones	4
Proterozoic sedimentary rocks (Earaheedy Group)	4
Yelma Formation	4
Frere Formation	4
Windidda Formation	4
Chiall Formation	5
Wongawol Formation	5
Kulele Limestone	5
Mulgarra Sandstone	5
Dolerite	5
Permian rocks (Paterson Formation)	5
Economic geology and mineralization	6
Geochemical surveys in open-file company reports	6
Regolith sampling and mapping	6
Regolith associated with Archaean granite and greenstone	7
Regolith of the Earaheedy Group and Paterson Formation	8
Regolith associated with lake systems	9
Discussion	9
Chemical analysis and quality control	10
Element-distribution maps	11
Major element oxides and loss-on-ignition	11
Trace elements	15
Discussion	17
Parent lithology (bedrock control)	17
Control exerted by regolith type	18
Statistical treatment of regolith chemical data	19
Comparison of various sandplain regolith populations	19
Comparison of greenstone belts	22
Downslope changes in regolith chemistry	22
Comparison of some depositional regime regolith units over Archaean granitoid	22
Speciality maps	28
Regolith pH and conductivity	28
Element-index maps	28
Chalcophile index	28
Mineralization potential	28
Summary and conclusions	32
References	34

Appendices

1. Gazetteer of localities	37
2. Gold production from mines and prospects on KINGSTON prior to December 1998	38
3. Open-file surface geochemistry for KINGSTON as at April 1999	39
4. Sampling, regolith-materials classification, quality control, and analytical procedures	45
5. Quality-control data (digital; disk in pocket)	

Plates (in pocket)

1. Simplified geology and sample locations (1:250 000)
2. Regolith materials (1:250 000)
3. Company projects with surface geochemistry data in open-file reports (at April 1999)

Figures (from p. 53)

1. Status of GSWA regional regolith and geochemical mapping program
2. Simplified locality plan
3. Simplified geological interpretation
4. Generalized regolith map

Element-distribution maps

5. TiO_2
6. Al_2O_3
7. Fe_2O_3
8. MnO
9. MgO
10. CaO
11. Na_2O
12. K_2O
13. P_2O_5
14. LOI
15. Ag
16. As
17. Au
18. Ba
19. Be
20. Bi
21. Cd
22. Ce
23. Co
24. Cr
25. Cu
26. Ga
27. In
28. La
29. Li
30. Mo
31. Nb
32. Ni
33. Pb
34. Pd
35. Pt
36. Rb
37. S
38. Sb
39. Sc
40. Se
41. Sn
42. Sr
43. Ta
44. Te
45. Th
46. U
47. V
48. W
49. Y
50. Zn
51. Zr
52. pH in regolith
53. Conductivity of regolith (mS/cm)
54. Chalcophile index ($\text{As} + \text{Sb} + \text{Bi} + \text{Mo} + \text{Ag} + \text{Sn} + \text{W} + \text{Se}$)

Tables

1. Regolith according to area and number of samples per regolith-materials unit	7
2. Samples with anomalous concentrations of analytes	12
3. Summary statistics for sandplain (<i>S</i>) over Archaean granitoid and sandplain elsewhere	20
4. Summary statistics for sandplain (<i>S</i>) over Paterson Formation and Archaean granitoid	21
5. Summary statistics for sandplain (<i>S</i>), and undulating sandplain (<i>SI</i>)	23
6. Summary statistics for regolith over the Gerry Well and Mount Eureka greenstone belts	24
7. Summary statistics for exposed regime regolith and colluvium (<i>Xfc</i> and <i>Cfc</i>) over the Frere Formation	25
8. Summary statistics for sheetwash (<i>W</i>) and colluvium (<i>Cfc</i>) over the Frere Formation	26
9. Summary statistics for exposed regime regolith and colluvium (<i>Xgp</i> and <i>Cgp</i>) over Archaean granitoid	27
10. Summary statistics for sheetwash in drainage depressions (<i>W_d</i>) and sandplain (<i>S</i>) over Archaean granitoid	29
11. Summary statistics for sheetwash in drainage depressions (<i>W_d</i>) and colluvium (<i>Cgp</i>) over Archaean granitoid	30
12. Summary statistics for sheetwash in drainage depressions over Archaean granitoid (<i>W_d</i>) and sheetwash from elsewhere (<i>W</i>)	31

Digital dataset (in pocket)

- 1. KINGSTON regional regolith geochemical data (KINGSTON.CSV)
- 2. Appendix 5 (quality-control data)

Geochemical mapping of the Kingston 1:250 000 sheet

by

K. J. Pye, P. A. Morris, and S. A. McGuinness

Abstract

Regolith and regolith geochemical mapping of the KINGSTON 1:250 000 map sheet has involved collection of 998 regolith samples (355 stream-sediment, 326 sheetwash, 227 sandplain, and 90 lake-sediment samples), sampled at a nominal density of one per 16 km². Each sample has been analysed for 48 components, acidity–alkalinity (pH), and conductivity. Results for major-element oxides (except SiO₂) and trace elements are represented as spot-concentration maps. Gold production data from greenstone-hosted mineralization is tabulated, as well as relevant open-file exploration company data.

Regolith on KINGSTON has been classified as either residual, exposed (corresponding to bedrock and subcrop), or depositional, and further subdivided largely on the basis of lithology, where appropriate. A regolith-materials map shows that the residual regime regolith only accounts for 2% by area on KINGSTON, with exposed regime regolith accounting for a further 13%. The remaining area is occupied by depositional regime regolith, of which the majority (28% of all regolith by area) is colluvium.

Regolith chemistry delineates the extent of bedrock, in particular two Archaean greenstone belts, which differ markedly in terms of bedrock chemistry and degree of weathering compared to the intervening granitoid rocks. Small areas of Proterozoic dolerite are also highlighted by a distinctive regolith chemistry (e.g. relatively high TiO₂, Sc, V), even for analytes at low concentrations, such as In and Se. Statistical analysis of regolith derived from shales and ferruginous sedimentary rocks of the Frere Formation, and Archaean granitoid rock, shows no difference in median values for exposed regime regolith relative to regolith further downslope, which is consistent with the dominance of physical rather than chemical weathering. Other statistical tests have been used to examine the chemistry of different sandplain deposits, showing that some of them are locally derived.

Precious-metal abundances are low in regolith on KINGSTON, reaching 4 ppb Au, 4 ppb Pd, and 9 ppb Pt. The highest values are in regolith over Archaean greenstone. Areas of multiple-element anomalism are confined to the Frere Formation and the siliciclastic- and carbonate-dominated Windidda Formation in the Wellington Range area, and over parts of the dominantly siliciclastic Wongawol Formation, and Kulele Limestone on the northern boundary with STANLEY. In the Wellington Range area, a chalcophile index has highlighted a possible area of sulfide-related mineralization, and this area coincides with regional- and local-scale deformation, involving brittle fracture and quartz veining. Areas of regolith with anomalous concentrations of some components over parts of the Wongawol Formation (K₂O, Ce, La, Li, Rb, Ta, Zn) and Kulele Limestone (TiO₂, MgO, K₂O, Ce, Pb, Rb, Ta, Zn) are contiguous with areas of regolith over manganiferous sedimentary rocks in the southern part of STANLEY, which also have anomalous concentrations of several components. These areas of anomalous concentrations in regolith in the southern part of STANLEY are discussed in terms of stratiform mineralization.

KEYWORDS: Kingston, regolith, geochemistry, mineralization, remote sensing.

Introduction

Regolith and geochemical mapping of the KINGSTON* 1:250 000 map sheet has been completed as part of the regional regolith and geochemical mapping program of the Geological Survey of Western Australia (GSWA). This program, commenced as part of GSWA's New Initiatives program in 1994, aims to collect and synthesize regolith chemical data to assist the mineral exploration industry, pastoralists, and environmental agencies.

To date, nineteen 1:250 000-scale map sheets have been sampled as part of this program, covering parts of the Archaean Yilgarn Craton, Proterozoic rocks of the Capricorn Orogen and Northampton Complex, part of the Proterozoic Albany–Fraser Orogen, and the Phanerozoic Carnarvon Basin. The KINGSTON regolith maps and explanatory notes extend and complement similar work on nearby map sheets (Fig. 1).

Jackson (1997) defined regolith as a 'general term for the layer or mantle of fragmental and unconsolidated rock material, whether residual or transported and of highly varied character, that nearly everywhere forms the surface

* Capitalized names refer to standard map sheets.

of the land and overlies or covers the bedrock'. Regolith materials include weathered rock in situ (e.g. saprock, saprolite), transported material (alluvial, colluvial, and windblown deposits), and chemical precipitates such as calcrete and various duricrusts (Ollier and Pain, 1996). Regolith blankets a significant area of Western Australia and commonly conceals bedrock mineralization. Geochemical signatures of mineral deposits, and related pathfinder elements, are diluted in regolith, or they concentrate differentially due to regolith-forming processes. Many exposed mineral deposits have been discovered in Western Australia; therefore, explorationists must increasingly look to regolith-dominated areas for deposits of economic significance. Thus, it is vital to understand the processes of regolith formation, and the behaviour of elements in the regolith environment. Geochemical mapping of regolith assists in this task and provides clues to the nature of underlying bedrock and potential mineralization.

Location and access

The KINGSTON 1:250 000 sheet (SF 50-10) lies between latitudes 26°00' and 27°00'S and longitudes 121°30' and 123°00'E (Fig. 2; Plate 1). Pastoral stations partly or wholly on KINGSTON include Lorna Glen, Prenti Downs, Old Windidda (abandoned), Windidda, Wongawol, and Yelma (abandoned). A gazetteer of localities is presented in Appendix 1.

Access to the project area is via the unsealed Wiluna to Carnegie Road, which crosses the northwest part of the map sheet. Approximately twenty kilometres south of Wongawol Homestead, an unsealed road branches east to Prenti Downs Homestead, providing access to the central and eastern parts of the map sheet. In the south of KINGSTON, an unsealed road links Laverton and Prenti Downs Homestead.

Station tracks provide access to most of the northern third of the map sheet, although low-lying areas adjacent to Lake Carnegie in the north of KINGSTON are inaccessible following rain. The southern third of the map sheet, where sand dunes and spinifex are prevalent, affords more limited access, and the few tracks in this area also become impassable after rain.

Physiography, vegetation, and soils

Physiography, vegetation, and soils have been discussed by Bunting (1986), Beard (1974), and Stace et al. (1968) respectively. KINGSTON can be divided into four main regions, each of which corresponds to distinctive geomorphological, vegetation, and soil types.

- Upland areas corresponding to resistant Proterozoic rocks, Permian rocks, and Archaean greenstone.
- Areas of sandplain and eolian material developed over Archaean and Permian rocks, such as in the southwest of the map sheet.

- Broad sheetwash plains and valleys, some of which are related to palaeodrainages that were probably active in the mid-Miocene.
- Areas proximal to and including salt lakes and playas.

Physiography

Relief on KINGSTON is typically subdued, with elevations ranging from 440 m Australian Height Datum (AHD) in low-lying areas surrounding Lake Carnegie to approximately 600 m AHD in areas such as the Princess Ranges and the Von Treuer Tableland (Plate 1). Topographically elevated regions are dominated by resistant sedimentary rocks of the Proterozoic Earaheedy Group. These rocks, which include iron formation, chert, and quartzite, commonly form rugged strike ridges and cuestas that occupy a broad northwest-trending tract through the centre of the map sheet. Flat-lying units of the Permian Paterson Formation, which are capped by iron- and silica-rich duricrusts, form mesas and breakaways, such as Tooloo Bluff and Panton Bluff. Shale units form low rounded hills. Archaean greenstones in the western part of KINGSTON form hills (up to 549 m AHD) capped by ferruginous duricrust.

Extensive areas of topographically subdued sandplain and dunefields have developed over Archaean granitoid rocks in the southwest of the map sheet. Sandplain and dunefields are also associated with backslopes of the Permian Paterson Formation in the central south and northwest parts of KINGSTON.

Broad sheetwash plains and valleys are widespread throughout the Earaheedy Group and commonly correspond to less resistant shale units of the Frere Formation. Channels incised in these valleys and plains commonly merge with major drainage systems that feed either Lake Carnegie in the north or Lake Wells in the east on ROBERT. Calcrete is a common feature of drainages and valley floors in the central west part of the map sheet and is particularly well developed in Banjo Creek. Playa-lake systems and associated landforms, including dunes and alluvial channels, are common in the central north and northeast parts of KINGSTON around Lake Carnegie. There are similar landforms (although less extensively developed) in the southeast of KINGSTON in the vicinity of Lake Wells extending onto ROBERT. These lakes were once part of a major drainage system that was active in the region until the middle Miocene. Calcrete-dominated valley floors and drainages are remnants of major drainage systems that flowed in the region until the middle Miocene.

Vegetation

Vegetation associated with saline playa systems and major valley floors includes saltbush (*Atriplex*), bluebush (*Kochia*), and samphire (*Arthrocnemum*) communities. These vegetation types are dominant in the northern part of the map sheet proximal to Lake Carnegie.

Mulga scrub (*Acacia aneura*) is the dominant vegetation type over resistant and more topographically elevated rocks of the Earaheedy Group. Calcrete-

dominated valley floors, which are mostly within the Earaheedy Group, are vegetated by mulga, saltbush, and samphire communities. Mulga and grass cover large areas of sheetwash and floodplain whereas eucalypts commonly line the major drainage systems.

The southern third of the map sheet is dominated by mulga (*Acacia aneura*), mallee (*Eucalyptus*), and spinifex (*Triodia*) developed on sandplain.

Soils

Stace et al. (1968) divided soils on KINGSTON into five types: lithosols, solonchaks, earthy sands, red earths, and red-brown earths. With the exception of red earths and red-brown earths, these soils display no profile development.

Lithosols, which are shallow sandy and loamy soils, are best developed over more hilly terrain on KINGSTON, such areas covered by the Frere Formation, the Princess Ranges Member of the Chiall Formation, and parts of the Wongawol Formation. This soil type, which is also developed over Archaean greenstones, is characterized by significant amounts of partially weathered rock fragments and mineral grains. Apart from the A horizon, there is no pedological development.

Solonchaks (saline loams) are well distributed around saline lake systems and their associated drainages, especially in the vicinity of Lake Carnegie and Lake Wells (on ROBERT). They range from brown to grey sandy clay loams to clays and may have salt encrustations at the surface as well as dessication cracks. At depths of greater than 20 cm, this soil type begins to more closely resemble the underlying parent material.

Earthy sands, which consist of clayey sands and light sandy loams, are widespread over granitoid rocks of the Yilgarn Craton in the southwest corner of the map sheet. This soil type is also developed over the Paterson Formation between Collurabbie Hills and Carclew Range in the central southern part of KINGSTON, where sandplain is extensively developed. These soils are siliceous, and individual grains are commonly coated with clay-rich material, some of which is also iron rich. They are commonly red, although in places yellow, and display uniform profile development.

The two other soil types (red-brown earths and red earths) are far more restricted than other soil types. Red-brown earths are in two areas in the northwest part of the map sheet. Both A and B horizons are developed, with the A horizon being mildly acidic to neutral and the B horizon being more alkaline with carbonate segregations. The A horizon is commonly loamy, and ranges in colour from grey-brown to red brown. Red-brown earths are derived from a wide variety of parent materials, and are commonly associated with alluvial and colluvial deposits. Red earths are located in three small areas—in the far northeast extending on to STANLEY, in the central part of KINGSTON, and in the central north-western region. They are commonly acidic, red to red-brown in colour, and porous with a sandy texture. Parent materials are characterized by

a high silica content and may include granites, quartz sandstones, and unconsolidated sedimentary material. These characteristics suggest that there may be some genetic relationship with the Permian Paterson Formation, which contains clasts of these rock types.

Climate

KINGSTON experiences an arid to semi-arid climate with hot summers and cool to mild winters. The hottest month is January with an average maximum of 38°C and minimum of 23°C. The coolest month (July) has average maximum temperatures of 20°C. In winter, low night temperatures (averaging 6°C in July) result in frosts in susceptible areas. Mean annual rainfall ranges from 200 to 250 mm, and is unreliable. The annual potential evaporation is about 2800 mm. The heaviest rainfall is experienced between December and May, and at times is associated with cyclonic activity, although rain also follows winter depressions. The area is prone to episodes of localized flooding following heavy rains, and periods of drought (Bunting, 1980).

Topographic and remote-sensing datasets

The regolith-materials map for KINGSTON (Plate 2) was compiled using Landsat Thematic Mapper (TM) images (rectified at level 9 and set to display bands 1, 4, and 7), and black and white aerial photographs at a scale of 1:80 200 (1974) and 1:86 000 (1993). Both datasets were obtained from the Western Australian Department of Land Administration (DOLA). Topographic information was supplied by the Australian Land Information Group (AUSLIG). Airborne radiometric and magnetic data from the Australian Geological Survey Organisation (AGSO) Australian regional coverage were also used. Other data include geological maps of Bunting (1980, 1986) and Myers and Hocking (1998).

Geology

A simplified geological map has been compiled (Fig. 3, Plate 1), based on Bunting (1980, 1986), and Myers and Hocking (1998). The 1:2 500 000 state map of Myers and Hocking (1998), 1:1 000 000 Eastern Nabberu Basin map of Bunting (1986), 1:250 000 KINGSTON geological map of Bunting (1980), and AGSO aeromagnetic and radiometric data were combined and the data from various scales rationalized to produce a map at the required scale of 1:250 000.

Four distinct geological associations have been identified on KINGSTON, comprising Archaean granite-greenstones of the Yilgarn Craton, sedimentary rocks of the Proterozoic Earaheedy Group (deposited in the Earaheedy Basin), dolerite sills that intrude the Earaheedy Group, and Permian rocks of the Paterson Formation (deposited in the Gunbarrel Basin).

The stratigraphic relationships on KINGSTON are shown on Plate 1. This stratigraphy is based on Bunting (1986), Pirajno (1998), and Jones et al., (2000). Comprehensive descriptions of the geology of KINGSTON are provided in Hall and Goode (1975), Hall et al. (1977), Bunting (1980, 1986), Gee (1990), and Jones et al. (2000). The following is largely taken from Bunting (1980, 1986) and Gee (1990).

Archaean granite-greenstones

The southwest part of KINGSTON is occupied by granitoid rocks and greenstones of the Archaean Yilgarn Craton that form the basement to Proterozoic rocks in the area. The majority of these rocks are deeply weathered with widespread development of kaolinization, ferruginization, and silicification.

Most of the Archaean rocks are granitoids that have a variety of compositions, grainsizes, and textures. Rocks include fine- to coarse-grained monzogranite with minor fluorite, and fine- to coarse-grained granitic rock with a strong gneissic foliation. Bunting (1980) compared coarse-grained adamellite (monzogranite) 9 km northwest of Yelma with the Mount Boreas Adamellite on DUKETON, which has a Rb-Sr age of 2480 Ma (Bunting and Chin, 1979). Nelson (1997) has recorded a sensitive high-resolution ion microprobe (SHRIMP) U-Pb zircon age of 2637 ± 8 Ma for a ‘Boreas suite’ granite from DUKETON (1:250 000). A SHRIMP age of 2651 ± 10 Ma has been recorded from a foliated biotite monzogranite near Mount Eureka on the western margin of KINGSTON (Nelson, 1998).

The two greenstone belts exposed on KINGSTON comprise the westerly Mount Eureka greenstone belt, and the Gerry Well greenstone belt in the central southern part of the map sheet. The greenstones are intruded by irregular plutons of syntectonic granitoid. The Mount Eureka greenstone belt, which consists of metamorphosed mafic, ultramafic, and sedimentary rocks (chert, shale, banded iron-formation (BIF), and possible felsic volcanic rocks), extends south onto DUKETON. The Gerry Well greenstone belt, which may be a northern extension of the Duketon belt, consists of BIF, chert, shale, amphibolite, dolerite, and felsic schist. AGSO airborne magnetic and gravity data indicate a continuation of the Gerry Well greenstone belt to the northwest, beneath rocks of the Earaheedy Group.

Proterozoic sedimentary rocks (Earaheedy Group)

The Earaheedy Group is a 5 km-thick sequence of Proterozoic, dominantly siliciclastic sedimentary rocks in the eastern part of the Earaheedy Basin. Based on stratigraphic correlations with the Yelma Formation at Mount Leake (north of Meekatharra), the group is probably younger than the c.1800 Ma Capricorn Orogeny. The Earaheedy Group pre-dates the c.1600 Ma Scorpion Group, and is unconformably overlain by the c.1200 Ma Collier Group on STANLEY.

Yelma Formation

The Yelma Formation is the basal unit of the Earaheedy Group. On KINGSTON, it rests unconformably on Archaean granite-greenstones of the Yilgarn Craton. Gee (1990) describes the Yelma Formation as a medium-grained, mature, slightly glauconitic and feldspathic quartz sandstone, cemented by authigenic silica. Towards the top of the sequence, the sandstone grades into shale and lenses of carbonate, the latter containing stratiform, domal, and digitate stromatolites (Grey, 1995).

The Yelma Formation is 150 m thick at the type section, 5 km northwest of Yelma, but decreases in thickness towards the southeast to 1–2 m, and is absent in some places. The formation was deposited at the start of an extensive marine transgression over a mature Archaean peneplain. Jones et al. (2000) discusses Pb mineralization in carbonate rocks of the Yelma Formation on NABBERU.

Frere Formation

The Frere Formation consists of buff, cream, and purple shales interbedded with iron formation and chert, and uncommon lenses of limestone. Towards the northwest, the ratio of iron formation to shale increases, but in southeast KINGSTON, the ratio is estimated at 1:50. This ratio increases to 1:1 along the northern edge of the Nabberu Basin.

Iron formation contains 1–2-m-thick bands of cherty, pelletal or oolitic granular material, with a steel-grey specular hematite alteration. Alternating shale units within the iron formation include siltstone, sandy siltstone, shale, and massive mudstone. Shales form valleys between resistant strike-ridges and cuestas of iron formation. Both massive and peloidal chert units are present in the Frere Formation. A distinctive marker band of green-grey chert at the top of the Frere Formation extends from 3 km south of Lorna Glen Homestead to Tooloo Bluff. Limestone and dolomite is exposed only in a few locations — a 10 m-thick lens of pink to grey, poorly laminated calcarenite is 8 km southwest of Old Windidda Homestead. Similar material is located at the western end of Wellington Range, where it forms a 5 m-thick lens at the top of the formation.

The Frere Formation represents a shallow marine-shelf deposit, with limited evidence for input of clastic material during a period dominated by precipitation of silica and iron. Oolite shoals and banks produced oolitic and pisolithic iron formation, especially in the area between northeast WILUNA (1:250 000) and central KINGSTON.

Windidda Formation

The Windidda Formation consists of interbedded, grey to pink, laminated, stromatolitic carbonate, and maroon, or grey-green micaceous mudstone and shale. It rests conformably on the Frere Formation. Bunting (1986) estimated a maximum thickness of 800 m at the type section near Windidda Homestead. The formation thins both east and west of the type section, and decreases to

300 m in thickness in the western part of ROBERT (1:250 000) and southeast NABBERU (1:250 000). The formation displays a distinctive striped pattern both on aerial photographs and satellite imagery, representing alternating layers of resistant carbonate-rich rock, and less resistant mudstone and shale. A barred basinal or lagoonal depositional setting during a period of regression is consistent with both the lack of current structures and coarse terrigenous sediment.

Chiall Formation

A reappraisal of Earaheedy Group stratigraphy by Pirajno (1998), Hocking and Jones (1998), and Jones et al. (2000) resulted in the designation of the Princess Ranges Quartzite and the overlying Wandiwarra Formation as members of the newly erected Chiall Formation. The Chiall Formation is a sandstone, siltstone, and shale unit that coarsens towards the top (Pirajno, 1998; Jones et al., 2000).

Wandiwarra Member

The Wandiwarra Member, which disconformably overlies the Windidda Formation, represents a period of rapid marine transgression over mudflats and carbonate shoals. The unit consists of quartz-rich sandstone (which may contain iron-oxide, glauconite, mica, feldspar, and carbonate cement), laminated micaceous shale, and minor carbonate-clast conglomerate. There is a locally developed glauconitic conglomerate at the base, which is interpreted as a submarine hardground rather than a disconformity (Jones, J. A., 2000, pers. comm.). The thickness of this member varies on KINGSTON from 500 m in the northwest to 350 m at the type section near Cork Tree Well. In the southeast, the unit thins considerably before grading laterally into the Princess Ranges Member. East of Prenti Downs Homestead near the sheet boundary, the Wandiwarra Member is absent and the Princess Ranges Member overlies the Windidda Formation. Potassium–argon dating by Horwitz (1975) dated rocks of the Wandiwarra Member in the Princess Ranges at 1685 ± 35 Ma.

Princess Ranges Member

The Princess Ranges Member prograded over the Wandiwarra Member during a slow shoreline regression in shallow-marine to coastal conditions. It consists of well rounded, fine- to medium-grained, silica-cemented quartz arenite, interbedded with white to cream kaolinitic and micaceous siltstone, and fine-grained feldspathic sandstone. The thickness of the unit ranges from about 280 m at the type section (an unnamed creek that crosses the Princess Ranges) to 600 m in the eastern part of KINGSTON.

Wongawol Formation

The Wongawol Formation, which conformably overlies the Chiall Formation, is about 1500–2000 m thick. In ascending stratigraphic order, it consists of lithic

sandstone, shale, mudstone, and carbonate (Bunting, 1986). This fining-upwards sequence is transitional from deposition of mature clastic debris of the Princess Ranges Member to carbonate-dominated deposition of the overlying Kulele Limestone. The Wongawol Formation was most likely deposited in sheltered lagoonal conditions. The type section extends from 1 km south of Wongawol Homestead, north along the Wiluna to Carnegie Road, to 1 km east of Thuraguddy Bore on STANLEY.

Kulele Limestone

The Kulele Limestone, which is the uppermost carbonate formation of the Earaheedy Group, is about 300 m thick. It consists of alternating bands of shale and limestone representing regular metre-scale cyclic fluctuations in sea level in a coastal to nearshore setting.

Mulgarra Sandstone

The Mulgarra Sandstone rests with apparent disconformity (Bunting, 1986) on the Kulele Limestone and was probably deposited in shallow-marine conditions. Lithologies include medium-grained, ferruginous quartz arenite with minor glauconite, shale, and pinkish limestone. Sandstone dominates the lower 20 m of the sequence, and is overlain by thin arenaceous beds containing shale and limestone. Sandstone is also the dominant lithology in the top part of the sequence. Bunting (1986) estimated the total thickness of the Mulgarra Sandstone to be 100 m.

Dolerite

In the eastern part of the map sheet, the Earaheedy Group is intruded by a number of fine-grained dolerite sills, which may be part of the intrusive suite in the nearby Sunbeam Group (Bagas et al., 1999) on STANLEY. Bunting (1980) describes the dolerites as texturally and mineralogically homogeneous, consisting of subophitic intergrowths of pyroxene and saussuritized plagioclase. A Rb–Sr mineral isochron age of 1050 ± 50 Ma was obtained for a dolerite sill on ROBERT by Compston (1974). AGSO airborne magnetic data indicate the likelihood of a large subsurface dolerite sill in the vicinity of Top Fourteen Mile Well near the southern shores of Lake Carnegie.

Permian rocks (Paterson Formation)

The Permian Paterson Formation is a sequence of mostly flat-lying fluvial and glaciogene deposits. Deep weathering is common, and in many places a resistant silcrete or laterite cap has developed resulting in mesas with steep-sided breakaways (e.g. Panton bluff).

The dissolution of the sandy clay matrix to these glaciogene sediments has resulted in a boulder lag of various rock types, including granitoid, quartzite, iron

formation, chert, and less common mafic and felsic volcanic rocks. The distribution of these rock types indicates that glaciation proceeded in a north to northeasterly direction, with many rock types sourced from the Archaean Yilgarn Craton (Bunting, 1980).

Economic geology and mineralization

KINGSTON forms part of the Mount Margaret and East Murchison Goldfields. The only recorded mineral production is from the Mount Eureka gold mining centre in the Mount Eureka greenstone belt, where 20.06 kg of gold was extracted from 941.0 t of ore. Mining was undertaken between 1932 and 1937.

Gold production data for the Mount Eureka gold mining centre is tabulated in Appendix 2, which is a collation of all available data as reported to the Department of Minerals and Energy (DME). Small operators whose production was limited to 50 t of ore per year for no more than two years were responsible for producing a significant amount of gold. Production from these operators is combined and reported in Appendix 2 as 'Sundries'.

The gold at Mount Eureka is in quartz veins in silicified talc–carbonate schist of the Mount Eureka greenstone belt, commonly at the contacts with thin chert bands. Quartz reefs east of Mount Eureka hosted by deeply weathered metasedimentary rocks also contain gold (Bunting, 1980).

Geochemical surveys in open-file company reports

To comply with the Mining Act of 1978, mineral exploration companies lodge reports with DME detailing exploration activity. These are listed in the GSWA Western Australian mineral exploration (WAMEX) database as either open-file or confidential reports. Details of open-file company reports that contain surface or near-surface geochemical data are listed in Appendix 3. For each project, surface geochemical exploration metadata (including shallow drilling) are captured to a maximum depth of 4 m. Projects with fewer than 30 samples have been omitted.

Each project has been assigned an identification number that is shown, along with project boundaries, on Plate 3.

The projects listed in Appendix 3 are arranged in order of increasing M number for the period 1985 to 1996. When reports are released to open-file, projects are assigned an Item number, with the highest Item number denoting the latest release. Gaps in reporting result from the failure of some tenement holders to lodge reports or because mineral claim holders were not required to report all of their exploration results prior to 1978.

Regolith sampling and mapping

Regolith sampling on KINGSTON was carried out in April 1999 by six, two-person sampling teams, each comprising a field assistant and geologist, using two Bell Jet-Ranger helicopters. The sample-site form (for recording information about regolith and geology at each sample site) and sampling methodology are detailed in Appendix 4, which also contains information about the regolith-materials mapping scheme and its evolution.

A regolith-materials map (Plate 2) has been produced for KINGSTON using Landsat TM imagery, synthetic stereo pairs, aerial photographs, airborne magnetic and radiometric data, and field observations recorded at each sample site. Sample numbers with their corresponding regolith codes are listed in the accompanying datafile (KINGSTON.CSV). The regolith units and their map codes are described in the reference for Plate 2 and in Appendix 4. For some sample sites, the scale difference between field-recorded data and remotely sensed mapping causes discrepancies between the regolith code assigned by the sampling geologist and the unit shown on the interpreted regolith-materials map. A generalized version of the regolith-materials map depicting residual, exposed, and depositional regolith is presented as Figure 4. Table 1 details regolith units by area as well as the number of samples per regolith unit.

Residual regime regolith (*R*) on KINGSTON covers approximately 2% of the sheet by area and is limited to iron-rich duricrust over greenstones (*Rf*), siliceous cap rock developed over Archaean granitoids (*Rz*), and relict regolith derived from various sedimentary rocks of the Paterson Formation (*Rls*). Exposed rock (*X*) accounts for about 13% of the map sheet and is most widespread in the vicinity of the Earaheedy Group along with smaller areas of Archaean granite–greenstone in the southwest of the map sheet. The majority of the map sheet (approximately 85%) is covered by depositional regime regolith, comprising colluvial, sheetwash, alluvial, floodplain, lacustrine, and sandplain deposits. Sandplain (*S*) and sheetwash (*W*) account for approximately 19% and 14% of total regolith respectively. Colluvial deposits (*C*) form aprons around outcrop of the Earaheedy Group, Archaean granite–greenstone, and rocks of the Permian Paterson Formation, and account for about 28% of total regolith. Regolith materials associated with lake systems (*L*) account for 16% of total regolith, and alluvial (*A*) and floodplain (*F*) deposits account for a further 9% of regolith.

Regolith over KINGSTON is described according to three main regions as follows:

- Regolith over Archaean rocks (occupying approximately one quarter of the map sheet) in the southwest where the topography is subdued and dominated by sandplain of both residual (derived from Archaean granite) and eolian origin.
- Regolith over Earaheedy Group rocks (approximately one half of the map sheet) occupying a broad northwesterly trending tract in the centre of the map

sheet. Regolith in this area is at higher elevations than in other regions on the map sheet, although relief is still quite subdued. Regolith associated with the Paterson Formation, and dolerites (although not part of the Earaheedy Group), is also discussed in this

section since it is spatially associated with regolith of the Earaheedy Group.

- Regolith developed in low-lying areas surrounding and including lake systems, especially in the northeast of the map sheet in the vicinity of Lake Carnegie, and in the east near Lake Wells (ROBERT).

Table 1. Regolith according to area and number of samples per regolith-materials unit

Regolith code	Area (km ²)	No. of samples	% of total regolith	% of regime
Residual regime				
Rf	51	2	0.31	15.2
Rls	242	4	1.47	72.2
Rz	42	5	0.25	12.6
Total	335	11	2.03	
Exposed regime				
Xcm	1	—	0.01	< 0.1
Xfc	508	19	3.07	23.1
Xgp	130	16	0.79	5.9
Xgs	427	19	2.58	19.4
Xgv	< 1	—	< 0.1	< 0.1
Xkc	184	10	1.11	8.4
Xmh	47	4	0.28	2.1
Xmm	4	—	< 0.03	0.2
Xqs	886	36	5.35	40.3
Xu	2	—	< 0.01	0.1
Xzc	12	—	0.07	0.5
Total	2201	104	13.29	
Depositional regime				
Colluvial				
Cd	465	33	2.81	10.2
Cf	229	13	1.38	5.0
Cfc	1 285	85	7.76	28.3
Cgp	666	37	4.02	14.6
Cgs	368	17	2.22	8.1
Ckc	95	7	0.58	2.1
Cl	373	21	2.25	8.2
Cls	416	22	2.51	9.2
Cmh	13	1	0.08	0.3
Cqs	638	41	3.85	14.0
Subtotal	4 548	277	27.47	
Alluvial				
A	485	109	2.93	12.9
Floodplain				
F	698	46	4.21	18.5
Ff	49	—	0.30	1.3
Fk	240	20	1.45	6.3
Sheetwash				
W	2 191	114	13.23	58.1
W _d	108	9	0.65	2.9
Subtotal	3 771	298	22.77	
Lacustrine				
L _t	1 088	29	6.57	41.1
L _m	1 558	117	9.41	58.9
Subtotal	2 646	146	15.98	
Sandplain and eolian				
S	2 551	134	15.41	83.5
Sl	505	28	3.05	16.5
Subtotal	3 056	162	18.46	
Total	14 021	883	84.68	
TOTAL		998	100.00	

Regolith associated with Archaean granite and greenstone

The southwest of KINGSTON is largely occupied by Archaean granite-greenstone blanketed by residual and eolian sand. Sandplain comprises nearly 19% of all regolith on KINGSTON, and most of this is developed over Archaean granitoids. Relief is minimal throughout most of this region.

Bunting (1980) notes that most of the Archaean rocks on KINGSTON are deeply weathered, involving kaolinization with subsequent ferruginization and silicification. However, for the majority of Archaean rocks, the parent lithology can be deduced, and an appropriate secondary compositional qualifier can be used (e.g. Xgp for exposed quartzofeldspathic plutonic rocks). The parentage of a metasedimentary, schistose, kaolinitic rock (designated As and Ast by Bunting (1980)) is uncertain, and the secondary 'c' (i.e. clay-rich) qualifier has been applied here.

Greenstones comprise a sequence of variably metamorphosed ultramafic (Xu) and mafic rocks (Xmm) through to felsic volcanic rocks (Xgv), schistose kaolinitic metasedimentary rocks (Xcm), and BIF (Xfc). Much of the sequence has been weathered to produce a massive and pisolithic ferruginous duricrust (Rf), which occupies topographic highs over the greenstones. This duricrust weathers to produce an iron-rich colluvium (Cf), which is readily identified using Landsat imagery bands 7, 4, and 1, where it appears as a pale brown material emanating from deep black-red outcrop (Rf). Small areas of colluvium of uncertain parentage surrounding felsic volcanic rocks (Xgv) and ultramafic rocks (Xu) have been designated Cd (undivided). Compositionally specific colluvial units (e.g. Cu for colluvium derived from ultramafic rocks, and Cgv for colluvium derived from quartzofeldspathic volcanic rocks), although recognizable at aerial photograph scale, cannot be shown at 1:250 000 scale, and therefore have been grouped as undivided colluvium (Cd). Heterogeneous colluvium (Cl) differs from undivided colluvium in that the parent material can be recognized. However, as this type of material is derived from a variety of rock types, a unique compositional qualifier cannot be used.

Weathered Archaean granite (Xgp) is capped by a siliceous duricrust (Rz), which forms a dendritic pattern on Landsat images and aerial photographs, similar to that described on PEAK HILL by Subramanya et al. (1995) in the Goodin Dome area. Subramanya et al. (1995) proposed that these silicified ridges may be remnants of an inverted drainage system.

Weathered Archaean granitoid rocks (Xgp, 6% of exposed regolith) are surrounded by low-angle slopes

blanketed by quartz- and feldspar-rich colluvium (*Cgp*, ~15% of colluvial regolith). In many areas, the colluvial slope is barely perceptible, and is a similar angle to that supporting the fine-grained, clay-rich material typical of distal sheetwash (*W*). Colluvium derived from granitoid rocks (*Cgp*) is best developed downslope of the breakaway face of weathered granite whereas the backslope is commonly covered by residual sand (*S*). These extensive sand sheets probably represent the breakdown products of granitic colluvium that has been progressively depleted in labile components to produce a quartz-rich material. Reworking of sandplain, particularly on backslopes, has formed numerous longitudinal and net dunes. In some areas, sandplain drapes over slope crests and onto the breakaway face. This suggests that eolian sand cover may once have been extensive in this region but has since been stripped away from the steeper breakaway faces. Some hills composed of granitoid rocks with less pronounced crests and breakaways are mostly covered by sandplain material (*S*). On the breakaway side of outcrop (*Xgp*), colluvium (*Cgp*) overlies sandplain (*S*) with a sharp boundary suggesting that erosion is active in these areas.

A number of sand- and colluvium-filled depressions in this region, which comprise less than 1% of total regolith, have been mapped as *W_d* (i.e. sheetwash in drainage depressions). These depressions, which are mostly between granite outcrops and probably represent old drainage lines, have been progressively filled with a mixture of both colluvial and eolian material. Recently developed drainages within these areas are visible on aerial photographs. Some of these depressions appear to have been linked to active alluvial channels that feed major salt-lake systems in the area (e.g. Lakes Carnegie and Wells) and were probably associated with middle Miocene palaeodrainages. The incursion of sand and colluvium, combined with the overall lower gradient in this area, has isolated them from present-day drainage systems. Sample-site observations reveal the predominance of quartz-rich sand in this unit, although scattered ferruginous granules are recorded at several sites. At sample site GSWA 166219 (MGA 399268E 7033091N), a ferruginous duricrust and hardpan material covers granitoid rock at 20 cm depth, and silcrete (e.g. also at GSWA 166611; MGA 366904E 7031299N) and calcrete (e.g. also at GSWA 166236; MGA 372466E 7028635N) have been recorded.

A transitional unit between sandplain and sheetwash has been designated *SI* (3% of total regolith). This unit represents mixed material and consists of distal sheetwash (*W*) covered by sand. It differs from the *W_d* unit in that it is developed in association with more poorly defined drainage systems such as those on broad sheetwash plains. The sandplain component is also far greater than that in the channel-like depressions of *W_d* regolith, which appear to have a greater colluvial component.

Regolith of the Earaheedy Group and Paterson Formation

Gently north-dipping, resistant bands of chert, iron formation, and quartz arenite of the Earaheedy Group exert a strong influence on topography (Bunting, 1980). The more resistant rock units form ridges and south-facing cuestas that are separated by less competent shale and carbonate units that occupy broad colluvial plains and valleys. The flat-lying Permian Paterson Formation typically occupies the highest part of the landform profile on KINGSTON. It rests unconformably on the Earaheedy Group and is commonly capped by silcrete or ferruginous duricrust, both of which form resistant mesas and breakaways.

Valley floors contain large areas of depositional regime regolith including colluvial (*C*), sheetwash (*W*), floodplain (*F*), and alluvial (*A*) material. The gradient of colluvium-draped slopes depends on bedrock type, but most slopes are gentle and grade downslope into extensive areas of distal sheetwash (*W*). This is the predominant depositional regolith type over rocks of the Earaheedy Group and is developed as broad, commonly clay-rich plains grading into floodplain and alluvial material downslope. Site observations include reference to locally abundant gravel and stones (commonly iron rich) in this regolith type. Clay, and mud cracks (indicative of standing water), were also recorded at a number of sample sites. Distal sheetwash is well developed downslope of iron-rich colluvium (*Cfc*) of the Frere Formation, and it is also close to Lake Carnegie (particularly in the northeast of KINGSTON), where it grades into dune and playa terrain (*L_m*). Valley floors, which are incised by drainage channels, are commonly flanked by floodplain deposits (*F*), some of which are calcareous (*Fk*). Calcrete is a prominent feature of many major valley-floors and drainage systems, and is well developed in floodplain deposits of Banjo Creek. Iron-rich floodplain material, predominantly sourced from the Frere Formation, has been designated *Ff*. There is a large area of this regolith type east of the confluence of Wongawol and Cole creeks. Major drainages, such as Wongawol Creek, contain abundant gravel-, stone-, and cobble-size rock fragments, and well-developed floodplain deposits. Drainages associated with distal sheetwash are either broad and shallow or braided, and mostly contain common to abundant clasts of gravel-grade material.

Sandplain development is limited over Earaheedy Group rocks, and most is associated with Permian rocks, commonly on backslopes. Sandplain units over Permian sedimentary rocks have been mapped as *S* in both the northwest and central southern regions of KINGSTON. This regolith unit includes both residual and eolian material. Eolian processes have been particularly active in the central southern area of sandplain with the presence of numerous longitudinal and net-like dunes.

Exposed quartz-rich sedimentary rocks of the Yelma Formation, Wandiwarra Member, Princess Ranges Member, and Mulgarra Sandstone have been mapped as *Xqs*, which accounts for 40% of all exposed rock on KINGSTON. The quartz-rich colluvium derived from these rocks (*Cqs*) makes up 14% of all colluvial regolith. These

* Locations mentioned in the text are referenced using Map Grid of Australia (MGA) coordinates, Zone 51. All locations are quoted to the nearest 100 m.

lithologies (in particular the Princess Ranges Member) weather to rugged ridges, hills, and cuestas, with rubbly skirts of colluvium.

Both the Windidda Formation and the Kulele Limestone have been mapped as carbonate-rich chemically precipitated or biochemical sedimentary deposits (*Xkc*), which account for just over 8% of exposed regolith and 1% of total regolith on KINGSTON. Associated colluvium (*Ckc*) is of limited extent, comprising about 2% of all colluvial regolith. The Windidda Formation, which occupies a broad valley floor between the Princess Ranges Member of the Chiall Formation and the Frere Formation, is largely obscured by sheetwash, floodplain, and alluvial material. There are small playas in areas of sheetwash, especially near lake systems, although at the scale of mapping these are too small to be represented. Where exposed, the Windidda Formation forms a subdued topography, and displays a distinctive striped appearance on both aerial photographs and Landsat imagery due to alternating units of resistant and more labile bedrock material. The Kulele Limestone occupies a slightly more elevated position and therefore produces a greater amount of colluvium (*Ckc*) than the Windidda Formation, although outcrops of the Kulele Limestone on KINGSTON are restricted to a small area in the northeast of the map sheet.

Exposed quartzofeldspathic sedimentary rocks of the Wongawol Formation are mapped as *Xgs*, constituting 19% of exposed regime regolith. The Wongawol Formation, which commonly forms low hills and ridges, occupies a low-lying area in the north of KINGSTON, which partly includes Lake Carnegie. Small areas of quartzofeldspathic colluvial material derived from this unit, where not obscured by lake sediments, have been mapped as *Cgs* (8% of all colluvial regime regolith).

The Frere Formation consists of alternating layers of iron formation and shale with less common chert and carbonate horizons. Iron formation is mapped as chemically precipitated iron-rich material (*Xfc*), which accounts for 23% of exposed regime regolith on KINGSTON. Resistant strike ridges of iron formation have weathered to produce extensive areas of iron-rich colluvium (*Cfc*, 28% of colluvial regolith). Some sample sites contain abundant pelletal ironstone, chert, shale, siltstone, and other ferruginous clasts in colluvium and sheetwash. Shale and siltstone horizons containing quartz, clay minerals, white mica, and minor feldspar, biotite, and chlorite are mapped as quartzofeldspathic sedimentary rocks (*Xgs*). Mass-wasting products derived from this rock type (*Cgs*) are well developed in the central part of the map sheet south of Bonython Bluff and near Old Windidda Homestead. Pale-green pelletal chert is mapped as chemically precipitated silica-rich material (*Xzc*) whereas carbonate-rich layers are mapped as *Xkc*. Both of these units are very restricted on KINGSTON. Less resistant materials of the Frere Formation have eroded to occupy lower parts of the landform profile, and are covered by sheetwash, floodplain, and alluvial deposits. Large areas of the Frere Formation are dissected by valleys and drainages, with associated floodplain and sheetwash deposits, many of which are calcrete-rich (*Fk*). Bunting (1986) suggested that these are remnants of major

drainage systems that were active until the middle Miocene, noting that modern drainage systems are re-incising these surfaces resulting in the preservation of calcrete remnants above present valley floors.

Mafic intrusive rocks mapped as dolerite sills by Bunting (1980) in the east of KINGSTON have been mapped as *Xmh*, with colluvial products designated *Cmh*.

The resistant mesa-like landforms of the Paterson Formation result from weathering of various rock types *in situ*, and the designated regolith code (*Rls*) reflects this heterogeneity. This unit accounts for less than 2% of total regolith and about 72% of residual regolith. Clasts of pelletal iron formation, chert, quartzite, quartz, granitoid rocks, and mafic and felsic volcanic rocks have been noted in these glaciogenic rocks (Bunting, 1980). On some areas of KINGSTON and STANLEY, a greater extent of these Permian rocks has been inferred from the presence of boulder lags or exotic blocks, which remain after the removal of the finer grained matrix (Hocking, R. M and Jones, J. A., 1999, pers. comm.). Colluvium derived from these Permian rocks has been mapped as *Cls* (i.e. colluvium derived from mixed sedimentary rocks). This unit constitutes almost 3% of total regolith and 9% of colluvial regime regolith.

Regolith associated with lake systems

Regolith associated with lake systems accounts for 16% of total regolith. It is in two main areas on KINGSTON — in the northeast in and around Lake Carnegie, and in the east occupying an area that drains into Lake Wells on ROBERT. The lakes are part of the extensive palaeodrainage system that was active in the area until the middle Miocene (Bunting, 1986). Numerous tributaries incising the Earaheedy Group and draining towards Lakes Carnegie and Wells were once connected to this system and are now represented by calcrete-rich valley floors, and isolated areas of playas and associated material. Sediments and evaporitic material in playas and claypans are designated *L_b*, and account for 41% of all lacustrine regolith on KINGSTON. Dune and playa terrain adjacent to salt lakes is designated *L_m* and constitutes 59% of lacustrine regolith.

Discussion

Regolith on KINGSTON is dominated by redeposited material (depositional regime regolith), which accounts for over 80% by area of all regolith. Regolith formed by weathering *in situ* (i.e. residual regime regolith) accounts for only about 2% of regolith by area, although sandplain — which has a residual component — accounts for almost 19% of regolith by area. The remaining area is exposed rock, subcrop or bouldery lag (exposed regime regolith).

Residual regime regolith largely comprises material derived by the weathering of heterogeneous sedimentary rocks of the Paterson Formation (72% of residual regime regolith) *in situ*, the flat-lying disposition of which is well

suites to development of this regolith type. Ferruginous duricrust developed over greenstones, and siliceous duricrust developed over Archaean granitoid and parts of the Paterson Formation, make up the remaining residual material.

Topographic and lithologic control on the type and distribution of regolith is shown in some areas of the Earaheedy Group (e.g. Frere Formation compared to the Windidda Formation), which can be attributed to variable resistance of bedrock units to weathering, and distinctive compositions. The imprint of composition can be traced downslope from outcrop (e.g. Fe-rich regolith of the Frere Formation as *Xfc*), through to colluvium (*Cfc*) into floodplain areas (*Ff*).

Sand-dominated regolith is largely over Archaean granitoid, with smaller areas over the Paterson Formation and over parts of the Earaheedy Group in the northeast of the map sheet. Sandplain over Archaean granitoid, which accounts for 19% of regolith by area, is mainly on the backslopes of breakaways developed on granitoid and the Paterson Formation. Dune forms in these and other areas of sandplain attest to some eolian reworking, and the relationships with adjacent colluvium and sheetwash indicate the sandplain may be a remnant of a more extensive cover. Sandplain with less well-developed dune systems and more clay-rich colluvium (*Sl*) more strongly resembles a sandy loam, similar to locally derived material described from the Fraser Range area by Morris et al. (2000b). If areas of sandplain are to be sampled for regional geochemical exploration, it is clearly important to identify characteristics that identify the relative contributions of in situ and transported components — a recent study by Pell et al. (1999) has suggested that sand overlying the Yilgarn Craton is of local derivation. A sheetwash unit developed only over granitoid units in drainage depressions (*Wd*) consists of a variety of material, including saprock and eolian sand.

Regolith associated with lake systems (16% of all regolith) is typically saline, gypsiferous, and carbonate rich, with no macroscopic features indicative of its parentage. As with sandplain, this may prove to be a difficult sample medium in mineral exploration (in that it is unrepresentative of any one bedrock type), although the thin cover in lake systems (through which bedrock structure can be seen on aerial photographs) indicates that sampling by shallow drilling may be effective.

Chemical analysis and quality control

Nine hundred and ninety-eight samples from KINGSTON were analysed in nine separate batches by Genalysis Laboratories, Maddington, Perth. The samples comprise 355 stream-sediment samples, 326 sheetwash samples, 227 sandplain samples, and 90 lake-sediment samples. Analyses of three GSWA standards were carried out with each batch, along with analyses of laboratory duplicates, standards, and blanks. Ten samples with anomalously high

concentrations of some analytes were submitted to Amdel Laboratories, Wangara, for re-analysis. Five of these samples were submitted to Analabs in Welshpool, for further re-analysis. Laboratory procedures and quality-control methods are summarized in Appendix 4. Samples were also measured for conductivity and alkalinity-acidity (pH) as described in Appendix 4.

Quality-control data (replicates, duplicates, blanks, and standards) are presented as a series of digital files (Appendix 5 on the accompanying floppy disk). Table_5_1.txt of Appendix 5 summarizes the structure of this digital appendix, which contains data discussed below.

In most cases, analytical precision is satisfactory, and where this is not the case, concentrations are commonly close to the lower prescribed limit of ten times the detection level (Appendix 4). The few deviations are commonly at concentrations very close to the prescribed limits (Appendix 5).

For replicate analyses carried out by Genalysis, the greatest deviation from acceptable limits is shown by As, W, and P₂O₅, although in all cases, concentrations of the analytes in question are close to the ten times detection-level limit, and the deviation from prescribed limits is small. GSWA standards analysed by Genalysis show good reproducibility, apart from small variations in W for IQC47 (laterite) and IQC45 (gossan) across the nine batches, although concentrations are at low levels. (For the laterite standard, W values range from 0.8 to 1.7 ppm with a relative standard deviation percent (RSD%) of 26, whereas for the gossan, standard values have a range of 2–3 ppm resulting in a RSD% of 27.) Blanks analyses from the beginning of each analytical run are generally good, with the exceptions listed in Appendix 5. There are some minor deviations from prescribed limits for other standards. In batch 8, SY-4 yielded a W result of 0.6 ppm, which is lower than the results from other batches (6 ppm). For standard SO2, As showed poor precision, but concentrations are only marginally above the ten times detection-level limit. Some blank values were slightly above the designated thresholds (Appendix 5).

Analyses of standards and replicates from Genalysis, Amdel, and Analabs are presented in Appendix 4, including analyses that fall outside of the prescribed limits. Samples GSWA 166526, 166548, 166570, 166659, and 166714 were analysed by all three laboratories, and the precision of analysis was assessed using the RSD%, which should be less than 20 if the analyte is at least ten times the detection level. Samples GSWA 166230, 166247, 166592, 166698, and 166713 were analysed by Genalysis and Amdel, and precision was assessed using the percent half relative deviation (HRD), which should not exceed 10 for analytes at concentrations greater than ten times the detection level. Only a few samples fell outside of these limits, with the biggest inter-laboratory variations for As, Ba, Cr, Cu, Nb, Pb, and Zr. During the analysis check procedure carried out by Amdel and Analabs, the GSWA standard IQC42 (amphibolite) was analysed by all laboratories. Results from Analabs and Amdel were compared with the average of nine determinations of this standard made by Genalysis during the course of analysis

of the 998 samples from KINGSTON. Between-laboratory variations were noted for Cr, Ni, Zr, and Ag. Chromium displayed the greatest disparity between laboratories (21 RSD%), with Genalysis returning 1571 ppm (detection level of 2 ppm), Amdel 1830 ppm (2 ppm), and Analabs 1180 ppm (10 ppm). Nickel results ranged from 283 ppm (Analabs, 2 ppm detection level), to 423 ppm (Amdel, 2 ppm), and 428 ppm (Genalysis, 1 ppm). Zirconium results produced an RSD% for the three laboratories of 47, although it should be noted that the concentrations reported by Amdel and Analabs are less than ten times the detection level (5 ppm) — results ranged from 17 ppm at Analabs to 22 ppm at Amdel and 40 ppm at Genalysis (detection level of 1 ppm). For Ag, Genalysis and Analabs (detection level: 0.01 ppm) produced results of 4.7 and 7.2 ppm respectively, whereas Amdel (detection level: 0.1 ppm) produced a result of 5.3 ppm.

Element-distribution maps

Regolith geochemistry on KINGSTON is shown as a series of spot-concentration maps relative to simplified geology in Figures 5–51. The maps are presented as major-element oxides and loss-on-ignition (LOI), followed alphabetically by trace elements. Silica dioxide has been omitted due to consistently high values in all samples. The diameter of the circles on the spot-concentration maps corresponds to the concentration of the analyte, unless the analyte concentration is more than 2.5 standard deviations above the mean, where it is termed anomalous and shown as a star. Exact element values can be determined by identifying the relevant GSWA sample number from Plate 1 and then referring to the digital dataset (KINGSTON.CSV), which also lists exact locations for each sample. Table 2 lists samples with anomalous analyte concentrations, along with sample medium, and the underlying geological unit.

Major element oxides and loss-on-ignition

Titanium concentrations in regolith are highest over Archaean greenstone (including one anomalous concentration), in marked contrast to regolith over adjacent Archaean granitoid rocks (Fig. 5). Three anomalous samples form a tight cluster around dolerite near Prenti Downs Homestead, and there are several high TiO_2 values in regolith over the Kulele Limestone in the vicinity of Mount Throssell Well. Values are typically low over Archaean granitoid and in lake-sediment samples.

Apart from most regolith samples over Archaean granitoid rocks, the central Frere Formation, and in lake sediments (which have low Al_2O_3 levels), Al_2O_3 shows a limited concentration range in most regolith samples on KINGSTON. There are anomalous values in regolith over parts of the Mount Eureka greenstone belt, Archaean granitoid, and the Frere and Wongawol Formations (Fig. 6).

Most high Fe_2O_3 values in regolith are over Archaean greenstone and the western part of the Frere Formation,

with the latter containing four anomalous samples (Table 2 and Fig. 7) ranging from 40.14 – 43.53% Fe_2O_3 . Several high values are in regolith close to dolerite at Prenti Downs Homestead, and values are low over Archaean granitoid rocks.

Most MnO values in regolith are less than 0.5% (Fig. 8), apart from several high and anomalous values in regolith samples from between Mount Wellesley and Christmas Bore, largely over the Windidda Formation.

Magnesium contents in regolith are typically low on KINGSTON (Fig. 9), and there is a poor contrast in MgO between regolith over Archaean granitoid rocks and greenstones. There are several high values (two of which are anomalously high) in regolith samples near Mount Throssell Well (Kulele Limestone), and there is an isolated anomalous value in a sheetwash sample in the southeast part of the Frere Formation. A series of relatively high values extend southeast from Mount Wellesley over the Windidda Formation, and another series of high values is recorded in lake sediments from Lake Carnegie.

All high values for CaO in regolith are in lake sediments (Fig. 10, Table 2), most of which are from the Lake Carnegie area.

Four of the five anomalous Na_2O values in regolith come from lake sediments in the vicinity of Lake Carnegie, whereas the remaining anomalous sample is a stream sediment from 7 km east of Burel Pool over the Princess Ranges Member of the Chiall Formation (Fig. 11). Elsewhere, Na_2O values in regolith are low, apart from a few relatively high values in regolith from the Wellington Range area.

There is a group of relatively high K_2O values in regolith near Mount Wellesley, and two anomalous values are close to the contact of Archaean granitoid and the Mount Eureka greenstone belt (Fig. 12). Other high values come from regolith in the vicinity of the Wongawol Formation and Kulele Limestone northeast of Bummer Pool. A series of relatively high values are grouped near dolerite near Prenti Downs Homestead. Potassium values are typically low over Archaean granitoid rocks, Archaean greenstones, the eastern part of the Frere Formation, and in lake-sediment samples.

Despite low concentrations, P_2O_5 provides a marked contrast in lithology between Archaean greenstones and granitoid rocks (Fig. 13). There are three anomalous P_2O_5 values in regolith samples from over the Frere Formation (Table 2). Phosphorus values are slightly lower in lake sediments.

Several high LOI values have been obtained from regolith samples recovered from the Lake Carnegie area (Table 2 and Fig. 14). Two nearby samples from over the Windidda Formation between Jackie Lookout and Christmas Bore have high LOI values, along with a sheetwash sample over the Frere Formation, southeast of Bilgarrie Cutarrie Pool. Loss-on-ignition provides only a weak contrast between regolith over greenstones and granitoid rocks.

Table 2. Samples with anomalous concentrations of analytes

GSWA No.	<u>MGA coordinates</u>		1	2	3	4	5	6	7	8	9	10	Regolith	Medium	Map code	Geology
	Easting	Northing														
166124	356714	7063280	Ni	Ta	-	-	-	-	-	-	-	-	Cf	Stream sediment	Ab	Archaean greenstone
166126	356461	7048321	Au	-	-	-	-	-	-	-	-	-	Cgp	Sheetwash	Ag	Archaean granitoid
166135	360368	7036128	Al ₂ O ₃	La	-	-	-	-	-	-	-	-	Cfc	Lake sediment	PEf	Frere Formation
166155	359937	7114844	Ba	-	-	-	-	-	-	-	-	-	W	Stream sediment	PEw	Wandiwarra Member
166162	372388	7113329	MnO	Co	-	-	-	-	-	-	-	-	Cqs	Stream sediment	PEw	Wandiwarra Member
166165	360754	7100060	Sn	-	1	-	-	-	-	-	-	-	L _m	Sheetwash	PEd	Windidda Formation
166184	425020	7025561	Nb	Ta	-	-	-	-	-	-	-	-	W	Sheetwash	PEf	Frere Formation
166185	424494	7016981	As	Sb	-	-	-	-	-	-	-	-	Xfc	Sheetwash	Ab	Archaean greenstone
166212	393378	7053449	Ba	-	-	-	-	-	-	-	-	-	Cfc	Sheetwash	PEf	Frere Formation
166226	352023	7060765	K ₂ O	-	-	-	-	-	-	-	-	-	Xgp	Sheetwash	Ab	Archaean greenstone
166229	352801	7028272	TiO ₂	Fe ₂ O ₃	Cr	Ga	Pt	Te	-	-	-	-	Sl	Sheetwash	Ab	Archaean greenstone
166230	352750	7020343	Pd	Sn	-	-	-	-	-	-	-	-	Cf	Sheetwash	Ab	Archaean greenstone
166233	372171	7016704	Al ₂ O ₃	Pd	Sn	Ta	Nb	-	-	-	-	-	Xgp	Sheetwash	Ag	Archaean granitoid
166242	375759	7060302	Se	-	-	-	-	-	-	-	-	-	W	Sheetwash	PEy	Yelma Formation
166247	353606	7076092	Cr	Cu	Ni	Pd	Pt	Sc	Zn	-	-	-	W	Sheetwash	Ag	Archaean granitoid
166248	352982	7084403	MgO	-	-	-	-	-	-	-	-	-	L _m	Sheetwash	PEf	Frere Formation
166282	428122	7020166	Cr	-	-	-	-	-	-	-	-	-	Cf	Sheetwash	Ab	Archaean greenstone
166291	380078	7079409	Ba	-	-	-	-	-	-	-	-	-	W	Sheetwash	PEf	Frere Formation
166294	403492	7080708	Sn	-	-	-	-	-	-	-	-	-	Cfc	Stream sediment	PEf	Frere Formation
166296	416141	7084223	Cd	-	1	-	-	-	-	-	-	-	W	Sheetwash	PEd	Windidda Formation
166325	356335	7076353	Cu	Sc	-	-	-	-	-	-	-	-	L _m	Sheetwash	Ag	Archaean granitoid
166337	376084	7111319	Mo	-	-	-	-	-	-	-	-	-	Cqs	Stream sediment	PEw	Wandiwarra Member
166338	366918	7111087	Pb	-	-	-	-	-	-	-	-	-	Cqs	Stream sediment	PEw	Wandiwarra Member
166341	360256	7095942	Ga	Th	-	-	-	-	-	-	-	-	W	Sheetwash	PEd	Windidda Formation
166347	373760	7096614	MnO	Be	Ce	Co	Li	Pb	-	-	-	-	Xkc	Stream sediment	PEd	Windidda Formation
166348	377559	7098927	K ₂ O	Ni	Rb	-	-	-	-	-	-	-	A	Stream sediment	PEd	Windidda Formation
166366	385649	7087474	Fe ₂ O ₃	Sb	Te	Th	-	-	-	-	-	-	A	Stream sediment	PEf	Frere Formation
166387	426078	7081437	MnO	LOI	-	-	-	-	-	-	-	-	Xkc	Sheetwash	PEd	Windidda Formation
166389	387929	7060948	P ₂ O ₅	Bi	Se	-	-	-	-	-	-	-	Cfc	Stream sediment	PEf	Frere Formation
166394	399884	7065356	Ga	Th	-	-	-	-	-	-	-	-	Cgs	Sheetwash	PEf	Frere Formation
166405	352877	7039834	Pd	-	-	-	-	-	-	-	-	-	Cf	Sheetwash	Ab	Archaean greenstone
166406	353185	7031865	Pt	-	-	-	-	-	-	-	-	-	Cf	Sheetwash	Ab	Archaean greenstone
166408	351512	7014387	Pt	-	-	-	-	-	-	-	-	-	Cgp	Sheetwash	Ag	Archaean granitoid
166417	372948	7048146	Ag	-	-	-	-	-	-	-	-	-	Cgp	Sandplain	Ag	Archaean granitoid
166423	372339	7093041	Co	-	-	-	-	-	-	-	-	-	Xfc	Sheetwash	PEf	Frere Formation
166425	377509	7097474	Ce	-	1	-	-	-	-	-	-	-	A	Sheetwash	PEd	Windidda Formation
166442	384889	7093766	Pd	-	-	-	-	-	-	-	-	-	W	Sheetwash	PEd	Windidda Formation
166450	420263	7029876	Ni	-	-	-	-	-	-	-	-	-	Cd	Sheetwash	Ab	Archaean greenstone
166523	368070	7071921	Fe ₂ O ₃	-	-	-	-	-	-	-	-	-	Cgs	Stream sediment	PEf	Frere Formation
166525	352027	7071911	Rb	-	-	-	-	-	-	-	-	-	W	Sheetwash	Ab	Archaean greenstone
166526	353478	7079481	K ₂ O	Bi	Mo	Nb	U	Zr	-	-	-	-	Xgp	Stream sediment	Ag	Archaean granitoid
166528	352785	7096087	U	-	-	-	-	-	-	-	-	-	Cfc	Sheetwash	PEf	Frere Formation
166546	377596	7088130	As	Th	-	-	-	-	-	-	-	-	A	Stream sediment	PEf	Frere Formation
166547	368414	7087491	As	Bi	Ga	Ta	Th	-	-	-	-	-	A	Stream sediment	PEf	Frere Formation

Table 2. (continued)

GSWA No.	<i>MGA coordinates</i>		<i>I</i>	<i>2</i>	<i>3</i>	<i>4</i>	<i>5</i>	<i>6</i>	<i>7</i>	<i>8</i>	<i>9</i>	<i>10</i>	<i>Regolith</i>	<i>Medium</i>	<i>Map code</i>	<i>Geology</i>
	<i>Eastings</i>	<i>Northing</i>														
166548	369942	7095572	MnO	Be	Cd	Ce	Co	La	Li	Ni	Y	Zn	<i>Cl</i>	Stream sediment	Pa	Paterson Formation
166558	415813	7123098	K ₂ O	La	Nb	Rb	Y	-	-	-	-	-	<i>Xgs</i>	Stream sediment	EEo	Wongawol Formation
166559	420527	7119443	As	-	-	-	-	-	-	-	-	-	<i>L_m</i>	Sandplain	EEo	Wongawol Formation
166570	400341	7080161	Fe ₂ O ₃	Sn	W	-	-	-	-	-	-	-	<i>Cfc</i>	Stream sediment	EEf	Frere Formation
166571	409522	7082214	U	-	-	-	-	-	-	-	-	-	<i>F</i>	Stream sediment	EEd	Windidda Formation
166578	423714	7084197	LOI	Ce	Pb	-	-	-	-	-	-	-	<i>A</i>	Stream sediment	EEd	Windidda Formation
166584	439486	7103798	Sr	-	-	-	-	-	-	-	-	-	<i>L_t</i>	Lake sediment	EEo	Wongawol Formation
166585	438969	7088171	Na ₂ O	-	-	-	-	-	-	-	-	-	<i>L_t</i>	Stream sediment	EEp	Princess Ranges Member
166592	400025	7077643	Fe ₂ O ₃	P ₂ O ₅	As	Sb	Se	-	-	-	-	-	<i>Xfc</i>	Stream sediment	EEf	Frere Formation
166593	399969	7071971	Al ₂ O ₃	-	-	-	-	-	-	-	-	-	<i>Fk</i>	Stream sediment	EEf	Frere Formation
166594	405598	7076720	Se	-	-	-	-	-	-	-	-	-	<i>Xfc</i>	Stream sediment	EEf	Frere Formation
166600	424962	7077621	Be	Rb	Y	-	-	-	-	-	-	-	<i>Cl</i>	Stream sediment	EEd	Windidda Formation
166602	357034	7061697	Cu	-	-	-	-	-	-	-	-	-	<i>Cf</i>	Stream sediment	Ab	Archaean greenstone
166605	356566	7035786	Cr	V	-	-	-	-	-	-	-	-	<i>Sl</i>	Sheetwash	Ab	Archaean greenstone
166624	372539	7086472	Y	-	-	-	-	-	-	-	-	-	<i>Cl</i>	Stream sediment	EEf	Frere Formation
166627	373435	7104583	V	-	-	-	-	-	-	-	-	-	<i>Xkc</i>	Stream sediment	EEd	Windidda Formation
166629	389435	7102707	V	-	-	-	-	-	-	-	-	-	<i>Xqs</i>	Stream sediment	EEw	Wandiwarra Member
166635	408475	7123118	Rb	Ta	-	-	-	-	-	-	-	-	<i>Xgs</i>	Sheetwash	EEo	Wongawol Formation
166659	431654	7016578	Ag	Cr	Sb	Sc	Te	V	-	-	-	-	<i>Cf</i>	Sheetwash	Ab	Archaean greenstone
166660	431968	7023589	La	-	-	-	-	-	-	-	-	-	<i>Sl</i>	Sandplain	EEf	Frere Formation
166672	403505	7072215	Sr	-	-	-	-	-	-	-	-	-	<i>A</i>	Lake sediment	EEf	Frere Formation
166676	413027	7076412	Se	-	-	-	-	-	-	-	-	-	<i>Cfc</i>	Stream sediment	EEf	Frere Formation
166678	419017	7077935	Be	W	Y	-	-	-	-	-	-	-	<i>Xkc</i>	Stream sediment	EEd	Windidda Formation
166680	429522	7076908	Ag	-	-	-	-	-	-	-	-	-	<i>A</i>	Stream sediment	EEd	Windidda Formation
166689	472475	7061939	Sb	-	-	-	-	-	-	-	-	-	<i>A</i>	Stream sediment	EEf	Frere Formation
166704	420516	7084603	W	-	-	-	-	-	-	-	-	-	<i>Xkc</i>	Sheetwash	EEd	Windidda Formation
166713	428364	7084208	Pb	-	-	-	-	-	-	-	-	-	<i>Ckc</i>	Sheetwash	EEw	Wandiwarra Member
166714	472254	7063196	W	-	-	-	-	-	-	-	-	-	<i>W</i>	Stream sediment	EEf	Frere Formation
166732	489145	7032805	P ₂ O ₅	-	-	-	-	-	-	-	-	-	<i>Cl</i>	Stream sediment	EEf	Frere Formation
166733	493073	7036541	Mo	-	-	-	-	-	-	-	-	-	<i>W</i>	Sheetwash	EEf	Frere Formation
166734	488118	7040067	Ce	La	-	-	-	-	-	-	-	-	<i>F</i>	Sheetwash	EEf	Frere Formation
166747	464784	7032388	Li	U	-	-	-	-	-	-	-	-	<i>L_t</i>	Lake sediment	EEf	Frere Formation
166753	472127	7036057	U	-	-	-	-	-	-	-	-	-	<i>L_m</i>	Lake sediment	EEf	Frere Formation
166767	499316	7107881	Mo	-	-	-	-	-	-	-	-	-	<i>W</i>	Sheetwash	EEm	Mulgarra Sandstone
166776	475471	7104258	W	-	-	-	-	-	-	-	-	-	<i>L_m</i>	Sandplain	EEk	Kulele Limestone
166806	440239	7108820	Zr	-	-	-	-	-	-	-	-	-	<i>L_m</i>	Lake sediment	EEo	Wongawol Formation
166818	439179	7020690	Zn	-	-	-	-	-	-	-	-	-	<i>Cl</i>	Sheetwash	EEf	Frere Formation
166828	497712	7036437	Zn	-	-	-	-	-	-	-	-	-	<i>Cl</i>	Sheetwash	EEf	Frere Formation
166845	480446	7024619	Ba	Nb	Zr	-	-	-	-	-	-	-	<i>Cl_s</i>	Sheetwash	Pa	Paterson Formation
166849	471612	7040260	Zr	-	-	-	-	-	-	-	-	-	<i>W</i>	Sandplain	EEf	Frere Formation
166857	484689	7065477	TiO ₂	Cu	-	-	-	-	-	-	-	-	<i>Cmh</i>	Sheetwash	EEp	Princess Ranges Member
166935	481310	7065188	TiO ₂	Ga	Sc	V	-	-	-	-	-	-	<i>Cl</i>	Stream sediment	EEp	Princess Ranges Member
166945	459503	7104273	Na ₂ O	-	-	-	-	-	-	-	-	-	<i>L_t</i>	Lake sediment	EEo	Wongawol Formation

Table 2. (continued)

GSWA No.	<i>MGA coordinates</i>		1	2	3	4	5	6	7	8	9	10	<i>Regolith</i>	<i>Medium</i>	<i>Map code</i>	<i>Geology</i>
	<i>Easting</i>	<i>Northing</i>														
166954	442689	7112052	Na ₂ O	Sr	—	—	—	—	—	—	—	—	L _t	Lake sediment	PEo	Wongawol Formation
167004	496444	7015275	Zr	—	—	—	—	—	—	—	—	—	S	Sheetwash	Pa	Paterson Formation
167013	467519	7088532	Al ₂ O ₃	Li	—	—	—	—	—	—	—	—	C _f	Sheetwash	PEo	Wongawol Formation
167015	468857	7103802	LOI	—	—	—	—	—	—	—	—	—	L _m	Sheetwash	PEo	Wongawol Formation
167020	460694	7107862	CaO	S	Sr	—	—	—	—	—	—	—	L _t	Lake sediment	PEo	Wongawol Formation
167021	460215	7099405	LOI	—	—	—	—	—	—	—	—	—	L _t	Lake sediment	PEo	Wongawol Formation
167029	445426	7116088	MgO	Na ₂ O	—	—	—	—	—	—	—	—	L _t	Lake sediment	PEo	Wongawol Formation
167034	496484	7084302	CaO	S	Sr	—	—	—	—	—	—	—	L _t	Lake sediment	PEo	Wongawol Formation
167036	492773	7100589	CaO	S	—	—	—	—	—	—	—	—	L _t	Lake sediment	PEk	Kulele Limestone
167048	489225	7087890	P ₂ O ₅	Be	—	—	—	—	—	—	—	—	X _{gs}	Sheetwash	PEo	Wongawol Formation
167056	486065	7069291	TiO ₂	—	—	—	—	—	—	—	—	—	W	Sheetwash	PEp	Princess Ranges Member
167102	432308	7076680	Ba	—	—	—	—	—	—	—	—	—	A	Stream sediment	PEd	Windidda Formation
167125	484625	7040473	MgO	LOI	Li	—	—	—	—	—	—	—	L _m	Sheetwash	PEf	Frere Formation
167129	464754	7044364	MgO	—	—	—	—	—	—	—	—	—	W	Sheetwash	PEf	Frere Formation
167133	485520	7059316	Cu	—	—	—	—	—	—	—	—	—	X _{fc}	Stream sediment	PEf	Frere Formation
167142	465648	7122605	MgO	—	—	—	—	—	—	—	—	—	X _{kc}	Stream sediment	PEk	Kulele Limestone
167148	455496	7089410	Pb	—	—	—	—	—	—	—	—	—	C _{qs}	Stream sediment	PEp	Princess Ranges Member
167149	456345	7101017	CaO	S	—	—	—	—	—	—	—	—	L _t	Lake sediment	PEo	Wongawol Formation
167218	473018	7123776	K ₂ O	—	—	—	—	—	—	—	—	—	X _{qs}	Stream sediment	PEm	Mulgarral Sandstone
167230	448045	7099735	Na ₂ O	—	—	—	—	—	—	—	—	—	L _t	Lake sediment	PEo	Wongawol Formation
167248	480244	7104340	CaO	S	—	—	—	—	—	—	—	—	L	Lake sediment	PEk	Kulele Limestone

Trace elements

Seventy-one percent (706) of regolith samples from KINGSTON have Ag contents less than detection level (0.1 ppm), and the maximum value is only 0.6 ppm in a sandplain sample over Archaean granitoid (Fig. 15). Most detectable Ag in regolith is from samples over Archaean greenstones.

Many high As values are in regolith samples in the western part of the Frere Formation (Fig. 16 and Table 2), including anomalous values ranging from 42.7 to 54.4 ppm. There are also anomalous values in two regolith samples from over the Gerry Well greenstone belt, and relatively high As values have been recorded from regolith over the Mount Eureka greenstone belt. Arsenic concentrations are low in samples over Archaean granitoid, and in lake sediments.

The maximum value for Au in regolith is only 4 ppb, in sample GSWA 166126 close to the Archaean greenstone–granitoid contact near the Mount Eureka greenstone belt (Fig. 17). Seventy percent of samples — 696 of the 998 samples — have gold contents less than detection level (1 ppb), and most samples with detectable gold show no clear relationship with any particular lithology.

Many high Ba values are from regolith samples over the Windidda Formation (Fig. 18 and Table 2), although some scattered anomalous values of 3605.0 ppm (GSWA 166291) and 4387.7 ppm (GSWA 166212) are from the western part of the Frere Formation. It is notable that these scattered values are not accompanied by other high-Ba samples. Other anomalous values are in samples over the Paterson Formation (3879.3 ppm) and Wandiwarra Formation (maximum value of 4494.5 ppm). Barium in regolith is low over both Archaean greenstone and granitoid rocks, and the eastern part of the Frere Formation.

Beryllium in regolith reaches a maximum value of 5.4 ppm, and is low over Archaean granitoid rocks and in lake-sediment samples (Fig. 19). Samples from Mount Wellesley and near Shed Bore over the Windidda Formation have anomalous Be concentrations, and several high values are recorded from regolith north and northwest of Prenti Downs Homestead. A few scattered high values are in the western part of the Frere Formation.

Most high Bi values are in regolith over the western part of the Frere Formation (Fig. 20), including three anomalous values between 1.5 and 1.8 ppm in the vicinity of the Wellington Range. Some high Bi values are also in regolith on or close to the Mount Eureka greenstone belt, but Bi values are relatively low in regolith over Archaean granitoid, and in lake-sediment samples.

Eighty-one percent of regolith samples (808) have less than detection level values (0.1 ppm) for Cd, and the maximum value is only 0.3 ppm in samples from Mount Wellesley and 5 km east of Quartz Well (Fig. 21 and Table 2).

Most high or anomalously high Ce values are in regolith samples on or near to the Windidda Formation

(Fig. 22 and Table 2), especially in the vicinity of Mount Wellesley, where there are three closely spaced anomalous values ranging between 110.2 (GSWA 166425) and 191.1 ppm (GSWA 166548). Several other high values are in samples located near to Shed Bore, also over the Windidda Formation. An isolated anomalous value of 103.6 ppm is from a sample in the eastern part of the Frere Formation, but, in general, the western part of this formation has higher Ce values in regolith. Small groups of high Ce values are in regolith samples over the Wongawol Formation northeast of Bummer Pool, and near the Wongawol Formation and Kulele Limestone in the northeast of KINGSTON, near Mount Throssell Well.

A group of three samples with anomalous Co concentrations, ranging from 45.9 to 122.4 ppm, are from the Mount Wellesley area (Fig. 23 and Table 2), and another anomalous value is in regolith a further 16 km to the north over the Wandiwarra Formation. A cluster of relatively high Co values have been measured from some samples near Shed Bore over the Windidda Formation, including one anomalous value of 56.7 ppm. A few high Co values are in some of the regolith samples over the Mount Eureka greenstone belt, but most Co values on KINGSTON are less than 15 ppm.

Chromium in regolith highlights the two Archaean greenstone belts on KINGSTON (Fig. 24 and Table 2), and provides a sharp contrast between areas of greenstone and Archaean granitoid rocks. Apart from a few high values in regolith over the western part of the Frere Formation, and over parts of the Windidda Formation, Cr values in regolith are low in the project area overall.

Relatively high Cu values are common in regolith either close to or overlying the Mount Eureka greenstone belt (Fig. 25 and Table 2), including the maximum value of 203 ppm in sheetwash sample GSWA 166247 from near Red Bluff. Other high values are spatially related to dolerite near Prenti Downs Homestead. Copper values are low over Archaean granitoid rocks and in lake sediments, but there are scattered high values over parts of the Windidda Formation.

Elevated Ga in regolith is largely confined to regolith over Archaean greenstones, and the western part of the Frere Formation (Fig. 26 and Table 2), with two values over the Frere Formation of 42.0 (GSWA 166547) and 40.2 ppm (GSWA 166394). There are also relatively high values near dolerite close to Prenti Downs Homestead, whereas Ga values are low over lake areas, Archaean granitoid, and in the eastern part of the Frere Formation. There are some elevated values over parts of the Windidda Formation.

Indium in regolith only reaches a maximum of 0.2 ppm, with a detection level of 0.1 ppm (Fig. 27), and 91% of samples (905) have In contents that are less than detection level. Samples with detectable In are in three areas on KINGSTON — over Archaean greenstones, in the western part of the Frere Formation, and overlying or close to dolerite near Prenti Downs Homestead.

The western part of the Frere Formation, and parts of the Windidda Formation (especially in the vicinity of

Mount Wellesley) have regolith samples with relatively high La concentrations (Fig. 28), with anomalous concentrations in several different types of sample media (Table 2). Parts of the Wongawol Formation northeast of Bummer Pool also have high La, and an isolated sample in the eastern part of the Frere Formation (GSWA 166734) has 54.8 ppm La.

Unlike many other analytes, Li shows only a weak contrast between regolith over Archaean greenstones compared to Archaean granitoid rocks (Fig. 29). A series of both high and anomalously high values are recorded from regolith samples near Mount Wellesley, extending southeast along the Windidda Formation towards Christmas Bore (Table 2 and Fig. 29). Other high values are over part of the Wongawol Formation northeast of Bummer Bore, and a few sheetwash samples over parts of the Frere Formation also have anomalously high concentrations of Li (Table 2).

Molybdenum in regolith highlights both greenstone belts on KINGSTON, where high Mo contents in regolith over the greenstone belts are in marked contrast to the low Mo concentrations over Archaean granitoid rocks (Fig. 30 and Table 2). Concentrations are higher in regolith over the western part of the Frere Formation (broadly west of a line south from Tooloo Bluff) than in the eastern part, although the maximum value is in a regolith sample over the Wandiwarra Formation west of Chiall Spring (GSWA 166337). Concentrations are particularly low in lake-sediment samples.

Apart from one anomalous value of 16.1 ppm (GSWA 166233), Nb in regolith is relatively low over Archaean granitoid rocks, as it is in lake sediments (Fig. 31 and Table 2). Anomalous values are also recorded from regolith either close to (e.g. Red Bluff) or over Archaean greenstones (Gerry Well greenstone belt). One anomalous Nb value is recorded from regolith over the Paterson Formation southeast of Warren Bore, and other high values are in regolith near the Kulele Limestone adjacent to STANLEY, and over the Frere and Windidda Formations.

Nickel in regolith shows a strong contrast between Archaean greenstones and granitoid rocks (Fig. 32), with anomalous values between 100 and 188 ppm recorded in regolith from greenstones (Table 2). There are other anomalous values over the Windidda Formation at Mount Wellesley, but, overall, values are low over most of the map sheet, especially in lake areas.

There are both high and anomalously high Pb values in regolith from near Mount Wellesley, and other anomalous samples over the Wandiwarra Member southwest of the Princess Ranges and at Christmas Bore near the contact of the Wandiwarra Member and Windidda Formation (Fig. 33 and Table 2). One anomalous sample is grouped with other high values close to the Kulele Limestone. The eastern part of the Frere Formation has lower Pb values than regolith to the west. In other parts of the Earaheedy Group, a band of high Pb values in regolith follows the Windidda Formation and Wandiwarra and Princess Ranges Members along the Princess and Wellington ranges. Lead also offers a sharp contrast between Archaean granitoids and greenstone.

Eighty-eight percent of samples (880) have Pd concentrations less than detection level (1 ppb) on KINGSTON. Four anomalous samples, each with 3 ppb Pd, are in regolith over Archaean rocks — three on or close to greenstones of the Mount Eureka greenstone belt, and one (GSWA 166233) over Archaean granitoid (Fig. 34 and Table 2). Most other samples with Pd above detection level are over greenstones, apart from the maximum value of 4 ppb, which is recorded from GSWA 166442 over the Windidda Formation 6 km west of Kepallin Spring.

Similar to Pd, a high proportion of regolith samples on KINGSTON (78% or 778) have Pt contents less than detection level (1 ppb), and most of those with detectable Pt are associated with greenstones of the Mount Eureka greenstone belt (Fig. 35 and Table 2). Other samples with Pt abundances above detection level are close to dolerite at Prenti Downs Homestead.

Rubidium contents are high in regolith over Archaean greenstones relative to Archaean granitoids (Fig. 36 and Table 2). Some high and anomalously high values come from regolith in the vicinity of Mount Wellesley, predominantly over the Windidda Formation. Two anomalous values have been recorded from regolith of the Wongawol Formation northeast of Bummer Pool, and there are several relatively high values in the vicinity of the Kulele Limestone near Mount Throssell Well. Scattered high values are strung out along the Windidda Formation, and the highest value of 227.5 ppm is over Archaean rocks near Red Bluff in the west of the map sheet.

All high and anomalously high S values are in lake sediments, all but one of which are located in Lake Carnegie (the anomalous values in Lake Carnegie range between 20.50 and 21.36% S; Fig. 37). The remaining values in regolith are less than or close to the detection level of 0.01%.

Two anomalous Sb values, including the highest value of 8.2 ppm (GSWA 166185), come from regolith samples over the Gerry Well greenstone belt (Fig. 38 and Table 2). High and anomalously high values stretch from Mount Wellesley east-southeast towards Gap Well, over the Windidda and Frere Formations. Antimony values are low over Archaean granitoid (in contrast to greenstones, where many regolith samples have Sb above detection level) and in lake-sediment samples. Concentrations are higher in the western part of the Frere Formation compared to eastern parts.

The largest concentration of elevated Sc values are in regolith on or close to Archaean greenstones (Fig. 39 and Table 2) including three anomalous values between 30 and 48 ppm. Scandium probably has the most stark contrast between Archaean greenstone and granitoid of all analytes. Other elevated values are in areas of dolerite near Prenti Downs Homestead, whereas Sc values are relatively low over the Paterson Formation and in lake sediments.

All of the anomalous Se values, and most of the high values, are in regolith over the western part of the Frere Formation (Fig. 40 and Table 2), including the maximum value of 7.9 ppm, 5 km northeast of Alf Bore (GSWA 166592). One anomalous value of 6.5 ppm is in regolith

over the Yelma Formation, but this sample is close to the contact with the Frere Formation southwest of Banjo Creek. Other relatively high values are in regolith close to dolerite at Prenti Downs Homestead, and over Archaean greenstones. Selenium concentrations are notably low in lake-sediment samples.

Overall, Sn concentrations in regolith are low on KINGSTON (Fig. 41), especially in lake-sediment samples. There is a marked contrast in values between regolith over the western part of the Frere Formation and the eastern part, although Sn concentrations do not have a strong contrast between regolith over Archaean greenstone and granitoid rocks.

High and anomalously high Sr values in regolith are restricted to lake-sediment samples, especially over Lake Carnegie, including the highest value of 987.4 ppm in GSWA 167034 (Fig. 42 and Table 2). Another anomalously high sample (GSWA 166672) is about 5 km southwest of Gap Well.

Tantalum in regolith (Fig. 43) reflects the lithological contrast between Archaean greenstones and granitoid rocks, with other high values over the Frere Formation (e.g. south of Mount Wellesley). Several relatively high values are in regolith samples over part of the Wongawol Formation northeast of Bummer Pool, and over the Kulele Limestone (Table 2).

The maximum value for Te in regolith is only 0.7 ppm (detection level 0.1 ppm) and 73% of samples (725) have Te contents less than detection level. There are high Te values in regolith over Archaean greenstones and the Frere Formation (Fig. 44 and Table 2). Despite the low levels, Te highlights the lithological contrast between Archaean granitoids and greenstones.

All five anomalous Th values in regolith, ranging from 48.4 to 71.7 ppm, are on or close to the Frere Formation (Fig. 45 and Table 2), with some high values on the adjacent Windidda Formation. Overall, values are low elsewhere on KINGSTON, especially in lake sediments, but relatively high in regolith on or close to dolerite near Prenti Downs Homestead.

Most samples with relatively high U are restricted to the western part of the Frere Formation, and the Windidda Formation (Fig. 46 and Table 2). Concentrations are low in samples from Lake Carnegie and over Archaean granitoid rocks, but two anomalous values are recorded from lake-sediment samples from near Warren Bore in the eastern part of the Frere Formation.

Vanadium is in notably high concentrations in regolith over Archaean greenstones and dolerite compared to other lithologies (Fig. 47 and Table 2), and ranges from 757 to 1170 ppm over the Mount Eureka greenstone belt. There is a marked contrast in V between regolith over Archaean greenstones and granitoid rocks. Vanadium values are slightly higher over the western part of the Frere Formation compared to the east, and low in lake-sediment samples.

Tungsten, which reaches a maximum of 8.5 ppm in regolith over the Windidda Formation (Fig. 48 and

Table 2), only highlights a weak contrast between Archaean granitoids and greenstones. An isolated anomalous value of 5.8 ppm is recorded from sandplain sample GSWA 166776 in Lake Carnegie.

A series of high and anomalously high Y values are in regolith samples over the Windidda Formation, the western part of the Frere Formation, and the Paterson Formation in the vicinity of Wellington Range, including the maximum value of 50.4 ppm in GSWA 166548. A series of relatively high values, including an anomalous value of 27.4 ppm (GSWA 166558), have been assayed from samples over part of the Wongawol Formation northeast of Bummer Pool (Fig. 49 and Table 2), and another group of high values is located over the Kulele Limestone near Mount Throssell Well.

Some anomalous Zn values in regolith are in samples spatially associated with Archaean greenstones, and in the Mount Wellesley area (Fig. 50 and Table 2). Other high values are near the contact of the Yelma and Frere Formations in the south central part of the map sheet, and near the contact of the Paterson and Frere Formations southeast of Bilgarrie Cutarrie Pool. Zinc values are notably lower over the eastern part of the Frere Formation, and in lake-sediment samples, but relatively high over the Windidda Formation and Kulele Limestone near Mount Throssell Well, and southeast of Princess Ranges.

There are no areas of notably high Zr content in regolith on KINGSTON (Fig. 51). Scattered high values are in lake-sediment samples of Lake Carnegie, and other high values are over parts of the Frere Formation, Paterson Formation, and near Red Bluff in the western part of the map sheet. A group of relatively high values are close to dolerite at Prenti Downs Homestead.

Discussion

Controls on the chemistry of regolith can be attributed to the combined contributions of two factors — parent lithology (i.e. bedrock control), and the processes of regolith formation (i.e. physical and chemical weathering). In some cases, it is possible to identify a simple relationship between bedrock composition and regolith chemistry, but in many cases, the bedrock signature has been overprinted or (in extreme cases) obliterated by regolith-forming processes. In addition, for the depositional regime, regolith chemistry may reflect the combined effects of the mixing of parent lithologies overprinted by physical and chemical weathering.

Parent lithology (bedrock control)

Archaean greenstone

The influence of bedrock control on the chemistry of regolith is well illustrated by the two Archaean greenstone belts on KINGSTON. The chemistry of regolith from these two greenstone belts contrasts markedly with that over the intervening Archaean granitoid. Nineteen components (TiO_2 , Fe_2O_3 , P_2O_5 , Ag, As, Bi, Co, Cr, Cu, Ga, Ni, Pb, Rb, Sb, Sc, Ta, Te, V, and Zn) are in relatively high concentrations in regolith over both the Gerry Well and

Mount Eureka greenstone belts relative to granitoid-derived regolith. This contrast is even demonstrated by analytes that are at concentrations close to detection level, such as Ta, Te, and Ag. This contrast also highlights the weathered nature of regolith over Archaean granitoids, where such weathering has resulted in the depletion of most analytes except SiO₂.

On NABBERU (1:250 000), Morris et al. (1997) used the concentrations of lithophile elements in granitoid-derived regolith (such as K₂O, Na₂O, Rb, and Sr) to distinguish various granitoid types. However, on KINGSTON, such components as K₂O and Rb are higher in greenstone-sourced regolith than that derived from granitoid rocks, consistent with the protracted weathering of Archaean granitoids and the possible metasomatic alteration of greenstones. The weathering of granitoid is confirmed by field observations, where much regolith is composed of quartz sand.

Proterozoic dolerite

Bedrock control on regolith is also shown for small areas of Proterozoic dolerite near Prenti Downs Homestead, which can be identified by relatively high concentrations of TiO₂, Fe₂O₃, K₂O, Cu, Ga, In, Pt, Sc, Se, and Zr compared to adjacent regolith. Similar to greenstones, several of these analytes, such as In, Pt, and Se, are typically at concentrations close to detection level, yet they remain useful in delineating the extent of mafic bedrock. The association of Fe₂O₃, TiO₂, Cu, Ga, In, Pt, Sc, and Se in regolith is typical of a mafic igneous association, but K₂O and Zr are unusual. The relatively high K₂O content could reflect the metasomatic alteration of dolerites, as reported from STANLEY (Pirajno, F., 1999, pers. comm.), and higher Zr could mean that the breakdown of dolerite involves the preferential concentration of zircon.

Compositional variations within the Frere Formation

An example of the modification of a bedrock signature in regolith is provided by comparing regolith chemistry from the eastern and western parts of the Frere Formation. Regolith samples from the western part of the Frere Formation have high concentrations of Fe₂O₃, K₂O, As, Ba, Be, Bi, Ce, Cr, Ga, In, La, Mo, Pb, Sb, Se, Sn, U, V, and Zn compared to samples from the eastern part. The lower concentrations in the eastern part can be attributed to input of regolith from the Paterson Formation, much of which is characterized by siliceous sandplain (S) material (Plate 2).

Other parts of the Earaheedy Group

Regolith from the upper part of the Frere Formation close to the contact with the overlying Windidda Formation in the Wellington Range area has relatively high concentrations of MnO, MgO, Ba, Ce, Co, Cr, Ga, Li, Pb, Rb, Sb, U, and W, extending east as far as Christmas Bore. The Mount Wellesley area in particular is characterized by high and anomalously high concentrations of MnO, MgO, K₂O, Co, La, Li, Ni, Pb, Rb, and W in regolith, and some samples have high concentrations of several of these

analytes (Table 2). As these high concentrations are localized, and transcend lithological boundaries, there is less convincing evidence for bedrock control alone on regolith chemistry. One possible explanation is provided by recent remapping of this area, which has identified intense folding and brittle deformation of rocks, with associated quartz veining (Jones, J. A., 2000, pers. comm.).

There are areally restricted groups of samples with high concentrations of several analytes over parts of the Wongawol Formation northeast of Bummer Pool (elevated K₂O, Ce, La, Li, Rb, Ta, and Zn), and over parts of the Kulele Limestone to the east in the vicinity of Mount Throssell Well (elevated TiO₂, MgO, K₂O, Ce, Pb, Rb, Ta, Zn). Morris et al. (2000a) discusses the development of similar localized anomalous in regolith over parts of the Wongawol Formation and Kulele Limestone on STANLEY, including elevated levels of Na₂O, K₂O, Ba, Be, Ce, Co, Cu, La, Li, Nb, Ni, Rb, Sn, Sr, Y, and Zn. On both KINGSTON and STANLEY, this anomalous is not restricted to any particular sample medium. Reconnaissance work on STANLEY (Pirajno, F., 1999, pers. comm.) has shown that high MnO contents in regolith over the Wongawol Formation in this area are consistent with the manganiferous nature of sedimentary rocks (Adamides and Pirajno, in prep.); however, the nature and extent of possible mineralization in this area is not known.

Control exerted by regolith type

Lake sediments

The clearest example on KINGSTON of the control on regolith chemistry exerted by regolith type is that provided by lake-sediment samples. Typically, lake-sediment samples (such as those from Lake Carnegie) have relatively low TiO₂, Al₂O₃, K₂O, P₂O₅, As, Be, Bi, Cu, Ga, Mo, Nb, Ni, Sb, Sc, Se, Sn, and Zn, and relatively high MgO, CaO, Na₂O, LOI, S, (and locally) U and Zr. These enrichments and depletions in analytes are similar to those recorded for lake-sediment samples on NABBERU (1:250 000; Morris et al., 1997), and illustrate the saline, gypsiferous, and carbonate-rich nature of these deposits. The relatively low concentrations of Al₂O₃, K₂O, and Be indicate a relatively low clay content. These characteristics of lake-sediment chemistry are different to other areas, such as the Fraser Range region (Morris et al., 2000b) — in the case of Fraser Range, lake-sediment compositions are similar to nearby bedrock, and it is likely that lakes have acted as local sinks into which locally derived, fine-grained debris has been deposited.

Sandplain

Sandplain regolith (S and SI) covers in excess of 3000 km² and accounts for 162 samples on KINGSTON (Table 1), the majority of which consist of a mixed eolian and residual material such as that over Archaean granitoid rocks, overlying the Paterson Formation (eastern Frere Formation), and in the northeast of the map sheet

(regolith unit *S* of Plate 2). Typically, this material is largely composed of SiO_2 , either derived by the intense weathering of bedrock *in situ* (such as in the case of Archaean granitoid), or through the combined input of bedrock and eolian processes in the case of the Paterson Formation in the northeast of KINGSTON. In the latter case, it is difficult to assess the relative contributions of bedrock and far-field transported windblown sand.

Statistical treatment of regolith chemical data

Although spot-concentration maps (Figs 5 to 51) allow a rapid comparison of regolith chemistry relative to bedrock geology, statistical analysis is necessary to determine differences in the chemistry of regolith populations according to such criteria as sample media, bedrock unit, or regolith unit. The problems of comparing datasets of unequal size, where the data are commonly positively skewed and follow a non-normal distribution, have been discussed by several authors (e.g. Koch and Link, 1970; Swan and Sandilands, 1995), and specifically addressed within the GSWA regolith program by Morris et al. (1998). In order to produce a dataset that more closely resembles a normal distribution, and avoid the problem of zero values, data can be log transformed after addition of a constant (Rock, 1988). Following this, geometric mean values can be calculated, and standard statistical tests can be carried out for comparison of mean values for two (Student's t-test) or more than two (Tukey's HSD, or Honestly Significant Difference) sample populations.

The application of this approach within the GSWA program is discussed in Morris et al. (1997, 1998). One major assumption of this approach is that addition of a constant and log normalization produces a sufficiently normally distributed dataset for the application of such parametric tests as Student's t-test and Tukey's HSD. When datasets are small or not normally distributed, non-parametric tests may be more appropriate. Amongst these is the non-parametric equivalent of the Student's t-test for independent samples known as either the Mann-Whitney U test or the Wilcoxon rank-sum test (Swan and Sandilands, 1995). Whereas the Student's t-test examines the hypothesis of equality of population means, the Mann-Whitney U test analyses for the equality of medians (i.e. the middle value in a set of ranked data).

For many geochemical datasets, particularly those containing large amounts of zero or near-zero data, use of such approaches as the Mann-Whitney U test (where data are ranked before being statistically compared) must take into account the problems introduced by having a significant number of data of the same value, commonly zero in the case of regolith geochemistry. In this situation, the Mann-Whitney approach may unrealistically highlight the importance of the few non-zero data. This must be borne in mind, although it is

accepted that the Mann Whitney U test is more appropriate for testing geochemistry, in that most such datasets are positively skewed. Tests of median equality have been carried out at the 99% probability level for data from KINGSTON. In order to avoid the influence of poorer precision and accuracy at low concentrations, only median values that are greater than ten times the detection level are discussed. It is unrealistic to report median values of trace elements to the level of precision presented in KINGSTON.CSV, and these median values are reported as integers in the relevant tables.

Comparison of various sandplain regolith populations

The association of dune forms with sandplain deposits is indicative of eolian input, and there is the possibility that eolian-derived quartz sand has acted as a dilutant, and that sandplain blankets locally derived regolith. Thus, determining how representative sandplain material is of the underlying bedrock is of great interest in mineral exploration and regional mapping.

Regolith designated as sandplain (*S*) on KINGSTON accounts for 134 samples and about 15% of all regolith. It is particularly well developed over Archaean granitoid, over parts of the Paterson Formation, and in the northeast of the map sheet (Plate 2). The mean, median, standard deviation, and skewness for sandplain samples (i.e. regolith type *S*) developed over Archaean granitoid and sandplain developed elsewhere on KINGSTON are shown in Table 3. The high SiO_2 content and low concentration of other analytes in these samples is shown by the positive skewness of all data apart from silica. A statistical comparison of median values using the Mann-Whitney U test shows a 99% or greater probability that TiO_2 , Ba, Li, Nb, Pb, Y, and Zr are lower and Al_2O_3 is higher in sandplain over Archaean granitoid compared to sandplain elsewhere on KINGSTON. These statistical results are consistent with field observations and spot-concentration maps that suggest that sand overlying Archaean granitoid rocks results from protracted weathering *in situ*, resulting in the loss of a wide range of analytes. Higher Al_2O_3 could be indicative of a higher clay content in regolith over granitoid rocks. This result is in marked contrast to regolith over Archaean granitoid on NABBERU (Morris et al., 1997), where chemistry was used to subdivide the underlying granitoid rocks.

Sandplain (*S*) developed over both Archaean granitoid and the Paterson Formation can be taken as material that has largely developed by weathering *in situ*, and a statistical comparison of these sample populations should provide information on the combined effects of bedrock chemistry and chemical weathering on regolith formation. Summary statistics for the two sample populations are shown in Table 4. Regolith over Archaean granitoid has lower median values for TiO_2 , As, Li, Mo, Nb, Th, and Zr compared to sandplain developed over the Paterson Formation. These differences in composition can be attributed to the combined effects of a more varied source lithology for Paterson Formation regolith, and the less intense weathering of this material to produce the

Table 3. Summary statistics for sandplain (S) over Archaean granitoid and sandplain elsewhere

Detection level	S over Ag (n=63)				S not over Ag (n=71)			
	Mean	σ	Median	Skewness	Mean	σ	Median	Skewness
Percent								
SiO ₂	0.1	91.37	5.31	92.40	-4.42	91.23	4.90	91.80
TiO ₂	0.01	0.20	0.08	0.19	2.25	0.25	0.08	0.24
Al ₂ O ₃	0.02	3.81	1.56	3.51	2.65	3.28	1.42	2.86
Fe ₂ O ₃	0.01	3.12	3.05	2.23	5.55	3.58	2.60	2.79
MnO	0.001	0.01	—	—	1.93	0.01	0.01	2.70
MgO	0.01	0.07	0.03	0.07	0.61	0.07	0.04	0.07
CaO	0.1	0.07	0.11	0.00	1.53	0.09	0.10	0.10
Na ₂ O	0.002	0.02	0.02	0.01	4.21	0.02	0.02	0.01
K ₂ O	0.02	0.20	0.16	0.15	2.59	0.21	0.18	0.16
P ₂ O ₅	0.002	0.01	0.01	0.01	6.07	0.01	0.01	0.01
LOI	0.01	1.66	0.78	1.49	3.18	1.50	0.73	1.25
Parts per million^(a)								
Ag	0.1	—	—	—	×	—	—	—
As	0.1	2	2	1	5	3	2	2
Au (ppb)	1	—	1	—	2	—	—	—
Ba	0.1	39	34	26	3	65	83	35
Be	0.1	—	—	—	×	—	—	—
Bi	0.1	—	—	—	×	—	—	—
Cd	0.1	—	—	—	×	—	—	—
Ce	0.1	7	3	6	3	9	5	7
Co	0.1	2	1	2	2	2	1	2
Cr	2	70	43	54	2	89	58	70
Cu	1	5	3	4	3	6	3	5
Ga	0.1	6	3	5	2	5	3	4
In	0.1	—	—	—	×	—	—	—
La	0.1	4	2	3	3	5	3	4
Li	0.1	5	2	4	2	5	2	5
Mo	0.1	—	—	—	×	—	—	—
Nb	0.5	3	1	3	2	5	2	5
Ni	1	8	3	7	2	7	3	6
Pb	0.1	7	3	6	2	8	3	7
Pd (ppb)	1	—	—	—	×	—	—	—
Pt (ppb)	1	—	—	—	×	—	—	—
Rb	0.1	11	7	9	2	13	9	11
S (%)	0.01	—	—	—	×	—	—	—
Sb	0.1	—	—	—	×	—	—	—
Sc	2	2	2	2	3	1	2	2
Se	0.5	—	—	—	×	—	—	—
Sn	0.1	1	1	1	2	1	—	1
Sr	0.1	8	4	6	2	9	7	6
Ta	0.1	—	—	—	×	—	—	—
Te	0.1	—	—	—	×	—	—	—
Th	0.1	4	2	4	2	5	3	4
U	0.1	—	—	—	×	—	—	—
V	2	48	34	36	2	53	38	42
W	0.1	1	—	1	2	1	1	1
Y	0.1	2	1	2	3	3	1	3
Zn	1	12	6	10	3	13	11	12
Zr	1	97	32	94	1	131	98	108

NOTE: (a) unless otherwise shown
 n number of samples
 ppb parts per billion
 — less than detection level
 σ standard deviation
 \times insufficient data for calculation of meaningful skewness

Table 4. Summary statistics for sandplain (S) over Paterson Formation and Archaean granitoid

Detection level		Paterson Formation (n=13)				Archaean granitoid (n=63)			
		Mean	σ	Median	Skewness	Mean	σ	Median	Skewness
Percent									
SiO ₂	0.1	91.29	4.34	91.70	-1.32	91.37	5.31	92.40	-4.42
TiO ₂	0.01	0.29	0.13	0.24	1.97	0.20	0.08	0.19	2.25
Al ₂ O ₃	0.02	3.45	1.50	3.03	1.78	3.81	1.56	3.51	2.65
Fe ₂ O ₃	0.01	3.38	1.64	2.98	1.05	3.12	3.05	2.23	5.55
MnO	0.001	0.01	0.01	0.00	2.87	0.01	0.00	0.00	1.93
MgO	0.01	0.07	0.04	0.08	-0.56	0.07	0.03	0.07	0.61
CaO	0.1	0.12	0.09	0.10	-0.34	0.07	0.11	—	1.53
Na ₂ O	0.002	0.01	0.01	0.01	1.57	0.02	0.02	0.01	4.21
K ₂ O	0.02	0.16	0.06	0.15	0.57	0.20	0.16	0.15	2.59
P ₂ O ₅	0.002	0.01	0.01	0.01	1.35	0.01	0.01	0.01	6.07
LOI	0.01	1.70	1.07	1.43	2.64	1.66	0.78	1.49	3.18
Parts per million^(a)									
Ag	0.1	—	—	—	×	—	—	—	×
As	0.1	4	3	3	3	2	2	1	5
Au (ppb)	1	—	—	—	×	—	1	—	×
Ba	0.1	41	33	29	2	39	34	26	3
Be	0.1	—	—	—	×	—	—	—	×
Bi	0.1	—	—	—	×	—	—	—	×
Cd	0.1	—	—	—	×	—	—	—	×
Ce	0.1	9	6	7	2	7	3	6	3
Co	0.1	2	1	1	0	2	1	2	2
Cr	2	95	60	67	2	70	43	54	2
Cu	1	5	2	5	2	5	3	4	3
Ga	0.1	6	3	6	2	6	3	5	2
In	0.1	—	—	—	×	—	—	—	×
La	0.1	5	3	4	2	4	2	3	3
Li	0.1	5	1	5	1	5	2	4	2
Mo	0.1	1	—	1	×	—	—	—	×
Nb	0.5	6	2	5	1	3	1	3	2
Ni	1	6	2	6	2	8	3	7	2
Pb	0.1	9	4	7	1	7	3	6	2
Pd (ppb)	1	—	—	—	×	—	—	—	×
Pt (ppb)	1	—	—	—	×	—	—	—	×
Rb	0.1	10	4	8	1	11	7	9	2
S (%)	0.01	—	—	—	×	—	—	—	×
Sb	0.1	—	—	—	×	—	—	—	×
Sc	2	1	2	—	1	2	2	2	3
Se	0.5	—	1	—	×	—	—	—	×
Sn	0.1	1	—	1	1	1	1	1	2
Sr	0.1	7	4	5	1	8	4	6	2
Ta	0.1	—	—	—	×	—	—	—	×
Te	0.1	—	—	—	×	—	—	—	×
Th	0.1	7	4	5	2	4	2	4	2
U	0.1	1	—	—	×	—	—	—	×
V	2	62	39	48	1	48	34	36	2
W	0.1	1	—	1	×	1	—	1	×
Y	0.1	3	2	2	1	2	1	2	3
Zn	1	19	24	14	3	12	6	10	3
Zr	1	187	177	133	3	97	32	94	1

NOTE: (a) unless otherwise shown
 n number of samples
 ppb parts per billion
 — less than detection level
 σ standard deviation
 \times insufficient data for calculation of meaningful skewness

overlying regolith. In particular, the higher Nb and Zr in regolith over the Paterson Formation would be consistent with a higher concentration of resistate mineral phases.

Sanders and McGuinness (2000) carried out detailed work on different sandplain regolith units on KINGSTON, subdividing this material in terms of geomorphology and composition. On KINGSTON, two types of sandplain have been identified — sandplain characterized by dune forms, which ranges from eolian deposits through to residual material with some eolian reworking (*S*); and sandplain with sand- and clay-rich colluvium or sheetwash (*SI*). Summary statistics for samples collected from these two regolith types are shown in Table 5. Immediately apparent is the relatively wide range in the concentrations of Fe_2O_3 , Ba, Cr, Cu, Ni, Pb, Sr, V, Zn, and Zr, especially for the undulating sandplain unit (*SI*), shown by the standard deviation values. A statistical comparison of median values shows that there is a 99% or better probability that TiO_2 , Al_2O_3 , Fe_2O_3 , K_2O , LOI, As, Ba, Ce, Co, Cr, Ga, La, Li, Pb, Rb, Sr, Th, V, Y, Zn, and Zr are all higher and SiO_2 lower in the undulating sandplain unit (*SI*) than in the residual sandplain unit (*S*). This suggests that the undulating unit is more immature (in that it represents a mixture of sand and sheetwash), and has a more localized provenance (consistent with the majority of this regolith type overlying the ferruginous Frere Formation in the central southern part of KINGSTON). In contrast, although it has a residual component, the residual unit also has higher SiO_2 , which is consistent with its derivation from granitoid rocks, its mineralogical maturity (in that it lacks a sheetwash component), and the unit having undergone some eolian reworking, as shown by the presence of net-like dunes.

Comparison of greenstone belts

Spot-concentration maps show that greenstone belts on KINGSTON have a distinctive chemistry. In Table 6, summary statistics are presented for regolith samples over both the Gerry Well ($n = 7$) and Mount Eureka ($n = 22$) greenstone belts. There is a 99% or better probability that median values for Na_2O , K_2O , Ba, Li, Rb, and Sr are higher, and As and Sb lower in regolith over the Mount Eureka greenstone belt compared to that over the Gerry Well greenstone belt. The analytes with higher median values for the Mount Eureka greenstone belt indicate some felsic igneous input, and it is possible that some samples assigned to greenstone geology have in fact been sourced from the adjacent granitoid. Furthermore, the validity of the statistical approach must be viewed in terms of the unequal population sizes, and the small number of samples from the Gerry Well belt. Of note is the similarity in median values for such mafic-related components as Mg, Cr, Ni, Sc, and V, which suggests that the two greenstone belts are fundamentally similar in terms of their lithological content.

Downslope changes in regolith chemistry

Differences in the composition between exposed regime regolith and colluvium derived from the same parent

lithology can provide important information on downslope processes, including the relative importance of chemical versus physical weathering. Two statistical comparisons have been made to examine this issue — comparing exposed regime regolith, colluvium, and sheetwash over the Frere Formation, and comparing exposed regime regolith and colluvium over Archaean granitoid rocks.

Summary statistics for exposed regime regolith and colluvium sourced from the Frere Formation (i.e. X_{fc} and C_{fc} respectively) are shown in Table 7. Relatively high standard deviation values for Fe_2O_3 , Ba, Cr, Cu, Ni, Rb, Sr, V, Zn, and Zr indicate some heterogeneity in these sample populations, but application of the Mann Whitney U test shows that there is no difference in the median values of any analytes at the 99% or higher level of probability. This suggests that physical comminution of material, rather than chemical weathering, is the more important downslope process. The chemistry of colluvium (C_{fc}) and sheetwash (W) over the Frere Formation are shown in Table 8. As for exposed regime regolith and colluvium, there is no statistical difference between median values at the 99% or higher level for colluvium and sheetwash. This comparison shows that over an extended slope interval, spanning exposed rock through to distal sheetwash, the nature of regolith is largely controlled by physical breakdown of the parent rock rather than chemical weathering. This means that even distal depositional regime regolith can retain the chemical signature of the parent rock.

Summary statistics for exposed regime regolith and colluvium derived from Archaean granitoid rocks (X_{gp} and C_{gp} respectively) are shown in Table 9. Relatively high standard-deviation values for some analytes (e.g. Al_2O_3 , Fe_2O_3 , Ba, Ce, Cr, La, Ni, Rb, Sr, V, Zn, and Zr) indicate some heterogeneity, with analytes such as Fe_2O_3 , Cr, Ni, and Zn consistent with input from greenstone, and analytes such as Al_2O_3 , Ba, and Rb indicative of either the variable preservation of feldspar or variable clay contents. As for regolith from the Frere Formation, there are no statistical differences in median values for these two populations over Archaean granitoid. Compared to the Frere Formation, regolith over granitoid has developed in areas of lower relief, yet this statistical analysis shows that physical rather than chemical weathering is the dominant process for production of granitoid colluvium. However, the results from the analysis of sandplain developed over Archaean granitoid indicate regolith formation by protracted chemical weathering.

Comparison of some depositional regime regolith units over Archaean granitoid

Sheetwash in drainage depressions, termed W_d on KINGSTON, is restricted to areas of Archaean granitoid rocks (Plate 2). In order to investigate the relationship of this material to other depositional regime regolith units in this area, the regolith samples collected from this regolith type ($n = 8$) have been statistically compared to sandplain over

Table 5. Summary statistics for sandplain (S) and undulating sandplain (Sl)

Detection level	S (n=134)				Sl (n=28)				
	Mean	σ	Median	Skewness	Mean	σ	Median	Skewness	
Percent									
SiO ₂	0.1	91.30	5.08	92.35	-3.20	83.35	13.80	88.90	-2.52
TiO ₂	0.01	0.23	0.08	0.21	2.01	0.37	0.26	0.29	2.81
Al ₂ O ₃	0.02	3.53	1.51	3.17	2.04	5.06	2.15	4.38	0.82
Fe ₂ O ₃	0.01	3.36	2.82	2.56	4.25	8.45	10.69	4.83	2.69
MnO	0.001	0.01	0.01	0.01	3.53	0.02	0.02	0.01	3.92
MgO	0.01	0.07	0.04	0.07	0.91	0.10	0.04	0.09	0.75
CaO	0.1	0.08	0.10	0.00	1.20	0.12	0.09	0.15	-0.38
Na ₂ O	0.002	0.02	0.02	0.01	4.50	0.02	0.02	0.01	2.90
K ₂ O	0.02	0.21	0.17	0.15	2.80	0.27	0.13	0.23	1.65
P ₂ O ₅	0.002	0.01	0.01	0.01	4.03	0.03	0.02	0.02	2.12
LOI	0.01	1.57	0.75	1.43	2.71	2.40	1.00	2.13	0.68
Parts per million^(a)									
Ag	0.1	—	—	—	×	—	—	—	×
As	0.1	2	2	2	3	6	7	3	2
Au (ppb)	1	—	1	—	×	—	1	—	×
Ba	0.1	52	66	31	3	82	77	67	3
Be	0.1	—	—	—	×	—	—	—	×
Bi	0.1	—	—	—	×	—	—	—	×
Cd	0.1	—	—	—	×	—	—	—	×
Ce	0.1	8	5	7	2	13	5	13	1
Co	0.1	2	1	2	2	3	2	3	2
Cr	2	80	52	65	2	247	339	111	3
Cu	1	6	3	5	2	14	13	9	2
Ga	0.1	5	3	5	2	10	9	7	2
In	0.1	—	—	—	×	—	—	—	×
La	0.1	4	2	4	2	7	3	7	1
Li	0.1	5	2	5	2	6	2	6	1
Mo	0.1	—	—	—	×	1	1	—	×
Nb	0.5	4	2	4	1	5	2	5	0
Ni	1	7	3	7	2	11	6	10	2
Pb	0.1	8	3	7	2	12	6	10	2
Pd (ppb)	1	—	—	—	×	—	—	—	×
Pt (ppb)	1	—	—	—	×	1	1	—	×
Rb	0.1	12	8	9	3	18	9	16	2
S (%)	0.01	—	—	—	×	—	—	—	×
Sb	0.1	—	—	—	×	1	1	—	×
Sc	2	2	2	2	2	6	6	4	2
Se	0.5	—	—	—	×	1	1	1	2
Sn	0.1	1	1	1	2	1	1	1	2
Sr	0.1	8	6	6	3	10	4	9	1
Ta	0.1	—	—	—	×	—	—	—	×
Te	0.1	—	—	—	×	—	—	—	×
Th	0.1	5	3	4	2	8	5	6	2
U	0.1	—	—	—	×	1	—	1	×
V	2	51	36	38	2	167	257	66	3
W	0.1	1	1	1	4	1	1	1	2
Y	0.1	3	1	2	2	4	2	4	1
Zn	1	13	9	11	6	19	9	17	1
Zr	1	115	77	101	6	135	47	135	1

NOTES: (a) unless otherwise shown
 n number of samples
 ppb parts per billion
 — less than detection level
 σ standard deviation
 × insufficient data for calculation of meaningful skewness

Table 6. Summary statistics for regolith over the Gerry Well and Mount Eureka greenstone belts

Detection level		Gerry Well (n=7)				Mount Eureka (n=22)			
		Mean	σ	Median	Skewness	Mean	σ	Median	Skewness
Percent									
SiO ₂	0.1	65.24	13.05	71.40	-1.20	64.31	13.46	65.30	-0.28
TiO ₂	0.01	0.72	0.28	0.58	1.20	0.70	0.27	0.65	0.64
Al ₂ O ₃	0.02	8.61	2.45	8.25	0.56	10.65	3.33	10.08	1.25
Fe ₂ O ₃	0.01	20.27	10.01	19.22	0.84	17.70	11.85	13.59	0.92
MnO	0.001	0.03	0.01	0.03	1.01	0.05	0.04	0.04	1.37
MgO	0.01	0.14	0.04	0.13	-0.09	0.30	0.32	0.16	1.76
CaO	0.1	0.10	0.10	0.10	x	0.11	0.10	0.10	0.03
Na ₂ O	0.002	0.03	0.03	0.03	2.21	0.14	0.21	0.05	2.78
K ₂ O	0.02	0.28	0.13	0.20	0.83	0.77	0.85	0.52	2.99
P ₂ O ₅	0.002	0.07	0.02	0.07	0.43	0.07	0.03	0.07	-0.21
LOI	0.01	4.30	1.22	4.54	-0.73	5.17	1.95	5.10	0.77
Parts per million^(a)									
Ag	0.1	—	—	—	x	—	—	—	x
As	0.1	28	15	22	0	12	7	10	0
Au (ppb)	1	1	1	1	0	1	1	1	0
Ba	0.1	86	93	54	2	221	270	147	3
Be	0.1	—	—	1	x	1	—	1	x
Bi	0.1	—	—	—	x	1	—	—	1
Cd	0.1	—	—	—	x	—	—	—	x
Ce	0.1	19	7	19	0	28	12	24	1
Co	0.1	7	3	7	1	11	7	8	1
Cr	2	676	366	507	1	559	404	573	1
Cu	1	45	15	51	-1	36	21	34	1
Ga	0.1	18	6	15	2	21	8	20	1
In	0.1	—	—	—	x	—	—	—	x
La	0.1	10	3	9	0	14	5	13	1
Li	0.1	7	2	7	0	11	6	9	2
Mo	0.1	1	—	1	1	1	1	2	0
Nb	0.5	6	2	6	-1	8	2	8	0
Ni	1	47	34	40	2	37	23	33	1
Pb	0.1	18	5	18	1	20	6	20	0
Pd (ppb)	1	1	1	1	1	1	1	1	1
Pt (ppb)	1	2	1	2	0	2	2	2	1
Rb	0.1	19	8	17	1	47	51	30	3
S (%)	0.01	—	—	—	x	—	—	—	x
Sb	0.1	3	3	3	1	1	1	1	1
Sc	2	17	8	13	1	17	8	16	0
Se	0.5	2	1	2	2	2	1	2	0
Sn	0.1	2	—	2	-1	2	2	2	3
Sr	0.1	11	4	10	1	31	27	25	3
Ta	0.1	—	—	—	x	1	1	1	4
Te	0.1	—	—	—	x	—	—	—	x
Th	0.1	11	6	10	1	12	4	11	1
U	0.1	1	1	1	0	2	1	2	1
V	2	399	268	308	1	368	287	276	1
W	0.1	1	1	1	1	2	1	2	1
Y	0.1	7	2	7	0	9	3	8	1
Zn	1	37	14	30	1	45	23	38	1
Zr	1	176	41	199	0	187	49	191	0

NOTES: (a) unless otherwise shown
 n number of samples
 ppb parts per billion
 — less than detection level
 σ standard deviation
 x insufficient data for calculation of meaningful skewness

Table 7. Summary statistics for exposed regime regolith and colluvium (X_{fc} and C_{fc}) over the Frere Formation

Detection level		X_{fc} (n=15)				C_{fc} (n=81)			
		Mean	σ	Median	Skewness	Mean	σ	Median	Skewness
Percent									
SiO ₂	0.1	65.77	14.57	68.50	-1.12	69.83	12.58	71.30	-0.31
TiO ₂	0.01	0.56	0.20	0.53	1.55	0.49	0.15	0.51	-0.37
Al ₂ O ₃	0.02	10.04	2.95	9.85	0.52	9.33	3.40	9.61	-0.31
Fe ₂ O ₃	0.01	16.20	9.93	14.62	1.52	14.38	8.70	11.02	1.07
MnO	0.001	0.10	0.12	0.05	1.80	0.07	0.11	0.03	5.83
MgO	0.01	0.33	0.43	0.17	2.98	0.22	0.17	0.19	1.92
CaO	0.1	0.26	0.52	0.10	3.52	0.10	0.10	0.10	0.40
Na ₂ O	0.002	0.09	0.13	0.04	2.89	0.08	0.15	0.04	4.52
K ₂ O	0.02	0.65	0.50	0.47	1.43	0.69	0.53	0.56	1.65
P ₂ O ₅	0.002	0.08	0.04	0.07	1.22	0.07	0.03	0.07	0.30
LOI	0.01	5.87	2.00	5.80	0.57	4.70	1.93	4.89	0.17
Parts per million^(a)									
Ag	0.1	—	—	—	×	—	—	—	×
As	0.1	15	13	11	2	12	8	10	1
Au (ppb)	1	1	1	—	×	—	1	—	×
Ba	0.1	289	276	168	1	285	502	178	7
Be	0.1	1	1	1	1	1	1	1	1
Bi	0.1	—	—	—	×	1	—	1	×
Cd	0.1	—	—	—	×	—	—	—	×
Ce	0.1	34	14	35	0	31	17	32	0
Co	0.1	10	11	6	3	7	4	6	1
Cr	2	209	101	176	1	247	139	222	1
Cu	1	28	24	20	2	18	10	19	0
Ga	0.1	18	8	16	1	16	7	15	0
In	0.1	—	—	—	×	—	—	—	×
La	0.1	15	6	14	0	16	8	16	1
Li	0.1	14	7	12	1	11	6	11	1
Mo	0.1	1	1	1	2	1	—	1	1
Nb	0.5	9	2	10	-1	9	3	9	0
Ni	1	23	17	19	3	19	8	18	1
Pb	0.1	25	6	23	1	23	9	23	0
Pd (ppb)	1	—	1	—	×	—	—	—	×
Pt (ppb)	1	1	1	1	×	1	1	—	×
Rb	0.1	43	28	36	1	46	30	41	1
S (%)	0.01	—	—	—	×	—	—	—	×
Sb	0.1	1	1	1	3	1	1	1	2
Sc	2	10	5	8	2	9	4	9	0
Se	0.5	2	2	2	2	2	1	1	1
Sn	0.1	2	1	2	1	2	1	2	1
Sr	0.1	23	20	18	3	25	20	18	2
Ta	0.1	1	—	1	×	1	—	1	×
Te	0.1	—	—	—	×	—	—	—	×
Th	0.1	16	7	15	1	16	8	15	1
U	0.1	2	1	2	0	2	1	2	0
V	2	180	104	167	1	159	85	136	1
W	0.1	2	1	1	2	2	1	2	2
Y	0.1	11	6	11	1	10	5	10	0
Zn	1	39	20	34	1	34	19	32	1
Zr	1	278	84	283	0	226	73	228	0

NOTES: (a) unless otherwise shown
 n number of samples
 ppb parts per billion
 — less than detection level
 σ standard deviation
 \times insufficient data for calculation of meaningful skewness

Table 8. Summary statistics for sheetwash (*W*) and colluvium (*Cfc*) over the Frere Formation

Detection level	Mean	σ	<i>W</i> (n=53)			<i>Cfc</i> (n=81)			
			Median	Skewness	Mean	σ	Median	Skewness	
Percent									
SiO ₂	0.1	73.17	11.22	71.80	0.12	69.83	12.58	71.30	-0.31
TiO ₂	0.01	0.48	0.17	0.49	-0.29	0.49	0.15	0.51	-0.37
Al ₂ O ₃	0.02	9.02	3.71	9.28	-0.10	9.33	3.40	9.61	-0.31
Fe ₂ O ₃	0.01	11.63	7.10	10.93	1.03	14.38	8.70	11.02	1.07
MnO	0.001	0.07	0.07	0.05	2.26	0.07	0.11	0.03	5.83
MgO	0.01	0.23	0.15	0.21	1.81	0.22	0.17	0.19	1.92
CaO	0.1	0.14	0.13	0.20	1.00	0.10	0.10	0.10	0.40
Na ₂ O	0.002	0.07	0.11	0.04	3.60	0.08	0.15	0.04	4.52
K ₂ O	0.02	0.65	0.36	0.58	0.88	0.69	0.53	0.56	1.65
P ₂ O ₅	0.002	0.06	0.02	0.06	0.37	0.07	0.03	0.07	0.30
LOI	0.01	4.42	1.85	4.54	-0.14	4.70	1.93	4.89	0.17
Parts per million^(a)									
Ag	0.1	—	—	—	×	—	—	—	×
As	0.1	10	7	9	1	12	8	10	1
Au (ppb)	1	1	1	—	×	—	1	—	×
Ba	0.1	416	598	205	4	285	502	178	7
Be	0.1	1	—	1	1	1	1	1	1
Bi	0.1	—	—	—	×	1	—	1	1
Cd	0.1	—	—	—	×	—	—	—	×
Ce	0.1	34	15	35	0	31	17	32	0
Co	0.1	7	4	6	1	7	4	6	1
Cr	2	236	136	226	1	247	139	222	1
Cu	1	18	9	19	0	18	10	19	0
Ga	0.1	16	8	16	0	16	7	15	0
In	0.1	—	—	—	×	—	—	—	×
La	0.1	17	7	17	0	16	8	16	1
Li	0.1	12	5	11	1	11	6	11	1
Mo	0.1	1	1	1	3	1	—	1	1
Nb	0.5	9	3	9	1	9	3	9	0
Ni	1	19	10	17	2	19	8	18	1
Pb	0.1	23	8	23	0	23	9	23	0
Pd (ppb)	1	—	—	—	×	—	—	—	×
Pt (ppb)	1	—	1	—	×	1	1	—	×
Rb	0.1	46	22	45	0	46	30	41	1
S (%)	0.01	—	—	—	×	—	—	—	×
Sb	0.1	1	—	1	1	1	1	1	2
Sc	2	9	4	9	0	9	4	9	0
Se	0.5	1	1	1	0	2	1	1	1
Sn	0.1	2	1	2	0	2	1	2	1
Sr	0.1	25	14	21	2	25	20	18	2
Ta	0.1	1	—	1	1	1	—	1	0
Te	0.1	—	—	—	×	—	—	—	×
Th	0.1	16	9	15	1	16	8	15	1
U	0.1	2	1	2	0	2	1	2	0
V	2	151	86	130	1	159	85	136	1
W	0.1	2	1	2	5	2	1	2	2
Y	0.1	11	4	10	0	10	5	10	0
Zn	1	35	14	35	1	34	19	32	1
Zr	1	217	68	214	0	226	73	228	0

NOTES: (a) unless otherwise shown
 n number of samples
 ppb parts per billion
 — less than detection level
 σ standard deviation
 \times insufficient data for calculation of meaningful skewness

Table 9. Summary statistics for exposed regime regolith and colluvium (X_{gp} and C_{gp}) over Archaean granitoid

Detection level		X_{gp} (n=15)				C_{gp} (n=35)			
		Mean	σ	Median	Skewness	Mean	σ	Median	Skewness
Percent									
SiO ₂	0.1	81.37	9.37	82.40	-0.99	82.46	7.58	83.20	-1.72
TiO ₂	0.01	0.38	0.13	0.38	0.26	0.38	0.14	0.36	1.22
Al ₂ O ₃	0.02	8.89	4.28	8.66	0.98	7.95	2.51	8.24	-0.15
Fe ₂ O ₃	0.01	4.43	4.85	3.31	3.66	5.08	4.71	3.90	3.48
MnO	0.001	0.02	0.01	0.01	1.47	0.02	0.02	0.01	2.11
MgO	0.01	0.13	0.06	0.14	0.01	0.12	0.05	0.12	0.42
CaO	0.1	0.14	0.09	0.20	-0.97	0.11	0.17	—	2.39
Na ₂ O	0.002	0.24	0.36	0.05	1.91	0.12	0.22	0.03	3.01
K ₂ O	0.02	0.82	0.81	0.71	2.54	0.62	0.47	0.42	1.32
P ₂ O ₅	0.002	0.03	0.02	0.03	1.02	0.03	0.02	0.03	1.68
LOI	0.01	3.89	2.06	3.82	1.27	3.44	1.24	3.41	0.22
Parts per million^(a)									
Ag	0.1	—	—	—	×	—	—	—	×
As	0.1	3	2	2	2	4	4	3	3
Au (ppb)	1	—	—	—	×	—	1	—	×
Ba	0.1	520	699	199	2	219	248	120	3
Be	0.1	1	—	1	2	—	—	—	×
Bi	0.1	—	1	—	4	—	—	—	×
Cd	0.1	—	—	—	×	—	—	—	×
Ce	0.1	27	22	24	2	19	9	17	1
Co	0.1	4	3	3	3	3	2	3	1
Cr	2	196	354	59	2	113	137	73	3
Cu	1	17	14	12	1	12	7	11	2
Ga	0.1	13	5	14	0	12	5	12	2
In	0.1	—	—	—	×	—	—	—	×
La	0.1	14	10	13	1	10	5	10	1
Li	0.1	7	3	7	0	7	2	8	0
Mo	0.1	1	1	1	2	1	—	1	3
Nb	0.5	8	7	7	2	6	2	6	1
Ni	1	15	14	10	2	13	5	12	1
Pb	0.1	15	9	14	2	14	9	12	3
Pd (ppb)	1	—	1	—	×	—	—	—	×
Pt (ppb)	1	—	1	—	×	—	1	—	×
Rb	0.1	43	40	32	2	30	17	27	1
S (%)	0.01	—	—	—	×	—	—	—	×
Sb	0.1	—	—	—	×	—	—	—	×
Sc	2	6	5	4	2	5	4	5	2
Se	0.5	1	1	1	0	1	1	1	2
Sn	0.1	2	1	1	3	2	1	2	1
Sr	0.1	61	137	22	4	24	22	16	2
Ta	0.1	1	—	1	2	—	—	—	×
Te	0.1	—	—	—	×	—	—	—	×
Th	0.1	10	10	7	3	7	4	6	3
U	0.1	2	1	1	2	1	1	1	3
V	2	88	89	64	3	93	99	67	3
W	0.1	1	1	1	2	1	—	1	1
Y	0.1	7	5	6	1	5	2	6	0
Zn	1	26	15	22	1	20	8	19	1
Zr	1	215	202	181	3	161	58	151	1

NOTES: (a) unless otherwise shown
 n number of samples
 ppb parts per billion
 — less than detection level
 σ standard deviation
 \times insufficient data for calculation of meaningful skewness

granitoid (S ; Table 10) and granitoid-sourced colluvium (Cgp ; Table 11). Compared to sandplain over granitoid, samples from the sheetwash unit in drainage depressions (W_d) have higher K_2O , Ba, Ce, La, Li, Rb, Sr, and Y. Higher K_2O , Ba, Rb, and Sr could indicate that the sheetwash unit has a higher feldspar content (i.e. is less weathered) than sandplain, whereas La and Y are consistent with a higher proportion of resistate phases. Site observations indicate a variety of materials, ranging from quartz-sand dominated regolith, through to thin sand cover over granitoid saprock, and areas with notable silcrete or ferruginous granules. Compared to granitoid-sourced colluvium (Cgp), the sheetwash unit (W_d) has statistically lower median values for TiO_2 , Al_2O_3 , K_2O , Ba, Ce, Ga, La, Pb, Th, Y, and Zr. The difference in some of these components, such as Al_2O_3 , K_2O , and Ba, between the regolith types could mean that the colluvium has a higher feldspar content and is thus less chemically weathered than the sheetwash unit. This is consistent with the production of colluvium from physical rather than chemical weathering, discussed in terms of the relationship between exposed regime regolith and colluvium derived from Archaean granitoid rocks (Xgp and Cgp) above.

Compared to sheetwash units in general on KINGSTON, the median values for sheetwash in drainage depressions over Archaean granitoid (W_d ; Table 12) have a 99% or greater probability of being lower for TiO_2 , Al_2O_3 , Fe_2O_3 , Na_2O , K_2O , P_2O_5 , LOI, As, Ba, Ce, Co, Cr, Ga, La, Li, Pb, Rb, Sr, Th, V, Y, Zn, and Zr than in sheetwash from elsewhere (W). The large number of analytes for which there are differences in median values suggests a local provenance for the sheetwash in drainage depressions (W_d), compared to sheetwash (W) in general. These differences are exaggerated by the likely dilution of sheetwash in drainage depressions by SiO_2 from nearby sandplain.

Speciality maps

Regolith pH and conductivity

Contoured maps of regolith pH and conductivity (mS/cm) are presented as Figures 52 and 53 respectively. Low pH values (typically less than 6) are largely in regolith over Archaean granitoid rocks, associated with areas of colluvium in the western part of the Frere Formation, along the Frere Formation towards Prenti Downs Homestead, and in the northeast part of the map sheet in areas of sandplain and sheetwash adjacent to Lake Carnegie. More alkaline regolith (i.e. pH > 7) is located over Lake Carnegie, and associated with lacustrine regolith in the southeast part of the Frere Formation and in drainage-related areas in the vicinity of Banjo Creek.

The majority of regolith samples on KINGSTON have conductivity values of less than 1 mS/cm (Fig. 53). Values ranging from 1 to the maximum value of 18.6 mS/cm in GSWA 167029 (MGA 445426E 7116088N) largely trace out the extent of Lake Carnegie, with especially high values in the north-central part of the map sheet. Other high values are in drainage in the western and southeastern parts of KINGSTON.

Element-index maps

Smith and Perdrix (1983) and Smith et al. (1989) showed how pathfinder elements and additive indices could be used to highlight areas of mineralization in arid terrains of the Yilgarn Craton. Although they concentrated on limited types of sample media (predominantly ferruginized duricrust or laterite), the use of additive indices has here been adapted and extended to include all media types sampled in the GSWA's regional regolith and geochemical mapping program. For example, Kojan et al. (1996a,b) show how a greenstone chalcophile index could be used to identify areas of known and potential gold mineralization on SIR SAMUEL (1:250 000). Indices are commonly additive (i.e. element a + element b + element c), but account must be taken of the relative concentration and concentration range of each element. This is accomplished by firstly log transforming the data, which reduces the effect of extremely high or low values. The transformed data are then standardized, which involves expressing each value as a standard normal deviate, thus allowing direct comparison of elements regardless of concentration (Rock, 1988). Standardized scores are then summed to create an additive index.

Chalcophile index

A contoured chalcophile-index plot (i.e. summed standard scores for As, Sb, Bi, Mo, Ag, Sn, W, and Se; Fig. 54) reveals low scores for areas of Archaean granitoid, lake sediments of Lake Carnegie, and lacustrine-, sandplain-, or sheetwash-dominated regolith over the Paterson Formation and underlying Frere Formation in the south-central and southeast part of KINGSTON. The index provides a marked contrast between the two Archaean greenstone belts and the intervening Archaean granitoid rocks. There are particularly high chalcophile-index scores over the upper part of the Frere Formation and lower Windidda Formation, in an east-southeasterly trending belt near the Wellington Ranges. This area coincides with closely spaced regional-scale faults and folds (also shown on Fig. 54), and is an area of relatively intense folding, brittle deformation, and related quartz veining, the development of part of which has been attributed to a competency contrast with overlying, less ferruginous rocks (Jones, J. A., 2000, pers. comm.).

Mineralization potential

The only recorded mineral production on KINGSTON is from gold workings in the Mount Eureka area, where structurally hosted gold mineralization is hosted by Archaean greenstones. Despite the kilometre-scale sample spacing and elongation of greenstone belts, regolith chemistry can be used to delineate the extent of greenstone belts on KINGSTON, because there is a strong lithological contrast between greenstones and adjacent Archaean granitoid rocks. Thus, further exploration for structurally hosted gold mineralization in these greenstone belts could be assisted by the use of regolith chemistry as a first-pass approach in determining the extent of greenstones.

Table 10. Summary statistics for sheetwash in drainage depressions (W_d) and sandplain (S) over Archaean granitoid

Detection level	Mean	σ	W_d (n=8)			S (n=63)		
			Median	Skewness	Mean	σ	Median	Skewness
Percent								
SiO ₂	0.1	87.90	5.77	89.70	-0.91	91.37	5.31	92.40
TiO ₂	0.01	0.23	0.09	0.21	1.20	0.20	0.08	0.19
Al ₂ O ₃	0.02	5.05	2.70	3.95	2.02	3.81	1.56	3.51
Fe ₂ O ₃	0.01	2.86	0.78	2.80	0.27	3.12	3.05	2.23
MnO	0.001	0.01	0.01	0.01	2.47	0.01	0.00	0.00
MgO	0.01	0.25	0.34	0.12	1.82	0.07	0.03	0.07
CaO	0.1	0.64	1.45	0.15	2.78	0.07	0.11	0.00
Na ₂ O	0.002	0.02	0.01	0.02	1.03	0.02	0.02	0.01
K ₂ O	0.02	0.30	0.16	0.24	2.23	0.20	0.16	0.15
P ₂ O ₅	0.002	0.02	0.01	0.02	1.09	0.01	0.01	0.01
LOI	0.01	2.98	2.22	2.07	1.21	1.66	0.78	1.49
Parts per million^(a)								
Ag	0.1	—	—	—	×	—	—	—
As	0.1	2	1	2	1	2	2	1
Au (ppb)	1	—	—	—	×	—	1	—
Ba	0.1	66	34	61	1	39	34	26
Be	0.1	—	—	—	×	—	—	—
Bi	0.1	—	—	—	×	—	—	—
Cd	0.1	—	—	—	×	—	—	—
Ce	0.1	11	5	10	1	7	3	6
Co	0.1	3	1	2	2	2	1	2
Cr	2	61	8	58	1	70	43	54
Cu	1	8	4	7	1	5	3	4
Ga	0.1	7	3	6	2	6	3	5
In	0.1	—	—	—	×	—	—	—
La	0.1	6	3	6	1	4	2	3
Li	0.1	7	4	6	2	5	2	4
Mo	0.1	—	—	1	×	—	—	—
Nb	0.5	4	2	4	0	3	1	3
Ni	1	10	6	9	2	8	3	7
Pb	0.1	7	3	7	1	7	3	6
Pd (ppb)	1	—	—	—	×	—	—	—
Pt (ppb)	1	—	—	—	×	—	—	—
Rb	0.1	18	11	16	2	11	7	9
S (%)	0.01	—	—	—	×	—	—	—
Sb	0.1	—	—	—	×	—	—	—
Sc	2	3	2	2	1	2	2	2
Se	0.5	—	—	—	×	—	—	—
Sn	0.1	1	1	1	1	1	1	1
Sr	0.1	19	13	15	1	8	4	6
Ta	0.1	—	—	—	×	—	—	—
Te	0.1	—	—	—	×	—	—	—
Th	0.1	4	1	4	0	4	2	4
U	0.1	1	—	1	×	—	—	—
V	2	44	13	43	0	48	34	36
W	0.1	1	1	1	2	1	—	1
Y	0.1	3	2	3	2	2	1	2
Zn	1	17	10	14	2	12	6	10
Zr	1	112	30	109	1	97	32	94

NOTES: (a) unless otherwise shown
 n number of samples
 ppb parts per billion
 — less than detection level
 σ standard deviation
 \times insufficient data for calculation of meaningful skewness

Table 11. Summary statistics for sheetwash in drainage depressions (W_d) and colluvium (Cgp) over Archaean granitoid

Detection level	Cgp (n=35)				W_d (n=8)				
	Mean	σ	Median	Skewness	Mean	σ	Median	Skewness	
Percent									
SiO ₂	0.1	82.46	7.58	83.20	-1.72	87.90	5.77	89.70	-0.91
TiO ₂	0.01	0.38	0.14	0.36	1.22	0.23	0.09	0.21	1.20
Al ₂ O ₃	0.02	7.95	2.51	8.24	-0.15	5.05	2.70	3.95	2.02
Fe ₂ O ₃	0.01	5.08	4.71	3.90	3.48	2.86	0.78	2.80	0.27
MnO	0.001	0.02	0.02	0.01	2.11	0.01	0.01	0.01	2.47
MgO	0.01	0.12	0.05	0.12	0.42	0.25	0.34	0.12	1.82
CaO	0.1	0.11	0.17	0.00	2.39	0.64	1.45	0.15	2.78
Na ₂ O	0.002	0.12	0.22	0.03	3.01	0.02	0.01	0.02	1.03
K ₂ O	0.02	0.62	0.47	0.42	1.32	0.30	0.16	0.24	2.23
P ₂ O ₅	0.002	0.03	0.02	0.03	1.68	0.02	0.01	0.02	1.09
LOI	0.01	3.44	1.24	3.41	0.22	2.98	2.22	2.07	1.21
Parts per million^(a)									
Ag	0.1	—	—	—	—	—	—	—	×
As	0.1	4	4	3	3	2	1	2	1
Au (ppb)	1	—	1	—	—	—	—	—	×
Ba	0.1	219	248	120	3	66	34	61	1
Be	0.1	—	—	—	—	—	—	—	×
Bi	0.1	—	—	—	—	—	—	—	×
Cd	0.1	—	—	—	—	—	—	—	×
Ce	0.1	19	9	17	1	11	5	10	1
Co	0.1	3	2	3	1	3	1	2	2
Cr	2	113	137	73	3	61	8	58	1
Cu	1	12	7	11	2	8	4	7	1
Ga	0.1	12	5	12	2	7	3	6	2
In	0.1	—	—	—	—	—	—	—	×
La	0.1	10	5	10	1	6	3	6	1
Li	0.1	7	2	8	0	7	4	6	2
Mo	0.1	1	—	1	3	—	—	1	0
Nb	0.5	6	2	6	1	4	2	4	0
Ni	1	13	5	12	1	10	6	9	2
Pb	0.1	14	9	12	3	7	3	7	1
Pd (ppb)	1	—	—	—	—	—	—	—	×
Pt (ppb)	1	—	1	—	—	—	—	—	×
Rb	0.1	30	17	27	1	18	11	16	2
S (%)	0.01	—	—	—	—	—	—	—	×
Sb	0.1	—	—	—	—	—	—	—	×
Sc	2	5	4	5	2	3	2	2	1
Se	0.5	1	1	1	2	—	—	—	×
Sn	0.1	2	1	2	1	1	1	1	1
Sr	0.1	24	22	16	2	19	13	15	1
Ta	0.1	—	—	—	—	—	—	—	×
Te	0.1	—	—	—	—	—	—	—	×
Th	0.1	7	4	6	3	4	1	4	0
U	0.1	1	1	1	3	1	—	1	1
V	2	93	99	67	3	44	13	43	0
W	0.1	1	—	1	1	1	1	1	2
Y	0.1	5	2	6	0	3	2	3	2
Zn	1	20	8	19	1	17	10	14	2
Zr	1	161	58	151	1	112	30	109	1

NOTES: (a) unless otherwise shown
 n number of samples
 ppb parts per billion
 — less than detection level
 σ standard deviation
 \times insufficient data for calculation of meaningful skewness

Table 12. Summary statistics for sheetwash in drainage depressions over Archaean granitoid (W_d) and sheetwash from elsewhere (W)

Detection level	Mean	σ	W_d (n=8)			W (n=114)			
			Median	Skewness	Mean	σ	Median	Skewness	
Percent									
SiO ₂	0.1	87.90	5.77	89.70	-0.91	71.56	12.18	70.85	0.03
TiO ₂	0.01	0.23	0.09	0.21	1.20	0.50	0.18	0.53	0.69
Al ₂ O ₃	0.02	5.05	2.70	3.95	2.02	9.26	3.69	10.03	-0.21
Fe ₂ O ₃	0.01	2.86	0.78	2.80	0.27	12.73	7.90	11.08	0.87
MnO	0.001	0.01	0.01	0.01	2.47	0.07	0.06	0.05	1.89
MgO	0.01	0.25	0.34	0.12	1.82	0.24	0.23	0.19	5.79
CaO	0.1	0.64	1.45	0.15	2.78	0.16	0.26	0.20	6.83
Na ₂ O	0.002	0.02	0.01	0.02	1.03	0.07	0.10	0.04	3.46
K ₂ O	0.02	0.30	0.16	0.24	2.23	0.67	0.38	0.59	1.41
P ₂ O ₅	0.002	0.02	0.01	0.02	1.09	0.06	0.03	0.06	0.49
LOI	0.01	2.98	2.22	2.07	1.21	4.60	1.86	4.95	-0.22
Parts per million^(a)									
Ag	0.1	-	-	-	x	-	-	-	x
As	0.1	2	1	2	1	12	8	10	1
Au (ppb)	1	-	-	-	x	-	1	-	x
Ba	0.1	66	34	61	1	488	677	237	3
Be	0.1	-	-	-	x	1	-	1	x
Bi	0.1	-	-	-	x	-	-	-	x
Cd	0.1	-	-	-	x	-	-	-	x
Ce	0.1	11	5	10	1	35	15	35	0
Co	0.1	3	1	2	2	8	5	7	3
Cr	2	61	8	58	1	283	240	223	3
Cu	1	8	4	7	1	21	20	19	7
Ga	0.1	7	3	6	2	17	8	17	0
In	0.1	-	-	-	x	-	-	-	x
La	0.1	6	3	6	1	17	7	17	0
Li	0.1	7	4	6	2	12	5	11	1
Mo	0.1	-	-	1	0	1	1	1	2
Nb	0.5	4	2	4	0	9	3	9	0
Ni	1	10	6	9	2	21	19	18	7
Pb	0.1	7	3	7	1	23	8	23	0
Pd (ppb)	1	-	-	-	x	-	1	-	x
Pt (ppb)	1	-	-	-	x	1	1	-	x
Rb	0.1	18	11	16	2	47	28	44	3
S (%)	0.01	-	-	-	x	-	-	-	x
Sb	0.1	-	-	-	x	1	1	1	1
Sc	2	3	2	2	1	10	6	10	3
Se	0.5	-	-	-	x	1	1	1	1
Sn	0.1	1	1	1	1	2	1	2	0
Sr	0.1	19	13	15	1	32	43	23	8
Ta	0.1	-	-	-	x	1	-	1	x
Te	0.1	-	-	-	x	-	-	-	x
Th	0.1	4	1	4	0	18	10	16	1
U	0.1	1	-	1	1	2	1	2	0
V	2	44	13	43	0	176	118	144	2
W	0.1	1	1	1	2	2	1	1	4
Y	0.1	3	2	3	2	11	4	10	0
Zn	1	17	10	14	2	37	18	34	2
Zr	1	112	30	109	1	226	66	228	0

NOTES: (a) unless otherwise shown
 n number of samples
 ppb parts per billion
 - less than detection level
 σ standard deviation
 x insufficient data for calculation of meaningful skewness

Although sample populations are small, there appears to be few compositional differences between the two greenstone belts on KINGSTON, in terms of such components as MgO, Cr, Ni, Sc, and V in regolith.

There is a strong coincidence of high and anomalously high concentrations of several analytes in regolith from the Wellington Range area with areas of regional- and local-scale deformation, covering parts of the Frere and Windidda Formations. A combination of several analytes in the form of a chalcophile index also highlights this area, and these results indicate that there is some potential for structurally hosted sulfide-related mineralization in this area. Local changes from brittle to ductile behaviour may control the extent of deformation (Jones, J. A., 2000, pers. comm.). The coincidence of regional-scale deformation and high concentrations of some elements in regolith over parts of the Frere Formation has also been reported from east of Blue Hill on NABBERU (Morris et al., 1997; Pirajno, F., 2000, pers. comm.).

There are several regolith samples with high concentrations of some analytes over parts of the Wongawol Formation (K_2O , Ce, La, Li, Rb, Ta, and Zn) and Kulele Limestone (TiO_2 , MgO, K_2O , Ce, Pb, Rb, Ta, and Zn) in the northern part of KINGSTON. On STANLEY, regolith over parts of the Wongawol Formation, which contains manganiferous sedimentary rocks in part, in the south of the map sheet also has high concentrations of some analytes (including MnO, Na_2O , K_2O , Ba, Be, Ce, Co, Cu, La, Li, Nb, Ni, Rb, Sn, Sr, Y, and Zn). The controls on this anomalous regolith chemistry on both KINGSTON and STANLEY are unknown, and there is a need for detailed mapping and structural analysis in the area, combined with bedrock chemistry, to determine the nature and extent of any mineralization.

Summary and conclusions

Regional-scale regolith and geochemical mapping on KINGSTON is based on the collection of 998 regolith samples collected at a nominal sample density of one sample per 16 km^2 , and observations made at each sample site. Each sample has been analysed for 48 major-element oxides and trace elements, acidity–alkalinity (pH), and conductivity. Analytical precision and accuracy were monitored using a series of laboratory and GSWA reference materials, and by analysis of replicates and blanks. Only a few analytes in several samples failed to meet prescribed analytical conditions, and the concentrations of these analytes were commonly close to detection level.

In order to understand the chemistry of regolith, a detailed knowledge of the distribution of various regolith types is essential, and a regolith-materials map has been compiled using remotely sensed data and site observations. KINGSTON comprises small amounts of residual (2%) and erosional regime regolith (13%), with the latter corresponding to the extent of bedrock exposure. The remaining 85% of the map sheet comprises depositional regime regolith, divided into colluvium (28%), floodplain, alluvial, and sheetwash material (23%), sandplain (18%), and regolith associated with lake systems (16%).

Regolith chemistry reflects the combined contribution of bedrock composition and weathering. Regolith over the two Archaean greenstone belts on KINGSTON provides a good example of bedrock control on regolith chemistry, especially as greenstones are separated by Archaean granitoid, which has undergone intense weathering in situ leading to the depletion of most components, apart from SiO_2 . The chemistry of the two greenstone belts, which are presumed to be largely composed of mafic volcanic rocks, is similar in terms of MgO, Cr, Ni, Sc, and V, and contrasts markedly with adjacent granitoids. Areas of Proterozoic dolerite are also highlighted by a unique chemistry, even for elements such as In and Se, which are at levels close to detection limits.

Parts of the Frere Formation are characterized by a distinctive regolith chemistry, but the chemical signature of the eastern part of this formation has been modified where it is overlain in some areas by the Permian Paterson Formation (which is characterized by a SiO_2 -rich, sand-dominated regolith). Thus, understanding spatial variations in regolith chemistry relies on understanding the distribution of both bedrock and regolith.

Statistical tests show that the chemistry of bedrock or subcrop (i.e. exposed regime regolith) and downslope regolith (colluvium and in some cases sheetwash) over the Frere Formation and Archaean granitoid is largely controlled by physical rather than chemical weathering. For these rock types, transported regolith can retain the chemical signature of the parent material, although sandplain developed over Archaean granitoid is depleted in most components apart from SiO_2 relative to other regolith types, indicative of protracted chemical weathering in situ. This chemical weathering has been sufficiently intense that the chemistry of this material resembles that of eolian sand deposits from the Little Sandy Desert region of NABBERU (Morris et al., 1997). The contribution of bedrock to sandplain chemistry is shown in a statistical comparison of sandplain derived from granitoid rocks with regolith over the Paterson Formation. The diverse chemistry of the latter attests to derivation from various lithologies, typical of glaciogene deposits of the Paterson Formation. Similarly, the sandy loam material typical of sandplain with clay-rich material (*SL*) is compositionally more diverse than sandplain with net-like dunes (*S*), which is consistent with more input from various lithologies and sheetwash for the former, and eolian reworking of the latter.

In two particular cases, high concentrations of analytes in regolith do not correspond with either bedrock or regolith. In the Wellington Range area, there are high concentrations of MnO, MgO, Ba, Ce, Co, Cr, Ga, Li, Pb, Rb, Sb, U, and W over parts of the Frere and Windidda Formations. In the same area there are folds and faults indicative of both regional- and local-scale deformation. Parts of the Wongawol Formation and Kulele Limestone in the north of KINGSTON have regolith with high concentrations of several analytes (including K_2O , Ce, La, Li, Rb, and Ta). In this area, there appears to be little structural control on mineralization, and further work is warranted, especially as a contiguous area of STANLEY also shows anomalous in regolith chemistry. One possibility

is that parts of the Wongawol Formation host syngenetic stratiform mineralization.

Samples of lake sediment are saline, gypsiferous, and carbonate-rich, retaining virtually no bedrock signature. As these sediments commonly form only a veneer over bedrock, it may be possible to employ shallow-drilling techniques to recover more meaningful samples. Sampling in sand-dominated terrains requires precursory mapping of the regolith to understand the influence of eolian (i.e. potentially far-field) processes, the degree of local reworking, and the amount of locally sourced material. Sanders and McGuinness (2000) shows the validity of a detailed regolith mapping approach on AJANA in understanding regolith chemistry, and application of this approach has been useful in understanding chemistry on KINGSTON in terms of examining the two sandplain types.

In summary:

- Areas of potential mineralization on KINGSTON include: the Wellington Range area (chalcophile element anomalism is coincident with regional- and local-scale deformation); parts of the Wongawol Formation and Kulele Limestone; greenstones of the Mount Eureka and Gerry Well greenstone belts.

- Statistical analysis of regolith chemical data has shown that there is a relatively simple relationship between regolith chemistry and bedrock over parts of the Earaheedy Group, with downslope regolith-forming processes dominated by physical rather than chemical weathering. In other cases, the bedrock signature is overprinted or obliterated by weathering or input from other lithological units, such as the Paterson Formation.

- Sandplain units divided on geomorphological grounds have chemical characteristics indicative of various amounts of lithological input (more than one lithology), sheetwash contribution, and eolian reworking. Division of such sand-dominated regolith (which occupies 16% of KINGSTON) is an important step in determining how this material should be treated as a sampling medium in regional mineral exploration programs. Regolith associated with lake systems (16% of total regolith) also retains little information on the parent lithology, but because this is commonly developed as a thin veneer over bedrock, sampling using shallow drilling may be an effective exploration technique.

References

- ADAMIDES, N. G., and PIRAJNO, F., in prep., Manganese and base metal potential of the Earaheedy Basin, with comments on the significance of glauconite: Western Australia Geological Survey, Annual Review 1999–2000.
- BAGAS, L., GREY, K., HOCKING, R. M., and WILLIAMS, I. R., 1999, Neoproterozoic successions of the northwestern Officer Basin: a reappraisal: Geological Survey of Western Australia Annual Review 1998–9, p. 39–44.
- BEARD, J. S., 1974, The vegetation of the Great Victoria Desert, Explanatory notes to sheet 3: 1:1000000 Vegetation Series, Perth, Western Australia, University of Western Australia Press, 50p.
- BUNTING, J. A., 1980, Kingston, W.A.: Western Australia Geological Survey, 1:250 000 Geological Series Explanatory Notes, 16p.
- BUNTING, J. A., 1986, Geology of the eastern part of the Nabberu Basin, Western Australia: Western Australia Geological Survey, Bulletin 131, 130p.
- BUNTING, J. A., and CHIN, R. J., 1979, Duketon, W.A.: Western Australia Geological Survey, 1:250 000 Geological Series Explanatory Notes, 24p.
- COMPSTON, W., 1974, The Table Hill Volcanics of the Officer Basin – Precambrian or Palaeozoic?: Journal of the Geological Society of Australia, v. 21, p. 403–411.
- GEE, R. D., 1990, Nabberu Basin, in *Geology and Mineral Resources of Western Australia*: Western Australian Geological Survey, Memoir, 3, p. 202–210.
- GREY, K., 1995, Stromatolites from the Palaeoproterozoic Earaheedy Group, Earaheedy Basin, Western Australia: *Alcheringa*, v. 18, p. 187–218.
- HALL, W. D. M., and GOODE, A. D. T., 1975, The Nabberu Basin, a newly discovered Lower Proterozoic basin in Western Australia: 1st Australian Geological Convention, Adelaide, 1975, Abstracts, p. 88–89.
- HALL, W. D. M., GOODE, A. D. T., BUNTING, J. A., and COMMANDER, D. P., 1977, Stratigraphic terminology of the Earaheedy Group, Nabberu Basin: Western Australia Geological Survey, Annual Report 1976, p. 40–43.
- HOCKING, R. M., and JONES, J. A., 1998, Methwin, W.A. Sheet 3047: Western Australia Geological Survey, 1:100 000 Geological Series.
- HORWITZ, R. C., 1975, Provisional geological map at 1:2 500 000 of the north-east margin of the Yilgarn block, Western Australia: CSIRO, Minerals Research Laboratories, Division of Mineralogy.
- JACKSON, J. A., (editor), 1997, *Glossary of Geology* (4th edition): Alexandria, Virginia, American Geological Institute, 769p.
- JONES, J. A., PIRAJNO, F., and HOCKING, R. M., 2000, Stratigraphy, tectonic evolution, and mineral potential of the Earaheedy Basin, in GSWA 2000 extended abstracts: geological data for WA explorers in the new millennium: Western Australian Geological Survey, Record 2000/8, p. 11–13.
- KOCH, G. S., and LINK R. F., 1970, *Statistical analysis of geological data*: New York, John Wiley and Sons Incorporated, 375p.
- KOJAN, C. J., BRADLEY, J. J., FAULKNER, J. A., and SANDERS, A. J., 1996a, Targeting mineralization using a chalcophile index — results of regional and project scale regolith geochemistry in the northern Eastern Goldfields: Western Australian Geological Survey, Annual Review 1995–96, p. 124–134.
- KOJAN, C. J., FAULKNER, J. A., and SANDERS, A. J., 1996b, Geochanical mapping of the Sir Samuel 1:250 000 sheet: Western Australian Geological Survey, 1:250 000 Regolith Geochemistry Series Explanatory Notes, 69p.
- MORRIS, P. A., COKER, J., and FAULKNER, J. A., 1998, Geochemical mapping of the Mount Egerton 1:250 000 sheet: Western Australia Geological Survey, 1:250 000 Regolith Geochemical Series Explanatory Notes, 63p.
- MORRIS, P. A., SANDERS, A. J., and FAULKNER, J. A., 1997, Geochemical mapping of the Nabberu 1:250 000 sheet: Western Australia Geological Survey, 1:250 000 Regolith Geochemical Series Explanatory Notes, 63p.
- MORRIS, P. A., SANDERS, A. J., McGUINNESS, S. A., and COKER, J., 2000a, Geochemical mapping of the Stanley 1:250 000 sheet: Western Australia Geological Survey, 1:250 000 Regolith Geochemical Series Explanatory Notes, 51p.
- MORRIS, P. A., SANDERS, A. J., McGUINNESS, S. A., COKER, J., and KING, J. D., 2000b, Geochemical mapping of the Fraser Range region: Western Australia Geological Survey, 1:250 000 Regolith Geochemical Series Explanatory Notes, 45p.
- MYERS, J. S., and HOCKING, R. M., 1998, Geological map of Western Australia 1: 2 500 000 (13th edition): Western Australian Geological Survey.
- NELSON, D. R., 1997, Compilation of SHRIMP U–Pb zircon geochronology data, 1996: Western Australian Geological Survey Record 1997/2, 189p.
- NELSON, D. R., 1998, Compilation of SHRIMP U–Pb zircon geochronology data, 1997: Western Australian Geological Survey Record 1998/2, 242p.
- OLLIER, C., and PAIN, C., 1996, *Regolith, Soils and Landforms*: New York, John Wiley and Sons, 308p.
- PELL, S. D., CHIVAS, A. R., and WILLIAMS, I. S., 1999, Great Victoria Desert: development and sand provenance: Australian Journal of Earth Sciences, v. 46, p. 289–299.
- PIRAJNO, F., 1998, Nabberu, W.A. Sheet 3048: Western Australia Geological Survey, 1:100 000 Geological Series.
- PREISS, W. V., JACKSON, M. J., PAGE, R. W., and COMPSTON, W., 1975, Regional geology, stromatolite biostratigraphy and isotopic data bearing on the age of a Precambrian sequence near Lake Carnegie, Western Australia: 1st Australian Geological Convention, Adelaide, 1975, Abstracts, p. 92–93.

- ROCK, N. M. S., 1988, Numerical geology: Berlin, Springer-Verlag, 427p.
- SANDERS, A. J., and McGUINNESS, S. A., 2000, Geochemical mapping of the Ajana 1:250 000 sheet: Western Australia Geological Survey, 1:250 000 Regolith Geochemical Series Explanatory Notes, 55p.
- SMITH, R. E., BIRRELL, R. D., and BRIGDEN, J. F., 1989, The implications to exploration of chalcophile corridors in the Archaean Yilgarn Block, Western Australia, as revealed by laterite geochemistry: *Journal of Geochemical Exploration*, v. 18, p. 169–184.
- SMITH, R. E., and PERDRIX, J. L., 1983, Pisolitic laterite geochemistry in the Golden Grove massive sulfide district, Western Australia: *Journal of Geochemical Exploration*, v. 18, p. 131–164.
- STACE, H. C. T., HUBBLE, G. D., BREWER, R., NORTHCOTE, K. H., SLEEMAN, J. R., MULCAHY, M. J., and HALLSWORTH, E. G., 1968, A handbook of Australian soils: South Australia, Rellim Technical Publications, 435p.
- SUBRAMANYA, A. G., FAULKNER, J. A., and SANDERS, A. J., 1995, Geochemical mapping of the Peak Hill 1:250 000 sheet: Western Australia Geological Survey, 1:250000 Regolith Geochemistry Series Explanatory Notes, 59p.
- SWAN, A. R. H., and SANDILANDS, M., 1995, Introduction to geological data analysis: Oxford, Blackwell Science, 446p.

Appendix 1

Gazetteer of localities

<i>Locality</i>	<i>MGA coordinates</i>		<i>Locality</i>	<i>MGA coordinates</i>	
	<i>Easting</i>	<i>Northing</i>		<i>Easting</i>	<i>Northing</i>
Alf Bore	396850	7073587	Milga Milga Well	406209	7094018
Banjo Well	378900	7071339	Milgarrie Pool	476167	7082653
Barral Pool	458534	7079143	Mils Corner	411023	7094561
Beacon Hill	458636	7031438	Miningarra Pool	430703	7085770
Benstead Lagoon	404468	7114904	Mount Alexandra	411175	7094030
Beru Pool	364010	7076595	Mount Courtney	493354	7079411
Bilgarrie Cutarrie Pool	478080	7044402	Mount Draper	489149	7089078
Bingah Pool	400381	7110265	Mount Eureka	353908	7060334
Boondin	478995	7073074	Mount Throssell Well	467572	7121091
Bummer Pool	404882	7117074	Mount Wellesley	368590	7095187
Burel Pool	430998	7089954	No 10 Well	403738	7084737
Charlie Bore	469542	7086045	Old Windidda Homestead (abd)	406438	7054369
Chiall Spring	385748	7112043	Paddy Well	367125	7074749
Chowidda Pool	406832	7082360	Panton Bluff	472952	7053414
Christmas Bore	428021	7081869	Prenti Downs Homestead	480773	7066987
Coolali Soak	474600	7044200	Quartz Well	410273	7084292
Cork Tree Well	436312	7080950	Red Bluff	352464	7080537
Cottonbush Bore	440526	7080708	Rock and Roll Bore	477500	7044800
Curdle Well	361421	7102926	Sachse Bluff	460751	7054918
Dempsey Bore	442948	7073506	Shed Bore	422837	7081812
Double Hill	478209	7089744	Sholl Bore	397845	7123867
Double Hill	478089	7089951	Skull	367655	7119848
Federation Headland	412003	7093643	Sodary Pool	427800	7070400
Finger Flat Well	435085	7069229	Tambree Well	402133	7116193
Gap Well	408037	7074964	The Jump-up	479991	7056010
Jackie Lookout	419105	7085420	Tooloo Bluff	422568	7075325
Jackie Well	413755	7087338	Top Fourteen Mile Well	445732	7087041
Jamieson Well	470617	7063836	Twin Swamps Bore	461277	7066217
Joey Jarra Pool	465334	7049227	Wadjinyanda Pool	374549	7119430
Jones Bore	432000	7072200	Waggon Flat	450543	7087910
Jump Up Bore	479527	7052080	Waguin	408839	7061182
Kalyaltcha Waterhole	463651	7087641	Warren Bore	468000	7032200
Kepallin Spring	394000	7096200	Warriarra Pool	408041	7114552
Kundabiddi	474092	7080309	Windidda	421582	7081244
Kundabiddi Bore	477360	7080707	Wongawol	394133	7109894
Little Banjo Bore	381000	7083200	Yelma Soak	360129	7071074
Lorna Glen	356013	7098634	Yelma Homestead (abd)	369738	7064960
Lynne Bore	455042	7084547	Yilgarrie Hills	454730	7049842
Marianindie Pool	405637	7115379			

NOTE: (abd) abandoned

Appendix 2

Gold production from mines and prospects on KINGSTON prior to December 1998

<i>Mining centre</i>	<i>Years</i>	<i>Mine/prospect</i>	<i>Tenements</i>	<i>MGA coordinates</i>		<i>Production</i>	
				<i>Easting</i>	<i>Northing</i>	<i>Ore</i> (t)	<i>Metal</i> (kg)
Mount Eureka	1932	Little Greta	GML 53/450	355136	7061532	16.0	0.15
	1932–1933	Mount Eureka	GML 53/448	353940	7060556	59.0	1.61
	1936–1937	Wongawol	GML 53/621	(a)354531	7060618	70.0	1.24
	1936	Sundries	nd			796.0	17.06
Total						941.0	20.06

SOURCE: Department of Minerals and Energy (DME), unpublished records
 Location information from DME's electronic tenement-graphics system (TENGRAPH) unless otherwise stated

NOTES: Sundries include Prospecting Areas with production limited to 50 t of ore per year for no more than two years
 (a) Location of GML from public plan SP 91
 nd not determined

Appendix 3

Open-file surface geochemistry for KINGSTON as at April 1999

	<i>Key</i>
ID no.:	Project reference number allocated for these notes (see Plate 3)
M no.:	GSWA project reference number
	An asterisk beside the M number indicates that not all the samples for the listed activities fall within KINGSTON; that is, the total number of samples includes some taken on adjacent sheets
I no.:	The Item number, or the Department of Minerals and Energy's (DME's) library reference number for a group of related open-file reports on microfiche. This number replaces the M number for project identification
A no.:	GSWA report reference number
Year:	The year that the report was written
Activity type:	The geochemical exploration activity (drilling details are only included if analytical samples are taken within 0–4 m depth): NGRD: Includes rock-chip, lag, costean (up to 4 m depth), and grab samples RAB: Rotary air blast drilling RC: Reverse circulation drilling SOIL: Surface or shallow soil samples SSED: Stream sediment
No.:	The number of analytical samples
Method:	The analytical method used to determine the elements listed: AAS: Atomic absorption spectroscopy BCL: Bulk cyanide leach ETA: Electron thermal atomization FA: Fire assay ICP: Inductively coupled plasma MS: Mass spectrometry XRF: X-ray fluorescence
Activity elements:	The elements for which analyses were carried out
Analyst:	AAL: Australian Assay Laboratories ALS: Australian Laboratory Services CRAE: CRA Exploration Pty Ltd SGS: SGS Australia Pty Ltd
DD:	A 'Y' in this column indicates deep drilling has taken place in the activity area
Comment:	Various sample details such as the sieve size fraction, sample density, and so on, depending on the information provided in the report

NOTES: For public use all open-file company reports are provided on microfiche in the DME library at Mineral House. To locate a particular report on microfiche, the relevant Item number and A number are required

Appendix 3. Open-file surface geochemistry

ID No.	M No.	Item No.	A No.(s)	Year	Activity type	No.	Method	Activity elements
1	3393/2	3640	25258, 28191	1988	SOIL	153	ICP-MS	Au
2	3393/3	4031	21075 28190	1987 1988	RAB NGRD SOIL RC	336 7 214 16	FA " " " "	Au Ag,Au,Cu,Pb,Zn Au Au
3	3393/4	6255	17074	1985	NGRD	312	AAS	Au
4	4976	3330	22216	1987	SSED/SOIL	200		
5	5030/3	4248	31604	1990	SSED	169		
6	6163/1	6873	27114, 36946	1989	SOIL SOIL " " NGRD RAB	2131 140 XRF AAS 46 72	BCL/AAS BCL/AAS As Cu,Pb,Zn AAS Au,Cu,Ni,Pb,Zn AAS	Au Au As Cu,Pb,Zn Au,Cu,Ni,Pb,Zn Au,As
7	6163/2	3879	27116	1989	SSED " SOIL NGRD " RAB	75 49 3 5	BCL/AAS AAS BCL AAS AAS	Au Ag,Cu Ag,Au,Cu Au As, Cu,Ni,Pb,Zn Au
8	6353	4624	28680	1989	SSED SOIL	320 1362		
9	6688	5148	30989	1990	NGRD "	87	FA XRF	Au As,Cu,Ni,Pb,Sb,Zn
10	7533	6135	36395	1992	SOIL SSED	2250 160		
11	7889/1	9316	41124	1994	NGRD "	107	FA AAS	Au Co,Cu,Mo,Ni,Pb,Zn

survey for KINGSTON as at April 1999

Analyst	DD Description
Analytical Services	Au detection limit of 1 ppb, -20 mesh fraction, sample weight of 500 g
AAL	Y Au detection limit of 0.01 ppm, -80 micron fraction, sample weight of 50 g Au detection limit of 0.01 ppm
AAL "	Y Au detection limit of 2 ppb, -20 + 40 mesh fraction Au detection limit of 0.01 ppm, sample weight of 2-3 kg
SGS	Au detection limit of 0.01 ppm, sample weight of 50 g
	Stream and loam samples concentrated and inspected for heavy minerals, sample weight of 20 kg, -4 mm fraction
	Y Samples inspected for kimberlite indicator minerals, selected mineral grains analysed
ALS	Y Au detection limit of 50 ppt, sample weight of 2 kg, sampled over a 100 x 500 m grid Sieve -80 mesh
"	
"	
Rapley Wilkinson Laboratories Classic Comlabs Ltd	Au detection limit of 0.01 ppm Au detection limit of 0.02 ppm
Perth Metallurgical Laboratories	Y Au detection limit of 0.01 ppb, sieve -30 mesh, sample weight of 5 kg
"	
Rapley Wilkinson Laboratories	Sample weight of 2 kg Au detection limit of 0.01 ppm
"	Au detection limit of 0.02 ppm
	Samples inspected for ilmenite, spinel and garnet
"	
AAL SGS	Ironstone lag, Au detection limit of 1.0 ppb, sample weight of 1 kg
	Y Samples inspected for ilmenite, spinel and garnet
"	
Analabs	Y Lag
"	

ID No.	M No.	Item No.	A No.(s)	Year	Medium	No.	Method	Activity elements
12	8046	9733	53109	1997	SOIL	139	BCL/ETA	Ag,Au
				"			BCL/AAS	Cu
				"			ETA	Au
				"			AAS	As,Bi,Co,Cr,Cu,Ni,Pb,Zn
				"			FA	Au
				RAB		68	AAS	As,Co,Cr,Cu,Ni,Pb,Zn
				"			FA	Au
				"			AAS	As,Co,Cr,Zn
13	8630	7507	40845	1994	SOIL	34	FA/ICP-MS	Au,Pd,Pt
				"			AAS	Ag,Cr,Cu,Fe,Mn,Ni,Pb,Zn
				"			ICP-MS	Bi,Co,Mo,Sb,Th,U,V,W,Nb,Ti,Zr,Ba,Ce
				SOIL		26	XRF	As,Sn
14	9251	7802	43339	1994	SOIL	37		
				SSED		70	BCL	Au
				NGRD		21	FA	Au
15	10115/1	8910	47789	1996	SSED	34	ICP-MS	Ag,As,Au,Co,Cu,Mn,Ni,Pb,Zn,Ba
				SOIL		43	ICP-MS	Ag,As,Au,Co,Cu,Mn,Ni,Pb,Zn,Ba
				NGRD		67	ICP-MS	Ag,As,Au,Bi,Co,Cu,Fe,Mn,Mo,Ni,Pb,Sb,V,W,Zn,Ba,Cd,K,Mg,Na,P,S,Sr
16	10115/2	9138	49644	1996	NGRD	30	ICP	Ag,As,Au,Bi,Co,Cu,Fe,Mo,Ni,Pb,Sb,V,W,Zn,Ba,Cd,K,Mg,Na,P,S,Sr
				SOIL		21	ICP	Ag,As,Au,Co,Cu,Mn,Pb,Zn,Ba
17	10165	8692	48033	1996	SOIL	141	FA	Au,Pd
				"			ICP	Ag,As,Bi,Co,Cr,Cu,Mo,Ni,Pb,Sb,V,W,Zn,Ba,Cd,Zr
18	10167	8694	48035	1996	SOIL	67	FA	Au,Pd
				"			ICP	As,Bi,Co,Cr,Cu,Mo,Ni,Pb,Sb,V,W,Zn,Ba,Cd,Zr

(continued)

Analyst	DD	Comment on samples
Genalysis	Y	Au detection limit: 0.1 ppb, sieve fractions of -2 mm, -0.5 mm, -80 mesh
"		
"		Au detection limit of 1 ppb
"		
Minlabs		Au detection limit of 1 ppb
"		
"		Au detection limit of 1 ppb
"		
Analabs	Y	Sieve -20 mesh
"		
"		
"		
CRAE		Samples inspected for kimberlite indicator minerals, selected grains submitted for scanning-electron microscopy (SEM) analysis
Genalysis		Samples panned for gold on site, sample weight of 20 kg
"		Au detection limit of 1 ppb, sample weight of 1 kg, -2 mm fraction
"		Au detection limit of: 0.01 ppm
ALS	Y	Assay results submitted to DME in digital form
"		"
"		"
ALS	Y	Samples are composites of 4 samples taken at 50 m intervals
ALS		Au detection limit of 0.001 ppm, sieve -80 mesh, depth of sample 20 cm, sample weight of 100 g
"		
ALS		Au detection limit of 0.001 ppm, sieve -80 mesh, sample weight of 100 g, depth of sample 20 cm
"		

Appendix 4

Summary of sampling procedure, regolith classification, and analytical procedures

Regolith sampling

The aim of the Geological Survey of Western Australia's (GSWA's) regolith sampling program is to sample regolith from sites representative of the 4×4 km sampling polygon of interest. The preferred sampling medium is active stream sediment, sampled from lower order streams draining the sample polygon. In areas where drainage is absent or only weakly developed, sheetwash (colluvium), soil, sand, or lake sediment is sampled. Sampling sites are chosen using Landsat Thematic Mapper (TM) imagery and topographic maps, combined with a 4×4 km grid overlay. The site locations are digitized and assigned a unique site name made up of part of the relevant 1:100 000 map sheet name and a number. For example, GRA95 would correspond to site 95 on the GRANITE PEAK* 1:100 000 sheet (on the NABBERU 1:250 000 sheet).

The actual sampling site in the field is determined by the geologist, who can move the site from the designated position in order to facilitate access, or avoid areas of human or animal activity, or areas of standing water.

Stream sediments

Stream sediments in single, well-defined channels are sampled by trenching perpendicular to the flow direction. Narrow streams are sampled from pits excavated along their length, whereas braided stream systems are sampled from pits in several individual channels.

Sheetwash (colluvium) or soil

Sample sites are selected towards the centre of the 4×4 km polygon. Where a clear slope direction can be identified, regolith is composited from three pits excavated 30 m apart, perpendicular to the slope direction. Where no clear slope direction can be identified, regolith is sampled from three pits forming the apices of an equilateral triangle, whose sides are 30 m long.

Lake sediments

Lake sites are chosen to maximize ease of access. They are sampled as for sheetwash with no discernible slope.

Sandplain

In areas of active sand dunes, sandplain samples are taken from three pits along the swale. In sandplain areas lacking active dunes, sampling is carried out as for sheetwash sites.

Prior to excavating pits or trenches, the top 5–10 cm of material is removed to minimize any surface-related contamination. Pits and trenches are excavated to a depth of 30 cm. If the excavated material is sufficiently dry, it is sieved at the site to -6 mm through a plastic sieve into a graduated sieve pan, then thoroughly mixed using a small shovel. Regolith, either sieved or unsieved, is divided into an archive sample (weighing about 3 kg) and an analytical sample (weighing about 2 kg) using graduated rings in the sieve pan. Information such as the unique GSWA sample number, site number, a map sheet identifier, and the relevant geologist's initials are recorded on each bag. A soft aluminium tag, on which the GSWA number is written, is included with the analytical sample. Analytical and archive samples are distinguished by the use of different-coloured nylon bag ties.

Sample-recording form

An example of the sample-recording form is shown in Figure 4.1. At each sampling site, the sample's MGA coordinates (GDA94 grid, read from a hand-held GPS), the sample-site number, GSWA number, sampling date, sampler's initials, and nature of sample (e.g. stream, sheetwash, channel, or pit) are recorded. The cross section is used to record the position of the sample in an idealized landform profile. The composition of the regolith is recorded in terms of iron-rich, lithic, and non-lithic components, using a series of letters signifying abundance (i.e. Abundant: > 30%; Common: 5–30%; Rare: 1–5%; Trace: < 1%). Within each category, the relative abundance of each component is recorded using a numerical system from 1 (most abundant) to > 1 (least abundant), or the A, C, R, T designations. Fresh bedrock-fragment types (if present) are recorded in the same way. Fields also exist for recording the nature of the surrounding regolith, any grain coatings, nature of fine-grained material, nature and distribution of bedrock and secondary units, and characteristics of the stream site (if appropriate). A free-form section (Remarks) allows for specific entries pertinent to the site that are not covered in the preceding sections.

Regolith-materials classification

Three regolith-materials classification schemes have been used during the course of the GSWA regional regolith and geochemical mapping program. All three are based on the regolith–landform RED scheme of Anand et al. (1993) and

* Capitalized names refer to standard 1:100 000 and 1:250 000 map sheets.

Sheet SG51-10 Zone 51	Loc/n No _____	GSPA No _____	Date _____				
Site Ref _____	E	N	Sampler _____				
Photo Y/N (Describe)							
Gravity G1 G2 Channel <input type="checkbox"/> Pit/Hole <input type="checkbox"/> Single point <input type="checkbox"/> Multipoint <input type="checkbox"/> Shtwsh Creek Soil Lake Sand							
Site Description:							
CLASTS	Gravel (2-5 mm) <input type="checkbox"/> cobbles (64-256 mm) <input type="checkbox"/>	Stones (5-64 mm) <input type="checkbox"/> Boulders (>256 mm) <input type="checkbox"/>	Surrounding Regolith Code: Left _____ Right _____				
Abundant : >30%	Common : 5-30%	Rare : 1-5%	Trace : <1%				
Iron-rich	Abnt/Comm/Rare/Tr <input type="checkbox"/>	Lithic	Abnt/Comm/Rare/Tr <input type="checkbox"/>				
<input type="checkbox"/> Pisoliths	<input type="checkbox"/> Saprolite fragments						
<input type="checkbox"/> Nodules	<input type="checkbox"/> Ferrig/ granules	<input type="checkbox"/> Ferruginous Saprolite fragments					
<input type="checkbox"/> Ferrug. duricrust	<input type="checkbox"/> Saprocks						
<input type="checkbox"/> Gossan fragments	<input type="checkbox"/> Fresh b'rock fragments (below)						
<input type="checkbox"/> Ferrug. Lithic fragments	<input type="checkbox"/> Vein quartz	<input type="checkbox"/> Other silica					
Non-lith Abnt/Comm/Rare/Tr <input type="checkbox"/>	Clast lithology						
<input type="checkbox"/> Quartz (sand)	<input type="checkbox"/> Feldspar	<input type="checkbox"/> Mafic	<input type="checkbox"/> BIF	<input type="checkbox"/>			
<input type="checkbox"/> Calcrete	<input type="checkbox"/> Ultramafic			<input type="checkbox"/> Sandstone			
<input type="checkbox"/> Hardpan	<input type="checkbox"/> Felsic	<input type="checkbox"/> Ark / Gwk					
<input type="checkbox"/> MnO ₂	<input type="checkbox"/> Granite	<input type="checkbox"/> Shale/Siltstone					
<input type="checkbox"/> Silcrete	<input type="checkbox"/> Other _____	<input type="checkbox"/> Quartzite	<input type="checkbox"/> Chert				
Secondary coating	<input type="checkbox"/> Fe / Mn	<input type="checkbox"/> Siliceous	<input type="checkbox"/> Calcareous	<input type="checkbox"/> Clay			
-2 mm Material	<input type="checkbox"/> Sand (0.1-2 mm)	<input type="checkbox"/> Clay	<input type="checkbox"/> Other _____	Colour _____			
Rock O/c	Dist.	Dir.	Secondary Units Nearby		Heading _____	Width _____ m	
1.	_____ m	_____	Hardpan <input type="checkbox"/>	Consolidated colluvium <input type="checkbox"/>	<input type="checkbox"/> Single	<input type="checkbox"/> Braided	<input type="checkbox"/> Incised
2.	_____ m	_____	Calcrete <input type="checkbox"/>	Duricrust <input type="checkbox"/>	Sieved to size: Y/N Depth: _____		
3.	_____ m	_____	Mot zone <input type="checkbox"/>	Saprolite <input type="checkbox"/>	Saprock <input type="checkbox"/>	Osize: _____ %	Usize: _____ %
4.	_____ m	_____	Gyps dune <input type="checkbox"/>	Sand dune <input type="checkbox"/>	Salt <input type="checkbox"/>		

REMARKS: _____

Figure 4.1. Sample-recording form, KINGSTON

Anand and Smith (1994), where regolith is classified according to its position in an idealized landform profile as relict (R), erosional (E), or depositional (D). Relict-regime regolith is commonly in areas of higher topographic elevation (e.g. upland surfaces and plateaus), and includes areas of siliceous and ferruginous duricrust ('laterite'). The erosional regime includes areas of outcrop and subcrop where there is a net loss of material caused by downslope transport. Areas of net material gain comprise the depositional regime, including active alluvial channels, areas of sheetwash, overbank deposits, sandplain, and lakes.

The three schemes reflect an ongoing change in the focus of the GSWA's regolith geochemistry program, from relatively simple granite-greenstone associations of the Yilgarn Craton to more complex associations such as the Capricorn and Albany-Fraser Orogenes.

Maps produced early in the GSWA regional regolith and geochemical mapping program focused on Archaean granite-greenstone associations of the Yilgarn Craton (e.g. MENZIES 1:250 000: Kojan and Faulkner, 1994; LEONORA 1:250 000: Bradley et al., 1995), which had few regolith-landform divisions, reflecting the lack of relief and limited number of lithologies. Regolith was subdivided according to its landform position (using R, E, D), slope position, and lithology. For example, in the erosional regime, E2v corresponded to erosional-regime regolith (E) derived from mafic igneous rock (v) that was upslope (2) from lithologically similar material that would be termed E4v. Alluvium of the depositional regime was separated using numerical qualifiers, such as DA4 (alluvium in active alluvial channels), DA5 (overbank deposits), DA7 (playa lake and associated deposits), and DA8 (calcrete). Sandplain was denoted as D9. This system has drawbacks, in that it only works well for lithologically simple map sheets, relies on a qualitative determination of slope position, and requires identification of the parent rock type to indicate the composition of regolith — the latter was commonly difficult for fine-grained, better sorted regolith, such as that of the depositional regime.

The shift in focus of the GSWA's regolith geochemistry program to Proterozoic successions of the Capricorn Orogen involved a change to map sheets with a relatively diverse lithology and physiography, combined with a less arid climate. This resulted in an increase in the number of regolith-landform divisions and increasingly complex regolith-landform maps. Several factors prompted a revision of the regolith-classification scheme. These included a need to simplify the regolith-landform maps, produce a more objective classification scheme, and introduce criteria that would enable the compositional classification of regolith independent of parent rock type. This change in scheme also coincided with the need for a universal regolith-classification scheme that could be used throughout GSWA.

The revised scheme retained the regolith-landform approach, and used a set of 11 primary codes for the subdivision of regolith in terms of landform position (Table 4.1). These codes aimed to satisfy a wide range of physiographic associations. The issue of regolith composition was addressed by a series of secondary codes,

including some designations for common regolith types (e.g. h: hardpan; w: consolidated colluvium) that were not strictly compositionally based. These secondary codes highlighted the composition of the regolith rather than the parent rock type. In situations where the parent rock type was identifiable (usually in the erosional regime), this could be designated using a set of tertiary codes (Table 4.1)

This revised scheme relied on placing the regolith in an idealized landform profile, and making basic macroscopic and mesoscopic (hand lens) observations about regolith composition. The scheme did not rely on detailed knowledge of regolith-forming processes. The revised scheme resulted in a reduction in the number of regolith-landform types, and hence a more simple regolith-landform map. In addition, the revised scheme allowed a more rigorous approach to statistical analysis of regolith chemistry according to regolith type, as there were usually larger sample populations for each regolith-landform subdivision.

Following implementation of this revised regolith-classification scheme on several GSWA 1:250 000 regolith-landform maps (e.g. MOUNT EGERTON: Morris et al., 1998; TUREE CREEK: Coker et al., 1998), several improvements were made to the scheme, as discussed by Hocking et al. (in prep.). These changes included expansion and some modification of the primary (environment or process), secondary (compositional), and tertiary (parent rock or cement) code sets, and the optional use of subscripts to primary, secondary, and tertiary codes to allow further subdivision of regolith.

An example of this approach to describe a gravel bar in an alluvial channel derived from ferromagnesian volcanic rock (basalt) would result in the code A_gmv_b , where A is a primary code denoting an alluvial environment, and the subscript (g) indicates a gravel bar. The secondary code (m) defines the composition as ferromagnesian material, whereas the tertiary code (v) indicates derivation from volcanic parent rock. The subscript (b) denotes the parent lithology as basalt. Lists of primary codes, selected primary code qualifiers, secondary codes and qualifiers, and tertiary codes with common qualifiers are shown in Tables 4.2 to 4.5.

Quality control during the analysis of regolith

Quality control aims to assess the precision and accuracy of chemical analysis using a series of standards (for which compositions are known), replicate and duplicate samples, and blank determinations. Precision is the closeness of agreement of independent test results obtained under prescribed conditions, whereas accuracy is the closeness of agreement between the result of a measurement and the true value (Thompson and Ramsey, 1995). Both precision and accuracy can only be reliably assessed when the analyte concentration is sufficiently above the detection level, which is the lowest level at which the analyte can be reliably measured using the technique under consideration. Precision is assessed using a series of

Table 4.1. Primary, secondary, and tertiary codes, prior to revision

<i>Regolith code</i>	<i>Description</i>
Primary codes — environment	
R	relict
E	erosional
C	colluvial
W	diluvial
A	alluvial
O	overbank
L	lacustrine
S	
B	
T	
M	
Secondary codes — composition	
b	black soil, gilgai
c	clay-mineral rich
e	evaporite
f	iron rich (ferruginous)
g	quartzofeldspathic
h	hardpan
k	carbonate rich (including calcrete)
m	ferromagnesian
q	quartz rich
r	carbonaceous
u	ultramafic
w	compacted and/or weakly cemented material (includes consolidated colluvium)
x	mineral-rich material
y	gypsiferous
z	siliceous (including silcrete)
Tertiary codes — rock qualifiers and specified compositional qualifiers	
m	metamorphic
p	plutonic
v	volcanic
s	sedimentary
h	halite
a	aluminous
n	magnesite

GSWA and laboratory reference standards for which there are consensus or recommended values. In the GSWA regional regolith and geochemical mapping program, precision is deemed acceptable if the percent relative standard deviation ($RSD\% = (\text{standard deviation}/\text{mean}) \times 100$) is less than 20 for multiple analyses, provided the analyte concentration is more than 20 times (in some cases 10 times) the detection level. Measurement of a replicate sample (i.e. a second analysis of the same sample pulp) also assesses precision, as well as any change in analytical conditions during a sample run (machine drift), and any variation in analytical conditions between batches (batch effects). In future regolith programs carried out by GSWA, the Half Relative Difference (HRD) factor ((assay #1 – assay #2)/(assay #1 + assay #2) $\times 100$; Shaw et al., 1998) will be used to assess replication, with a value of 10% deemed acceptable.

Accuracy is assessed using GSWA and laboratory standard analyses, with an acceptable accuracy if the analyte concentration lies within 20% of the recommended or consensus value, provided the analyte concentration

is greater than 10 or 20 times the detection level. These data can also be used to assess machine drift and batch effects.

Background levels are assessed by periodic analysis of blanks, with acceptable background levels in the GSWA program being less than three times the detection level.

For each analytical batch of between 120 and 200 samples (batch size depends on the laboratory), up to three GSWA standards are included as blind checks (i.e. with the GSWA number only), resulting in about 10 standard analyses per map sheet. These standards include a laterite (IQC47), a gossan (IQC45), and an amphibolite (IQC42), which span a wide SiO_2 interval of 42–88%.

Rigorous application of criteria for acceptability of results in terms of accuracy and precision assumes sample homogeneity and the suitability of the analytical technique to the analyte under consideration. With a wide range in composition — Morris et al. (1997) reported a SiO_2 range of 7% to 96% for regolith on NABBERU (1:250 000) — and

the concentration of resistate phases (e.g. rutile, chromite, and zircon) lower in the landform profile, it is unlikely that one preparation or analytical technique is suitable for all samples. Morris et al. (1998) discussed this problem with regard to analysis of niobium on MOUNT EGERTON and TUREE CREEK (1:250 000). They concluded that precise and accurate analysis of high field strength elements such as niobium is difficult, as these elements were common in resistate phases, such as rutile, which are difficult to dissolve prior to analysis by inductively coupled plasma (ICP) techniques. One approach to reducing these problems is to use different preparation or analytical techniques depending on analyte concentration. For example, Morris et al. (1998) report chromium data for regolith on MOUNT EGERTON according to two techniques: for concentrations of less than 100 ppm, data are reported after mixed acid digestion and inductively coupled plasma mass spectrometric (ICP-MS) analysis; for values greater than 100 ppm, data are reported following fusion and mixed acid digest and inductively coupled plasma optical emission spectrometric (ICP-OES) analysis. Although this approach can produce more acceptable data, the niobium issue on MOUNT EGERTON and TUREE CREEK as discussed by Morris et al. (1998) was not resolved by using different preparation or analytical techniques. Another factor in this approach is that of cost, which increases with the number of sample digests or techniques employed.

Batch effects have been noted for gold in regolith on EDMUND (1:250 000; Pye et al., 1998) and GLENBURGH (1:250 000; Sanders et al., 1998). In both cases, gold at levels of less than 4 ppb (detection level of 1 ppb) were subject to batch control.

Quality-control data for regolith on KINGSTON are presented as a series of digital datafiles on the accompanying floppy disk. For GSWA standards, the consensus values are taken as averages of analyses carried out at individual laboratories during the course of the GSWA regolith program. Consensus values for laboratory standards have been provided by the respective laboratories.

Typical analytical schemes from three commercial laboratories are outlined below.

Genalysis Laboratory Services

All regolith samples were oven dried at GSWA's Carlisle base. Approximately 2 kg of each sample (either sieved to < 2 mm or to < 6 mm) was supplied to the laboratory. Following further drying, an aliquot of each sample was sieved to between 2 and 0.45 mm. This material was pulverized to < 75 µm in a zirconia ring mill (for analysis of SiO₂, TiO₂, Fe₂O₃, Al₂O₃, MnO, MgO, K₂O, and Cr), or a chrome-steel jumbo ring mill (for analysis of CaO, Na₂O, P₂O₅, Ag As, Ba, Be, Bi, Cd, Ce, Co, Cu, Ga, In, La, Li, Mo, Nb, Ni, Pb, Rb, Sc, Se, Sn, Sr, Ta, Te, Th, U, V, W, Y, Zn, and Zr).

Seven different analytical methods were used:

1. Silver, As, Ba, Be, Bi, Cd, Ce, Co, Ga, In, La, Li, Mo, Pb, Rb, Sb, Sn, Sr, Te, Th, U, W, and Y were analysed by ICP-MS using a combined mixed acid digest (Genalysis code A/MS). The pulverized sample was digested in a hydrofluoric–perchloric–nitric acid

Table 4.2. Revised primary regolith codes

<i>Primary landform code</i>	<i>Environment and process</i>	<i>Notes</i>
<i>R</i>	Residual	Principally relicts of an ancient weathered land surface, derived by in situ weathering. Includes overlying proximal disaggregated and reworked material. Does not refer to relict-depositional regimes
<i>X</i>	Exposed	Used for rock (optional) and weathered rock of uncertain protolith
<i>C</i>	Colluvial	Proximal mass-wasting deposits grading into sheetwash with a significant to perceptible slope
<i>W</i>	Low-gradient slope	Distal sheetwash and slope deposits where the gradient is minimal, and drainage is not clearly defined
<i>A</i>	Alluvial/fluvial	Alluvium in channels. Includes deltaic deposits
<i>F</i>	Floodplain/overbank	Floodplain deposits in recognizable drainage systems, alluvial terrace deposits Grades into alluvium
<i>L</i>	Lacustrine	Inland lakes, dune and playa terrain, and some coastal lakes (those not formed by coastal barring). Includes saline and fresh-water playas and claypans, and minor eolian deposits directly associated with the lake system (fringing gypsumiferous dunes, etc.)
<i>E</i>	Eolian	Eolian dunes, interdune areas, and sandplain
<i>S</i>	Sandplain	Dominantly sandplain, may be of residual or mixed origin
<i>B</i>	Wave-dominated coastal (beach)	Beaches, beach ridges, barrier bars and lagoons, and back-beach dunes
<i>T</i>	Tide-dominated coastal	Intertidal and supratidal flats and channels, estuaries, and mangrove flats
<i>M</i>	Marine	Marine deposits such as coralgal reefs, shell banks, and sea-grass banks

Table 4.3. Examples of primary code qualifiers

<i>Primary landform/process</i>	<i>Landform element or pattern</i>	<i>Suggested primary code</i>	<i>Suggested subscript code</i>
Colluvial (proximal slope)	Landslide	C	<i>C_l</i>
Wash (sheet-flood, distal slope)	Playa, pan	W	<i>W_p</i>
Floodplain	Delta Alluvial plain	F	<i>F_d</i> <i>F_p</i>
Alluvial	Stream channel Delta Alluvial fan Gravel bar	A	<i>A_c</i> <i>A_d</i> <i>A_f</i> <i>A_g</i>
Lacustrine	Fringing dunes Fringing bedded deposits Dune and playa terrain Lake, excluding fringing deposits Playa, pan	L	<i>L_d</i> <i>L_s</i> <i>L_m</i> <i>L_l</i> <i>L_p</i>
Eolian	Dunefield Dune Longitudinal dunefield Mobile dune Interdune pavements Lunette	E	<i>E_d</i> <i>E_e</i> <i>E_l</i> <i>E_m</i> <i>E_p</i> <i>E_u</i>
Sandplain, residual, uncertain, and mixed	Gravel deflation pavement	S	<i>S_p</i>
Wave-dominated coastal (beach)	Beach (foreshore) Mobile dunes	B	<i>B_f</i> <i>B_m</i>
Tide-dominated coastal	Tidal bar, in channel Tidal delta Estuary Lagoon	T	<i>T_b</i> <i>T_d</i> <i>T_e</i> <i>T_l</i>
Marine	Coral reef	M	<i>M_r</i>

mixture for at least 24 hours, evaporated to fume dryness and leached in hydrochloric acid.

2. Manganese oxide, Na₂O, P₂O₅, Cr, Cu, Ni, Sc, V, and Zn were analysed by ICP-OES using a mixed acid digest (Genalysis code A/OES). The pulverized sample was digested in a hydrofluoric–perchloric–nitric acid mixture for at least 24 hours, evaporated to fume dryness, and leached in hydrochloric acid.
3. SiO₂, TiO₂, Al₂O₃, Fe₂O₃, MgO, CaO, K₂O, and S were analysed by ICP-OES using an alkaline oxidative fusion with sodium peroxide in a nickel crucible followed by leaching with hydrochloric acid (Genalysis code DX/OES).
4. Niobium, Ta, and Zr were analysed by ICP-MS using an alkaline oxidative fusion with sodium peroxide

in nickel crucibles followed by leaching with hydrochloric acid (Genalysis code DX/MS).

5. The precious metals Au, Pd, and Pt were analysed by fire-assay lead collection and ICP-MS analysis (Genalysis code FA*MS).
6. Selenium was analysed by precipitation of selenium metal followed by aqua-regia digestion and ICP-MS analysis (Genalysis code A*MS)
7. Loss on ignition (LOI) was determined by gravimetric means (Genalysis code GRAV).

Analabs

The total sample was dried to 110°C, jaw crushed if necessary, split then milled in a chromium-free mill to a

Table 4.4. Revised secondary codes and qualifiers

Code	Composition	Qualifier	Composition
a	aluminous/bauxitic		
b	black soil, gilgai		
c	clay	c _c c _g c _i c _k c _m c _s	chlorite glaucite illite kaolin montmorillonite smectite
d	undivided		
e	evaporite	e _a e _g e _h	anhydrite gypsum halite
f	ferruginous		
g	quartzofeldspathic		
h	heavy mineral	h _a h _g h _i h _j h _m h _o h _r h _z	apatite garnet ilmenite leucoxene magnetite monazite rutile zircon
i	limonite		
k	carbonate	k _a k _c k _d k _m	aragonite calcite dolomite magnesite
l	heterogeneous		
m	ferromagnesian		
o	goethite		
q	quartz		
r	carbonaceous/organic	r _c r _h r _p	coal humus peat
u	ultramafic		
x	other mineral	x _i x _m	mica manganese
z	siliceous		

nominal particle size of 90% less than 75 µm. An analytical pulp of approximately 200 g was subsampled from the bulk and the milled residue and any split retained for future reference. All the preparation equipment was flushed with barren feldspar prior to the commencement of the job and after each batch.

The following analytical schemes were used:

1. Silica, TiO₂, Al₂O₃, Fe₂O₃, MnO, MgO, CaO, Na₂O, K₂O, and P₂O₅ were measured by X-ray fluorescence spectrometry (XRF) on a glass fusion disc (Analabs code X408).
2. Loss on ignition (LOI) was determined gravimetrically, by heating the sample to 1000°C (Analabs code V955).
3. A series of trace elements were measured by ICP-MS, following sample digestion with nitric, hydro-

chloric, hydrofluoric, and perchloric acids (Analabs code G104). Elements measured include: Ag, As, Ba, Be, Bi, Cd, Ce, Co, Ga, In, La, Li, Mo, Nb, Ni, Pb, Rb, Sb, Sc, Sn, Ta, Th, U, W, and Y (Analabs code M104).

4. The G104 digest (at 3. above) was used for the analysis of Sr, V, and Zr by ICP-OES (Analabs code I104).
5. An aliquot of the G104 digest (at 3. above) was analysed by atomic absorption spectrometry (AAS) for Cr, Cu, and Zn (Analabs code A104).
6. The volatile metals Se and Te were analysed by hydride generation AAS (Analabs code H109), from a chromate-enhanced hydrochloric and nitric acid digestion carried out at low temperature (Analabs code G109).

Table 4.5. Revised tertiary codes and qualifiers for parent rock or cement type

Parent rock or cement	Parent rock qualifier
a aluminous cement	
c chemical/biochemical sedimentary deposit	c _c c _d c _i c _l c _t
f duricrust	chert
h hyperbyssal	dolomite
i iron cement	iron-formation
k carbonate cement	limestone
m metamorphic	diatomite
o fossiliferous	
p plutonic	
s siliciclastic sedimentary rock	
u ultramafic	
v volcanic	
z silica cement	

c_c chert
c_d dolomite
c_i iron-formation
c_l limestone
c_t diatomite
h_d dolerite
h_p porphyry
m_g gneiss
m_p pelite
m_m psammite
m_s schist
o_s shells
o_c coral/coralgal
p_a alkali granite
p_g gabbro
p_d diorite
p_g granite
p_m monzogranite/monzonite
p_o granodiorite
p_s syenogranite/syenite
p_t tonalite
s_c conglomerate
s_m mudstone, siltstone, shale
s_s sandstone, arenite, wacke
u_d dunite
u_k komatiite
u_p peridotite
u_y pyroxenite
u_s serpentinite/talc rock
v_a andesite
v_b basalt
v_d dacite
v_i latite
v_r rhyolite
v_t trachyte
v_v volcaniclastic

7. Sulfur (as S) was evolved at high temperature in a stream of oxygen, and the resultant gas was measured in an infrared cell (Analabs code V821).
8. A 50 g subsample of the assay pulp was fused in a lead collection fire assay. The prill was dissolved in aqua regia (i.e. hydrochloric and nitric acid) and the resultant solution presented to an ICP-MS (Analabs code F627) for analysis of Au, Pd, and Pt.

Amdel Laboratories

Following oven drying, an aliquot of each sample was sieved to between 2 and 0.45 mm. This material was pulverized to < 75 µm in a chrome-free bowl pulverizer; imparted contamination during milling estimated by the manufacturer is 50 ppm Mn and 5000 ppm Fe, with no detectable contamination for Co, Cu, Mo, Ni, Pb, V, or Zn.

Six analytical methods were used:

1. Silica, TiO₂, Al₂O₃, Fe₂O₃, MnO, MgO, CaO, Na₂O, K₂O, and P₂O₅ were analysed by ICP-OES following a lithium metaborate fusion and dilute hydrochloric acid digestion (Amdel code IC4).
2. Silver, As, Bi, Cd, Ce, Co, Cu, Ga, In, La, Mo, Nb, Pb, Rb (up to 20 ppm; IC4M > 20 ppm), Sb, Se, Sn, Sr (up to 500 ppm; IC3E > 500 ppm), Te, Th, U, W, and Y were analysed by ICP-MS following mixed-acid sample digestion (hydrofluoric–perchloric–nitric–hydrochloric) for 24 hours. Samples were evaporated to fume dryness and dissolved in hydrochloric acid prior to analysis (Amdel code IC3M).
3. Barium, Be, Cr (up to 100 ppm; IC4E > 100 ppm), Li, Ni, S (up to 5 %; analysis by Leco (Amdel code VOL2) > 5 %), Sc, V, and Zn were analysed by ICP-OES (Amdel code IC3E). Samples were digested using a hydrofluoric–perchloric–nitric–hydrochloric acid mixture for 24 hours, then evaporated to fume dryness and dissolved in dilute hydrochloric acid.
4. Tantalum and Zr were analysed by ICP-MS following a lithium metaborate fusion and dilute hydrochloric acid digestion (Amdel code IC4M).
5. Gold, Pt, and Pd were collected in a lead collection fire-assay fusion. Following cupellation, the prill was dissolved in aqua regia (i.e. hydrochloric and nitric acids), then analysed by graphite furnace AAS (Amdel code FA3).
6. Loss on ignition (LOI) was determined by gravimetric means (Amdel code GRAV7).

Determination of regolith pH and total dissolved solids

The acidity–alkalinity (pH) and total dissolved solids (TDS) of all regolith samples were measured at the GSWA Carlisle base. For both types of measurements, a subsample was mixed with deionized water in the ratio of 1:5, then shaken vigorously. After standing overnight, the pH was

measured using a portable Jenway pH meter, calibrated using standard solutions of pH=4 and pH=7. The electrode was rinsed in deionized water between each measurement of unknowns. The conductivity of each sample (i.e. a measure of the TDS) was made using a SCAN4 conductivity meter, calibrated using a buffer solution of 11.67 millisiemens/centimetre (mS/cm). Electrodes were rinsed between every measurement of unknowns.

References

- ANAND, R. R., SMITH, R. E., PHANG, C., WILDMAN, J. E., ROBERTSON, I. D. M., and MUNDY, T. J., 1993, Geochemical exploration in complex lateritic environments of the Yilgarn Craton, Western Australia: Australia CSIRO, Division of Exploration and Mining, Report 442R, 297p.
- ANAND, R. R., and SMITH, R. E., 1994, Classification, origin and geochemistry of laterites and ferruginous regolith materials in the Yilgarn Craton — implications for exploration: Geological Society of Australia; 12th Australian Geological Convention, Perth, W.A., 1994; Abstracts no. 37, p. 7–8.
- BRADLEY, J. J., SANDERS, A. J., VARGA, Z. S., and STOREY, J. M., 1995, Geochemical mapping of the Leonora 1:250 000 sheet: Western Australia Geological Survey, 1:250 000 Regolith Geochemistry Series Explanatory Notes, 86p.
- COKER, J., FAULKNER, J. A., and SANDERS, A. J., 1998, Geochemical mapping of the Turee Creek 1:250 000 sheet: Western Australia Geological Survey, 1:250 000 Regolith Geochemistry Series Explanatory Notes, 65p.
- HOCKING, R. M., LANGFORD, R. L., THORNE, A. M., MORRIS, P. A., GOZZARD, J. R., and STRONG, C. A., in prep., A classification system for regolith in Western Australia: Western Australian Geological Survey, Record.
- KOJAN, C. J., and FAULKNER, J. A., 1994, Geochemical mapping of the Menzies 1:250 000 sheet: Western Australia Geological Survey, 1:250 000 Regolith Geochemistry Series Explanatory Notes, 55p.
- MORRIS, P. A., SANDERS, A. J., and FAULKNER, J. A., 1997, Geochemical mapping of the Nabberu 1:250 000 sheet: Western Australia Geological Survey, 1:250 000 Regolith Geochemistry Series Explanatory Notes, 63p.
- MORRIS, P. A., COKER, J., and FAULKNER, J. A., 1998, Geochemical mapping of the Mount Egerton 1:250 000 sheet: Western Australia Geological Survey, 1:250 000 Regolith Geochemistry Series Explanatory Notes, 63p.
- PYE, K. J., COKER, J., FAULKNER, J. A., and SANDERS, A. J., 1998, Geochemical mapping of the Edmund 1:250 000 sheet: Western Australia Geological Survey, 1:250 000 Regolith Geochemistry Series Explanatory Notes, 51p.
- SANDERS, A. J., FAULKNER, J. A., COKER, J., and MORRIS, P. A., 1998, Geochemical mapping of the Glenburgh 1:250 000 sheet: Western Australia Geological Survey, 1:250 000 Regolith Geochemistry Series Explanatory Notes, 33p.
- SHAW, W. J., KHOSROWSHAHI, S., HORTON, J., and WALTHO, A., 1998, Predicting and monitoring variability in sampling, sample preparation, and assaying, in More meaningful sampling in the mining industry edited by B. DAVIS and S. E. HO: Australian Institute of Geoscientists, Bulletin 22, p. 11–19.
- THOMPSON, M., and RAMSEY, M. H., 1995, Quality concepts and practices applied to sampling — an exploratory study: Analyst, v. 120, p. 261–270.

Figures

1. Status of GSWA regional regolith and geochemical mapping program
2. Simplified locality plan
3. Simplified geological interpretation
4. Generalized regolith map

Element-distribution maps

5. TiO_2
6. Al_2O_3
7. Fe_2O_3
8. MnO
9. MgO
10. CaO
11. Na_2O
12. K_2O
13. P_2O_5
14. LOI
15. Ag
16. As
17. Au
18. Ba
19. Be
20. Bi
21. Cd
22. Ce
23. Co
24. Cr
25. Cu
26. Ga
27. In
28. La
29. Li
30. Mo
31. Nb
32. Ni
33. Pb
34. Pd
35. Pt
36. Rb
37. S
38. Sb
39. Sc
40. Se
41. Sn
42. Sr
43. Ta
44. Te
45. Th
46. U
47. V
48. W
49. Y
50. Zn
51. Zr
52. pH in regolith
53. Conductivity of regolith (mS/cm)
54. Chalcophile index ($\text{As} + \text{Sb} + \text{Bi} + \text{Mo} + \text{Ag} + \text{Sn} + \text{W} + \text{Se}$)



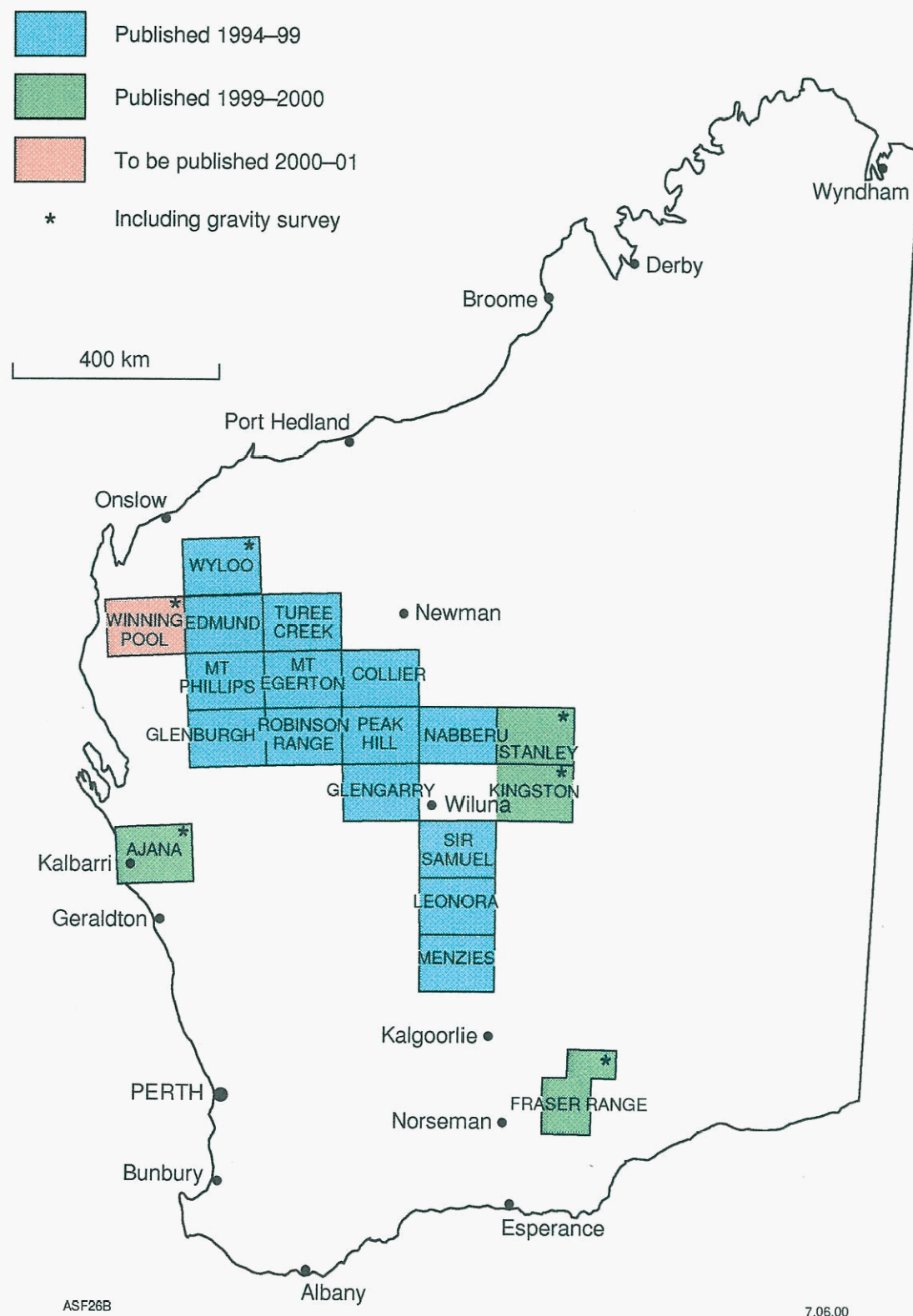


Figure 1. Status of GSWA regional regolith and geochemical mapping program

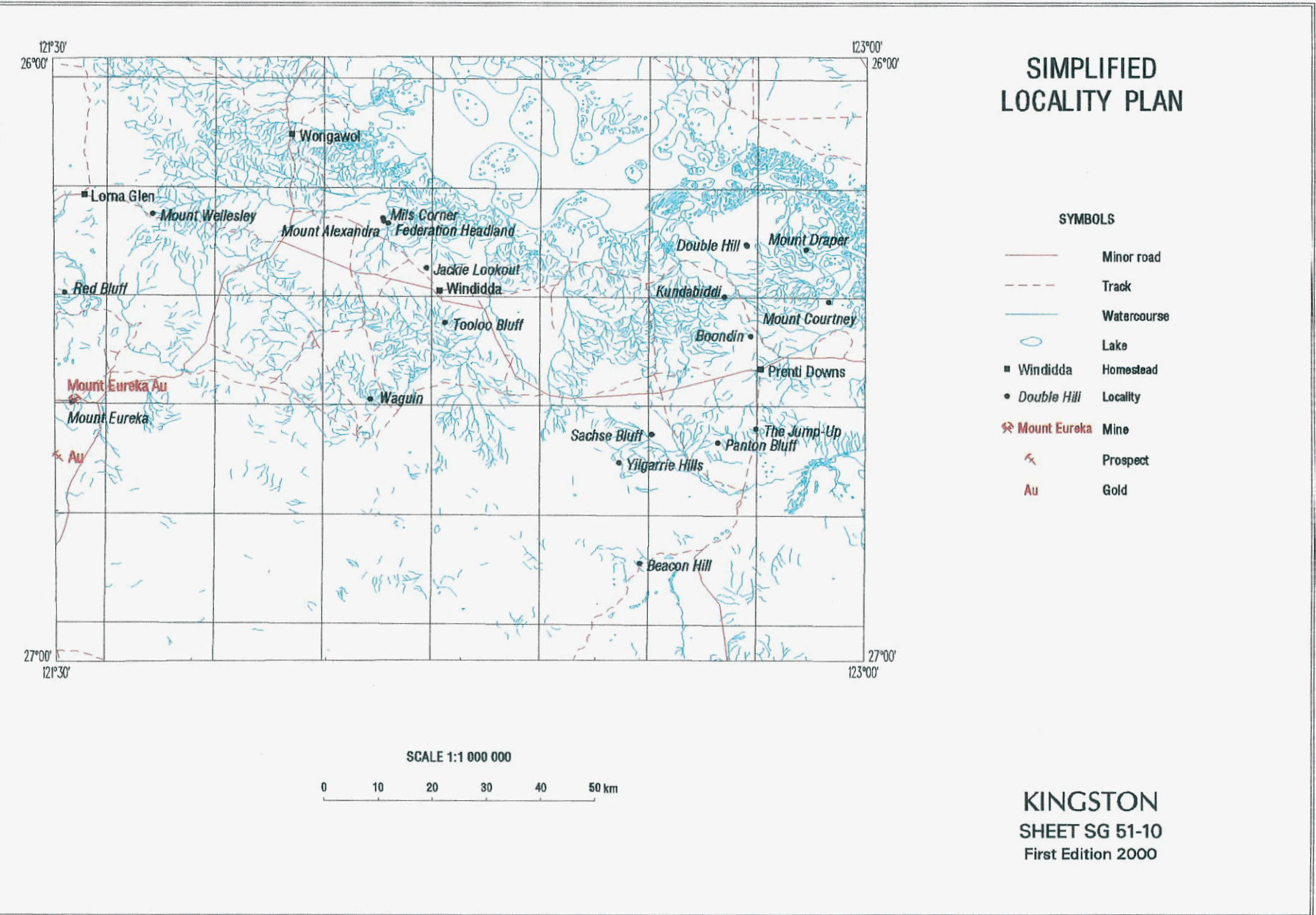
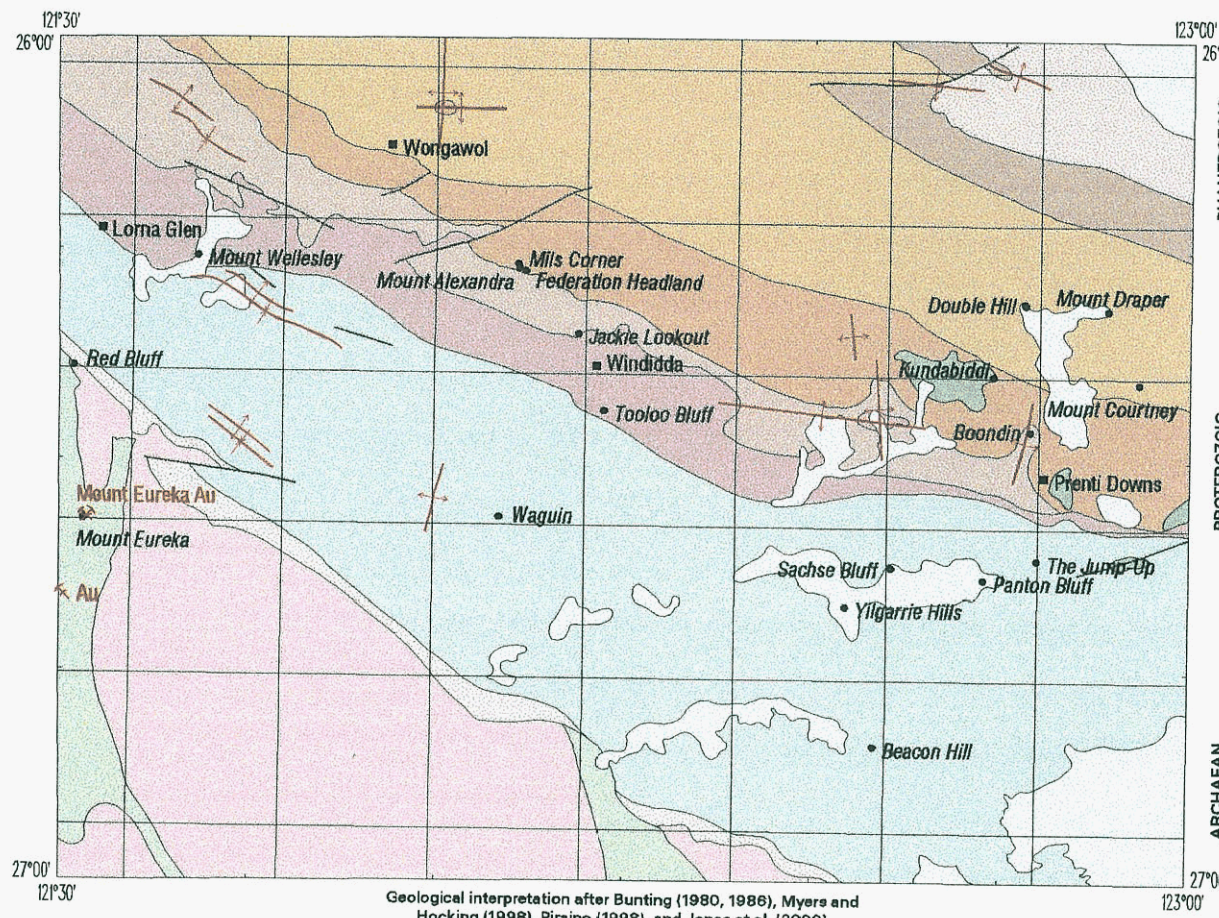


Figure 2

Figure 3



SIMPLIFIED GEOLOGICAL INTERPRETATION

PHANEROZOIC

PERMIAN

PATERSON FORMATION: fluvial or flavioglacial sandstone, conglomerate, and siltstone

Dolerite

Earaheedy Group

MULGARRA SANDSTONE: quartz sandstone; with minor shale and limestone

KULELE LIMESTONE: stromatolitic limestone, calcarenite, and mudstone; minor sandstone

WONGAWOL FORMATION: very fine-grained sandstone, shale, and minor carbonate-rich rocks

CHIALL FORMATION
Princess Ranges Member: quartz arenite with minor siltstone

Wandilla Member: sandstone, siltstone, and shale; locally glauconitic basal conglomerate

WINDIDDA FORMATION: limestone, shale, and chert; stromatolitic in part

FRERE FORMATION: granular iron-formation, hematitic shale, chert, and siltstone

YELMA FORMATION: sandstone and shale; minor chert, and stromatolitic carbonate

Granitoid rock

Greenstone: basalt, dolerite, ultramafic rock, metamorphosed sedimentary rocks, and felsic volcanic rock

Geological boundary

Anticline

Fault

Syncline

KINGSTON
SHEET SG 51-10
First Edition 2000

Windidda Homestead
Double Hill Locality

Mount Eureka Mine
Prospect
Au Gold

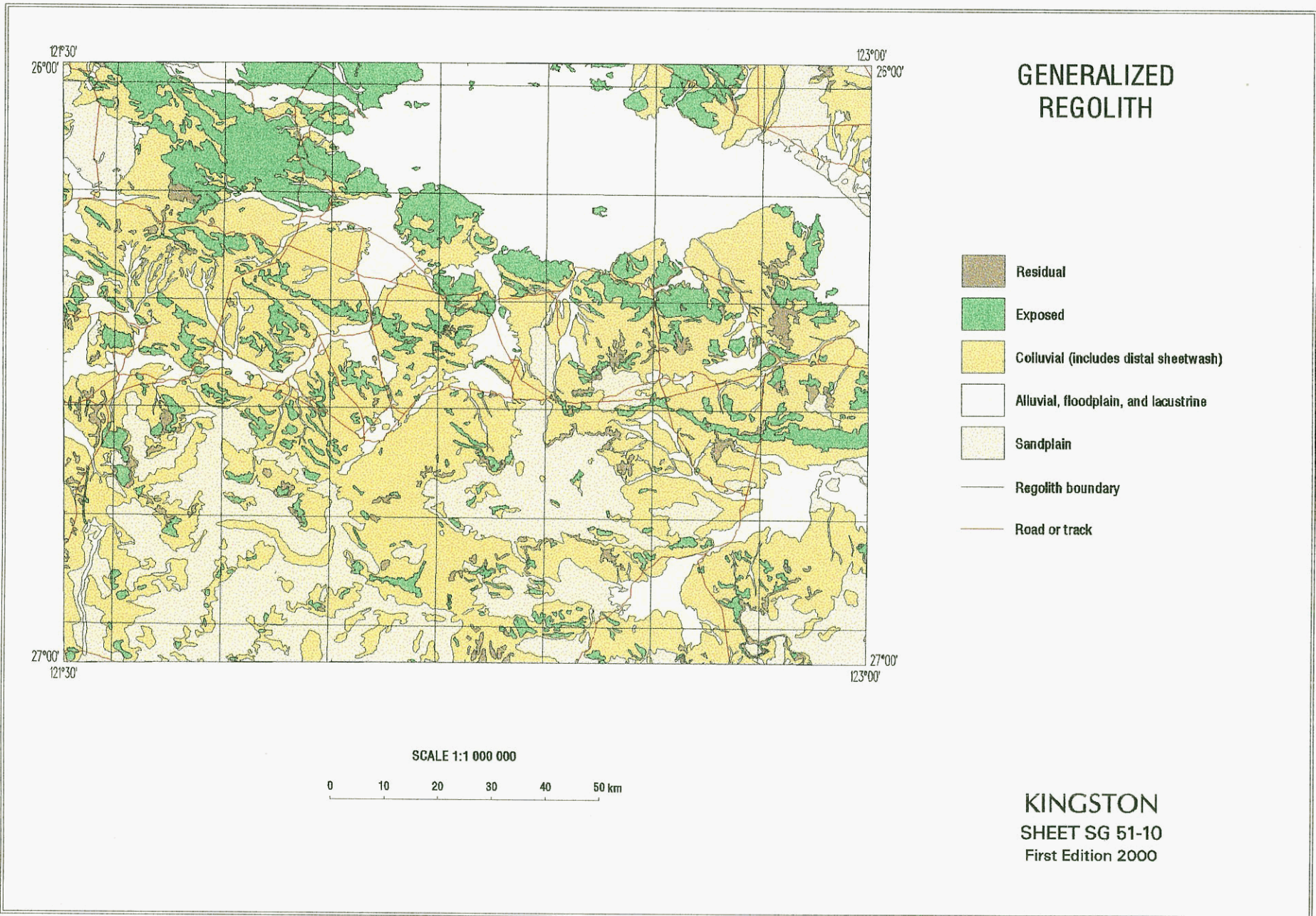


Figure 4

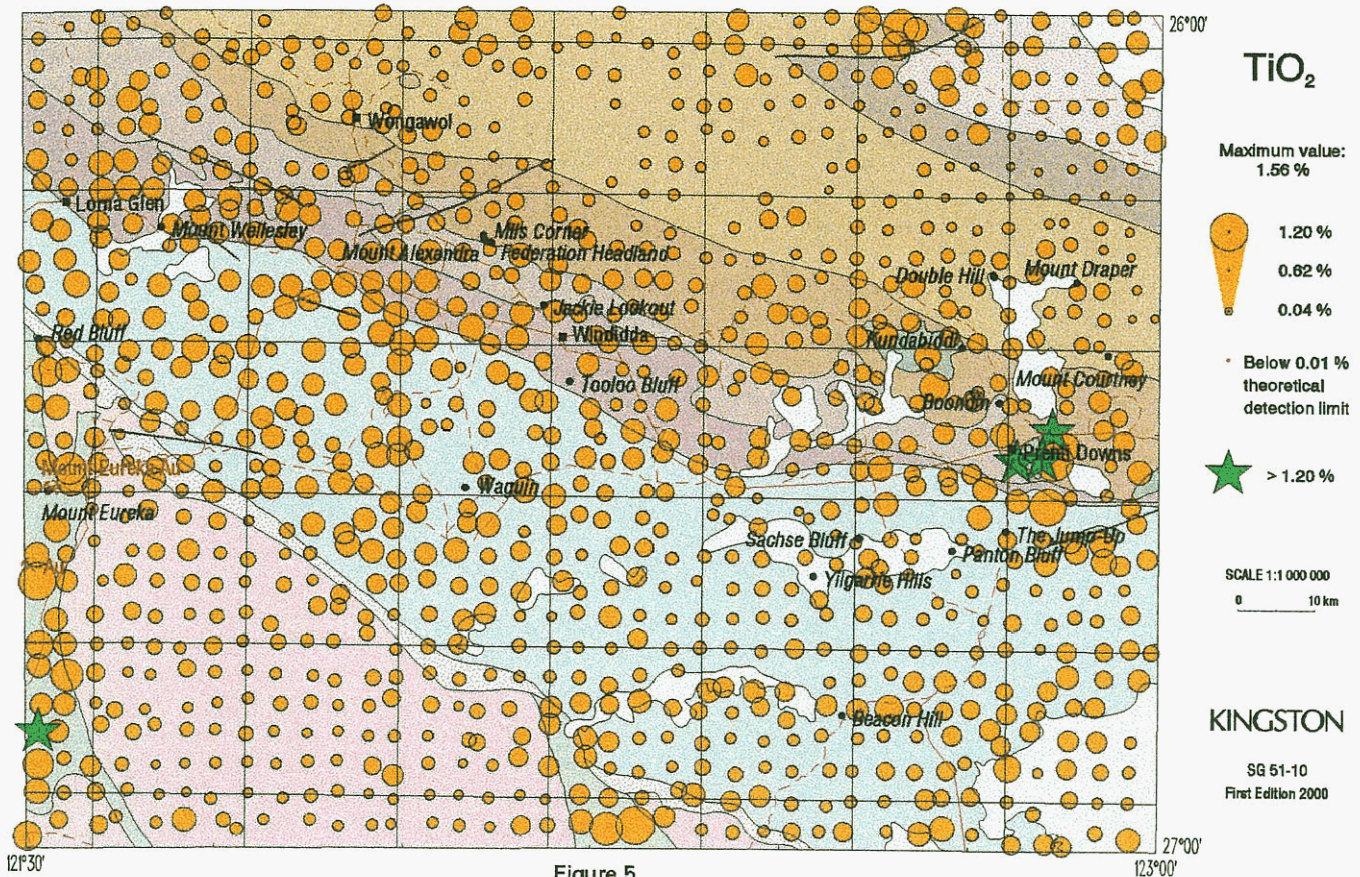


Figure 5

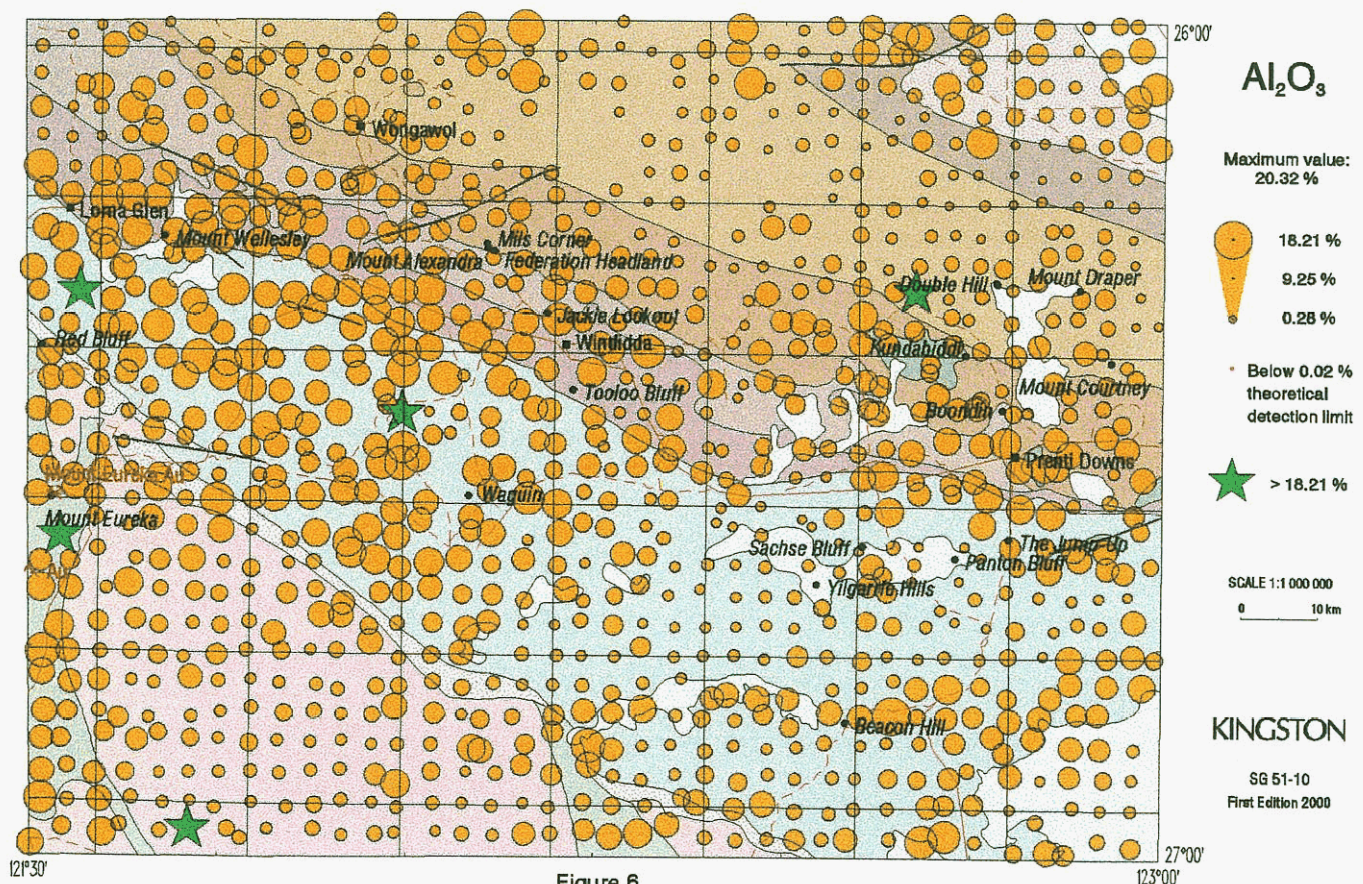


Figure 6

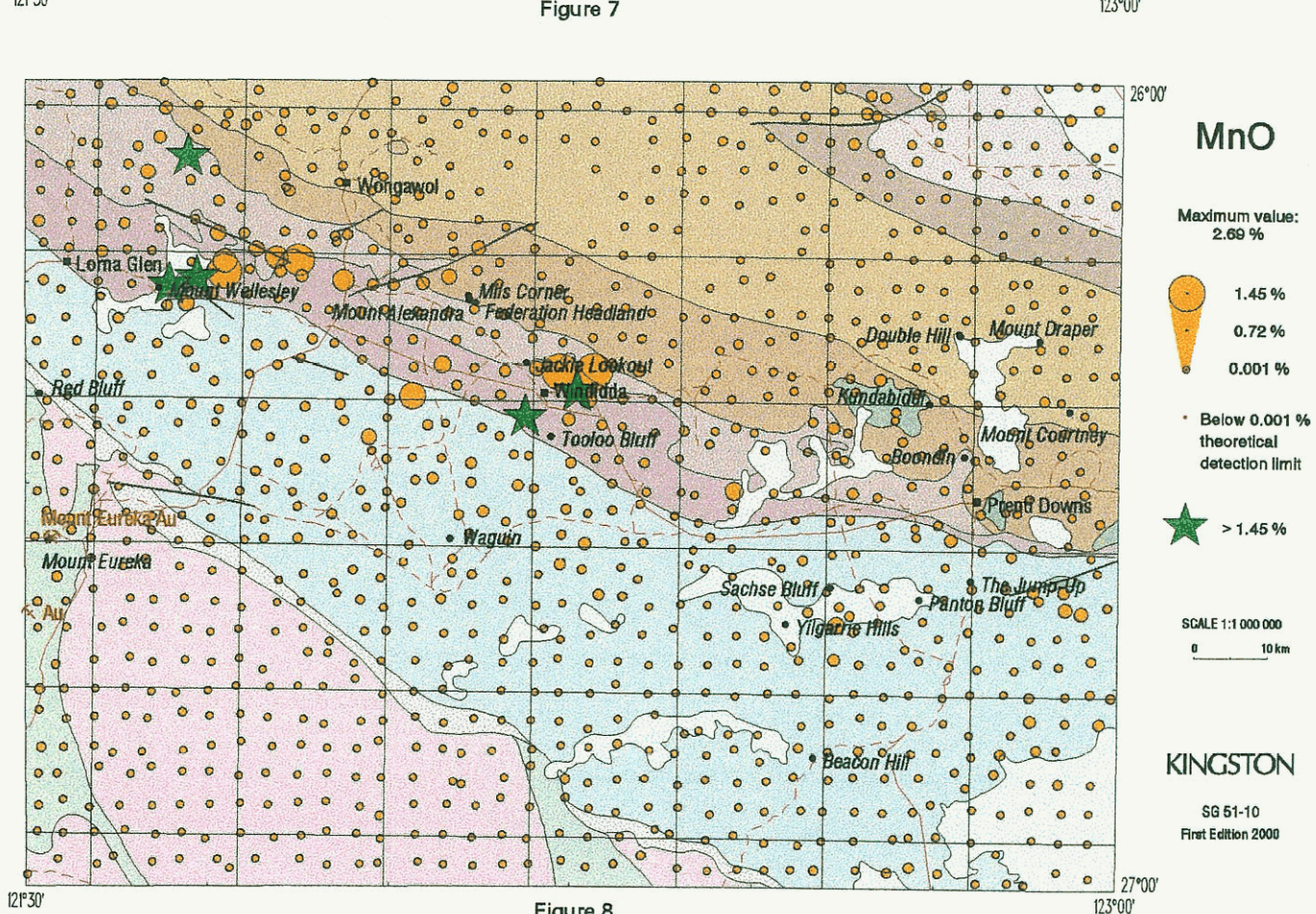
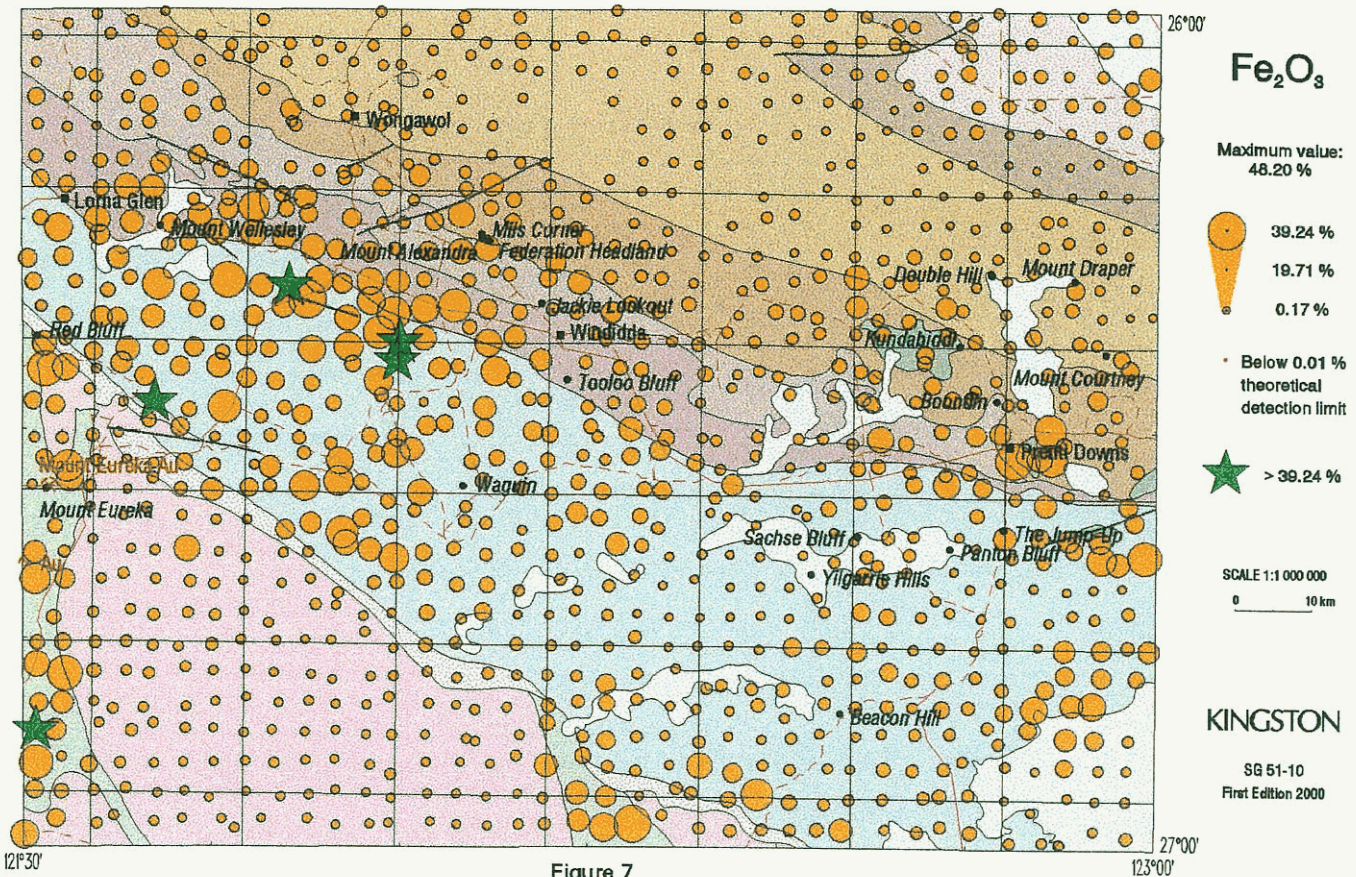


Figure 7

Figure 8

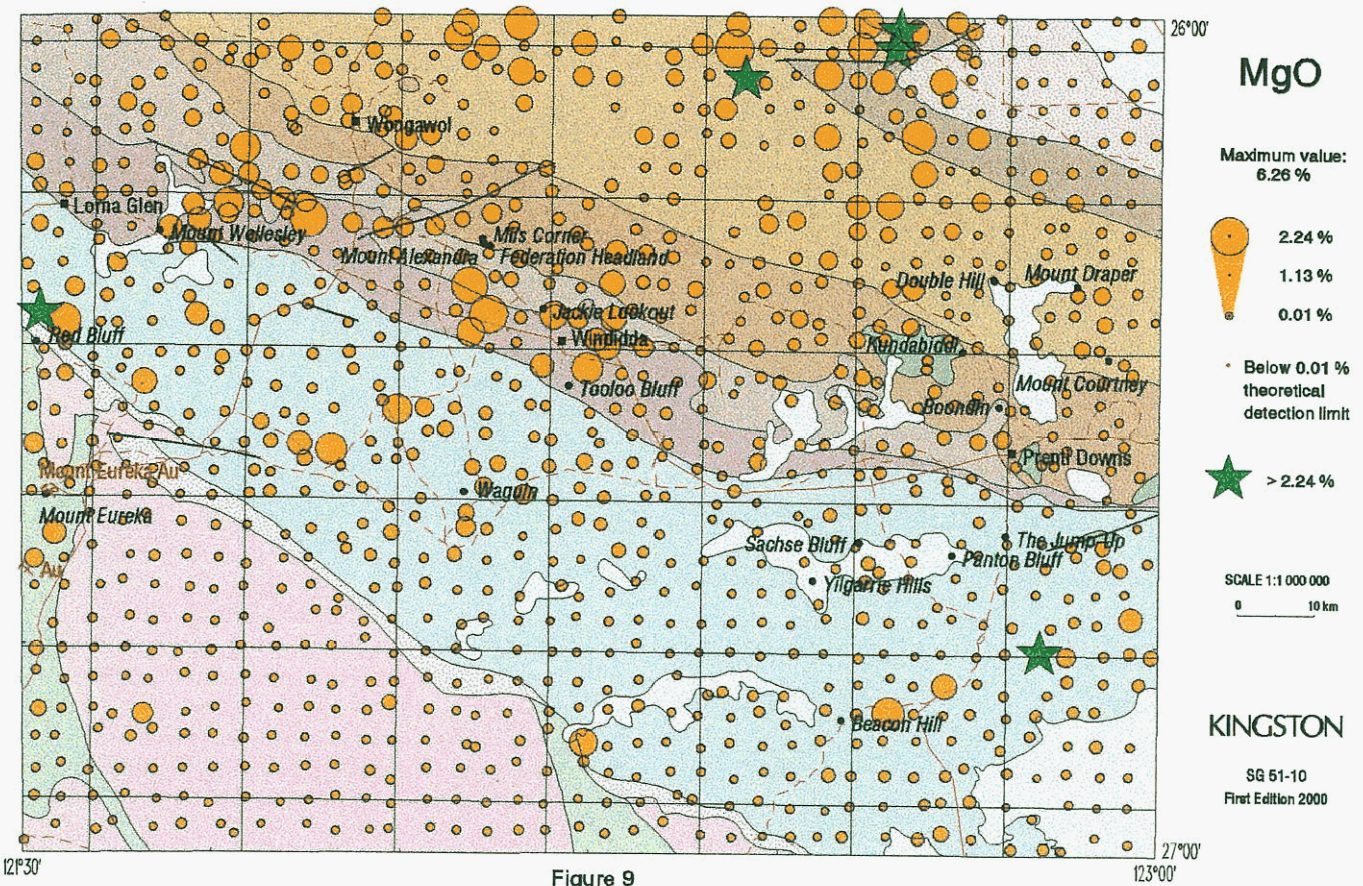


Figure 9

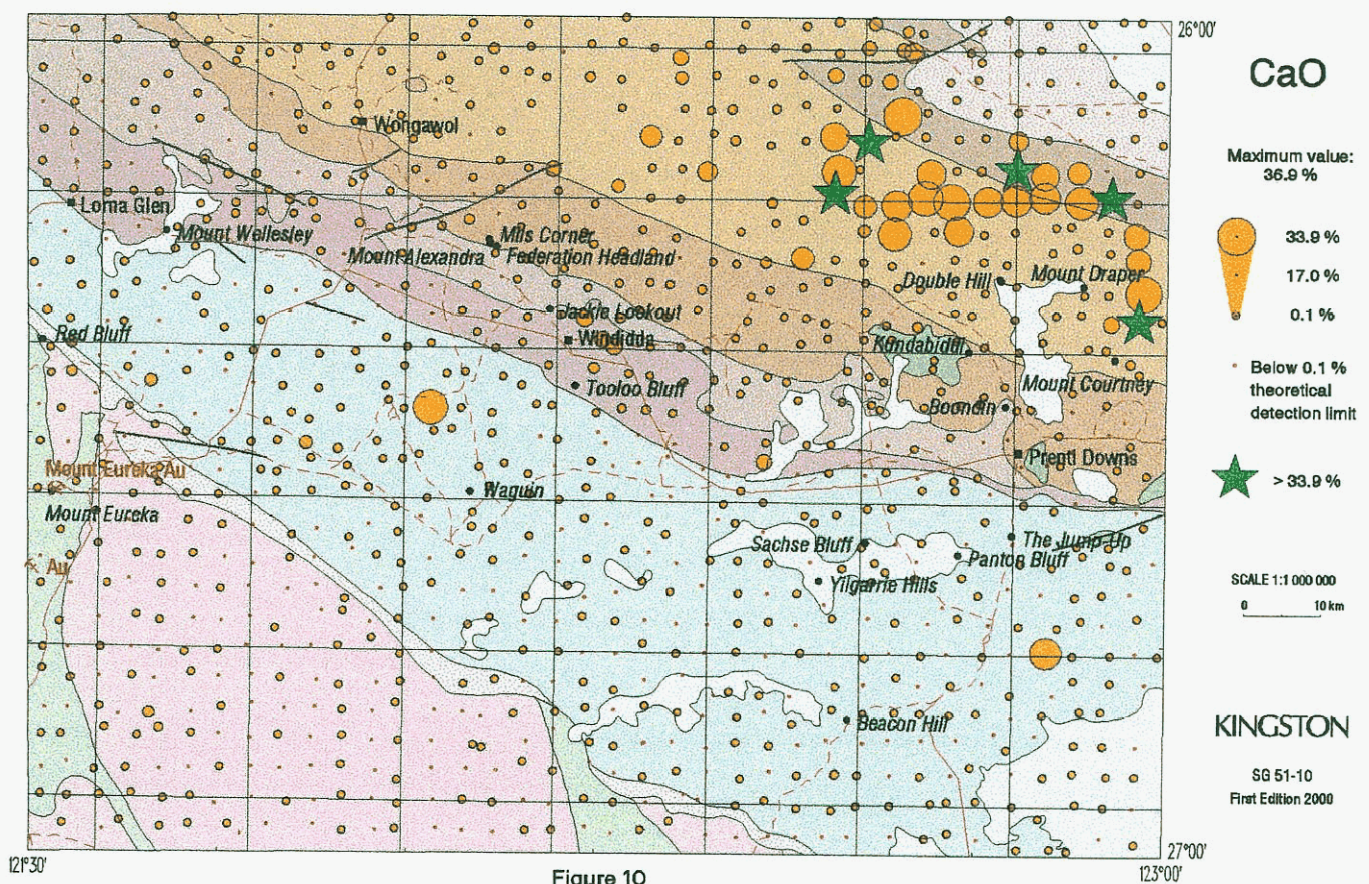


Figure 10

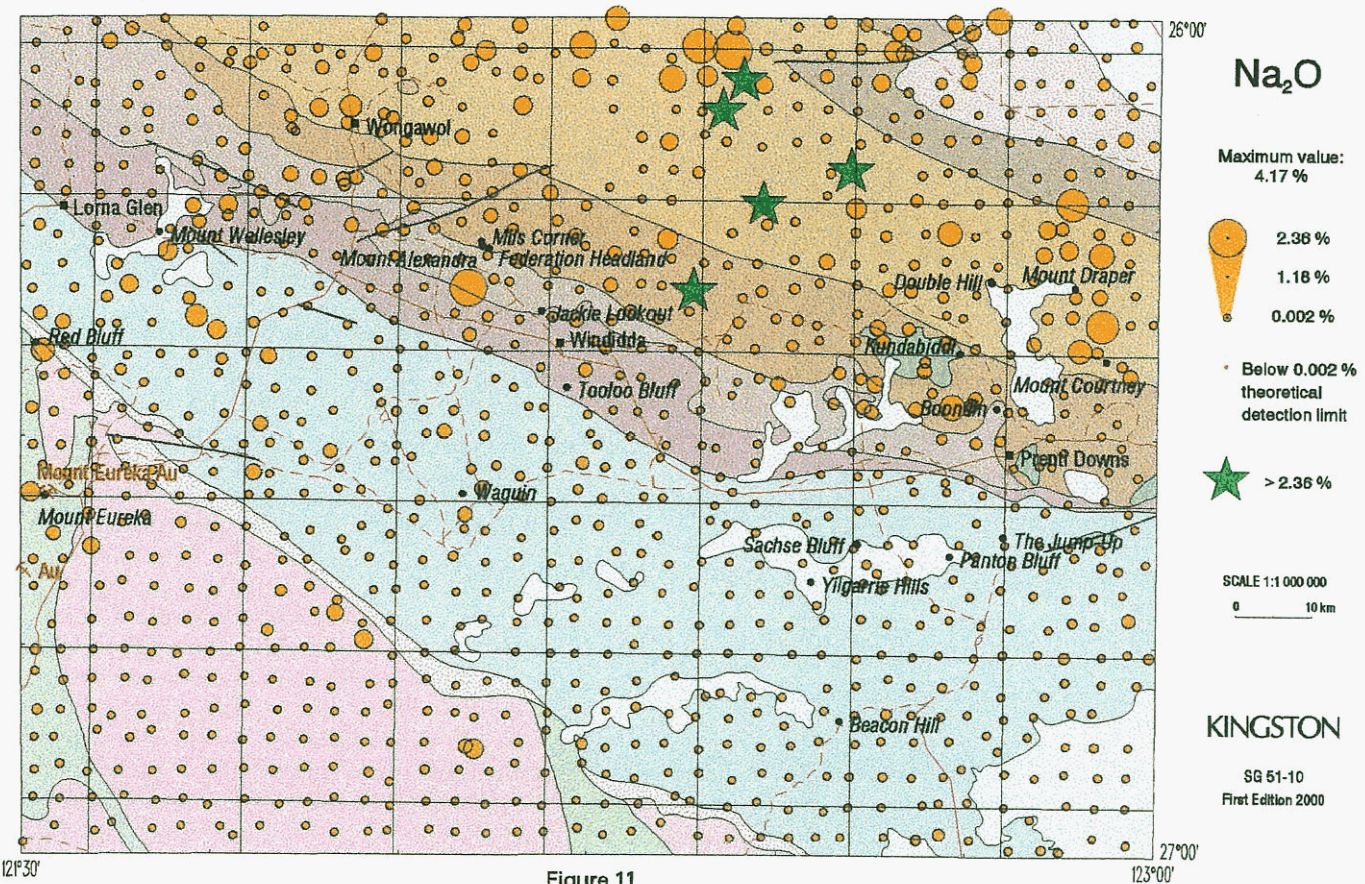


Figure 11

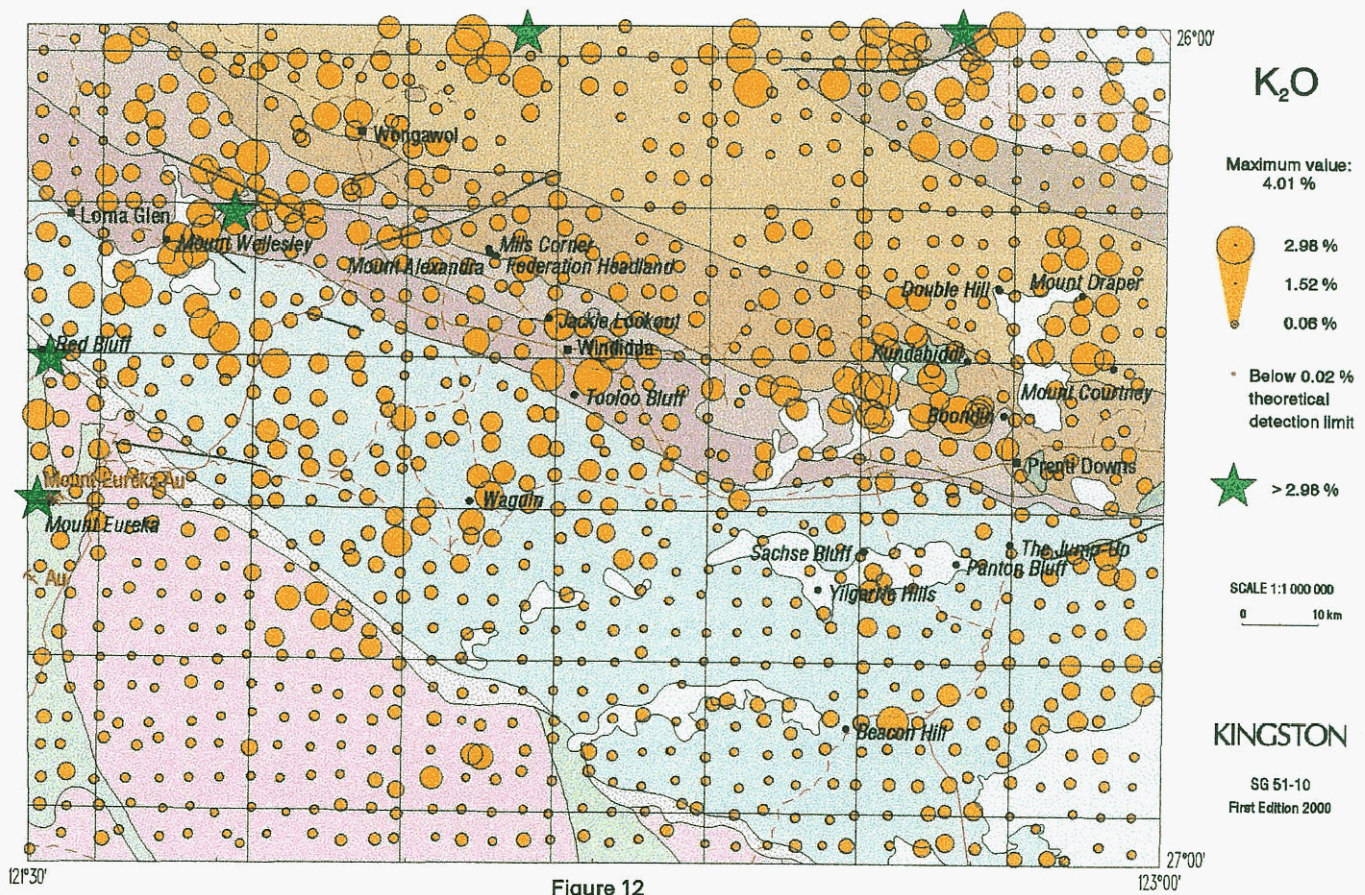


Figure 12

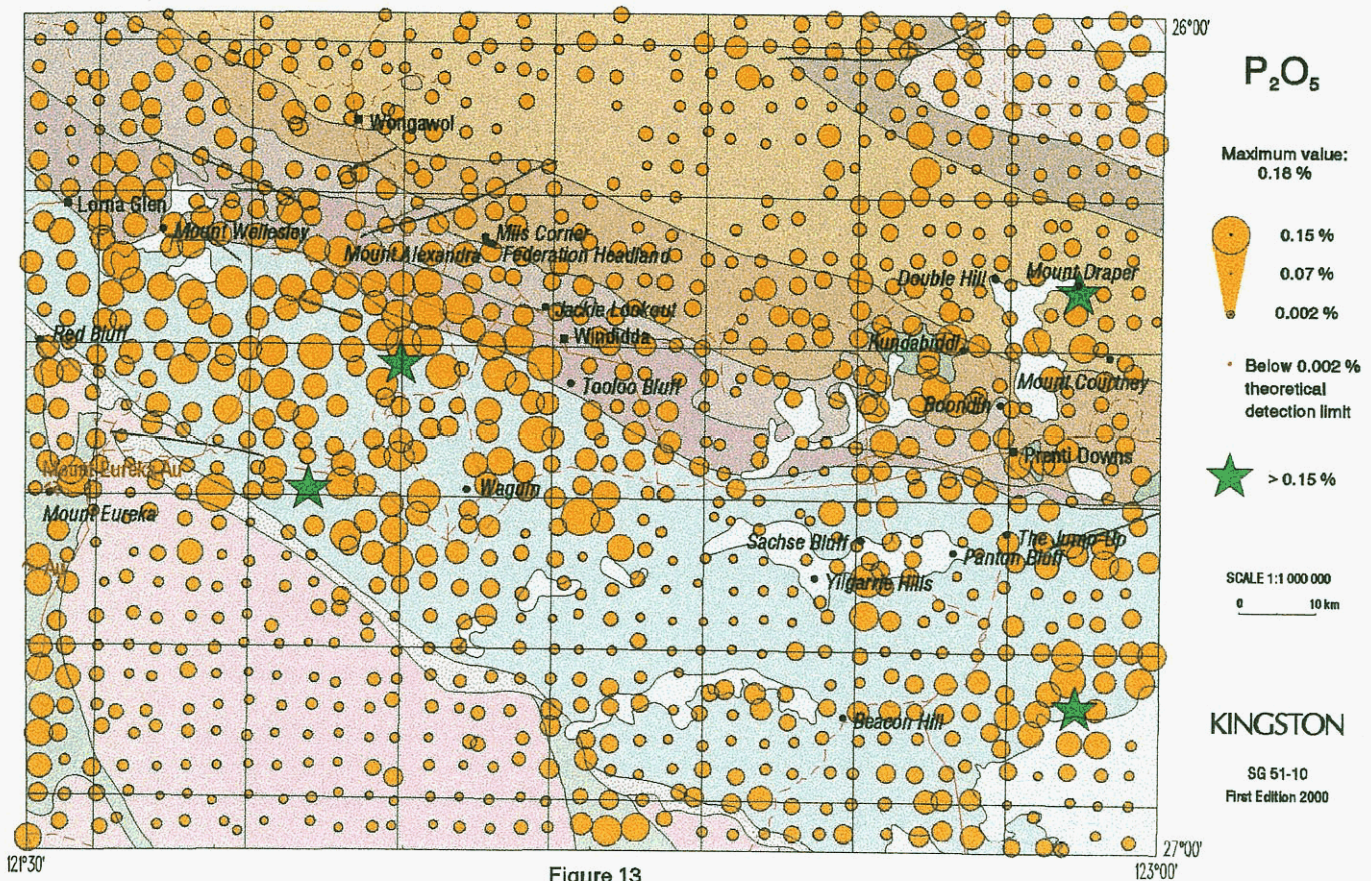


Figure 13

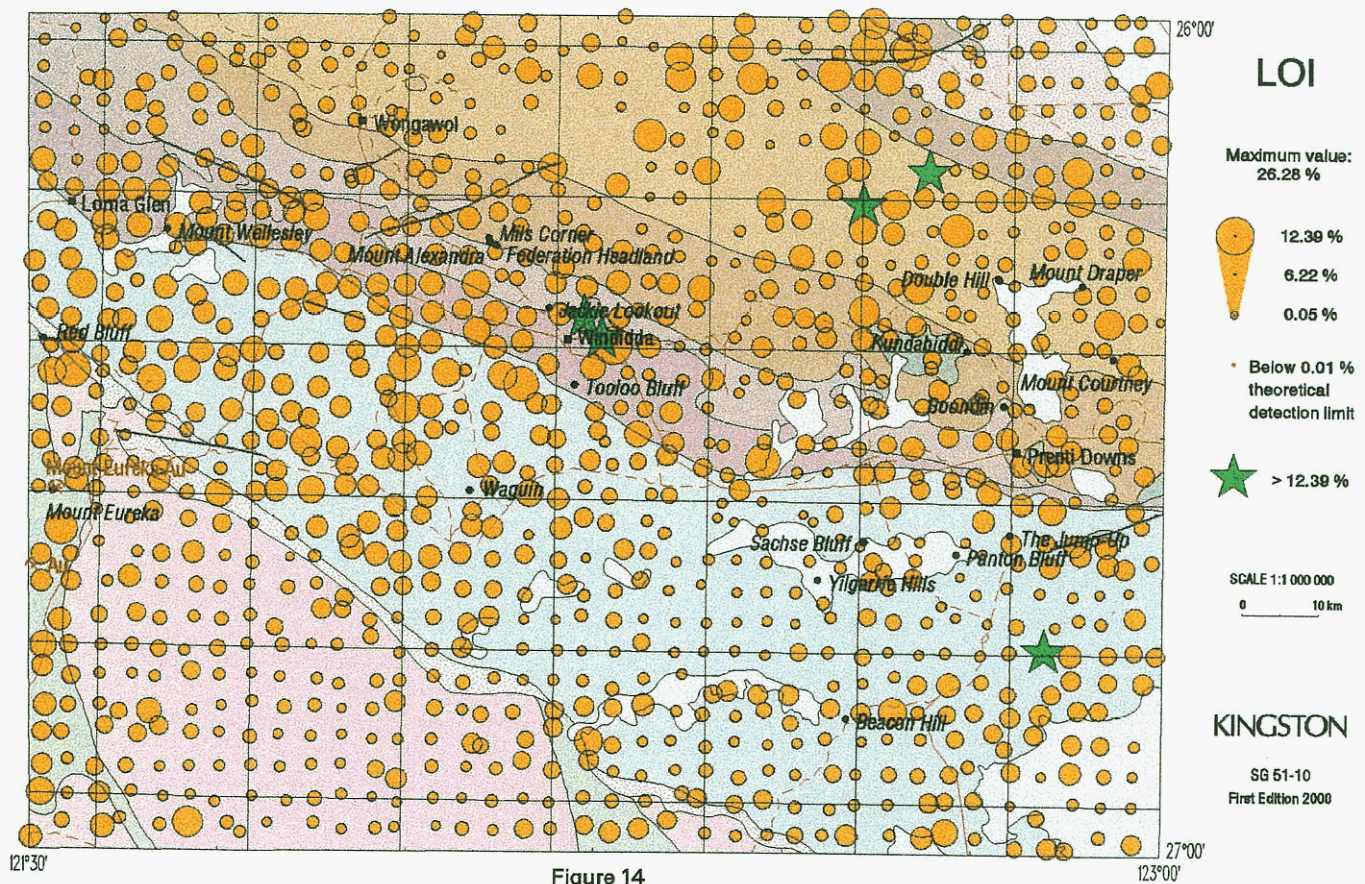
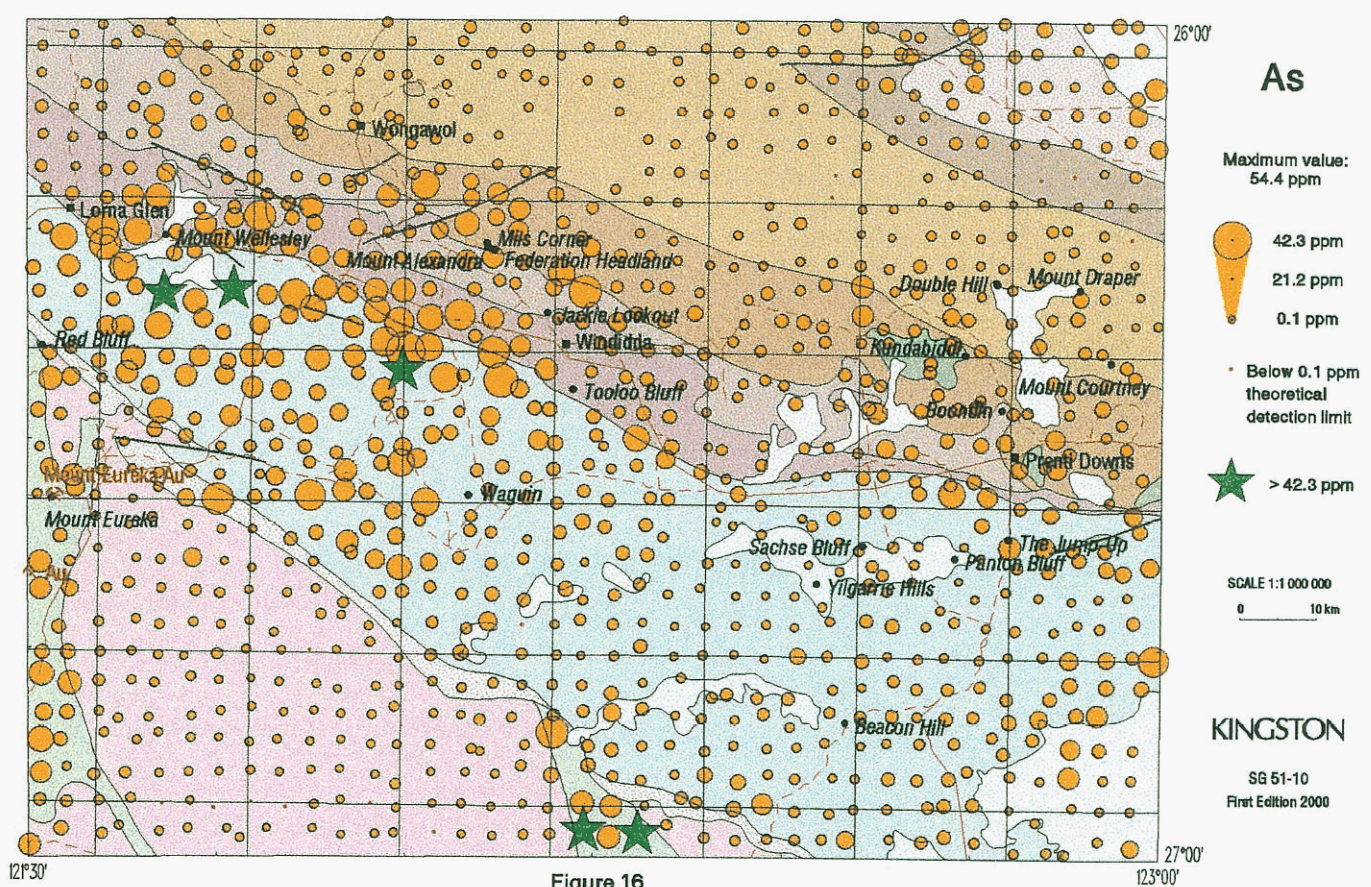
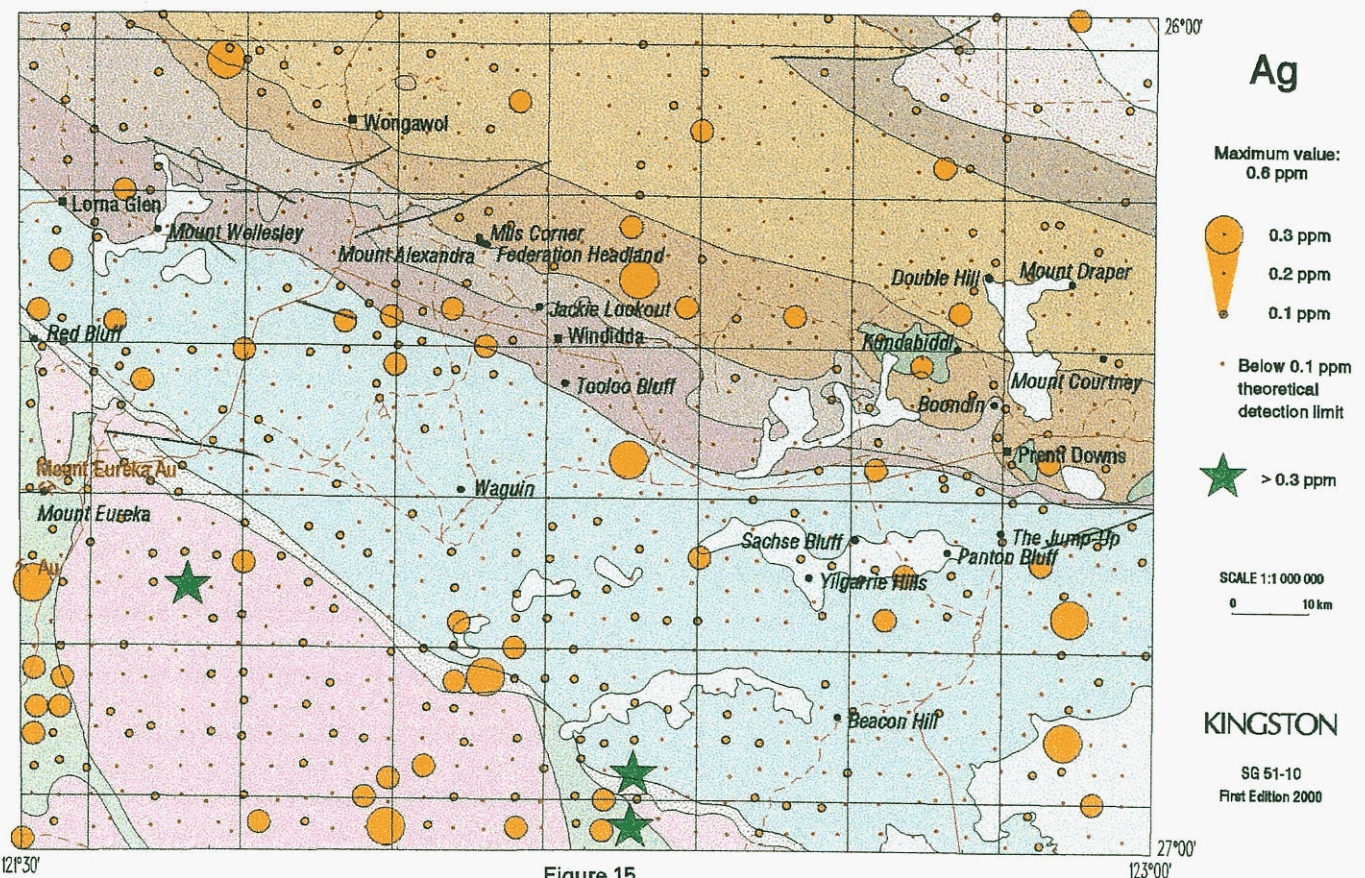


Figure 14



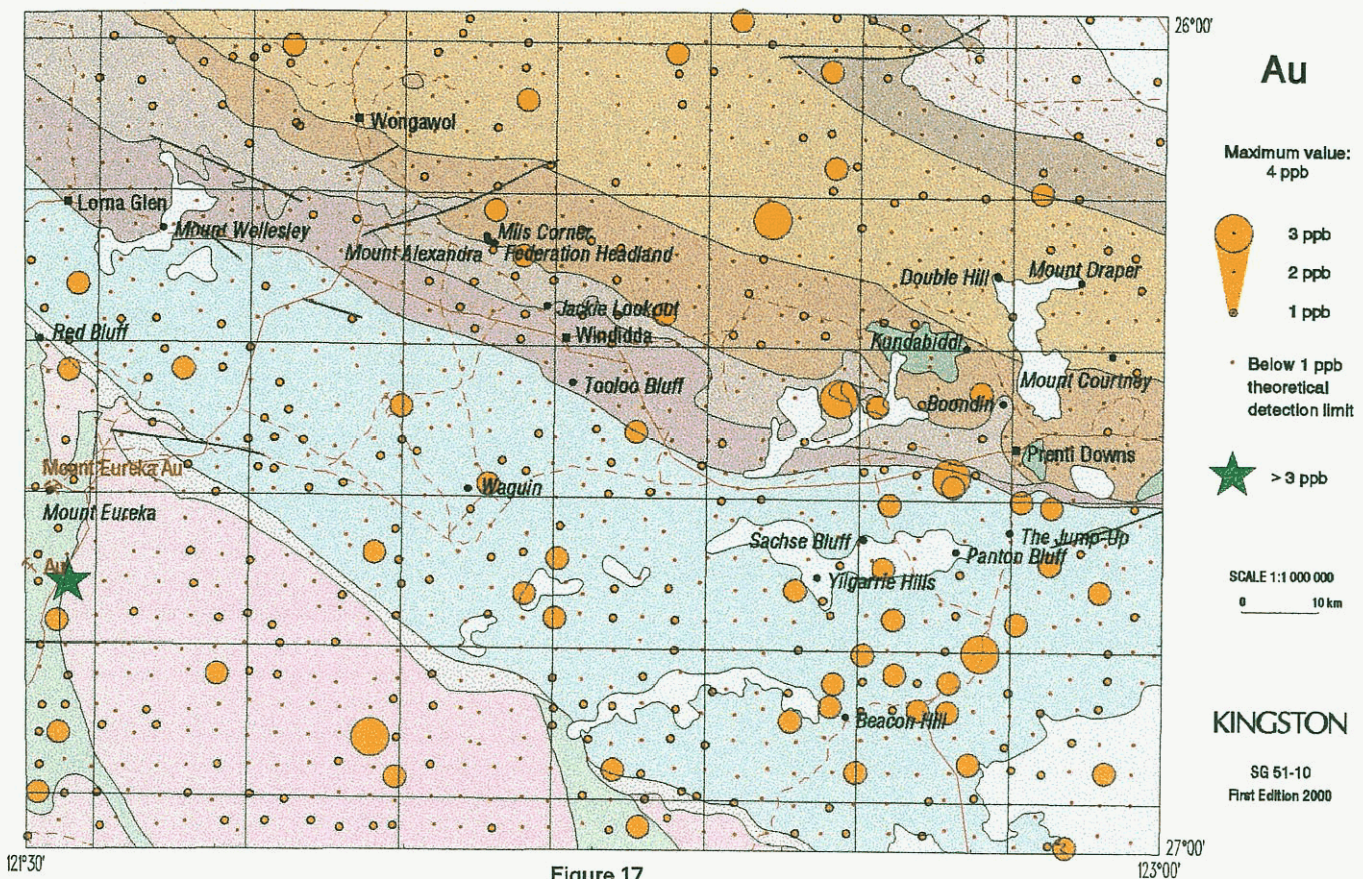


Figure 17

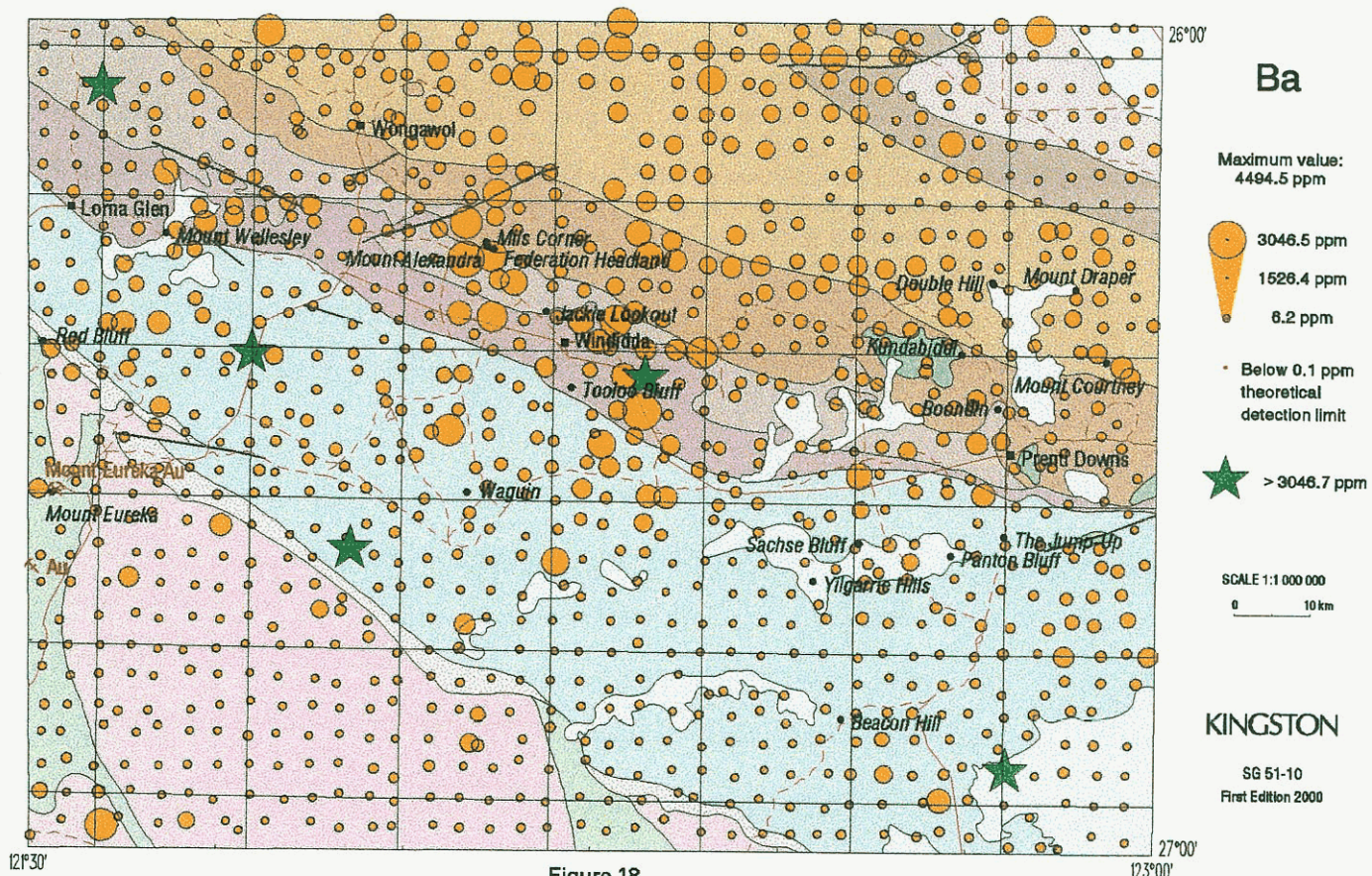


Figure 18

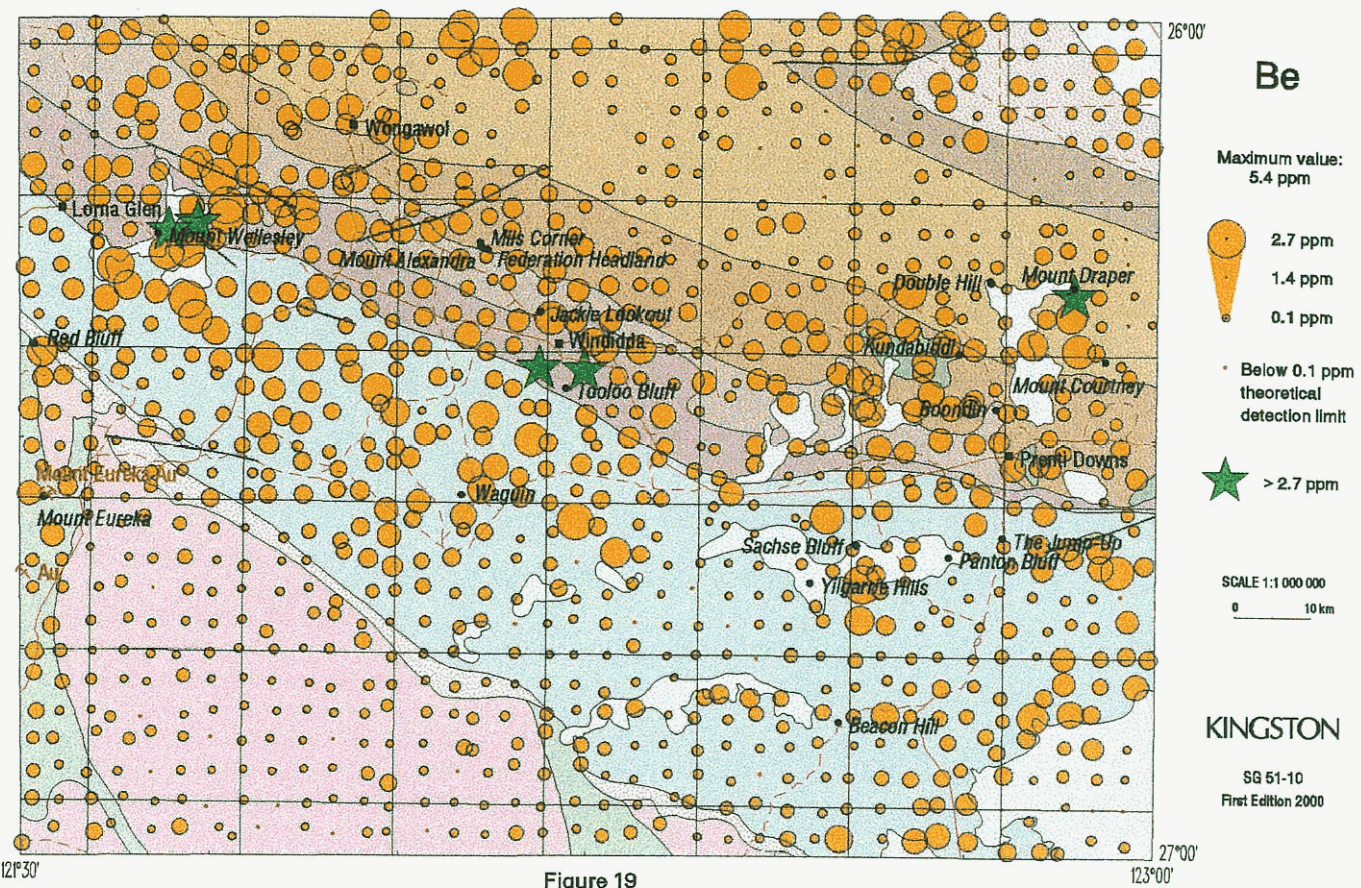


Figure 19

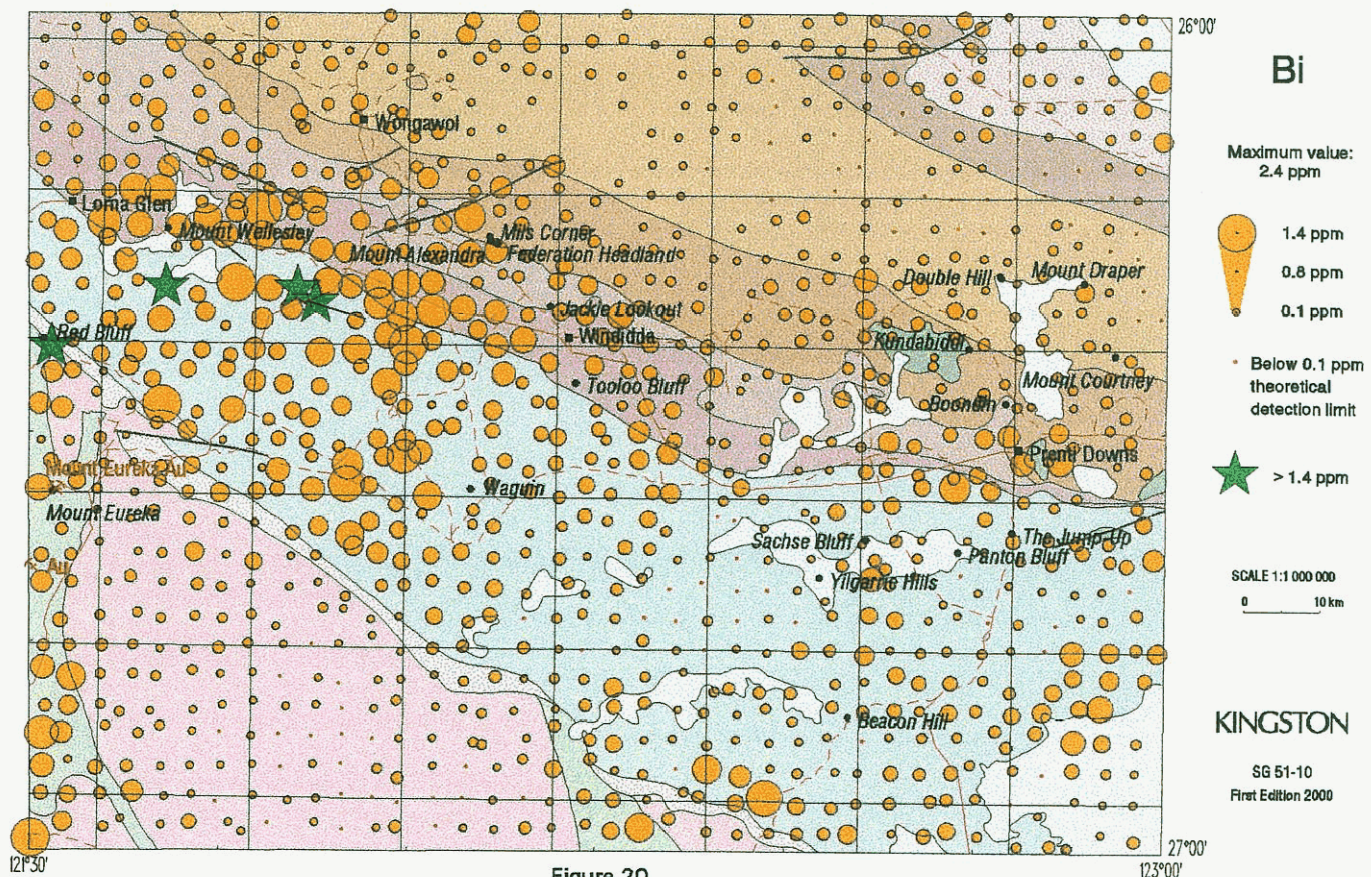
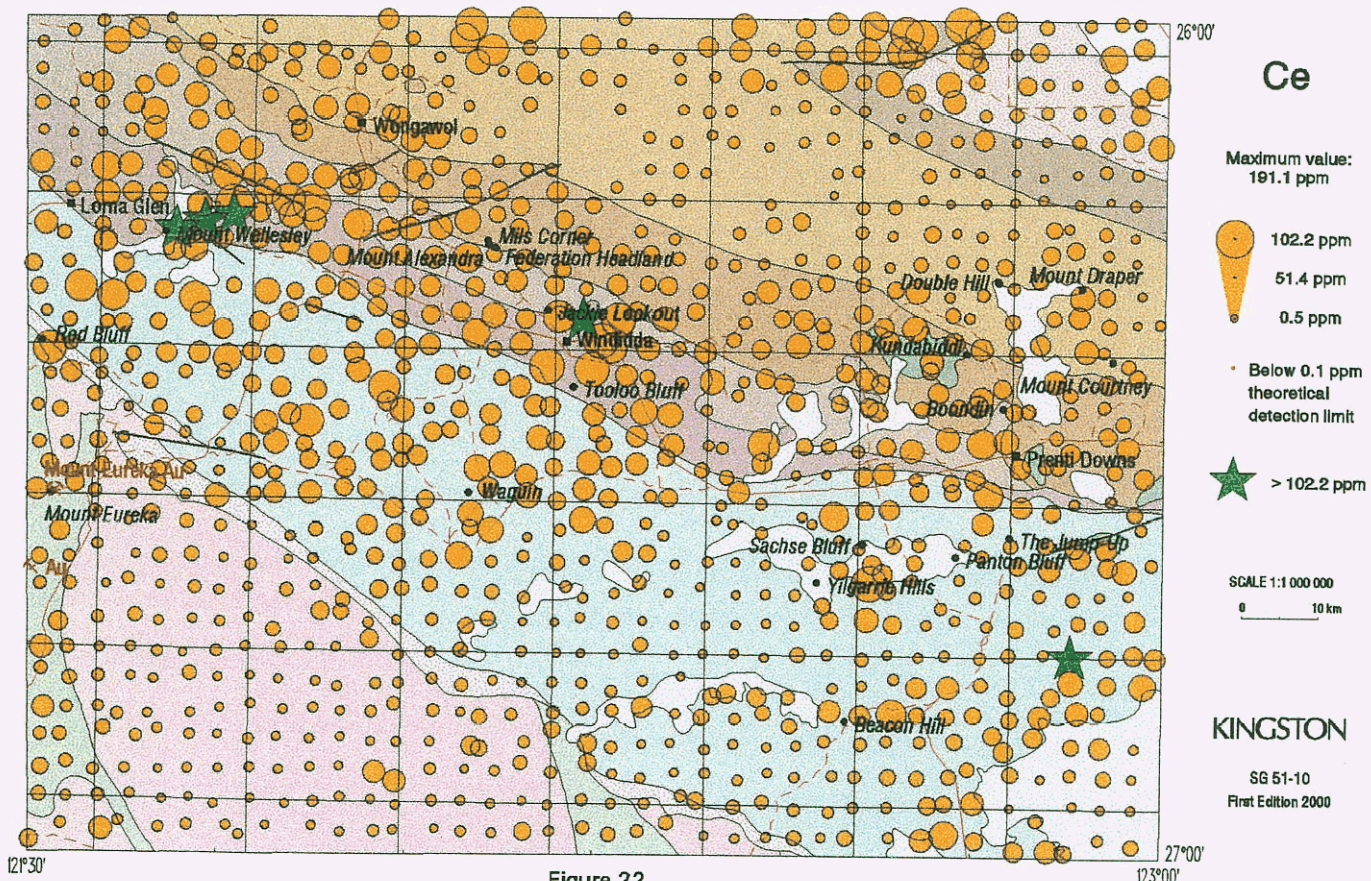
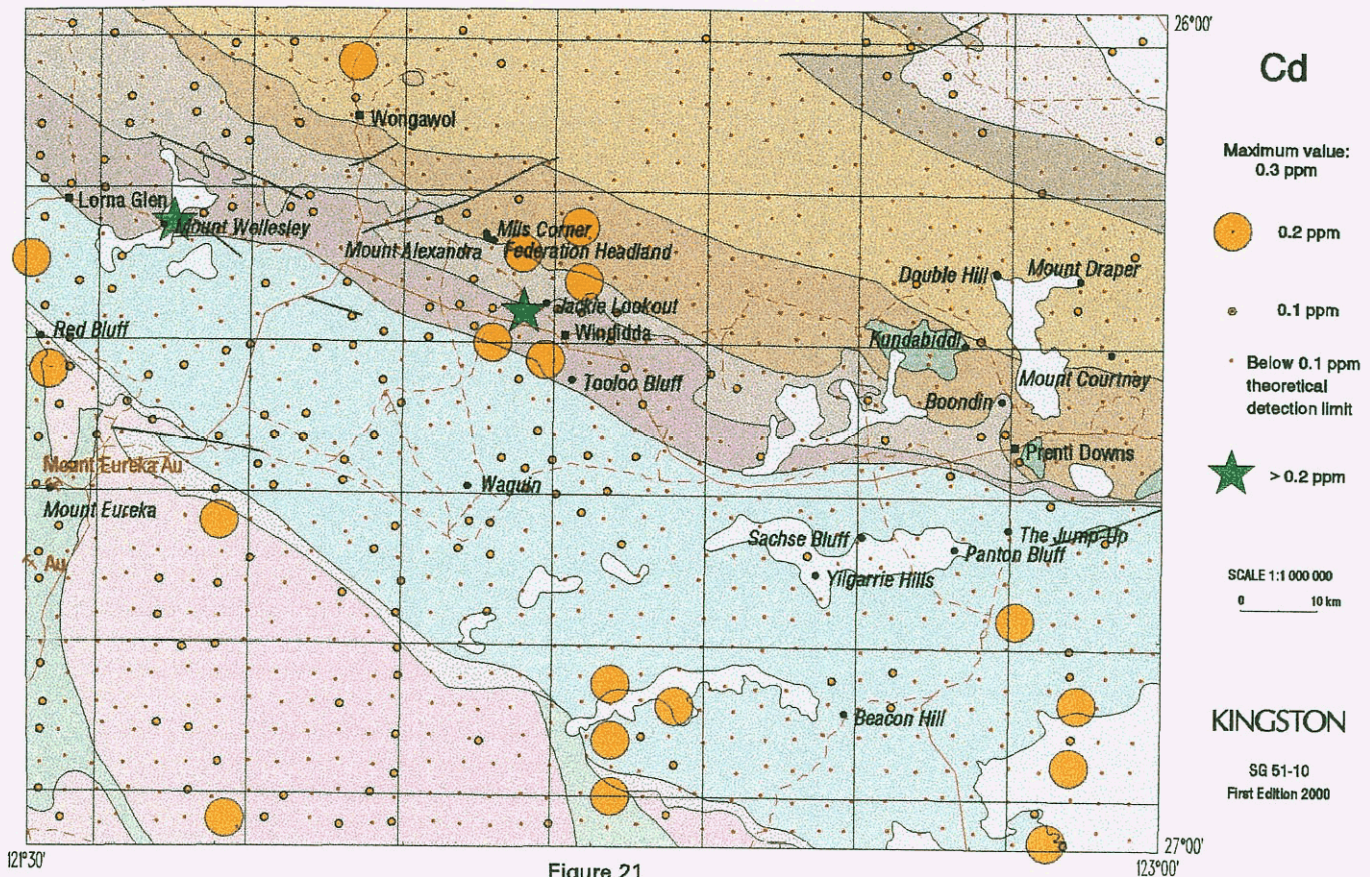


Figure 20



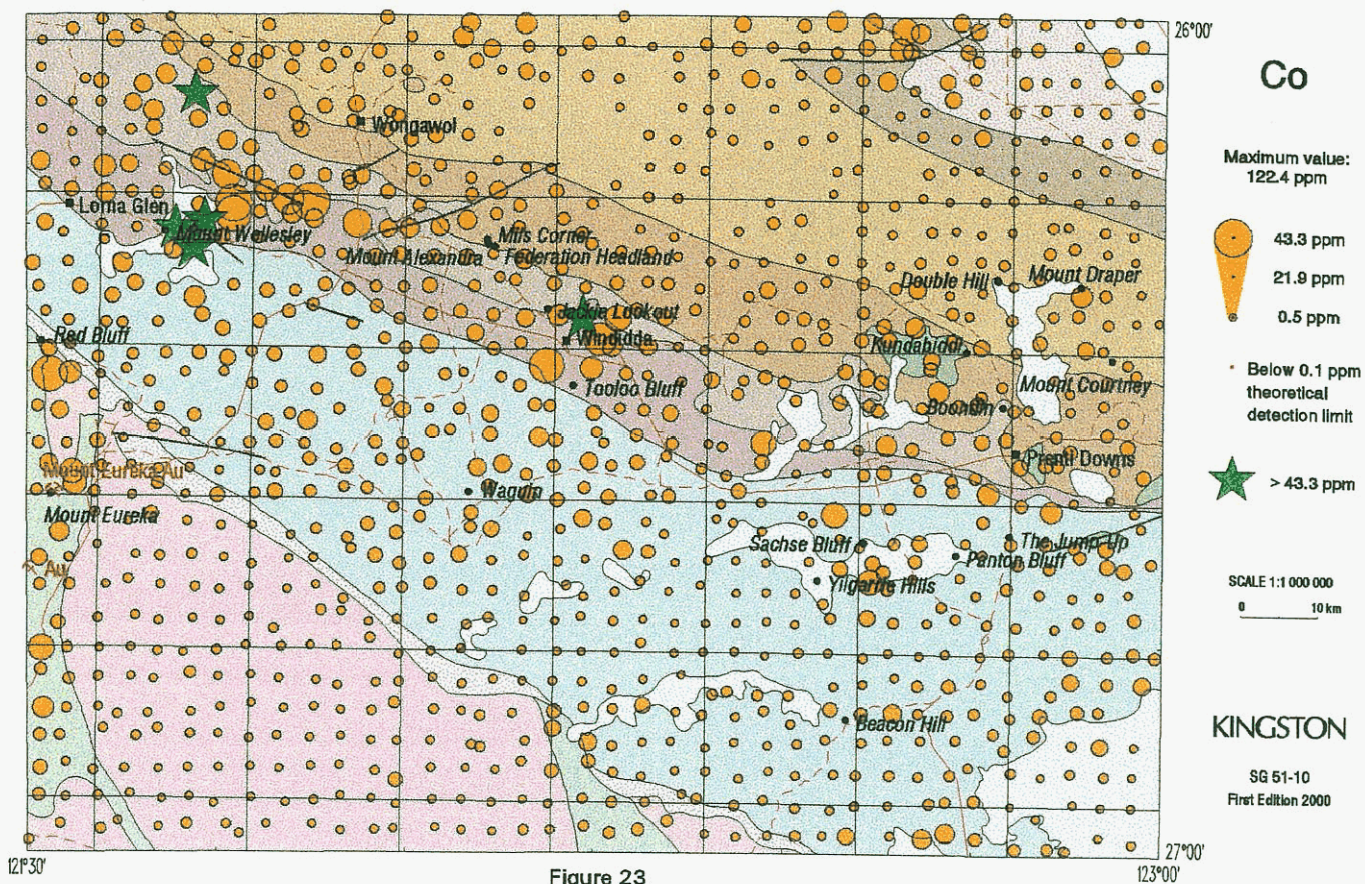


Figure 23

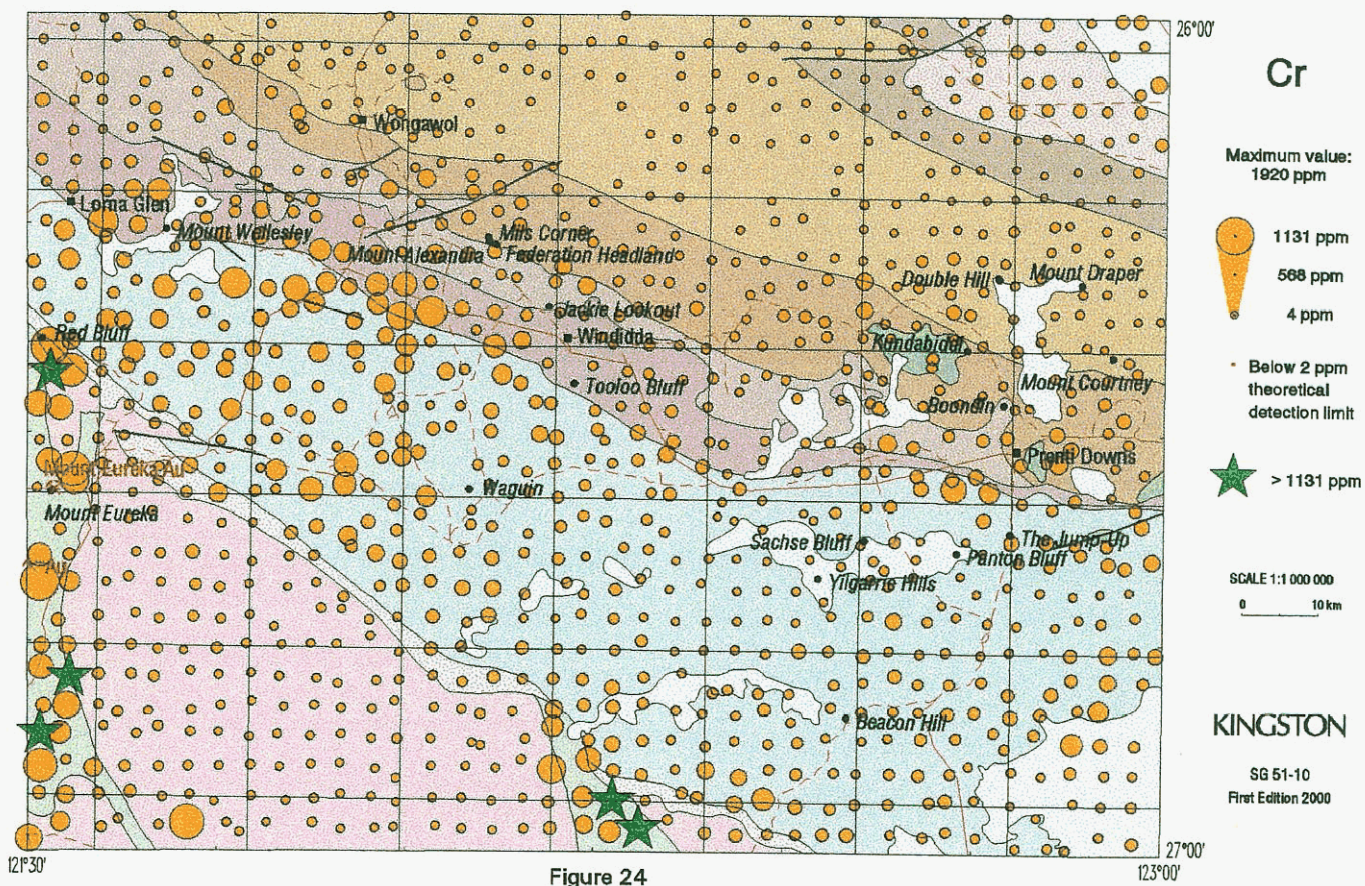


Figure 24

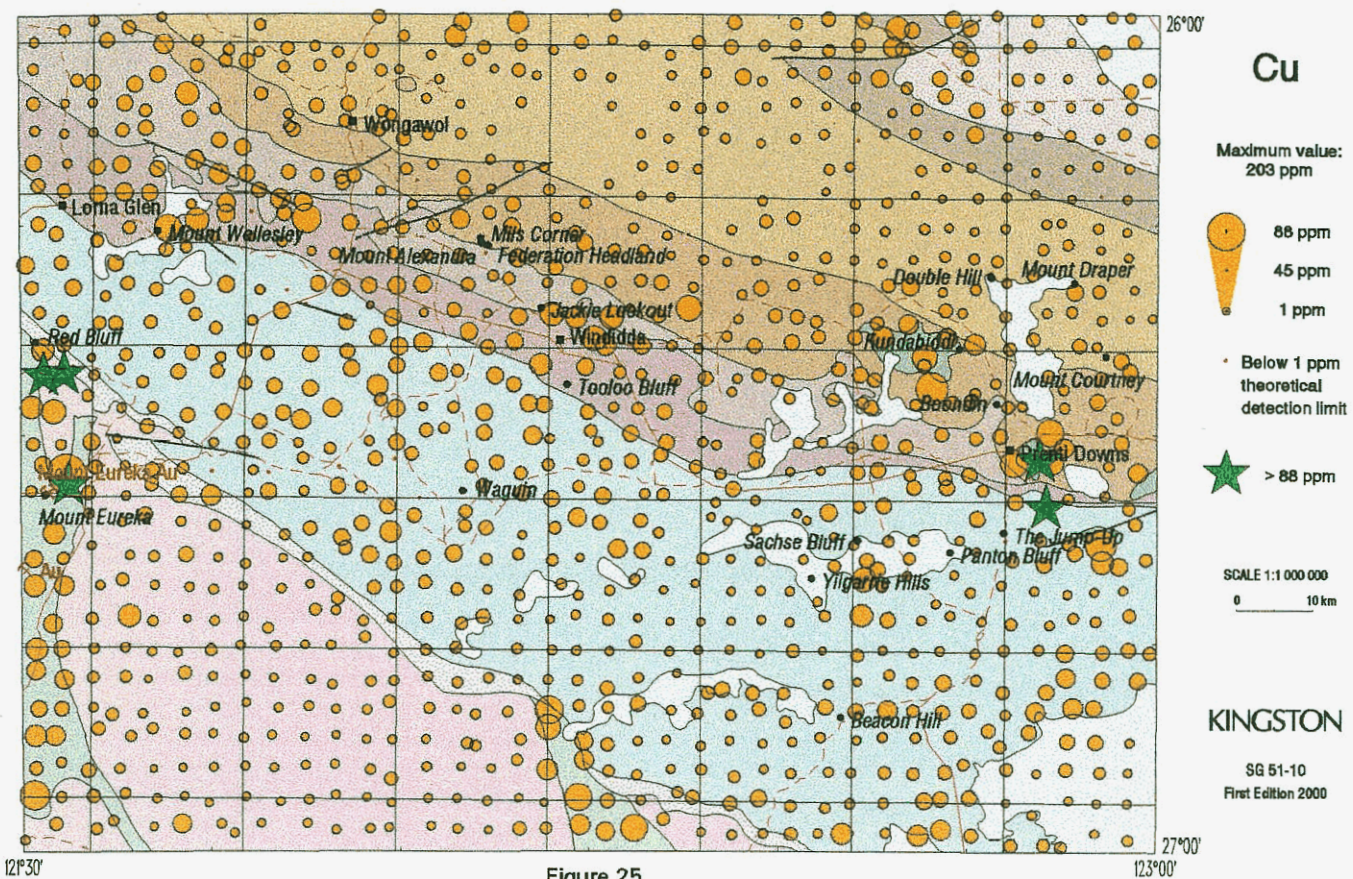


Figure 25

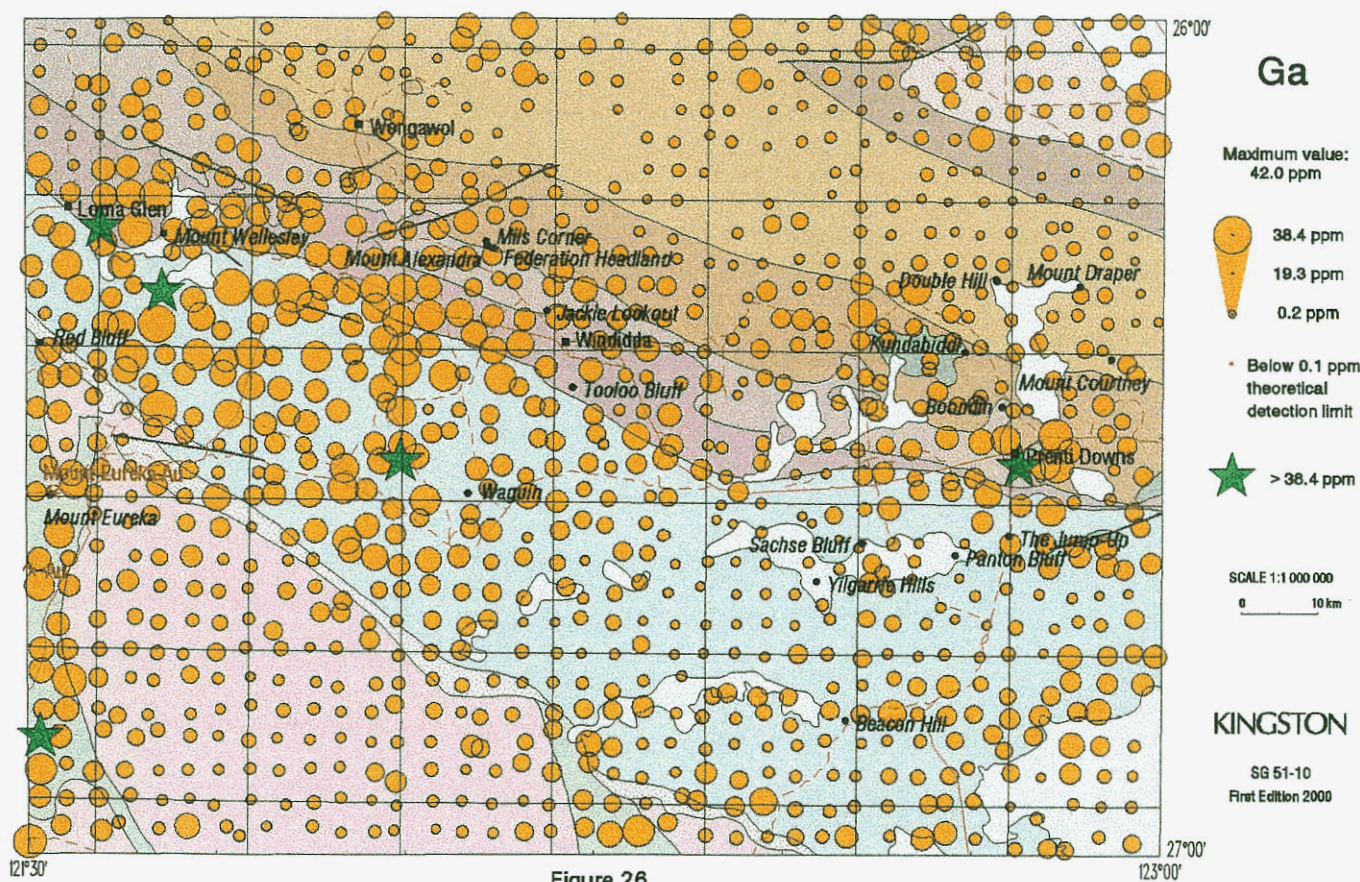


Figure 26

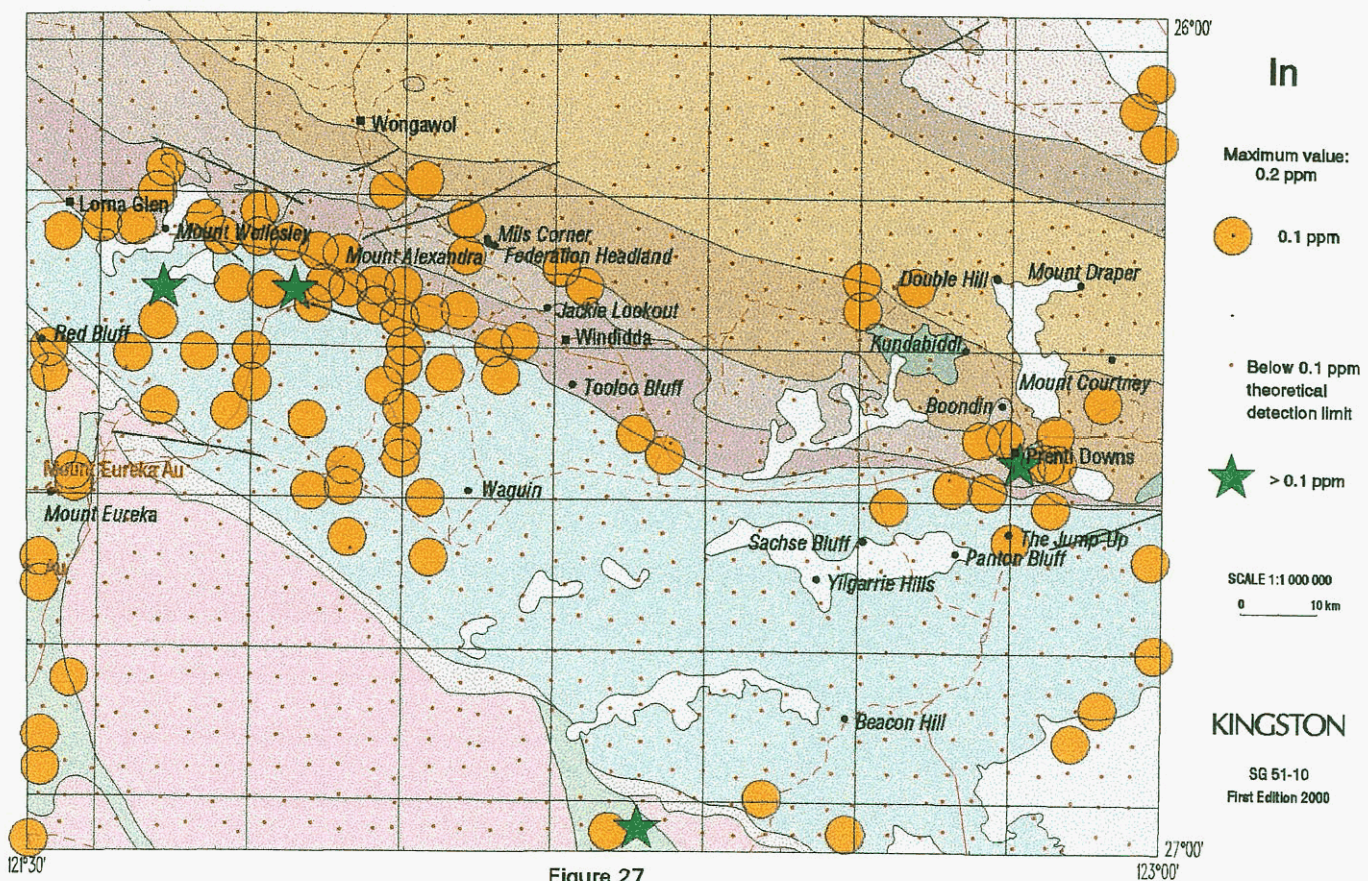


Figure 27

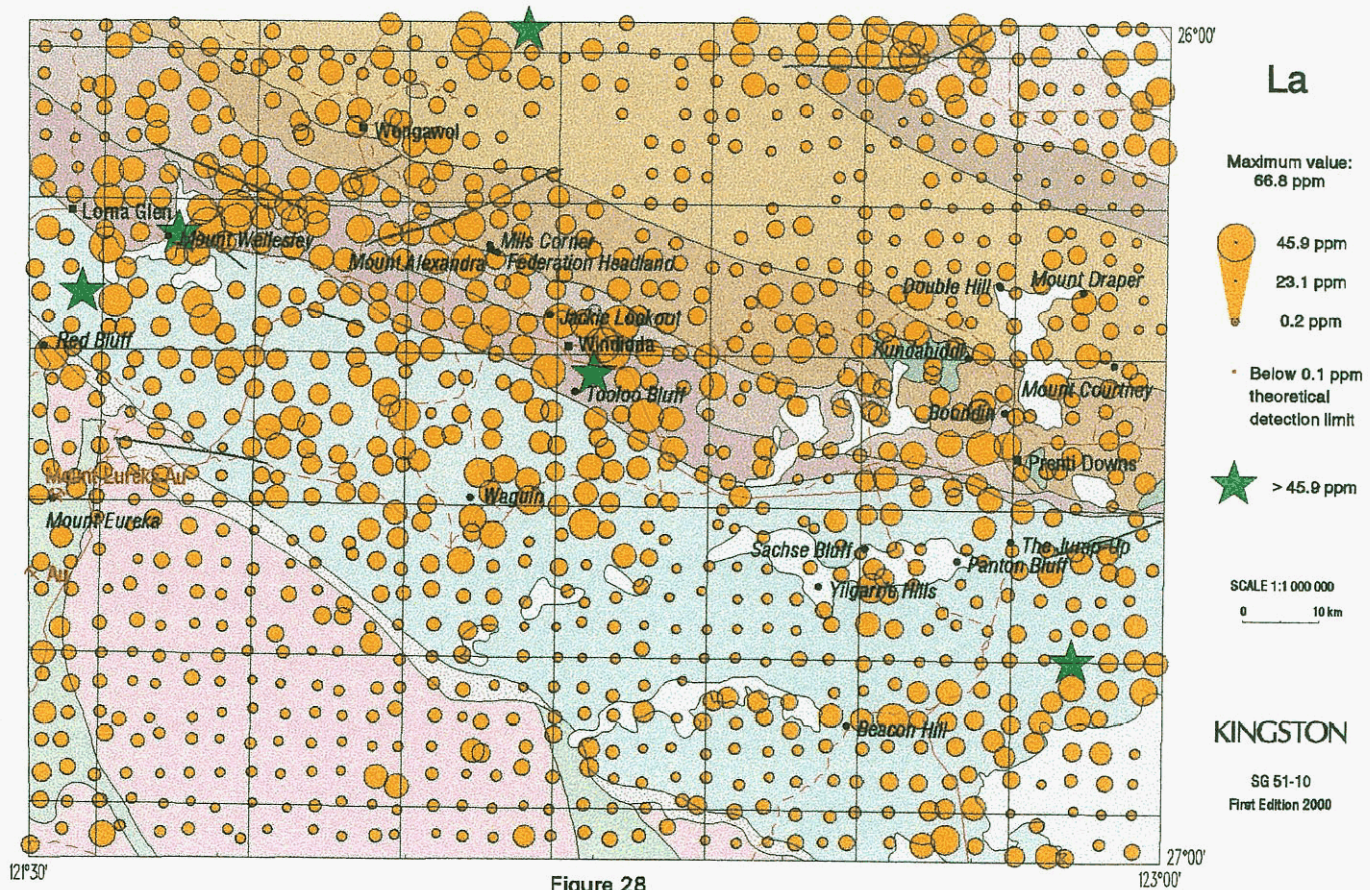
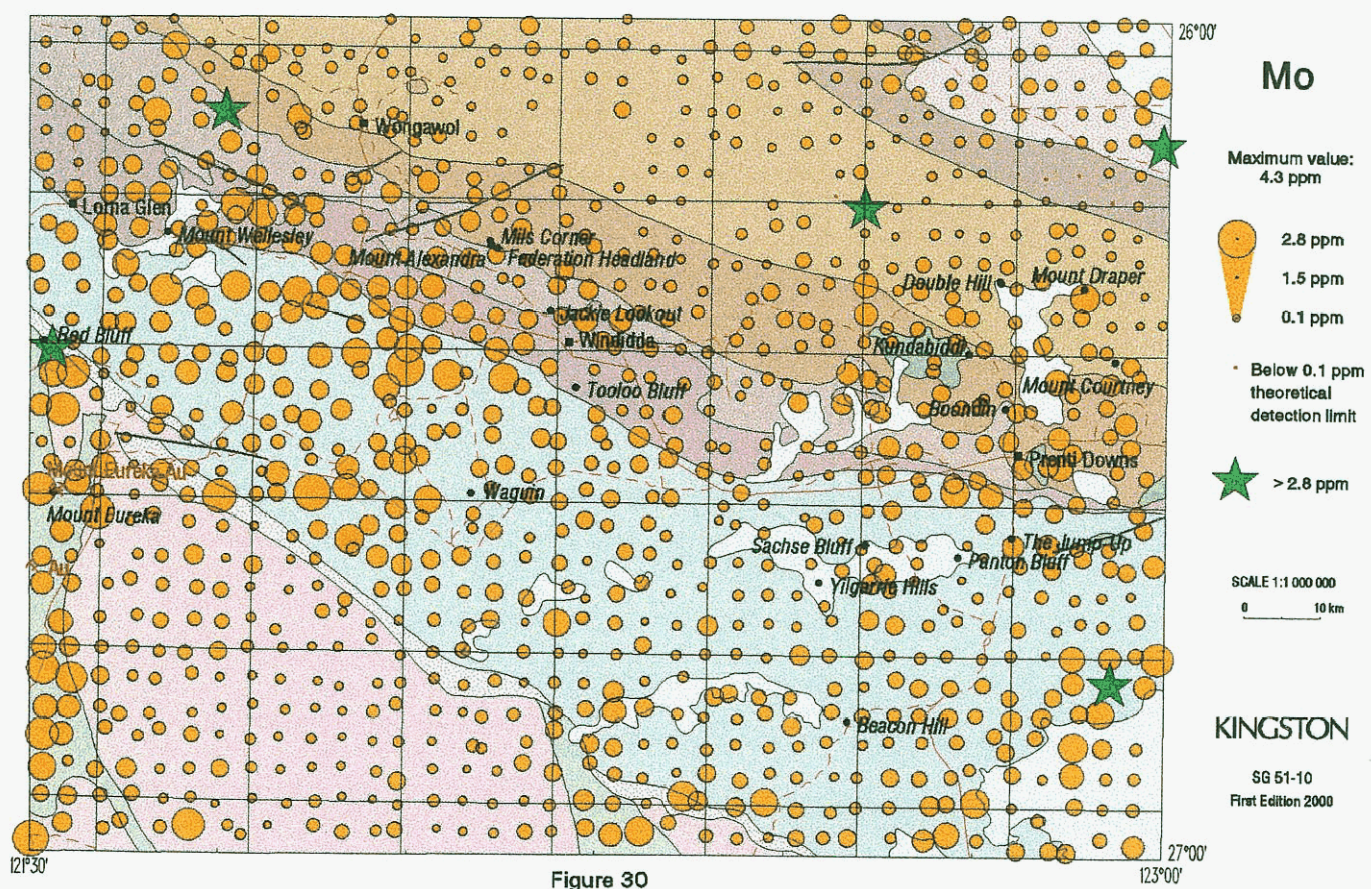
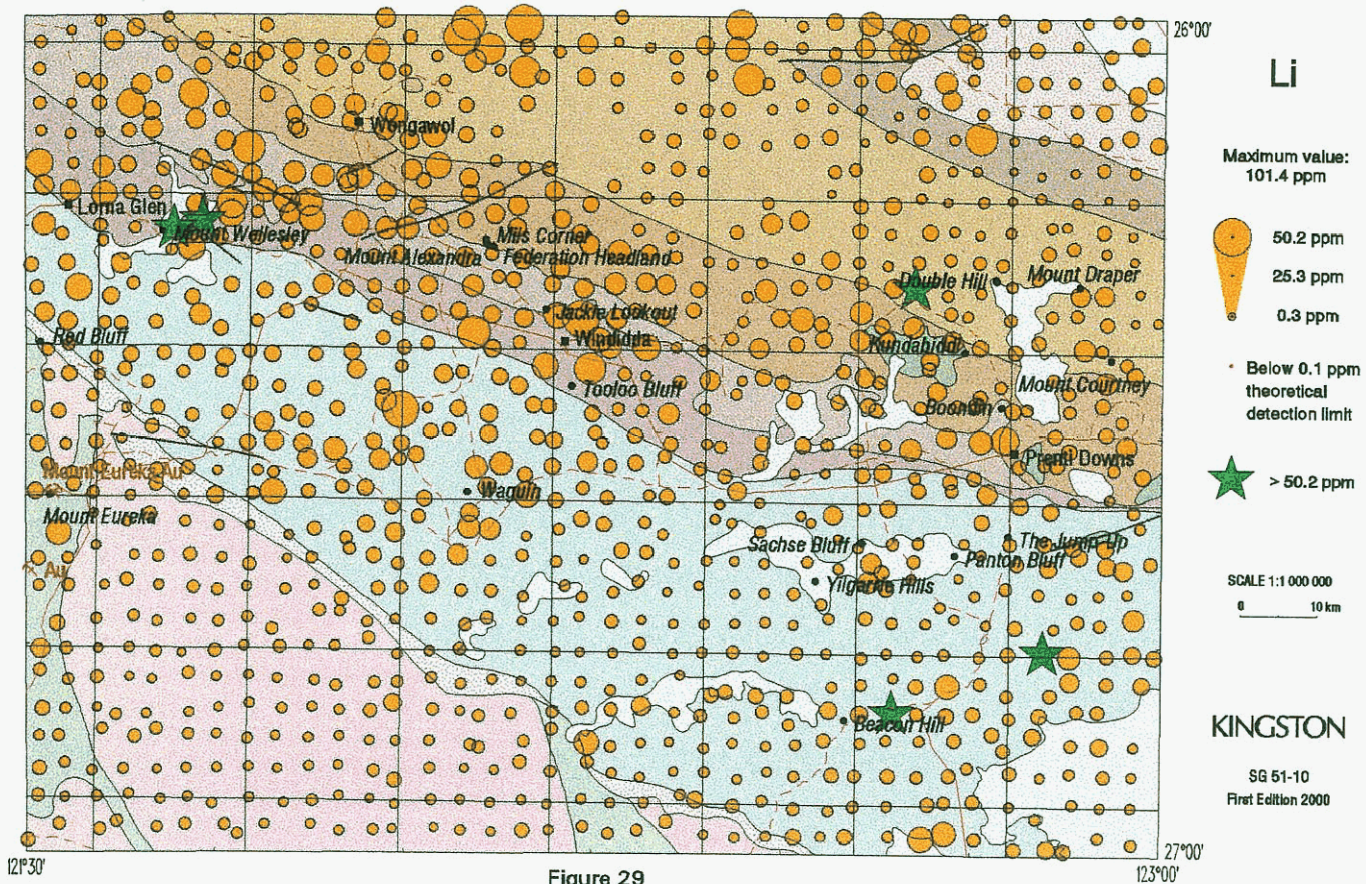
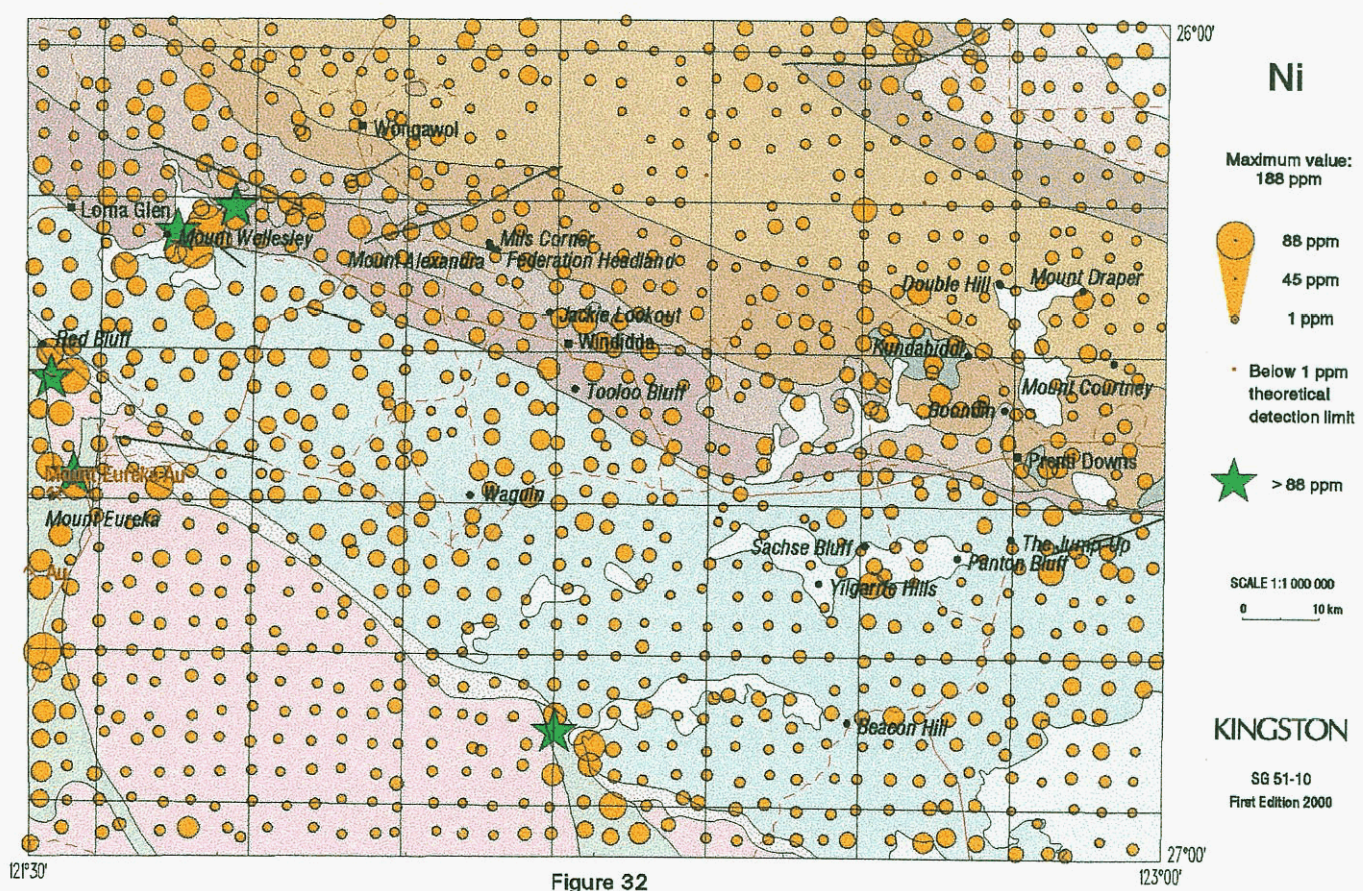
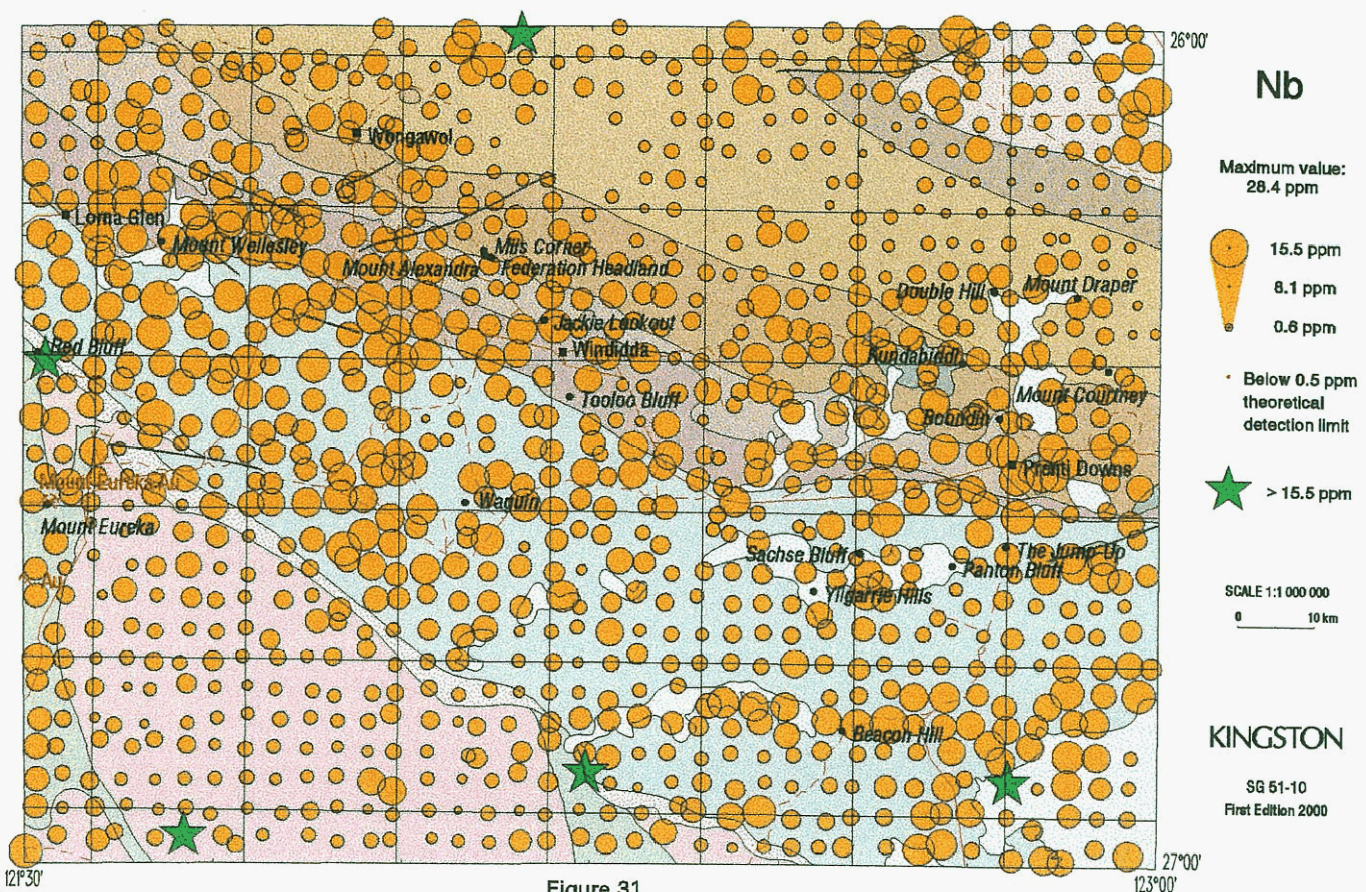
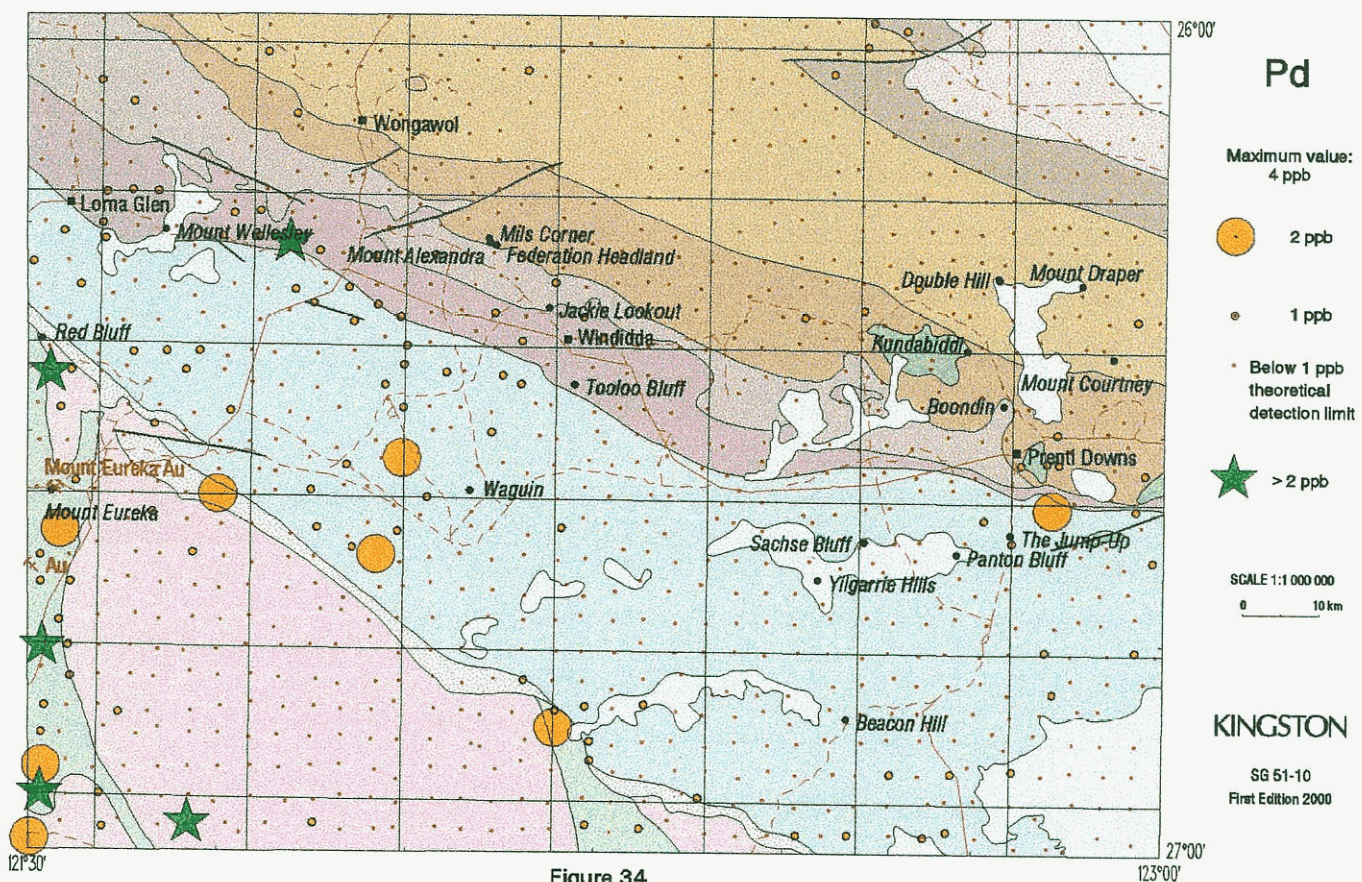
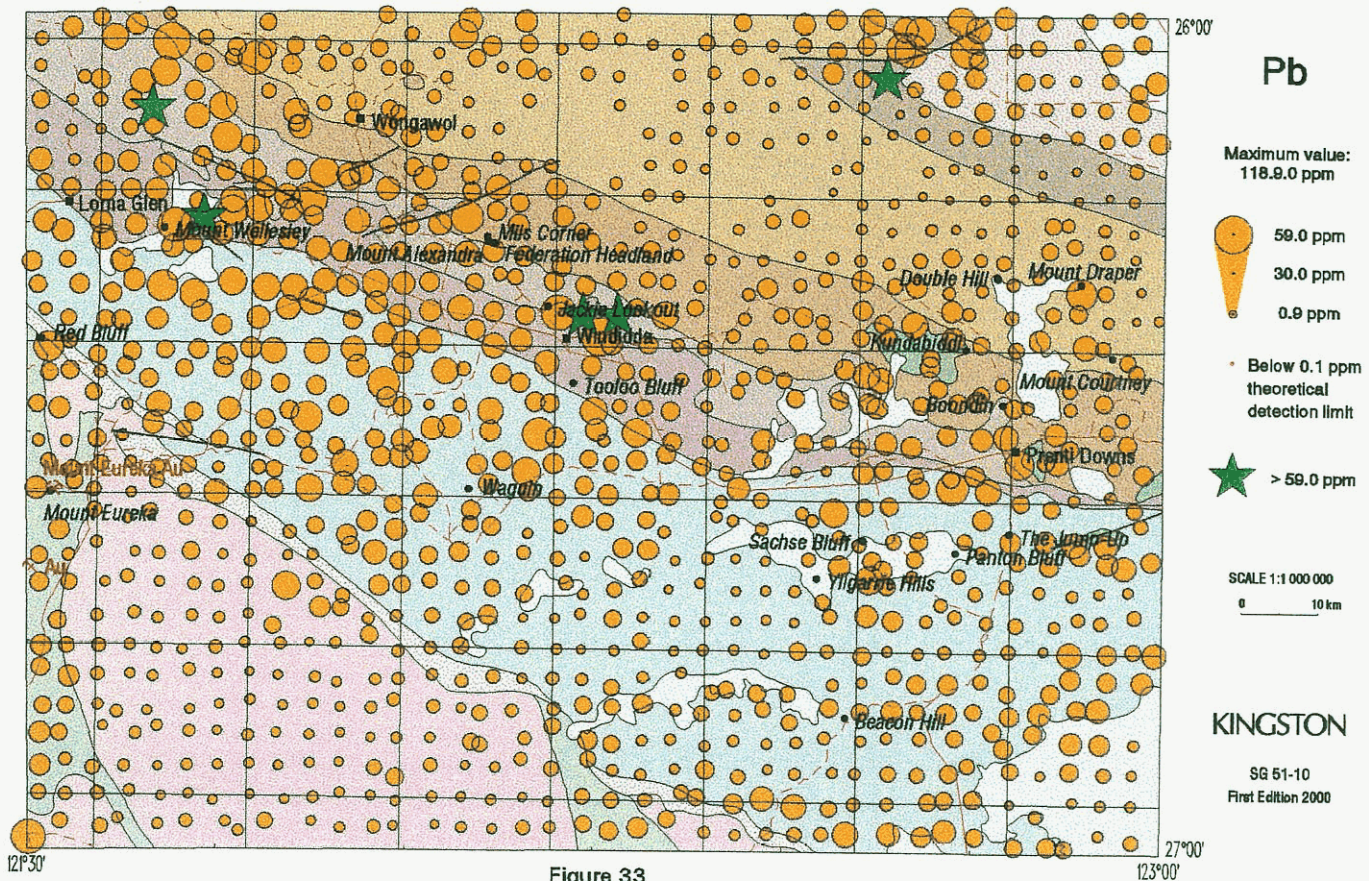


Figure 28







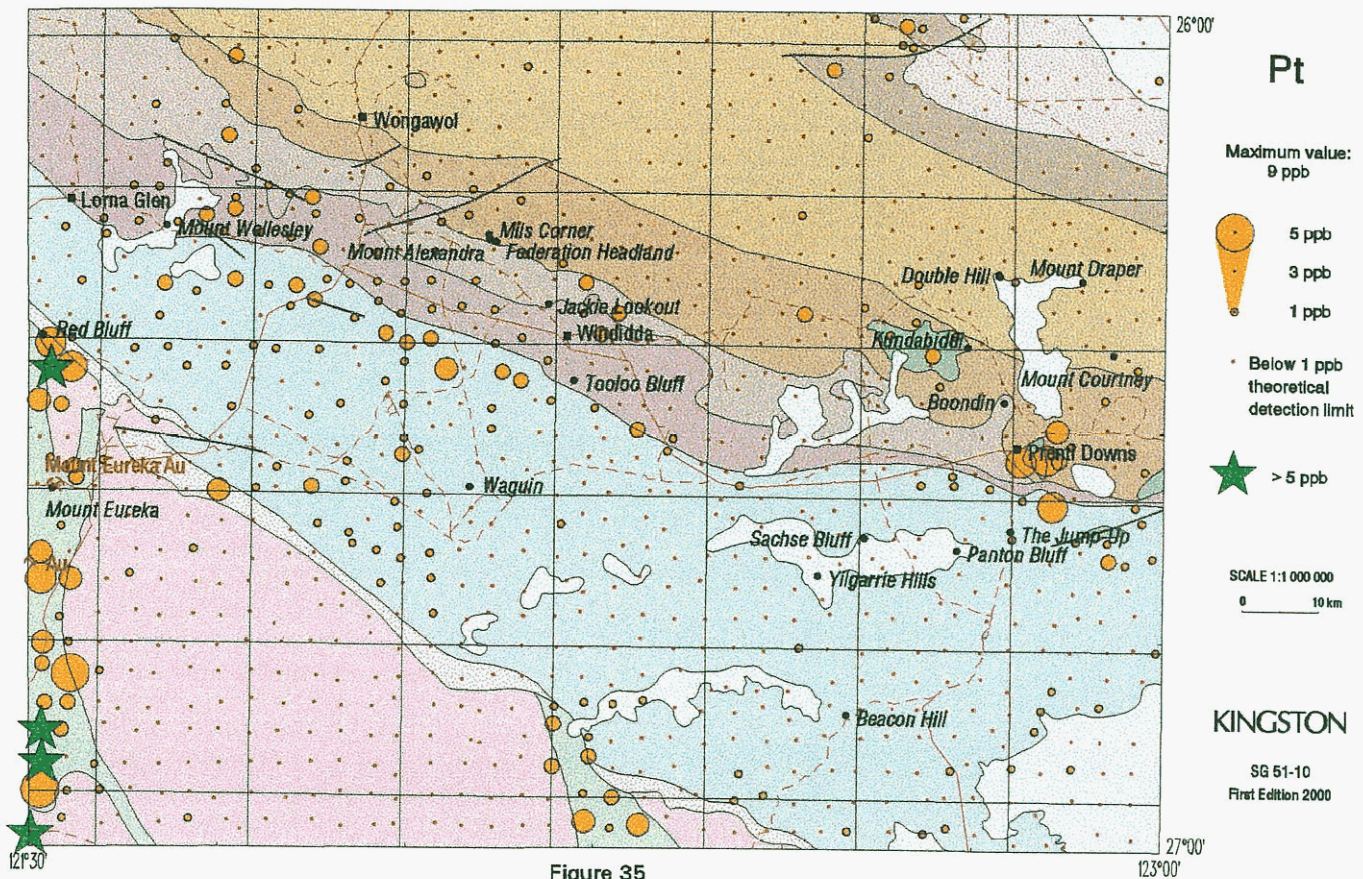


Figure 35

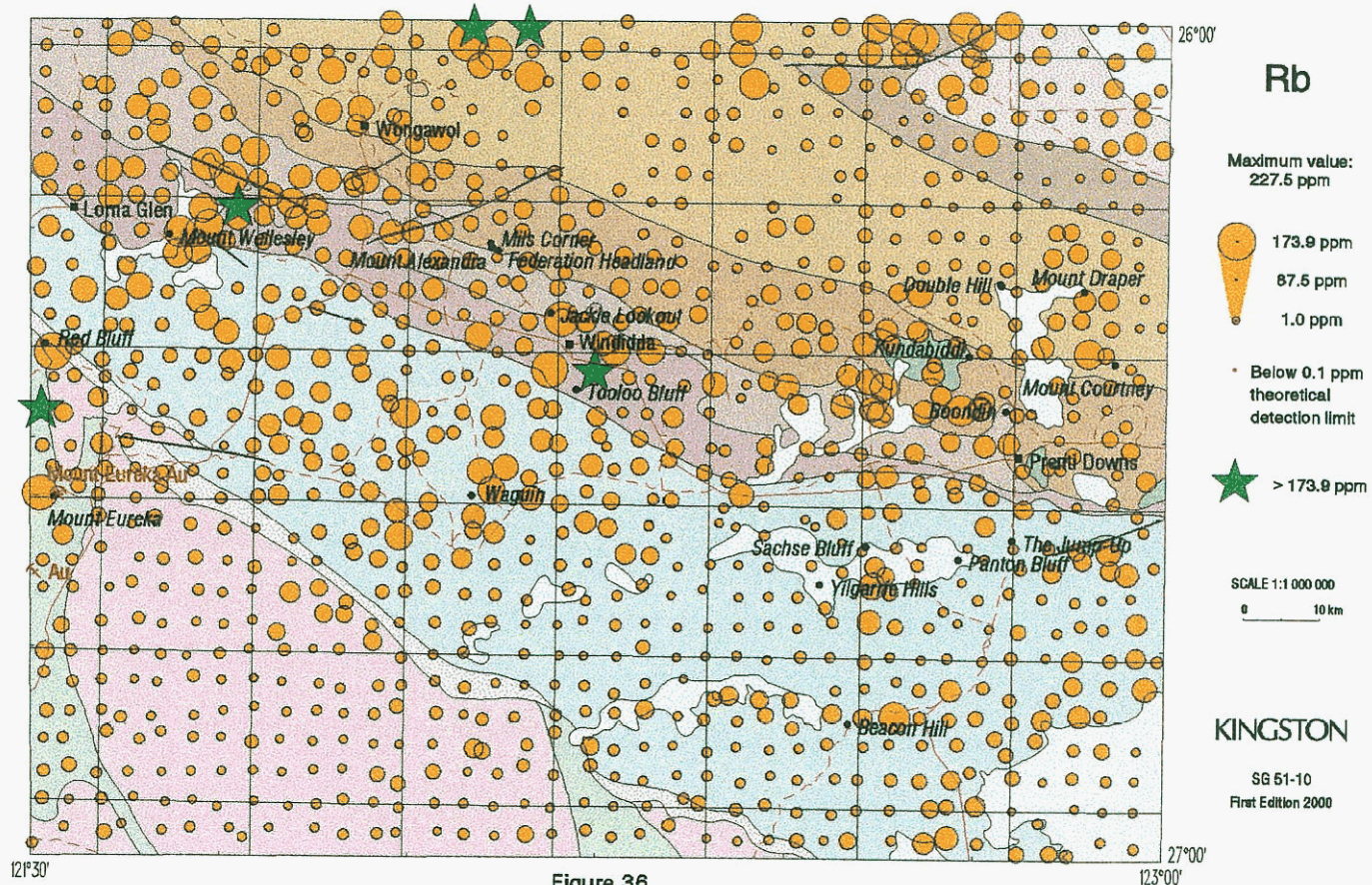


Figure 36

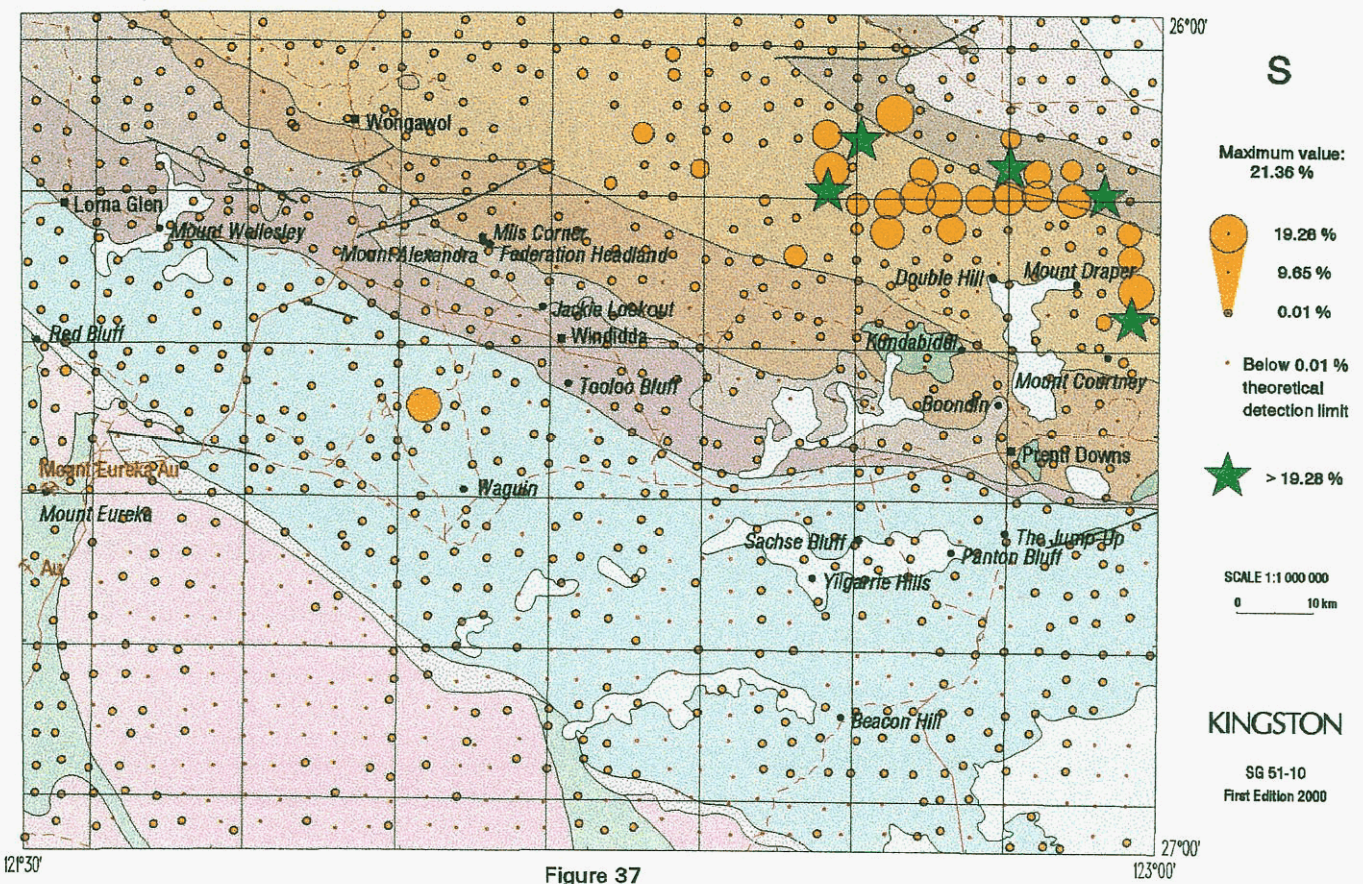


Figure 37

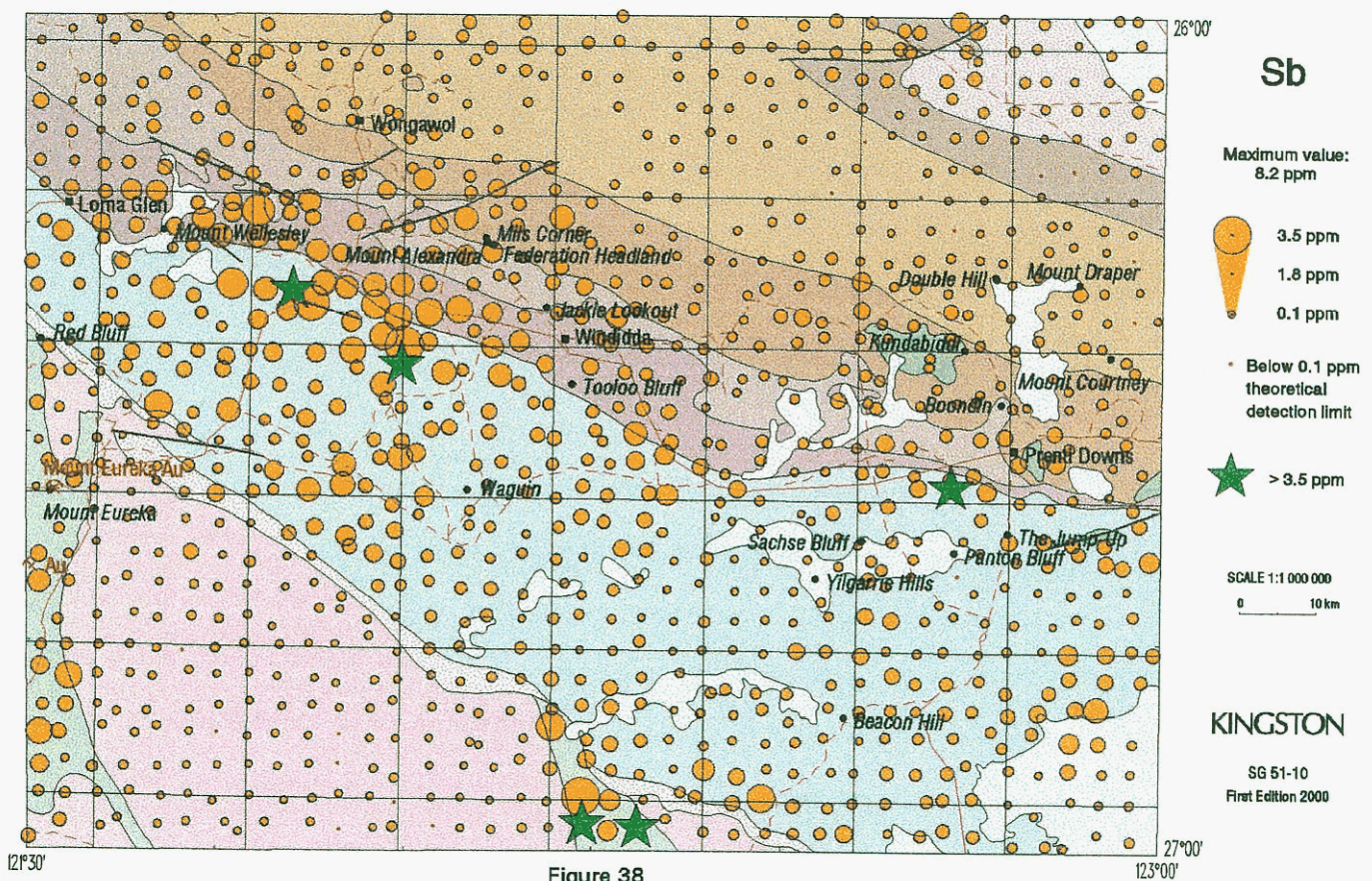


Figure 38

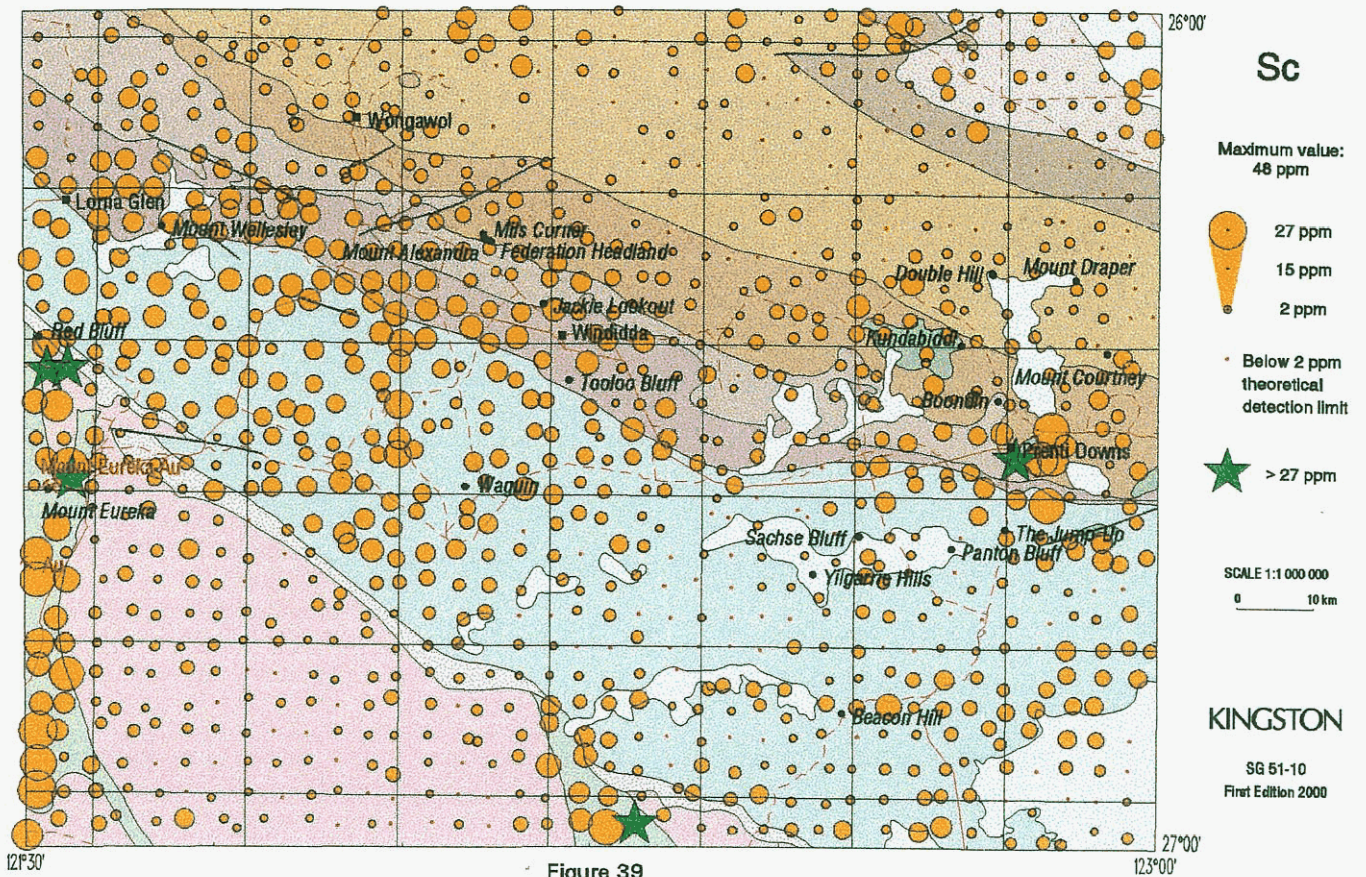


Figure 39

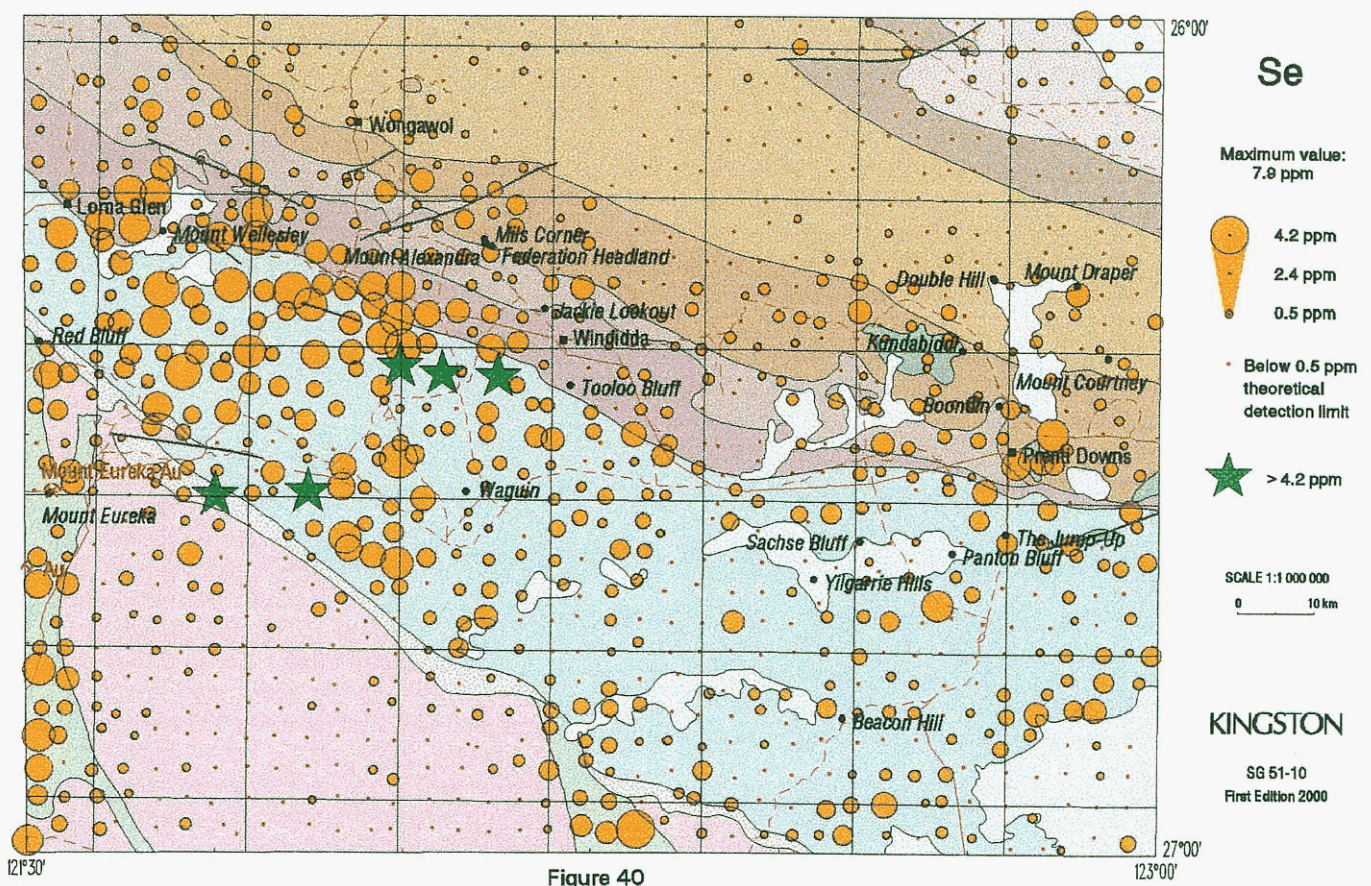


Figure 40

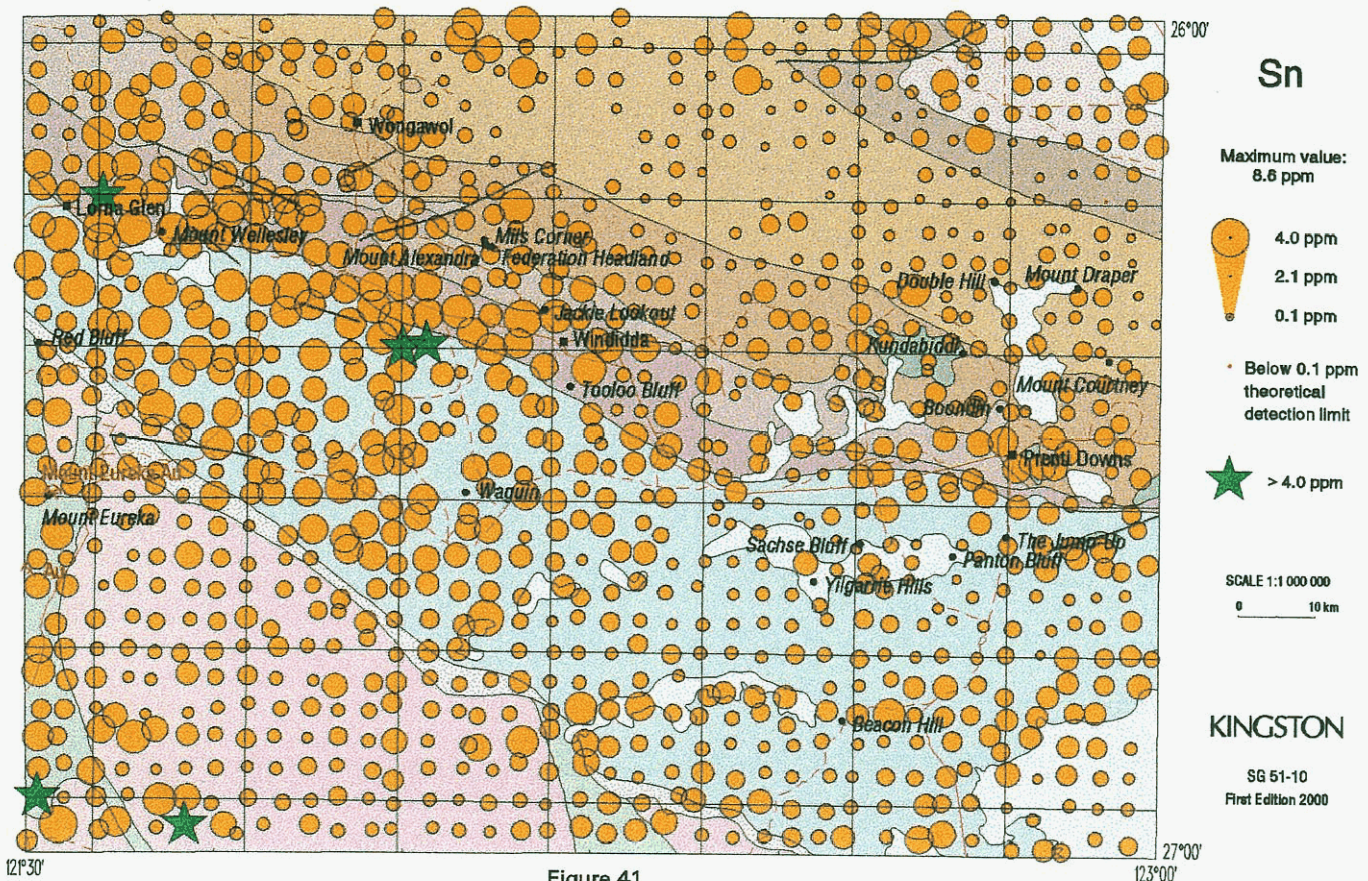


Figure 41

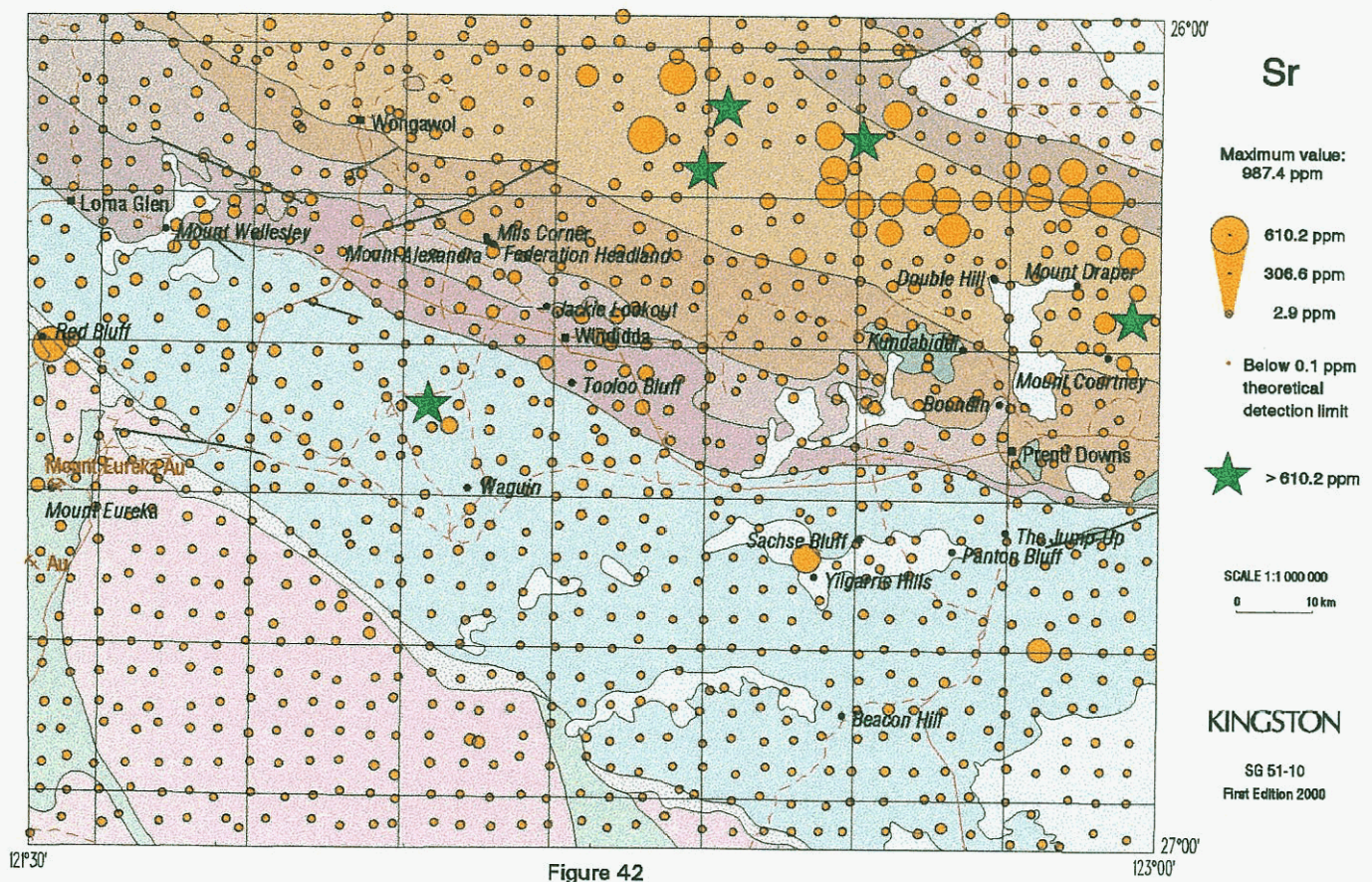


Figure 42

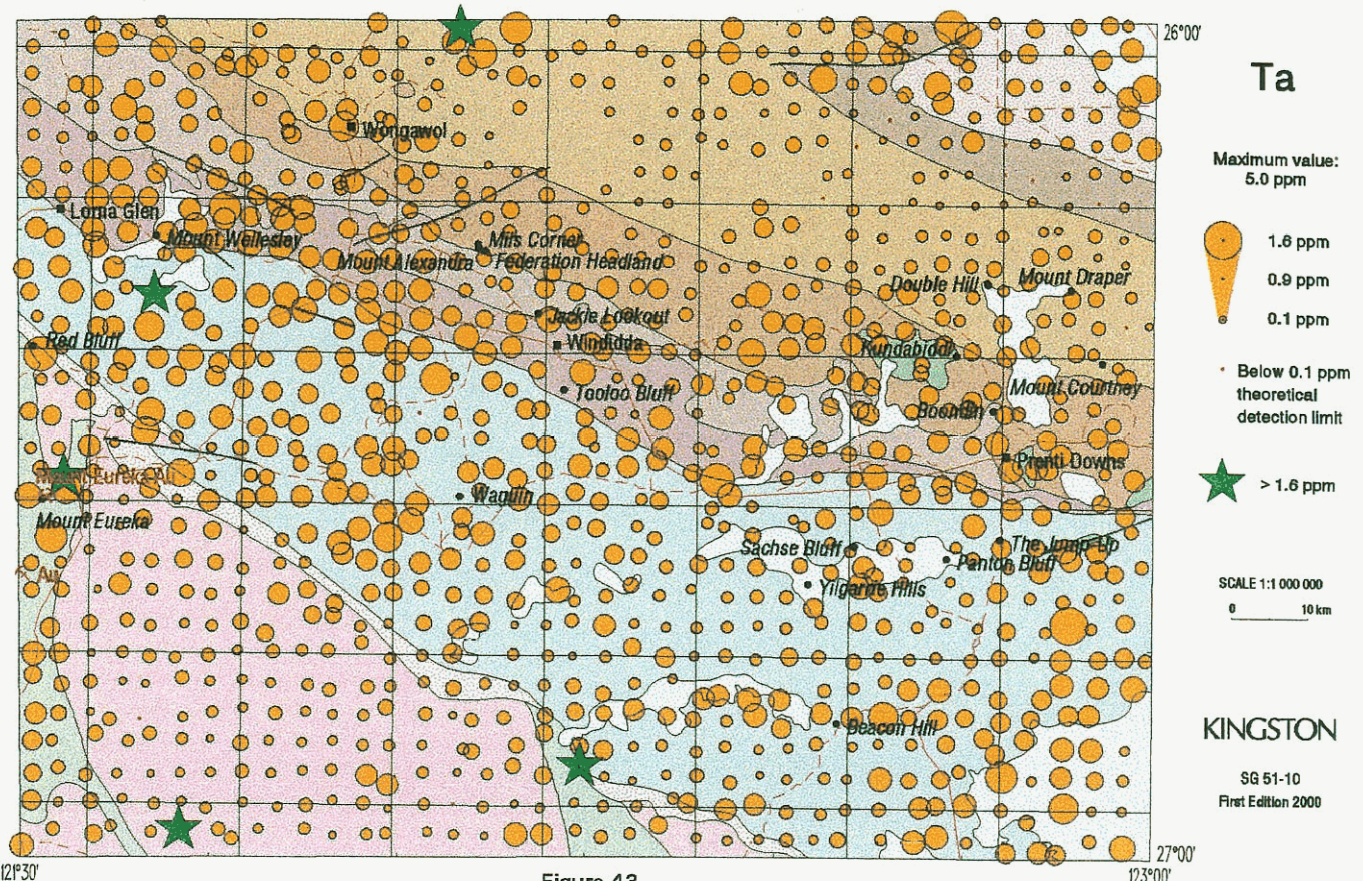


Figure 43

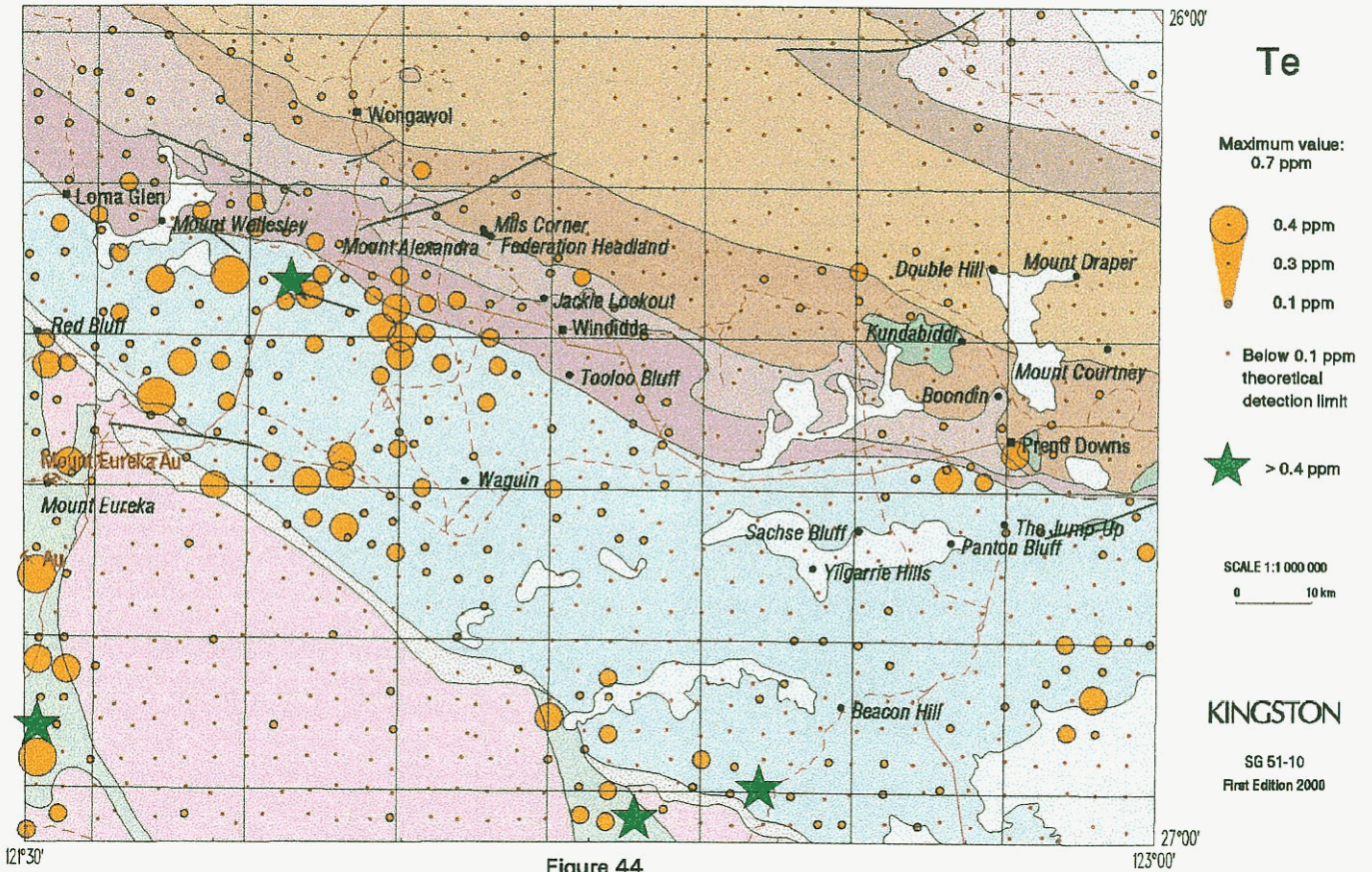


Figure 44

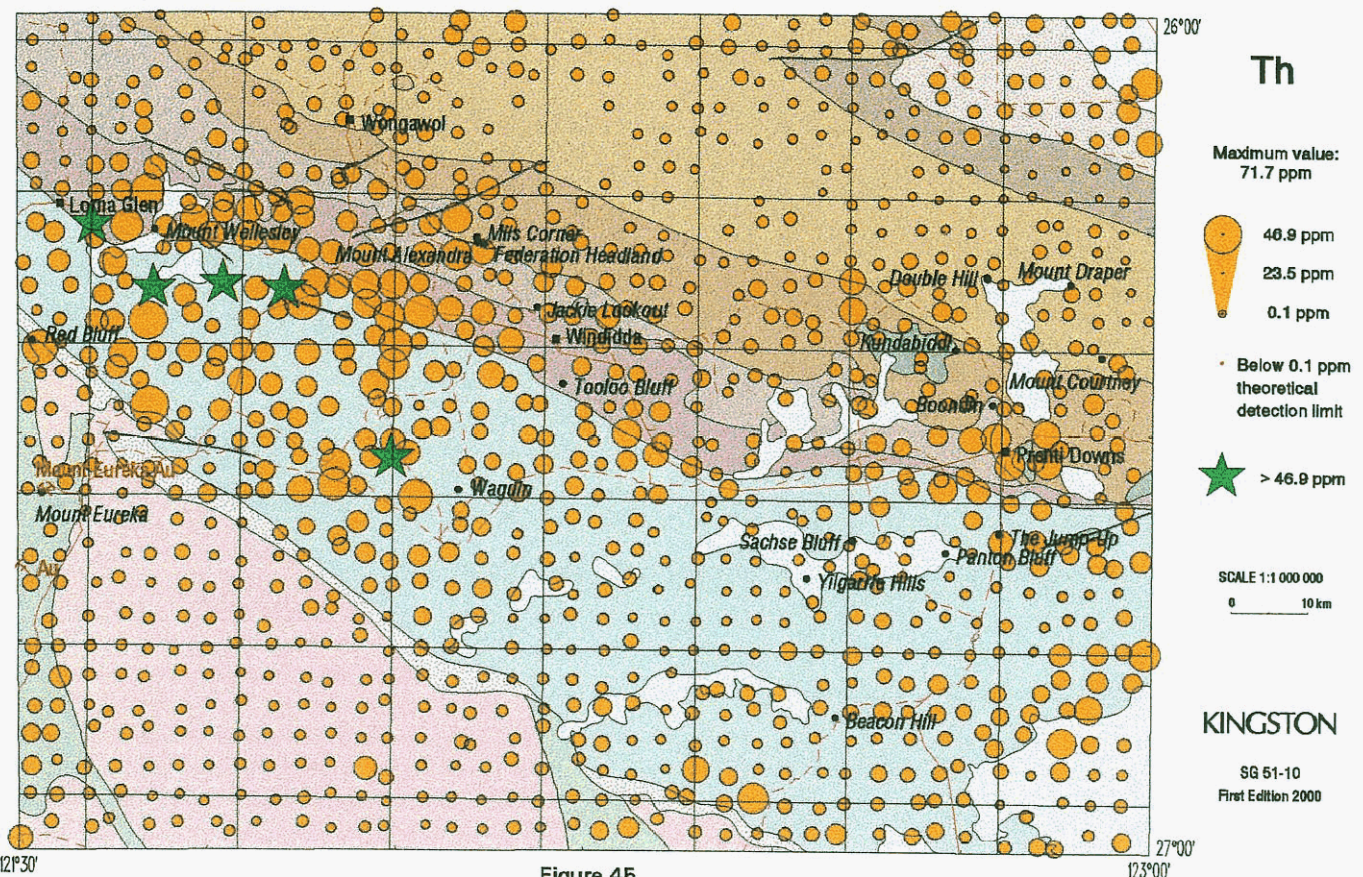


Figure 45

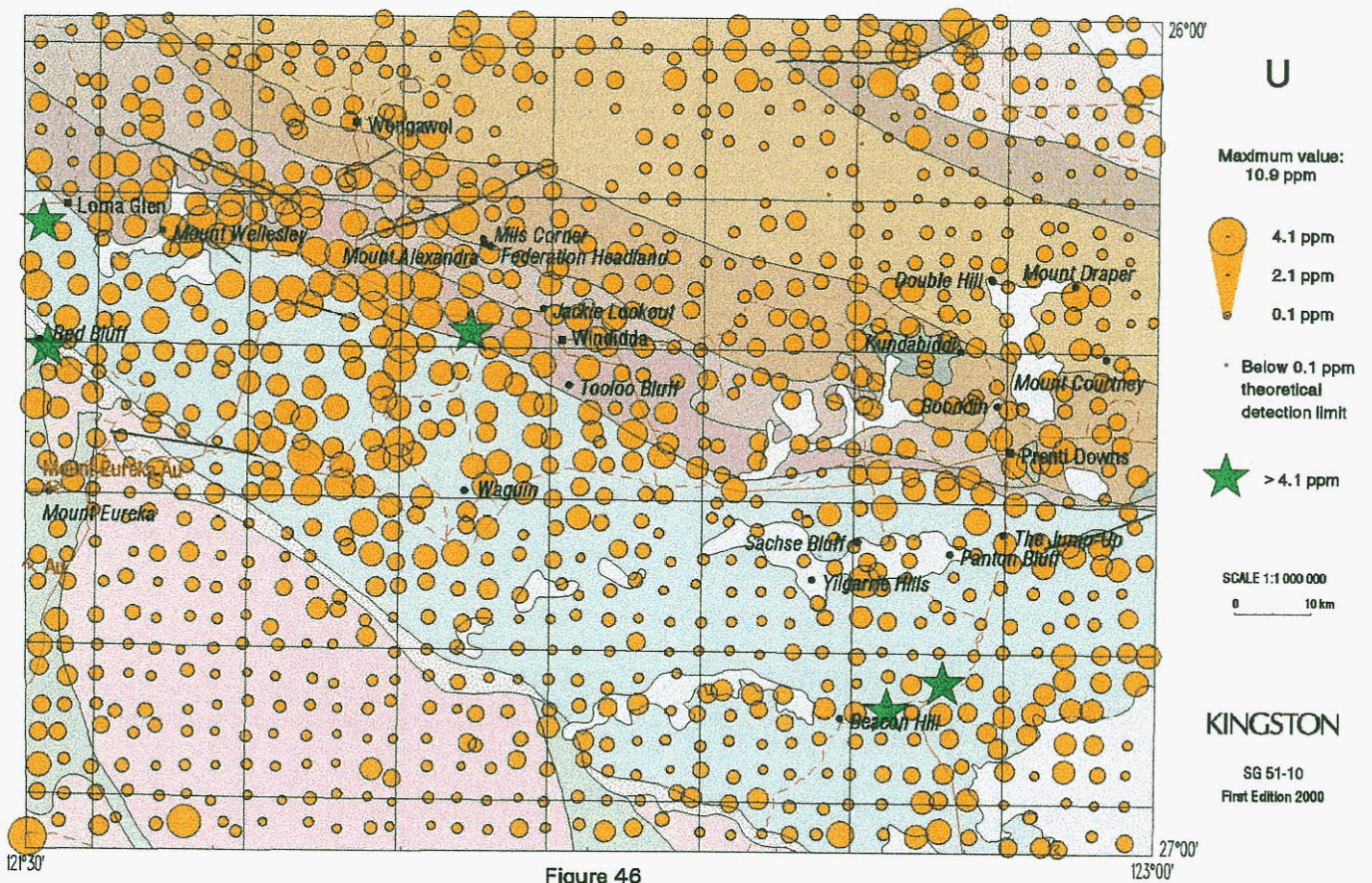


Figure 46

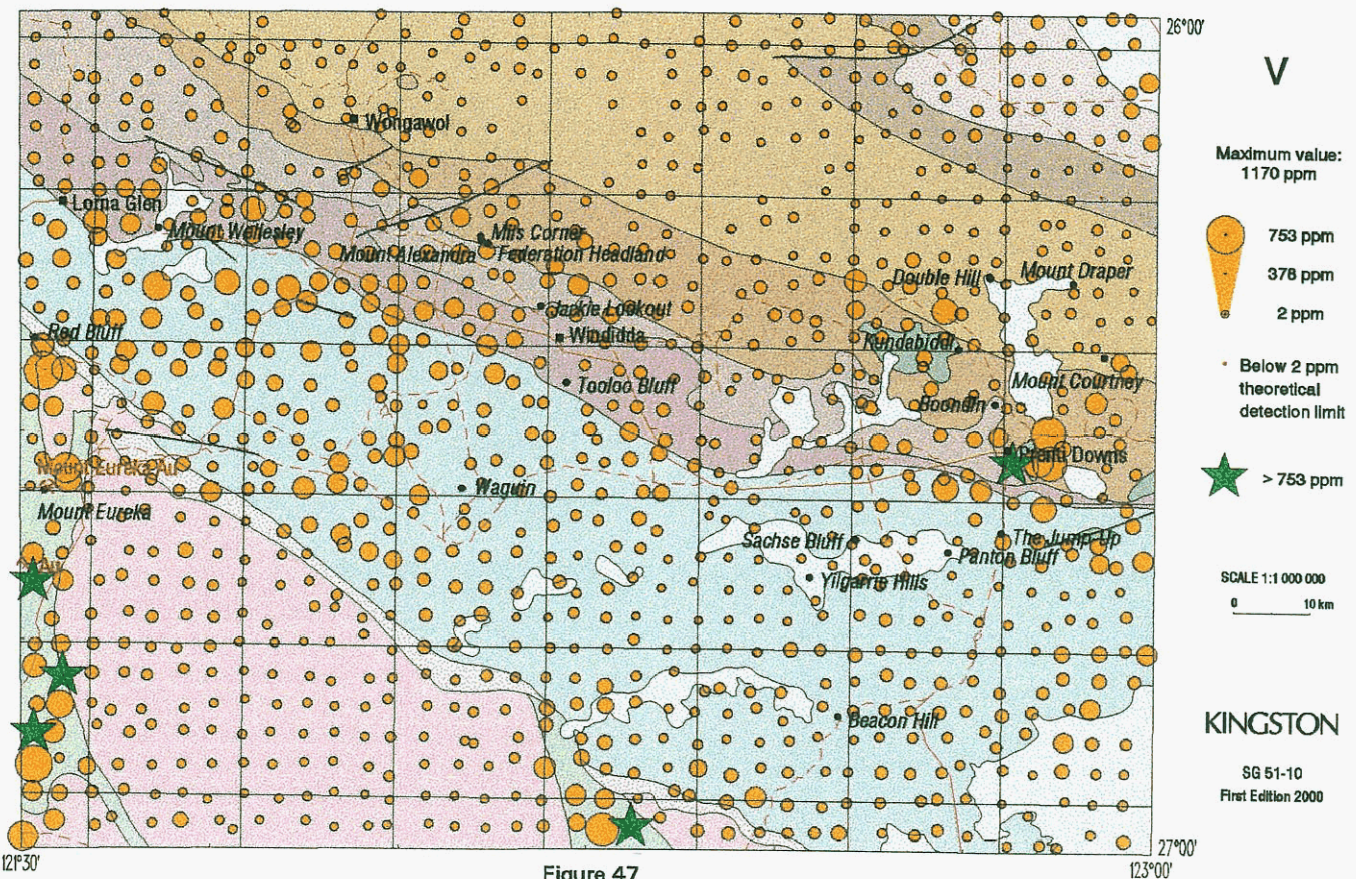


Figure 47

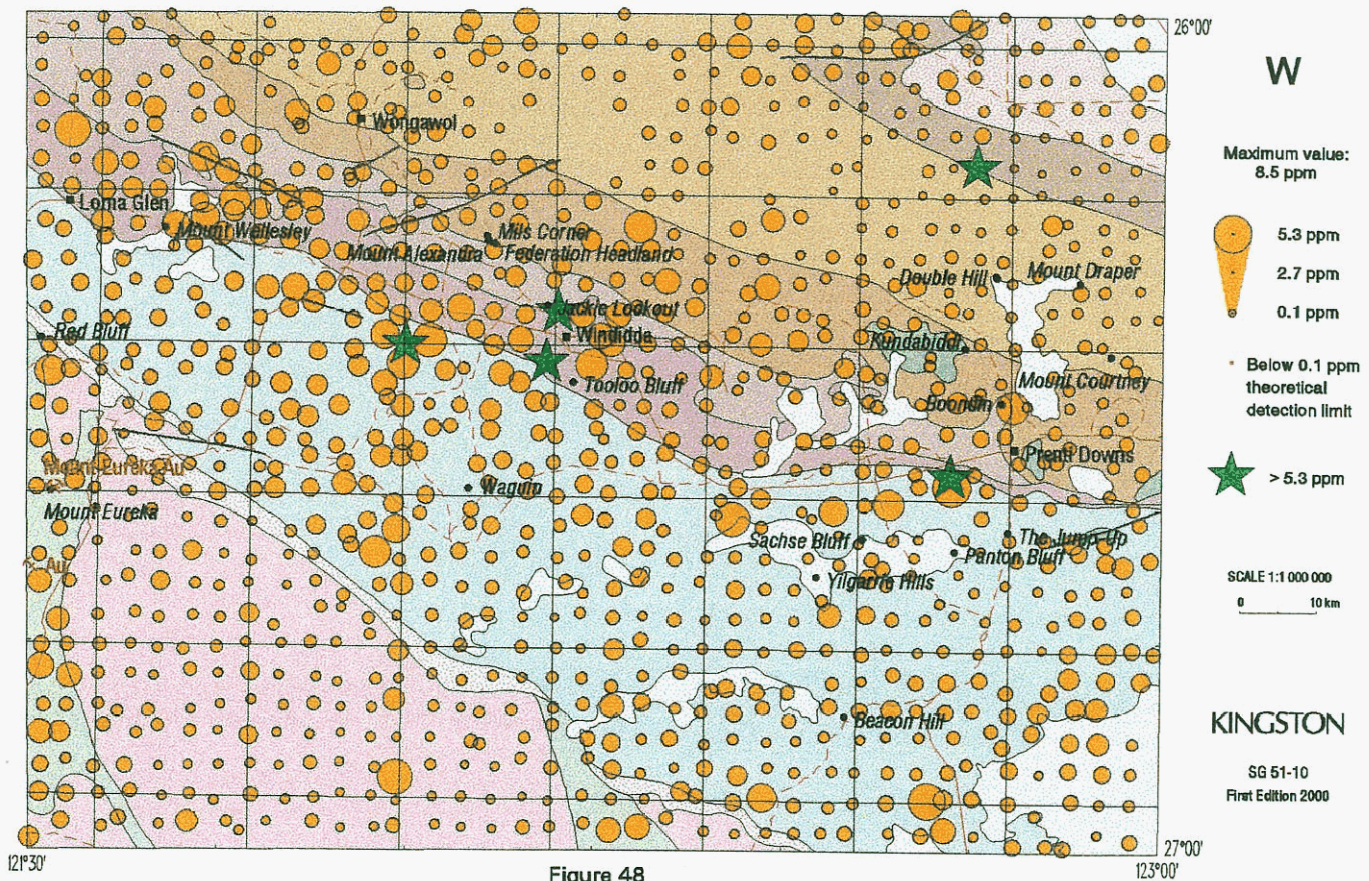


Figure 48

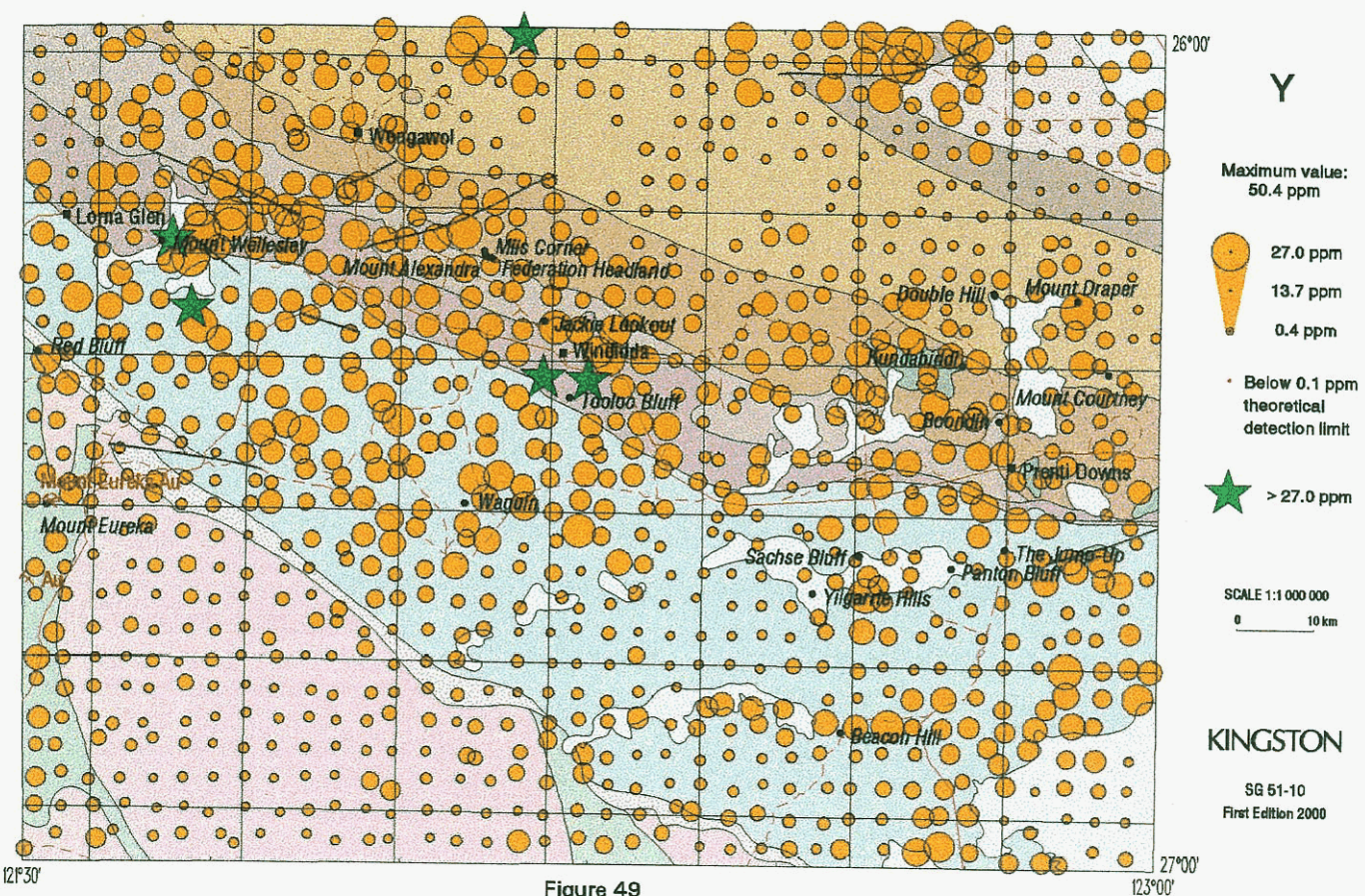


Figure 49

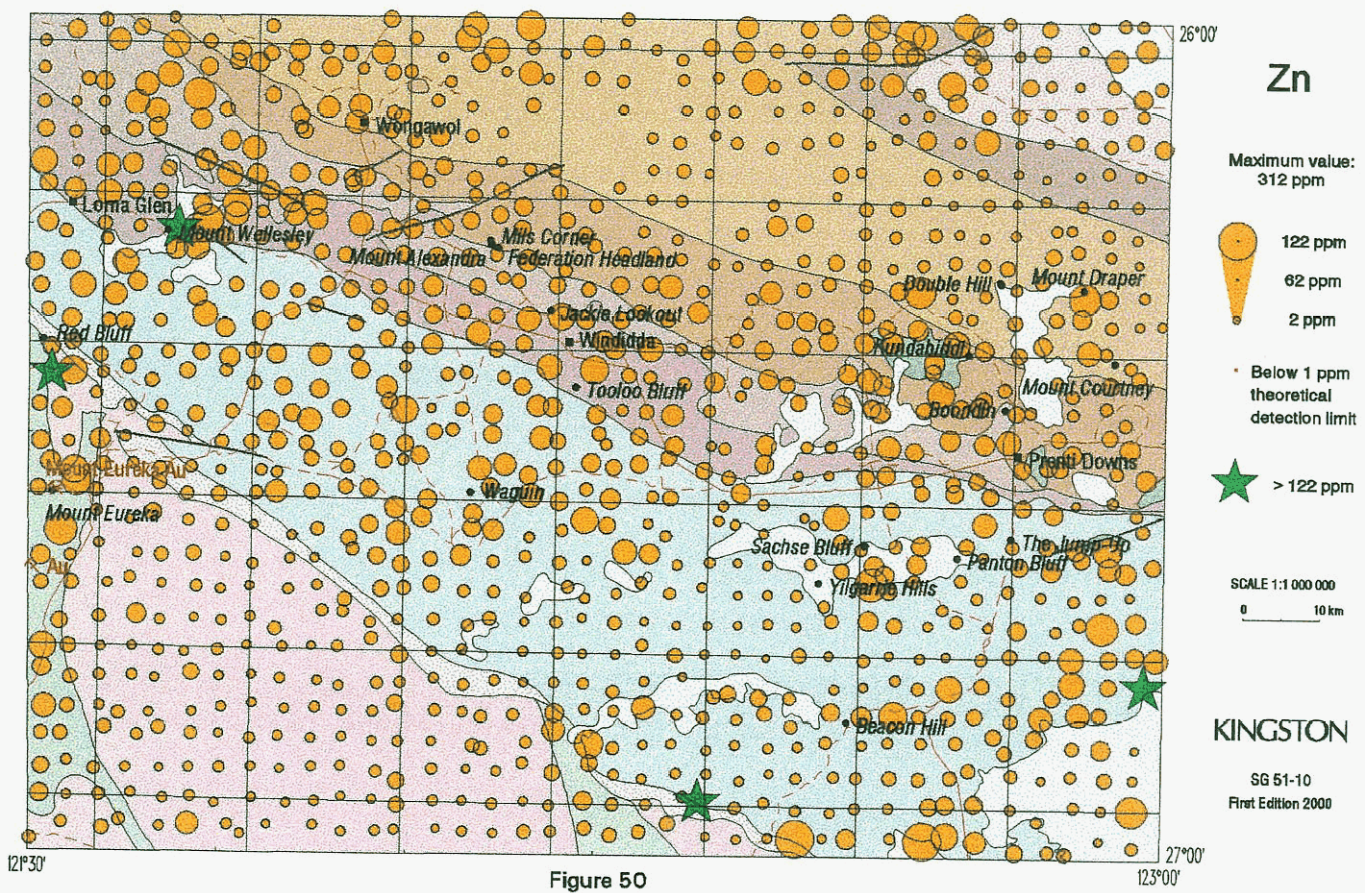


Figure 50

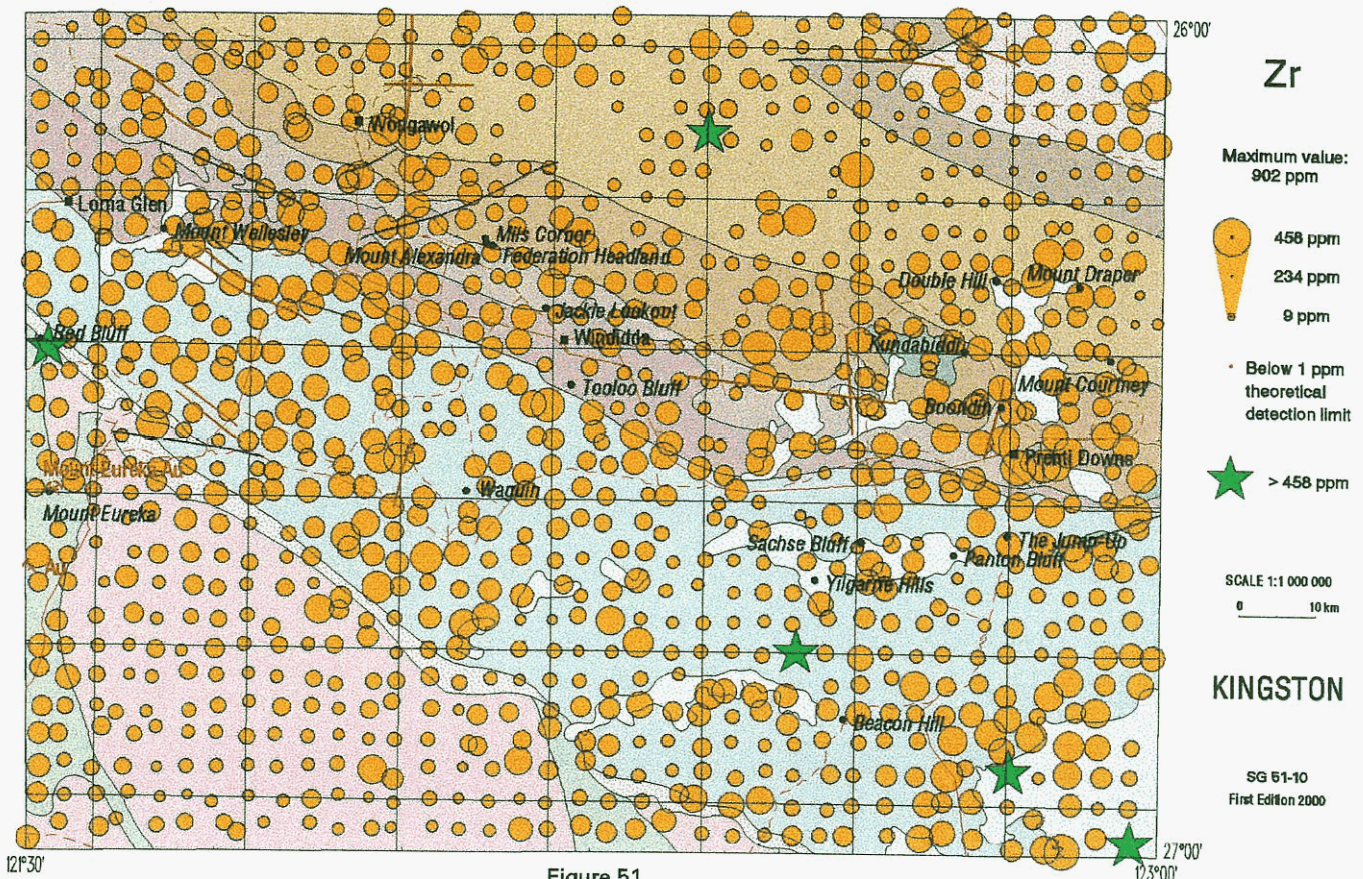


Figure 51

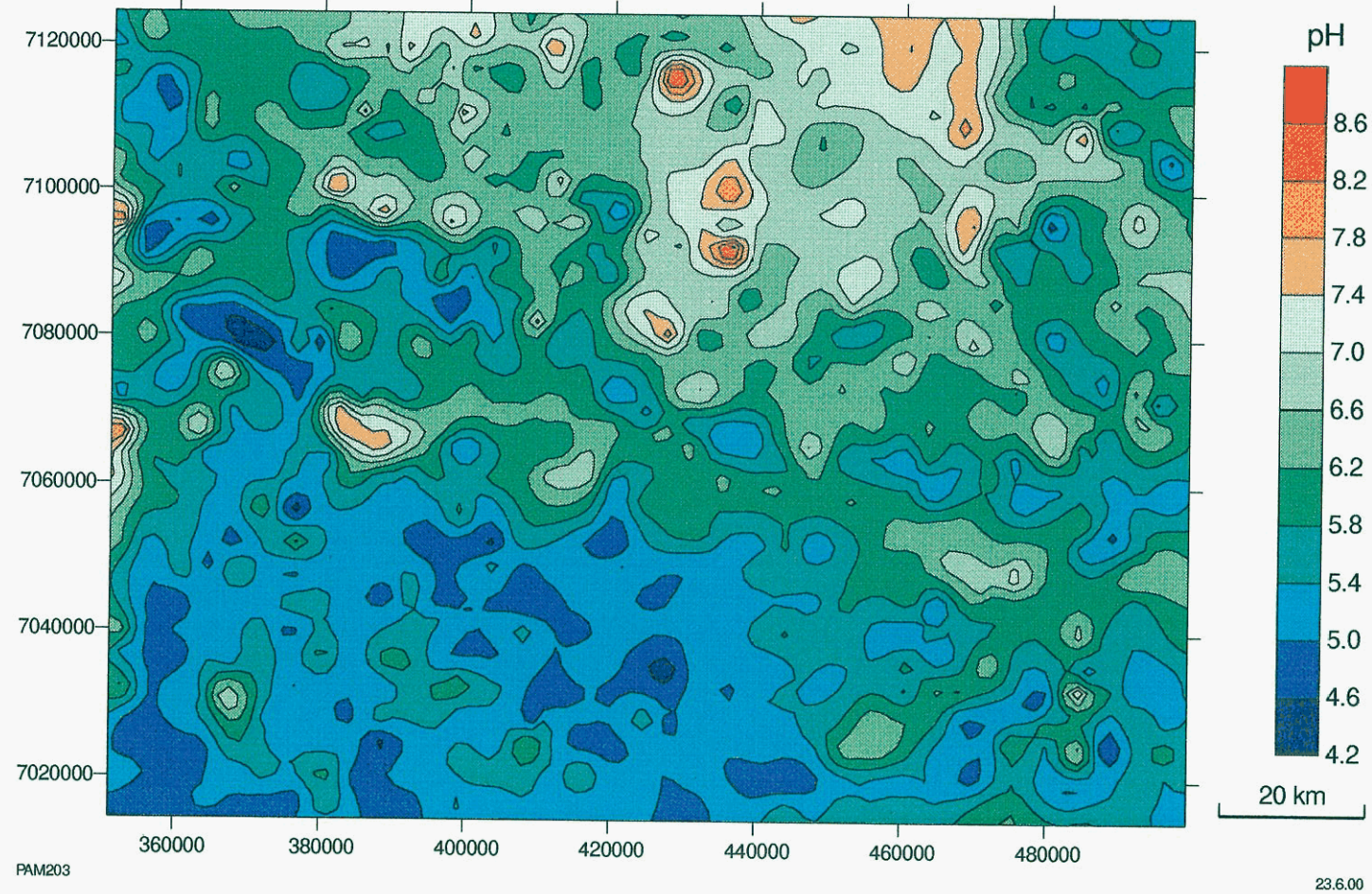


Figure 52. pH in regolith

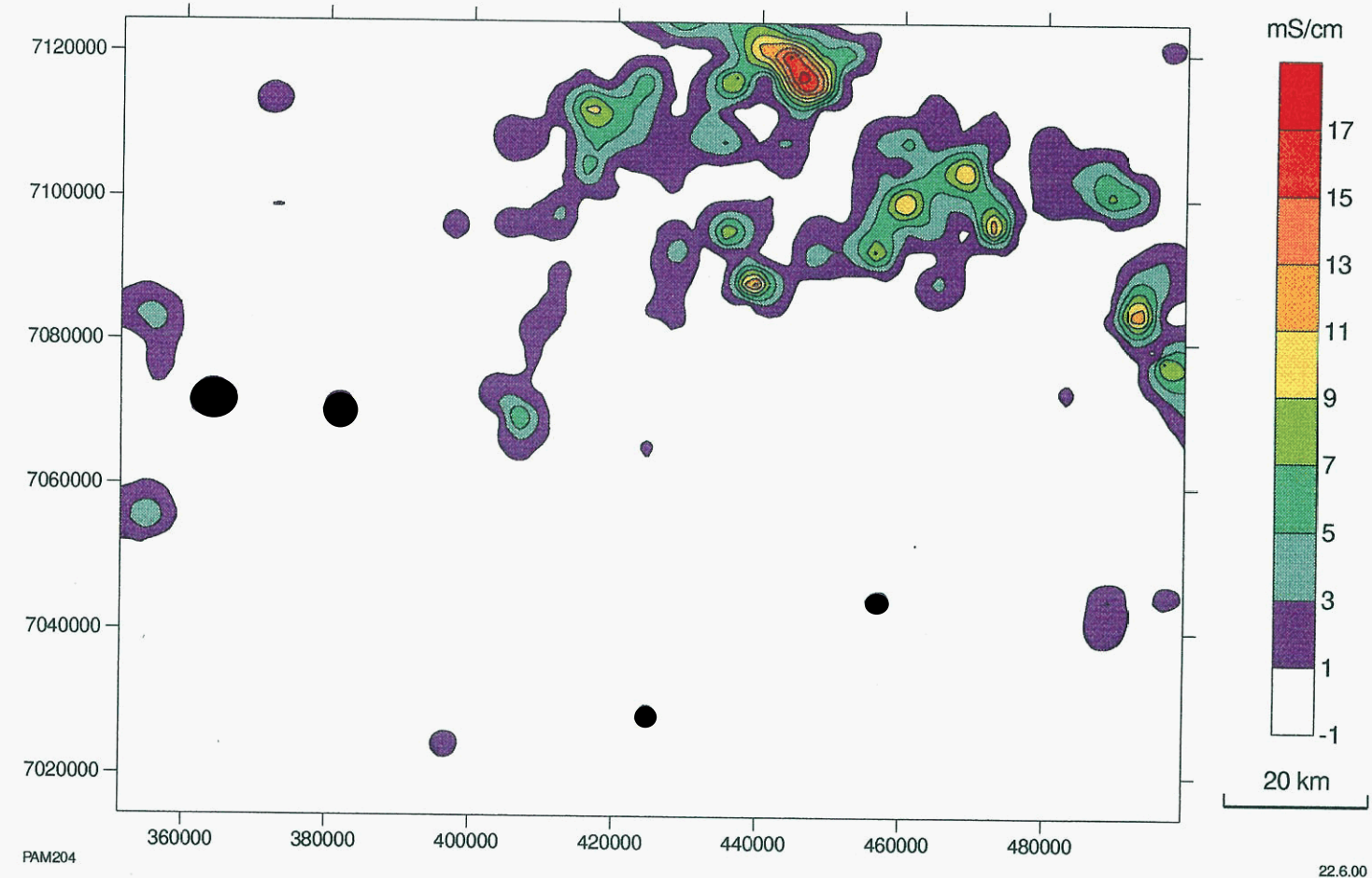


Figure 53. Conductivity of regolith (mS/cm)

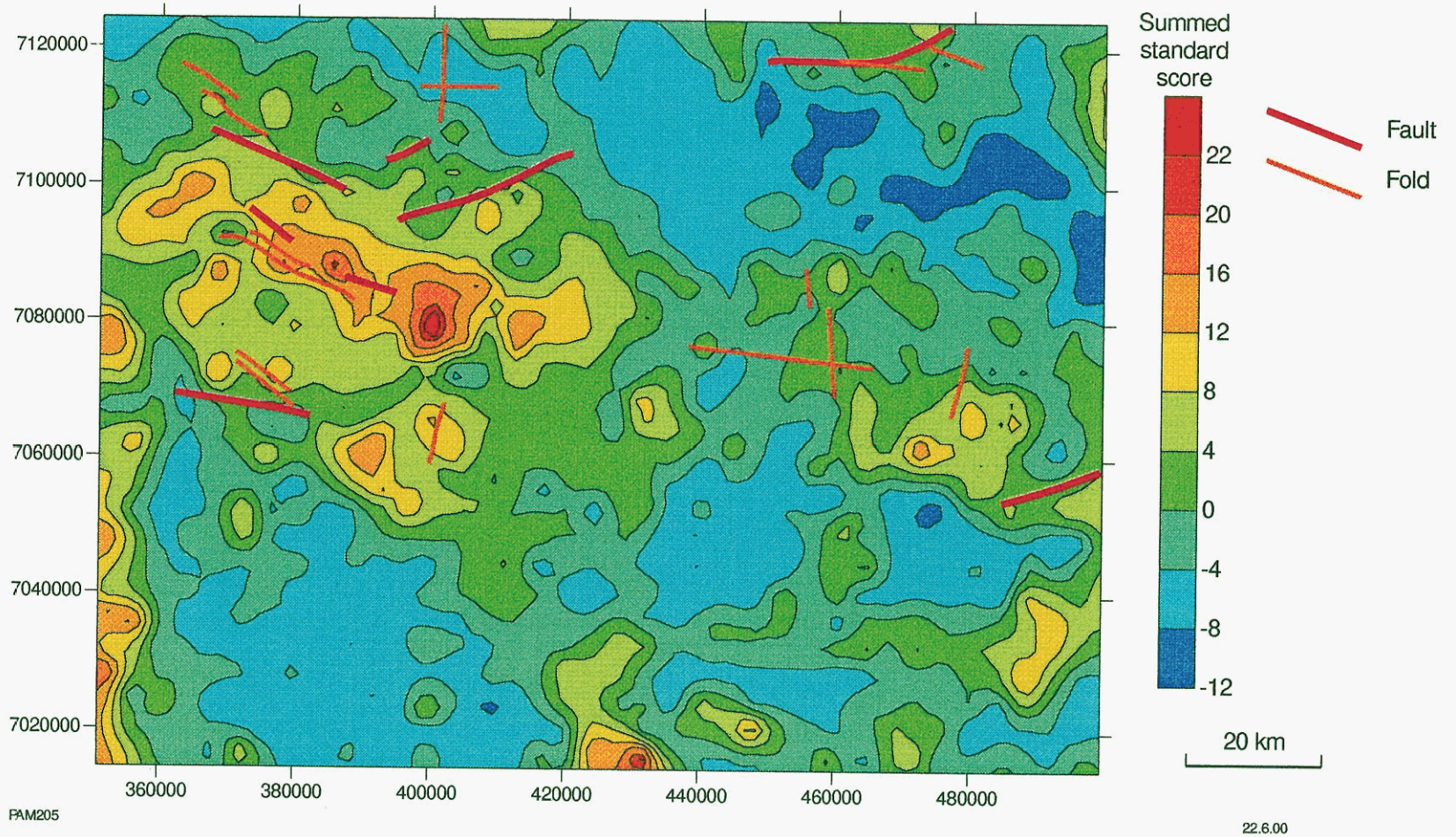


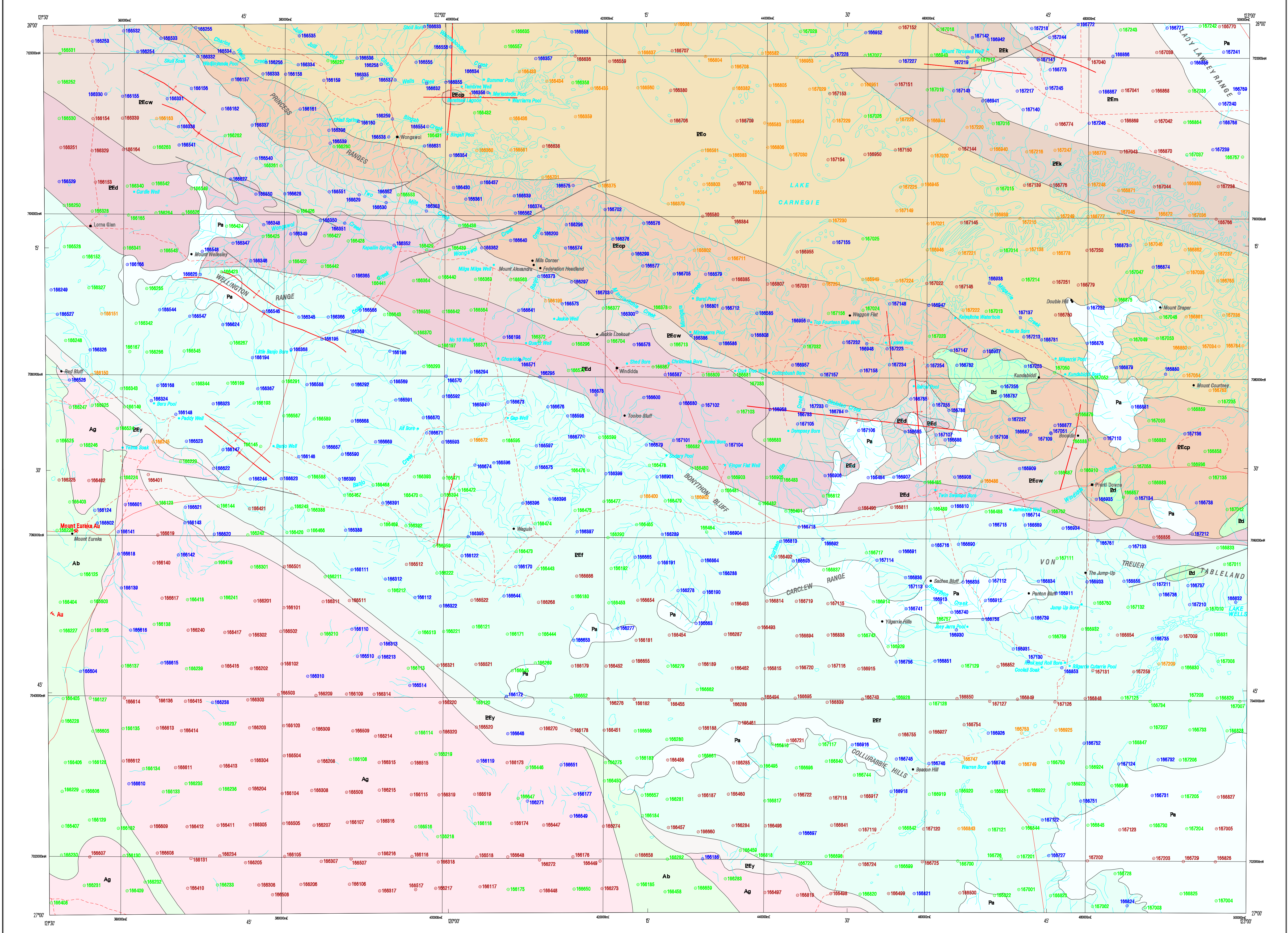
Figure 54. Chalcophile index ($\text{As} + \text{Sb} + \text{Bi} + \text{Mo} + \text{Ag} + \text{Sn} + \text{W} + \text{Se}$)

KINGSTON

GEOLOGICAL SURVEY OF WESTERN AUSTRALIA

SHEET SG 51-10

AUSTRALIA 1:250 000 REGOLITH GEOCHEMISTRY SERIES



Edited by N. Tetlow and G. Lowe

Cartography by G. Lowe

Topography from Australian Surveying and Land Information Group and modified from geological field survey (1988)

This map was compiled and produced using a Geographic Information System (ArcInfo), and the data are available in digital form

Published by the Geological Survey of Western Australia. Copies of this map, or extracts of the data, are available from the Information Centre, Department of Minerals and Energy, 100 Plain Street, East Perth, W.A., 6004. Phone (08) 9222 3456, Fax (08) 9222 3444

Compiled by K. J. Pye 1999

Sampling by S. Basajou, E. Bosanquet, J. Hansen, E. Mitnick, J. Moore, and N. Neave

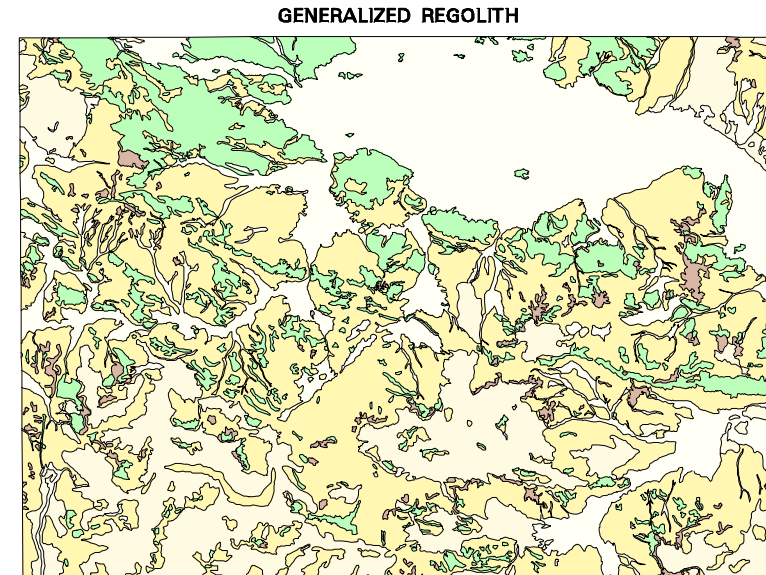
Total sample sites: 998; 329 sheetwash, 355 stream sediment, 227 sandplain, and 90 lake sediment

Analyse: Geology Laboratory Services.

Minimum sample size: 1.5 kg.

Fraction of sample analysed: >0.45 mm < 2 mm

Geological interpretation after Bunting (1980, 1988), Myers and Hocking (1989), Pirajno (1988), and Jones et al. (2000)

The recommended reference for this map is:
PYE, K. J., 2000, Sample locations, Kingston, W.A., sheet SG 51-10, A geological mapping of the Kingston 1:250 000 sheet by K. J. PYE, J. A. MORRIS, and S. A. JONES, Geological Survey of Western Australia, 1250 000 Regolith Geochemistry Series Explanatory Notes, Plate 1The recommended reference for this map is:
PYE, K. J., 2000, Sample locations, Kingston, W.A., sheet SG 51-10, A geological mapping of the Kingston 1:250 000 sheet by K. J. PYE, J. A. MORRIS, and S. A. JONES, Geological Survey of Western Australia, 1250 000 Regolith Geochemistry Series Explanatory Notes, Plate 1

GENERALIZED REGOLITH

GDA

SCALE 1:250 000

6000 METRES

0 5 10 15 20 25 30 KILOMETRES

UNIVERSAL TRANSVERSE MERCATOR PROJECTION

HORIZONTAL DATUM: GEOCENTRIC DATUM OF AUSTRALIA 1994

VERTICAL DATUM: AUSTRALIAN HEIGHT DATUM

Grid lines indicate 20 000 metre interval of the Map Grid Australia, Zone 51

The Map Grid Australia (MGA) is based on the Geocentric Datum of Australia 1994 (GDA94). GDA94 positions are compatible within one metre of the datum WGS84 positions

INDEX TO 1:100 000 MAP SHEETS

WONGAWOL 3446

WINDDOA 3446

CARNIE 3446

YELMA 3446

COLLARBIE 3446

VON TREUER 3446

WINDIDDY 3446

BIR SAMUEL 3446

DUKETON 3446

THROBBELL 3446

NARBERU 3446

STANLEY 3446

HERBERT 3446

WILNA 3446

KINGSTON 3446

ROBERT 3446

BIR SAMUEL 3446

DUKETON 3446

THROBBELL 3446

NARBERU 3446

STANLEY 3446

HERBERT 3446

WILNA 3446

KINGSTON 3446

ROBERT 3446

BIR SAMUEL 3446

DUKETON 3446

THROBBELL 3446

NARBERU 3446

STANLEY 3446

HERBERT 3446

WILNA 3446

KINGSTON 3446

ROBERT 3446

BIR SAMUEL 3446

DUKETON 3446

THROBBELL 3446

NARBERU 3446

STANLEY 3446

HERBERT 3446

WILNA 3446

KINGSTON 3446

ROBERT 3446

BIR SAMUEL 3446

DUKETON 3446

THROBBELL 3446

NARBERU 3446

STANLEY 3446

HERBERT 3446

WILNA 3446

KINGSTON 3446

ROBERT 3446

BIR SAMUEL 3446

DUKETON 3446

THROBBELL 3446

NARBERU 3446

STANLEY 3446

HERBERT 3446

WILNA 3446

KINGSTON 3446

ROBERT 3446

BIR SAMUEL 3446

DUKETON 3446

THROBBELL 3446

NARBERU 3446

STANLEY 3446

HERBERT 3446

WILNA 3446

KINGSTON 3446

ROBERT 3446

BIR SAMUEL 3446

DUKETON 3446

THROBBELL 3446

NARBERU 3446

STANLEY 3446

HERBERT 3446

WILNA 3446

KINGSTON 3446

ROBERT 3446

BIR SAMUEL 3446

DUKETON 3446

THROBBELL 3446

NARBERU 3446

STANLEY 3446

HERBERT 3446

WILNA 3446

KINGSTON 3446

ROBERT 3446

BIR SAMUEL 3446

DUKETON 3446

THROBBELL 3446

NARBERU 3446

STANLEY 3446

HERBERT 3446

WILNA 3446

KINGSTON 3446

ROBERT 3446

BIR SAMUEL 3446

DUKETON 3446

THROBBELL 3446

NARBERU 3446

STANLEY 3446

HERBERT 3446

WILNA 3446

KINGSTON 3446

ROBERT 3446

BIR SAMUEL 3446

DUKETON 3446

THROBBELL 3446

NARBERU 3446

STANLEY 3446

HERBERT 3446

WILNA 3446

KINGSTON 3446

ROBERT 3446

BIR SAMUEL 3446

DUKETON 3446

THROBBELL 3446

NARBERU 3446

STANLEY 3446

HERBERT 3446

WILNA 3446

KINGSTON 3446

ROBERT 3446

BIR SAMUEL 3446

DUKETON 3446

THROBBELL 3446

NARBERU 3446

STANLEY 3446

HERBERT 3446

WILNA 3446

KINGSTON 3446

ROBERT 3446

BIR SAMUEL 3446

DUKETON 3446

THROBBELL 3446

NARBERU 3446

STANLEY 3446

HERBERT 3446

WILNA 3446

KINGSTON 3446

ROBERT 3446

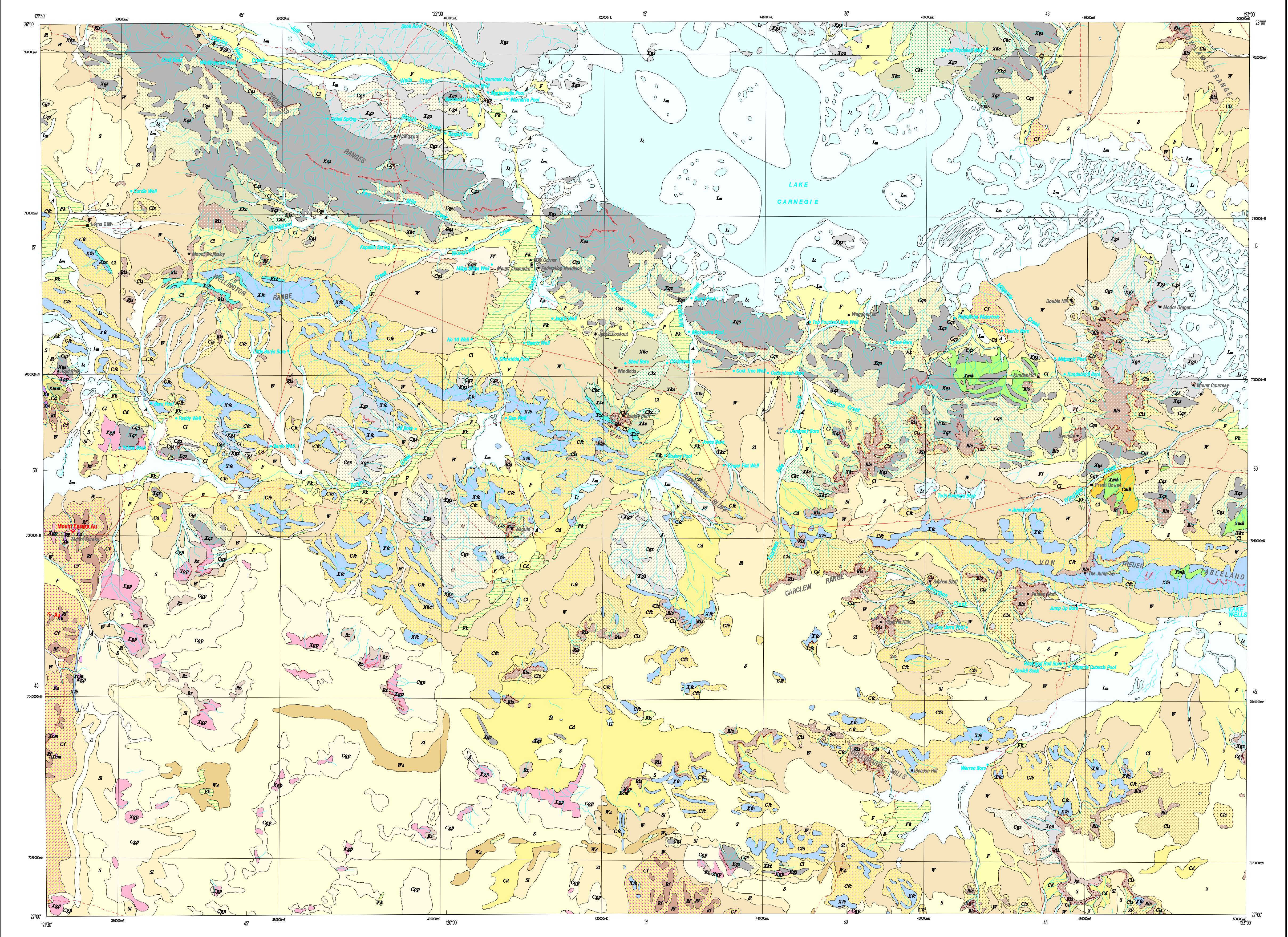
BIR SAMUEL

KINGSTON

GEOLOGICAL SURVEY OF WESTERN AUSTRALIA

SHEET SG 51-10

AUSTRALIA 1:250 000 REGOLITH GEOCHEMISTRY SERIES



REGOLITH MATERIALS

REFERENCE

RESIDUAL (R)	- Residual sand and duricrust and proximal reworked material derived by weathering in situ
Rf	- comprising mainly iron-rich material (ferriferous and ferruginous lag)
Rls	- derived from mixed sedimentary rock (Paternon Formation); locally silicified
Rz	- comprising mainly silica-rich material (albite and jasperoidal chaledony)
EXPOSED (X)	- Outcrop of bedrock, subcrop, and saprock with locally derived sand, silt, clay, and rubble
Xcm	- derived from clay-rich metamorphic rock (phyllite, kaolinized schist, and kaolinized volcanoclastic rock)
Xfe	- derived from iron-rich chemical sedimentary rock (pelletal and banded iron-formation, hematitic shale, and chert)
Xgp	- derived from quartzofeldspathic plutonic rock (granitoid rock); locally kaolinized, silicified, and ferruginized
Xgs	- derived from quartzofeldspathic siliciclastic sedimentary rock (sandstone, siltstone, and shale)
Xgv	- derived from quartzofeldspathic volcanic rock (lithic volcanic rock)
Xhc	- derived from carbonate-rich biochemical sedimentary rock (limestone, calcarenous, and dolomite)
Xmh	- derived from ferromagnesian hypabyssal rock (dolerite)
Xms	- derived from ferromagnesian metamorphic rock (metamorphosed tholeiitic basalt, metadolerite, and metagabbro)
Xqs	- derived from quartz-rich siliciclastic sedimentary rock (sandstone, quartzite, siltstone, and shale)
Xu	- derived from ultramafic rock (peridotite and metamorphosed ultramafic rock)
Xzc	- derived from aluminosilicate-rich chemical sedimentary rock (pelletal chert)
COLLUVIAL (C)	- Unconsolidated and semi-consolidated silt, sand, gravel, and rubble
Cd	- undivided
Cr	- comprising iron-rich material
Cfe	- derived mainly from iron-rich chemical sedimentary rock (pelletal and banded iron-formation, hematitic shale, and chert)
Cgp	- derived mainly from quartzofeldspathic plutonic rock (granitoid)
Cgs	- derived mainly from quartzofeldspathic sedimentary rock (sandstone)
Chc	- derived mainly from carbonate-rich biochemical sedimentary rock (limestone, calcarenous, and dolomite)
Clt	- derived from mixed parentage
Cls	- derived mainly from mixed sedimentary rock (Paternon Formation)
Cma	- derived mainly from ferromagnesian hypabyssal rock (dolerite)
Cqs	- derived mainly from quartz-rich siliciclastic sedimentary rock (sandstone, quartzite, siltstone, and shale)
DISTAL SHEETWASH (W)	- Sand- and clay-dominated colluvium or sheetwash
Wa	- Sand- and clay-dominated colluvium or sheetwash associated with depressions and drainages
ALLUVIAL (A)	- Cobble, gravel, sand, silt, and clay in alluvial channels
FLOODPLAIN (F)	- Overbank deposits; sand- or clay-rich alluvium and colluvium on floodplains
Ft	- Overbank deposits; sand- or clay-rich alluvium and colluvium on floodplains containing iron-rich material
Fk	- Overbank deposits; sand- or clay-rich alluvium and colluvium on floodplains containing carbonate-rich material (valley calcrete)
LACUSTRINE (L)	- Clay, silt, sand, and evaporitic material; locally saline and gypferous
Li	- In playas and claypanes
Lm	- In mixed dune and playa terrain proximal to lakes
SANDPLAIN (S)	- Reddish and eolian sand; dominated by undulating sandplain and eolian dunes
S	- Sandplain with clay-rich colluvium and sheetwash; minor solan reworking

SYMBOLS

Regolith boundary	Windidda	Homestead
Breakaway	Double Hill	Locality
Minor road	Mount Eureka	Mine
Track	Gold	Prospect
Watercourse	Au	
Pool, soak, spring bore, well		



REGOLITH MATERIALS

REGOLITH GEOCHEMISTRY SERIES

KINGSTON

SHEET SG 51-10
FIRST EDITION 2000
© Western Australia 2000

Edited by N. Tetlow and G. Lomax

Cartography by G. Jose

Topography from Australian Surveying and Land Information Group and modified from geological field survey (1988)

This map was compiled and produced using a Geographic Information System (ArcInfo), and the data are available in digital form

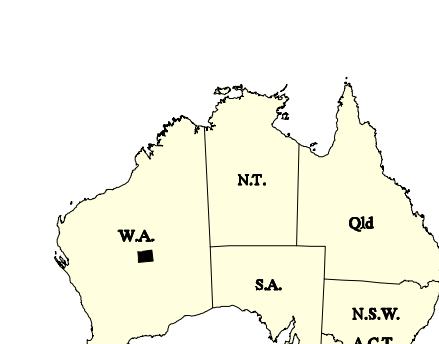
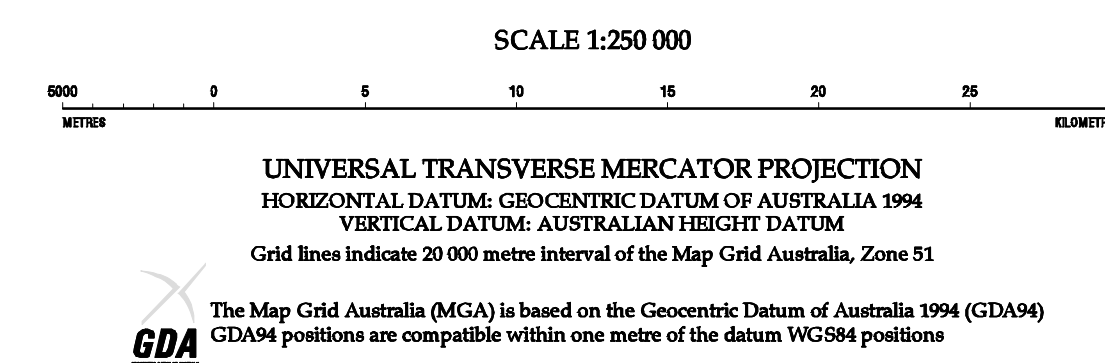
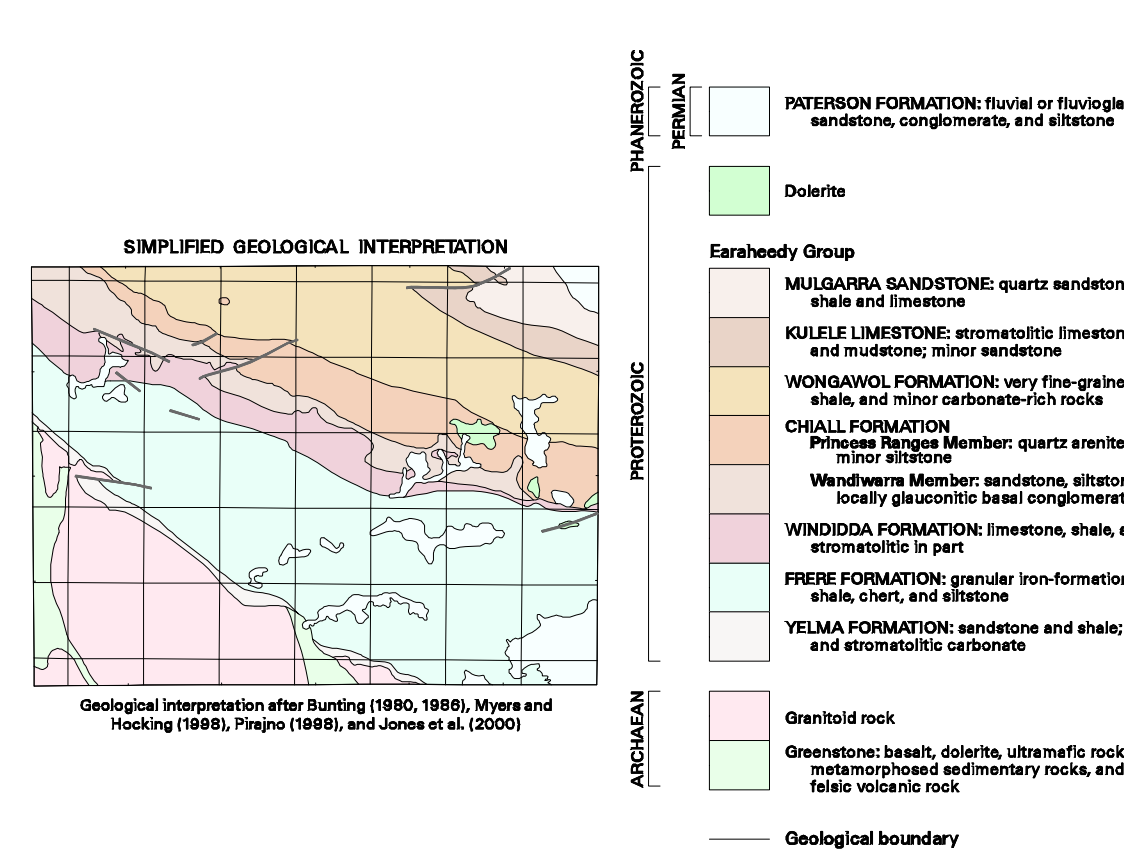
Published by the Geological Survey of Western Australia. Copies of this map, or extracts of the data, are available from the Information Centre, Department of Minerals and Energy, 100 Plain Street, East Perth, W.A., 6004. Phone (08) 9222 3456, Fax (08) 9222 3444

Compiled by S. A. McGuinness and K. J. Pye 1999

Sampling by S. Basajou, E. Bosanquet, J. Hansen, E. Mikucki, J. Moore, N. Neave

Comprising Landsat TM Images (1984 data), black and white aerial photography, 1:100 000 published GSWA 1:250 000 Geological Series maps and field observations 1998

The recommended reference for this map is: McGuinness, S. A. and Pye, K. J., 2000, Regolith materials, Kingston, W.A. sheet SG 51-10, In: Geochimical mapping of the Kingston 1:250 000 sheet by K. J. Pye, P. A. Morris, and S. A. McGuinness: Western Australia Geological Survey, 1:250 000 Regolith Geochemistry Series Explanatory Notes, Plate 2



SHEET INDEX		
WALES 60 51-4	STANLEY 60 51-4	HERBERT 60 51-7
WILLINA 60 51-9	KINGSTON 60 51-10	ROBERT 60 51-11
BIR SAMUEL 60 51-12	DUNTON 60 51-14	THROBELL 60 51-15

INDEX TO 1:100 000 MAP SHEETS		
WONGAWOL 3244	WINDIDDA 3244	CARNEGIE 3444
YELMA 3244	COLLARASIE 3244	VON TREUER 3444

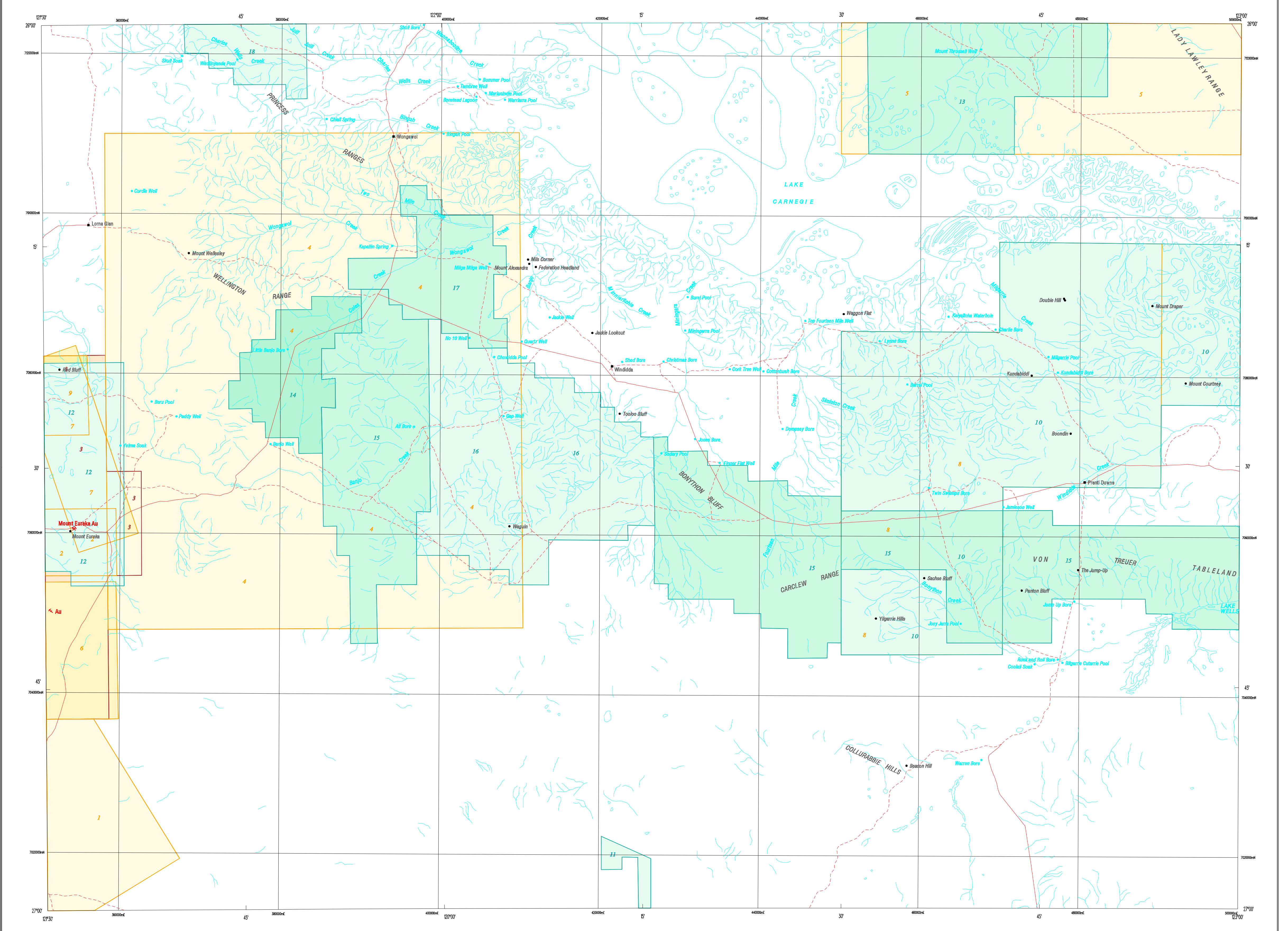
WARNING: Inks are water soluble and will fade with prolonged exposure to light

KINGSTON

GEOLOGICAL SURVEY OF WESTERN AUSTRALIA

SHEET SG 51-10

AUSTRALIA 1:250 000 REGOLITH GEOCHEMISTRY SERIES

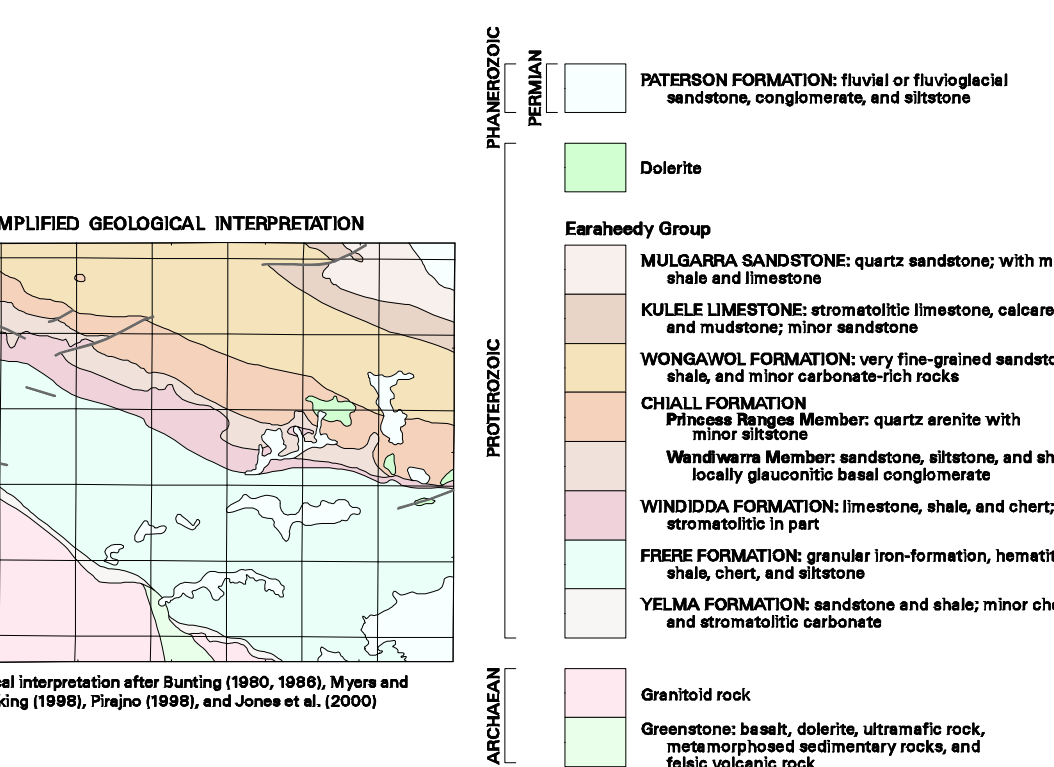


COMPANY PROJECTS WITH SURFACE GEOCHEMISTRY DATA IN OPEN-FILE REPORTS (at April 1999)

Project period reported within
(Various colour shades used for ease of project identification)

- 1966 - 1970
- 1971 - 1975
- 1976 - 1980
- 1981 - 1985
- 1986 - 1990
- 1991 - 1997

Number within project area is a database ID number (see Appendix 3 of the Explanatory Notes)



SYMBOLS	
Minor road	Windidda
Track	Double Hill
Watercourse	Locality
Lake	Mount Eureka
Pool, soak, spring bore, well	Mine
Au	Prospect
	Gold



COMPANY PROJECTS WITH SURFACE GEOCHEMISTRY DATA IN OPEN-FILE REPORTS (at April 1999)

Edited by N. Tetlow and G. Loan

Cartography by G. Jose

Topography from Australian Surveying and Land Information Group

and modified from geological map survey (1988)

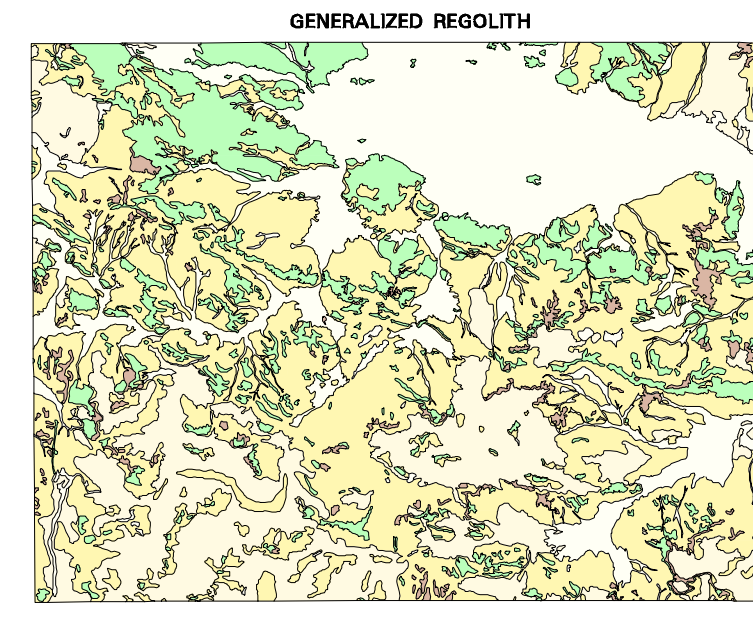
This map was compiled and produced using a Geographic Information System (ArcInfo), and the data are available in digital form

Published by the Geological Survey of Western Australia. Copies of this map, or extracts of the data, are available from the Information Centre, Department of Minerals and Energy, 100 Plain Street, East Perth, W.A. 6004. Phone (08) 9222 3456, Fax (08) 9222 3444

Compiled by S. A. McGuinness 1999

Compiled from open-file mineral exploration reports held by the Geological Survey of Western Australia

The recommended reference for this map is:
McGUINNESS, S. A., 2000. Company projects with surface geochemistry data in open-file reports (at April 1999). In: Geochimical mapping of the Kingston 1:250 000 sheet by K. J. PYE, P. A. MORRIS, and S. A. McGUINNESS. Western Australia Geological Survey, 1:250 000 Regolith Geochemistry Series Explanatory Notes, Plate 3



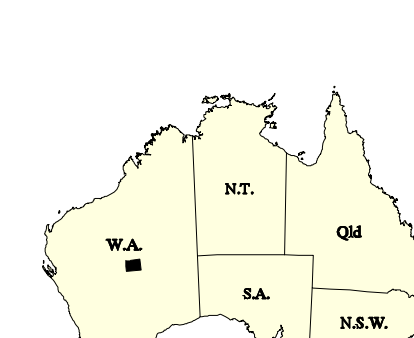
SCALE 1:250 000

6000 METRES 0 5 10 15 20 25 30 KILOMETRES

UNIVERSAL TRANSVERSE MERCATOR PROJECTION
HORIZONTAL DATUM: GEOCENTRIC DATUM OF AUSTRALIA 1994
VERTICAL DATUM: AUSTRALIAN HEIGHT DATUM
Grid lines indicate 20 000 metre interval of the Map Grid Australia, Zone 51

GDA

The Map Grid Australia (MGA) is based on the Geocentric Datum of Australia 1994 (GDA94). GDA94 positions are compatible within one metre of the datum WGS84 positions.



SHEET INDEX		
WA 51-4	STANLEY 51-14	HERBERT 51-17
WILNA 51-9	KINGSTON 51-10	ROBERT 51-11
BIR SAMUEL 51-15	DUNTON 51-14	THROBELL 51-16
INDEX TO 1:100 000 MAP SHEETS		
WONGAWOL 344	WINDIDDA 344	CARNEGIE 344
YELMA 344	COLLARBIE 344	VON TREUER 344

REGOLITH GEOCHEMISTRY SERIES
KINGSTON
SHEET SG 51-10
FIRST EDITION 2000
© Western Australia 2000

WARNING: Inks are water soluble and will fade with prolonged exposure to light